EXPLORING THE REPRODUCIBILITY AND ENVIRONMENTAL REALISM OF PESTICIDE FATE PROCESSES IN REGULATORY SYSTEMS

REBECCA VICTORIA SOUTHWELL

A thesis submitted for the degree of Doctor of Philosophy

School of Life Sciences, University of Warwick

February 2018

CONTENTS

LIST OF FIGURES

LIST OF TABLES

ACKNOWLEDGEMENTS

Firstly, I would like to thank my supervisors Gary Bending, Jonty Pearson, and Laurence Hand for their help, guidance, and advice over the last four years. I would also like to acknowledge the Biotechnology and Biological Sciences Research Council and Syngenta for providing funding for this project.

Being split between two departments at the University of Warwick could be challenging at times; however, I am eternally grateful to Ian Baylis at Warwick School of Engineering for his patience and expertise with silicone sealant. I would also like to thank Vassia Ioannidou and Joel Whittle. During my project, I was fortunate to spend three months working at Syngenta's Jealott's Hill International Research Centre. I would like to thank the Product Safety team for making me feel welcome during my time on site, with especial thanks to Harriet Moreland for giving up so much of her time. I would also like to acknowledge Kevin Thomas, Samantha Marshall, and Carol Nichols for their inputs in project meetings, particularly at the beginning of my PhD, and Mansoor Saeed for assistance with the LC-MS protocol.

From Warwick School of Life Sciences, I would like to thank past and present members of the Bending group. In particular, Sally Hilton for help with MiSeq library preparation, Emma Picot for being an R wizard, Paul Hunter for help with combustion analysis, and Chris Hale for general help, advice, and tea breaks. Very special thanks go to Mark Day for guidance with chemical analysis methods and for still replying to my questions when trekking around Asia. I would not have been able to carry out my many river sampling trips if it had not been for Helen Jones, Emily Stoakes, and Chris Hale; Helen in particular gave up a lot of time and rescheduled her own work to help with the massive feat that was sampling for the microflume experiment. Other acknowledgements include Hendrik Schäfer for help using ARB software, Martin Holdsworth for fixing my shaker multiple times and the idea of incorporating chillers on the microflume plumbing, Phil Young for statistical help, Robert Spooner for guidance with my teaching qualifications, and Andy Jukes, whom I never met, but he let me borrow his SPE manifold for three years! Thanks also to the technical and support staff in the School of Life Sciences, particularly Cathy Parry, and also Gill Scott, Tracy McCusker, and Gerrie Keene for allowing me to "borrow" multiple reagents and kit from the Teaching Laboratory.

Lastly, I would like to thank my family and friends for their continued support: my parents for their encouragement, Luke Southwell for his patience with maths questions, and Eric Melander for proof-reading the parts of my thesis I had time to pass on to him and distracting me with an unhealthy amount of comedy boxsets and heavy metal gigs.

DECLARATION

I declare that the work presented in this thesis was conducted by me under the direct supervision of Professor Gary D. Bending, Doctor Jonathan Pearson, and Laurence Hand, with the exception of those instances where the contribution of others has been specifically acknowledged. The work contained in this thesis has not been submitted previously for any other degree.

Rebecca Victoria Southwell

LIST OF ABBREVIATIONS

‘	Minutes of arc
‘’	Seconds of arc
<	Less than
>	More than
≤	Less than or equal to
$(NaPO_3)_6$	Sodium hexametaphosphate
$(NH_4)_6Mo_7O_{24}$	Ammonium molybdate
%	Percent
°	Degrees
°C	Degrees Celsius
$	United States dollar
^{14}C	The radioactive isotope Carbon 14
$^{14}CO_2$	Radioactive ^{14}C carbon dioxide
$^1O_2$	Singlet oxygen
5’	Five prime end
AI	Active Ingredient
AIDA	Advanced Image Data Analyzer
ANOVA	Analysis of Variance
AU	Arbitrary Units
BC	Before Christ
bp	Base pair
Bq	Becquerel
BSA	Bovine Serum Albumin
$C_{20}H_{23}F_2N_3O$	Isopyrazam
CAKE	Computer Aided Kinetic Evaluation
CFU	Colony Forming Units
CI	Confidence Interval
cm	Centimetre
cm^2	Square centimetre
cm^3	Cubic centimetre

CO_2	Carbon dioxide
d_{50}	Sediment particle size distribution
DAT	Days After Treatment
DDT	Dichlorodiphenyltrichloroethane
DEFRA	Department for Environment, Food & Rural Affairs
DegT50	Time to 50 % degradation of a chemical
DegT90	Time to 90 % degradation of a chemical
DES	DNase/Pyrogen Free Water
DNA	Deoxyribonucleic Acid
dsDNA	Double Stranded Deoxyribonucleic Acid
DT50	Time to 50 % dissipation of a chemical
ECETOC	European Centre for Ecotoxicology and Toxicology of Chemicals
EFSA	European Food Standard Authority
EPA	Environmental Protection Agency
EU	European Union
f	Forward primer
FAO	Food and Agriculture Organisation of the United Nations
FERA	The Food and Environmental Research Agency
FOCUS	Forum for the Co-ordination of Pesticide Fate Models and their Use
ft	Foot
g	Gram
h	Height
H_2O_2	Hydrogen peroxide
ha	Hectare
HCl	Hydrochloric acid
HPLC	High-Performance Liquid Chromatography
HS	High Sensitivity
I	Central axis
ICC	Ion Charge Control
J	Joules
K	Kinetic energy
k	Von Karman's Constant
k_1	Degradation according to first-order kinetics

K_d	Adsorption coefficient
kg	Kilogram
K_{oc}	Organic matter normalised adsorption coefficient
KOH	Potassium hydroxide
K_{ow}	Octanol-water partitioning coefficient
L	Litre
l	Length
lb	Pound
LC-MS	Liquid Chromatography-Mass Spectrometry
ln	Natural logarithm
Log	Logarithm
LSC	Liquid Scintillation Counting
LSU	Large Sub Unit
lux	Luminous emittance
M	Molar
M	Mass
m	Metre
m/z	Mass-to-charge ratio
m^2	Square metre
m^3	Cubic metre
MBq	Megabecquerel
mg	Milligram
min	Minute
mL	Millilitre
mm	Millimetre
mol	Mole
MRM	Multiple Reaction Monitoring
ms	Millisecond
N	North
N/A	Not applicable
NaOH	Sodium Hydroxide
NCBI	National Centre for Biotechnology Information
NER	Non-Extractable Residues

ng	Nanogram
nM	Nanomole
nm	Nanometre
NMDS	Non-metric Multidimensional Scaling
NO_3-	Nitrate
NRFA	National River Flow Archive
O_2	Oxygen
O_3	Ozone
OECD	Organisation for Economic Co-operation and Development
OTU	Operational Taxonomic Unit
p	Probability value (level of significance)
Pa	Pascal
PAR	Photosynthetically Active Radiation
PCR	Polymerase Chain Reaction
PERMANOVA	Permutational Analysis Of Variance
pK_a	Acid dissociation constant at logarithmic scale
PO_4	Phosphate
PPDB	Pesticides Properties DataBase
PPS	Protein Precipitation Solution
QIIME	Quantitative Insights Into Microbial Ecology
r	Reverse primer
r	Radius
R^2	Dissimilarity between groups (PERMANOVA)
r^2	Correlation between observed and expected values (kinetics)
r^2	Goodness of fit (linear regression)
R2A	Reasoner's 2A agar
Rf	Retention factor
rpm	Revolutions per minute
rps	Revolutions per second
rRNA	Ribosomal Ribonucleic Acid
s	Second
SD	Standard deviation
SFO	Single First-Order (kinetics)

SPE	Solid Phase Extraction
spm	Strokes per minute
SRA	Sequence Read Archive
TLC	Thin-Layer Chromatography
u	Cross-sectionally average velocity
u^*	Shear velocity
u_d	Depth mean velocity
UK	United Kingdom
US	United States
UV	Ultra Violet light (wavelength < 400 nm)
V	Volts
V	Velocity
v	Volume
W	Watt
W	West
w	Width
WWTP	Waste Water Treatment Plant
x g	Times gravity
z	Depth height at a particular velocity
z_o	Bottom roughness parameter
α	Alpha (diversity)
β	Beta (diversity)
µg	Microgram
µL	Microlitre
µm	Micrometre
µM	Micromole
π	Pi
χ^2	Goodness of fit (kinetics)
ω	Angular velocity

ABSTRACT

Pesticides are vital for controlling agricultural pests and increasing crop yields; however, they can have detrimental effects on the environment and human health. Regulatory laboratory studies need to be carried out to assess the risks of a pesticide before it can be produced and sold. These regulatory studies tend to poorly predict pesticide fate and degradation in the field, likely due to specified test conditions not accurately representing the environment. This thesis focuses on the potential for adding greater environmental realism to regulatory-type tests, using the fungicide isopyrazam in OECD 308- and 309-type studies.

Regulatory tests are carried out under dark conditions. Microcosm studies were conducted in the presence of non-UV light to minimise photolysis, yet include phototrophic transformation; there was significantly more biodegradation in illuminated microcosms compared to those carried out in the dark, in which there was little degradation. The effect was more pronounced in water-sediment microcosms compared to water-only microcosms, as the sediment provided a platform for phototrophic biofilm development. Regulatory tests do not consider temporal variation in the microbial composition of environmental inoculum. Experiments carried out over two years showed that the outcome of tests, in terms of both degradation and mineralisation, were variable with inocula collected at different time periods from the same river location.

Regulatory tests are also carried out statically. Recirculating microflume experiments showed that flowing water increased dissipation compared to static systems, regardless of light treatment. This suggests regulatory tests are not properly representing flowing aquatic systems, e.g. rivers. Lastly, regulatory tests are carried out on a small scale. Although there was little effect on pesticide decline in different sized microcosms, in the larger microflumes, dissipation occurred even under dark conditions. A number of Operational Taxonomic Units were specific to the microflumes suggesting that, on a larger scale, there was a wider variety of microorganisms that better reflected the environment.

This work provides evidence for potential modifications to regulatory tests and insight into non-standard tests that industry could include in regulatory submissions.

CHAPTER 1 – GENERAL INTRODUCTION

1.1 THE RISE OF PESTICIDE USAGE IN AGRICULTURE

1.1.1 The history of pesticides and the green revolution

Pests have plagued human populations for centuries with records of insects in human societies going as far back as 12,000 BC with *Cimex* infestations in the Middle East (Fishel, 2009, Miller, 2008). With the pests came a need to control them, and early pesticides were predominantly derived from plants and inorganic compounds (Fishel, 2009, Taylor *et al.*, 2007). In 1939, World War II helped drive new technologies in a bid for victory, and many chemicals developed for warfare during this time were later used in agriculture (Carson, 1962, Taylor *et al.*, 2007). DDT, an organochlorine, was synthesised in the laboratory in 1873, with its insecticidal properties researched between 1932 and 1939 (Carson, 1962, Fishel, 2009). By 1942, the United States military made it available for use with great success, leading to a plethora of other synthetic organic pesticides which were subsequently produced.

Pesticides have been defined by the United Nations (FAO, 2002) as:

"...Any substance or mixture of substances intended for preventing, destroying or controlling any pest, including vectors of human or animal disease, unwanted species of plants or animals causing harm during or otherwise interfering with the production, processing, storage, transport or marketing of food..."

The development of synthetic pesticides paved the way for the green revolution and the chemical industry as we know it today (Fishel, 2009). As these new pesticides were both cheap and successful, it meant that they soon became the main mechanism for pest control (Taylor *et al.*, 2007). As well as pesticides, other advances which led to increased crop yields included developments in plant breeding (Evenson and Gollin, 2003) and the use of fertilisers (Hazell, 2002). The human population is estimated to reach 9.1 billion by 2050 (Carvalho, 2006). Coupled with better health care and higher life expectancy (Hazell, 2002),

this number could be even greater than previously estimated, suggesting that the demand for food, and thus pesticides to aid in its production, will remain high (Sexton, 2007).

1.1.2 The pesticide industry and usage today

Pesticides form a multibillion-dollar industry and in 2012 worldwide expenditure on pesticides was estimated at $ 56 billion (Atwood and Paisley-Jones, 2017). Of this total, herbicides dominated, accounting for 44 % of the total worldwide pesticide usage in 2012. Insecticides, fungicides, and fumigants accounted for 29, 26, and 1 %, respectively (Atwood and Paisley-Jones, 2017).

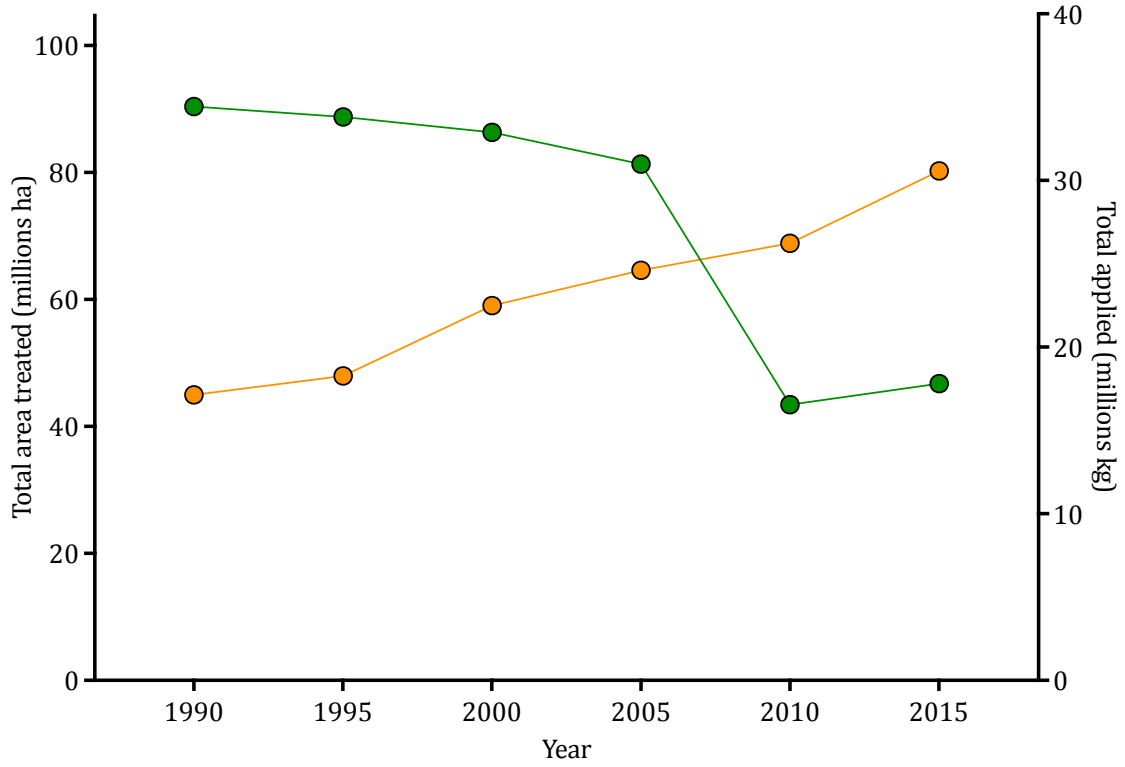

Figure 1.1: Total area treated with pesticide (orange) and total mass of pesticide applied (green) to all United Kingdom crops between 1990 and 2015. Data taken from FERA (2017).

In the United Kingdom, the total area of land treated with pesticides increased from 45.0 million hectares (ha) in 1990 to 80.3 million ha by 2015 (FERA (2017), **Fig. 1.1**). With the development of increasingly efficient and targeted pesticides (Yudelman *et al.*, 1998), however, the total volume of pesticides applied decreased from 34.4 million kg in 1990 to 17.8 million kg by 2015 (FERA (2017), **Fig. 1.1**).

1.2 THE FATE AND TRANSFORMATION OF PESTICIDES IN THE ENVIRONMENT

Agricultural pesticides are generally applied directly to the soil surface or the crop in a field (Herzfeld and Sargent, 2012). Pesticides can also be applied to seeds to counteract pests which target seeds or seedlings (TeKrony, 1976). Once present in the environment, pesticides have the potential to be transported elsewhere from the initial application site and become distributed in the water, air, soil, and biota (**Fig. 1.2**). Where a chemical is distributed and how it is subsequently transformed depends on both the environmental compartment the pesticide has been transported to and the properties of the chemical itself (Linde, 1994).

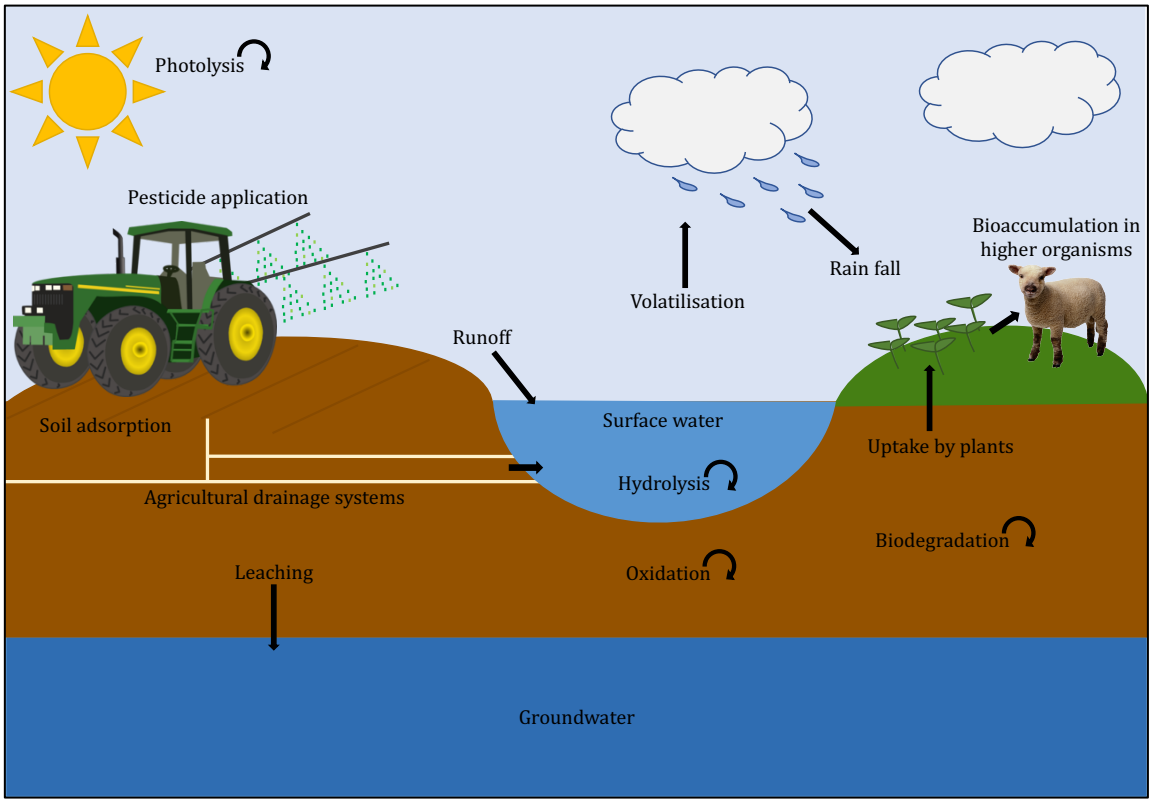

Figure 1.2: Fate and transformation of pesticides in the environment. Fate processes are shown by straight arrows and degradation processes by curved arrows. Created using Microsoft® PowerPoint for Mac.

This thesis primarily focuses on the fate and transformation of pesticides in aquatic systems. Fate in the environment can be determined by sorption processes, surface run off, leaching, uptake by organisms, and volatilisation (**Fig. 1.2**). Degradation of a pesticide in the environment can occur by both abiotic and biotic factors (Gao *et al.*, 2012); these processes in the environment will be described subsequently in detail. Within water bodies, there are

three main outcomes of pesticide fate and degradation: (i) the transformation of the parent compound to metabolites by both abiotic and biotic transformation, (ii) mineralisation to CO_2, water, or, in some rare cases, phosphate, and (iii) the formation of non-extractable residues (NER) bound to soil, plants, or animals (Linde, 1994, OECD, 2002b, OECD, 2004). NER can be classified into three different types: sequestered within soil organic matter (type I), chemically bound via covalent bonds (type II), and biogenic NER (type III) which result from conversion of the pesticide into microbial biomass (Kästner *et al.*, 2014). In this thesis, however, NER will refer to the proportion of an applied pesticide and its metabolites that are not recovered by solvent extraction methods.

1.2.1 Soil sorption

Adsorption is a process in which a molecule in soil or sediment pore water is attracted and retained onto the surface of a soil or sediment particle, organism, or humic material; this can be either a chemical or physical process (Gao *et al.*, 2012, Karickhoff, 1984). Absorption is the process of uptake into another substance (e.g. an organism) (Kamrin, 1997) and this will be discussed in more detail in section 1.2.4. These processes can be difficult to distinguish between and are therefore collectively referred to as sorption. The sorption coefficient (K_d) is used to quantity pesticide sorption to soil and indicates the ratio of sorbed pesticide to pesticide remaining in solution (Weber *et al.*, 2004). K_d is directly related to soil properties (organic matter and clay content) and is usually converted to an organic matter normalised coefficient (K_{oc}) in order to consider the amount of pesticide sorbed in relation to mass of organic carbon in the soil (ECETOC, 2013); this allows predictions to be made on pesticide mobility, and thus leaching potential (Weber *et al.*, 2004).

Multiple factors can influence pesticide sorption processes, such as surface area and soil particle size, soil pH, soil moisture content, surface charge of the soil particle, and solubility and polarity of the pesticide molecule, including the octanol-water partition coefficient (K_{ow}) (Gao *et al.*, 2012, Gavrilescu, 2005). Additionally, increased contact of a pesticide over time (aging) can lead to stronger sorption or a change in the sorption mechanism. This means that over time mobility of the pesticide is reduced as the desorption rate is lowered or the pesticide becomes bound to the soil or sediment (Cheng and Koskinen,

2010, Laird and Koskinen, 2008). If a pesticide can bind strongly to soil particles, it can decrease the bioavailability and mobility to other environmental compartments and, therefore, its impacts on human health and the environment (Gao *et al.*, 2012, Gavrilescu, 2005).

1.2.2 Surface runoff

If the precipitation rate exceeds the infiltration rate into the soil, pesticide can reach surface waters by overland flow (Gao *et al.*, 2012). This is problematic for several reasons; firstly, the pesticide is transported from its application site, reducing its effectiveness, and secondly, pesticides can cause contamination in the water body it is transported to, impacting aquatic flora and fauna (Gao *et al.*, 2012, Gavrilescu, 2005). Pesticide molecules can be present in surface runoff either in the dissolved phase, or associated with a particle or colloid that is also transported in the runoff (Gavrilescu, 2005). Surface runoff is dependent on soil and pesticide physicochemical properties, water flow, the slope of the land, the amount of rainfall and irrigation, and soil moisture content (Gao *et al.*, 2012, Gavrilescu, 2005, Sharpley, 1985). Agricultural management can also impact runoff, such as tillage practices and crop rotations (Gao *et al.*, 2012).

1.2.3 Leaching

If pesticide molecules have not sorbed to soil particles, as described in section 1.2.1, then there is the potential for leaching of the molecules into groundwater (Gao *et al.*, 2012). This is a mass transport process of downward water movement and can be dependent on physical, chemical, and biological properties of the pesticide and soil, and can also be impacted by rainfall post pesticide application (Flury, 1996, Seiber, 2002). For instance, sorption affinity of the pesticide molecule to the soil, or degradation rate as pesticides are transported through the soil profile, can determine the likelihood of a compound reaching groundwater (Gao *et al.*, 2012, Gavrilescu, 2005). Furthermore, agricultural drainage systems can similarly act as a transport mechanism into water bodies (Anderson, 2005, Gao *et al.*, 2012). Preferential flow is the phenomenon of a molecule moving rapidly through macropores in the soil profile, and this will decrease sorption or degradation potential; this can be dependent on size, geometry, and frequency of macropores in the soil profile

(Andreini and Steenhuis, 1990, Gao *et al.*, 2012, Gavrilescu, 2005). Matrix flow, however, causes slow water and chemical migration through the soil, meaning the pesticide will move with water into small pores, increasing the chance of contact with soil particles (Gavrilescu, 2005).

Groundwater can move slowly and, together with slow degradation in sub-surface environments, it results in long persistence of pesticides which reach groundwater through leaching. There can also be movement from groundwater to surface waters leading to further pollution of other aquatic environments (Nielsen and Lee, 1987). Groundwater is a vital drinking water resource and freshwater reserves are described as one of the most valuable resources we have on our planet (Catford, 2008). The European Commission Drinking Water Directive (European Commission, 1998) states that the maximal allowable concentration of pesticides in our water at the point of supply should be 0.5 μg/L for all pesticides and 0.1 μg/L for a single pesticide (DEFRA, 2012). These thresholds are commonly exceeded. For example, metaldehyde, which is used to control snails and slugs, is difficult to remove in treatment plants and has been widely detected in United Kingdom ground- and surface water, sometimes above the 0.1 μg/L limit (Stuart *et al.*, 2011).

1.2.4. Uptake by organisms

Organisms are able to take up pesticides from the surrounding environment. These include, for example, fish via gills in contaminated surface water or, most commonly, plants via the soil. This is influenced by the physicochemical properties of the pesticide and the soil, as well as the environmental conditions (Gao *et al.*, 2012, Gavrilescu, 2005). In particular, low pH has been shown to cause higher uptake of pesticides into plant seeds; however, the affinity of a pesticide to biochar, organic matter, and minerals in the soil can decrease uptake by a plant (Bewick, 1994, Gao *et al.*, 2012, Saha *et al.*, 1971, Yu *et al.*, 2009). Plant species and growth stage can determine pesticide uptake. Although plants can be capable of metabolising pollutants via enzymatic processes (Hoagland *et al.*, 2000), there can still be exposure to livestock (through consumption of animal feed) and, ultimately, humans (through consumption of food crops and animal products). Accumulation can continue up the ecosystem tropic levels, causing biomagnification at the top of the food chain. This can lead to persistence of the pesticide in the whole ecosystem (Franke *et al.*, 1994, Streit, 1992).

1.2.5 Volatilisation

Some pesticides are volatile and are released from the soil as a gas, which can be transported through the air. This distribution between the air and water is referred to as Henry's Law constant (Cetin *et al.*, 2006). This can cause higher dispersion of the residues and deposition back to the soil in rain (Gao *et al.*, 2012, Gavrilescu, 2005); this can be far from the initial application site (Gao *et al.*, 2012). Higher temperatures and low atmospheric humidity can increase volatilisation, and air movement can also be beneficial. Soil physicochemical properties can impact volatilisation rate, as pesticides that have strong sorption to soil particles are less likely to volatilise. If the pesticide is present in water, however, the depth of the water and water mixing can have an influence on volatilisation rate (Gao *et al.*, 2012, Gavrilescu, 2005, Seiber, 2002). Volatilisation rate is usually low and pesticide transportation in the atmosphere is typically via spray mist in windy conditions (Gao *et al.*, 2012, Gavrilescu, 2005).

1.2.6 Abiotic degradation

If microbial activity is low under certain conditions, abiotic degradation processes can aid in pesticide environmental transformation, with the main degradation pathways being oxidation, hydrolysis, and photolysis (Coats, 1991, Gao *et al.*, 2012, Gavrilescu, 2005, Seiber, 2002).

1.2.6.i Oxidation

Pesticide molecules can be oxidised and this involves electron transfer from a reduced species to an oxidised species. Molecular oxygen or its more reactive forms (e.g. O_3) react with the pesticide and this can be affected by oxygen availability. Oxidation occurs at a higher rate near the soil surface due to increased oxygen abundance. Oxygen abundance, and thus oxidation, decreases with soil depth. Similarly, oxygen levels are lower in water and so oxidation is less likely to occur under saturated soil conditions (Coats, 1991, Gao *et al.*, 2012, Kookana *et al.*, 1998). Oxidation is also impacted by metal ions which can act as catalysts in oxidation reactions (Barrett and McBride, 2005, Gao *et al.*, 2012, Gavrilescu, 2005, Nowack and Stone, 2000).

1.2.6.ii Hydrolysis

Pesticide molecules can similarly react with water molecules in aquatic environments or in soil pore water. This involves either protons, hydroxide or inorganic ions and, in some cases, metal ions acting as catalysts (Gao *et al.*, 2012, Mortland and Raman, 1967). Generally, a hydrolytic reaction occurs by replacing a chemical group in the pesticide structure with a hydroxyl group (Gavrilescu, 2005). The process is largely dependent on the pesticide chemical structure and the functional groups it possesses. Some pesticide groups, however, will not undergo hydrolysis. Environmental conditions, such as temperature and pH can also influence the process (Auld and Vallee, 1971, Coats, 1991, Gao *et al.*, 2012, Gavrilescu, 2005). Generally, degradation is quicker at higher temperatures (Comisar *et al.*, 2008) and both acidic and alkaline hydrolysis occur at acid and base pHs, respectively (Gao *et al.*, 2012). The properties of the pesticide can be altered during hydrolysis and the metabolites are usually less toxic than the parent compound (Carson, 1962, Gavrilescu, 2005).

1.2.6.iii Photolysis

Under high levels of UV radiation (< 400 nm), photolysis can have a major role in pesticide degradation in most environmental compartments, and this can occur both directly and indirectly (Bansal, 2012). The pesticide structure is broken up, or bonds in the structure are weakened, when the pesticide molecule receives energy in the form of photons, and becomes excited (Gao *et al.*, 2012, Gavrilescu, 2005). Direct photolysis occurs when the molecule absorbs the photons, while indirect photolysis occurs when another molecule absorbs the photons and produces reactive species which degrade the pesticide molecule (Gao *et al.*, 2012, Gavrilescu, 2005, Kelly and Arnold, 2012, Wallace *et al.*, 2010). It has been noted by Burrows *et al.* (2002), that only a small amount of short wavelength UV radiation reaches the Earth's surface, so direct photolysis in the real environment may only be relevant for some compounds. Indeed, studies by Romero *et al.* (1994) determined that photolysis in water was three times longer under natural than artificial light; however, lamps capable of simulating natural sunlight are used in regulatory studies which assess chemical phototransformation in water (OECD, 2008b).

Studies have found that pesticide photolysis rates differ between aqueous and solid phases, with different metabolites formed (Pirisi *et al.*, 1996). Cheng and Hwang (1996) showed that photolysis was quicker in the water fraction compared to the solid phase; however, Konstantinou *et al.* (2001) found the opposite was the case with soil and water. These interactions will largely be dependent on the factors influencing photolysis. Light intensity is a major influence on photolysis rates, and this is dependent on depth, time of day and year, and the amount of particulate matter within the water column. Additionally, exposure time, depth, soil moisture, environmental and pesticide properties, and pesticide application techniques (e.g. application to the plant rather than soil increases light exposure) can influence degradation by photolysis (Frank *et al.*, 2002, Gao *et al.*, 2012, Gavrilescu, 2005, Graebing *et al.*, 2003). Lastly, photosensitisers, such as humic acids, can accelerate the process, as they generate reactive oxidative species (e.g. H_2O_2 and $^1O_2$), which react with the pesticide and degrade it (Gao *et al.*, 2012, Konstantinou *et al.*, 2001). In particular, nitrate can act as a photosensitiser, and this will be present in higher concentrations in water bodies near agricultural land due to fertiliser use (Hand and Oliver, 2010, Wallace *et al.*, 2010). In this case, hydroxyl radicals are presumed to be the most important reactive intermediate produced. These are known to react with electron-rich aromatic organic compounds and, therefore, have an important role in pesticide transformation (Wallace *et al.*, 2010).

1.2.7 Biotic degradation

Biotic degradation is usually the most important transformation process in the environment, particularly in the water and the soil (Bansal, 2012, Fenner *et al.*, 2013). Microbes include bacteria, fungi, protozoa, and algae, and these communities have high species diversity in nature. This means there is also a high diversity of genes present in the community, which increases community metabolic potential and thus the probability of a pesticide being degraded (Bansal, 2012, Thouand *et al.*, 1995, Wang *et al.*, 2017). Microbes absorb the pesticide and use enzymes to metabolise the pesticide into smaller fragments and, eventually, to CO_2, water, or minerals (Bansal, 2012). Pre-existing enzymes with promiscuous activities can be utilised to detoxify environmental pollutants. For microbes to possess complete degradative capabilities, however, multiple pathways need to evolve. Large microbe population size and rapid growth rates result in high mutation frequency, meaning there is a greater chance these pathways will evolve (Bansal, 2012, Copley, 2009,

Hibbing *et al.*, 2010). Many different types of biotic degradation reactions have been observed depending on the pesticide and degradation pathway; these include dealkylation, conjugation, hydrolysis, hydroxylation, oxidation, reduction, and ring cleavage (Bansal, 2012).

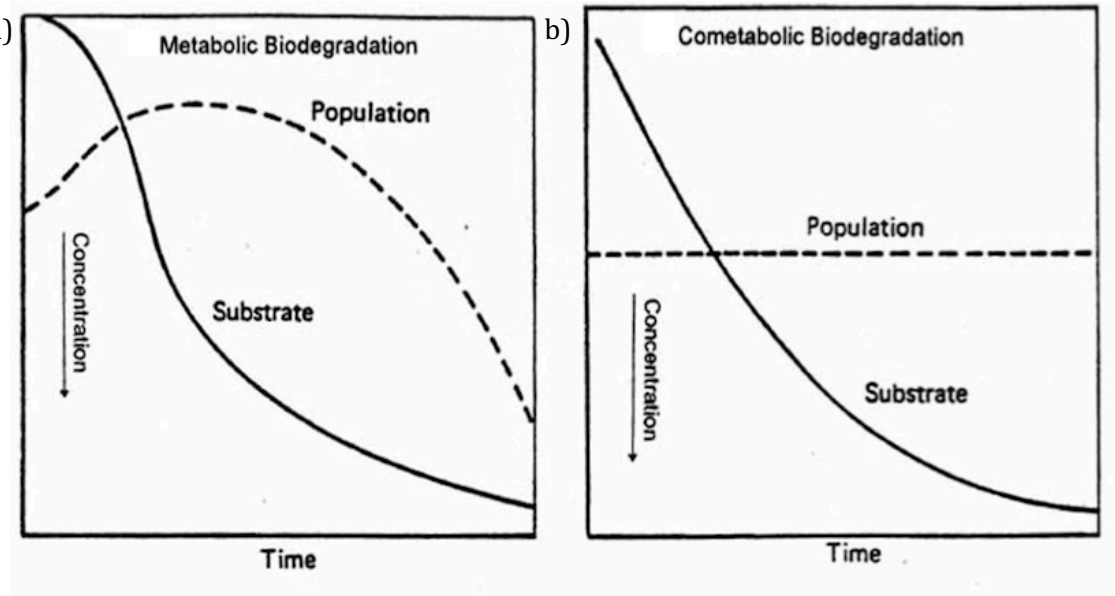

Figure 1.3: Conceptual diagram of pesticide degradation and bacterial population size under (a) growth-linked metabolic biodegradation and (b) co-metabolic biodegradation. Taken from (Scow, 1982).

Biotic degradation can be growth linked, in which the pesticide is used as a carbon or nitrogen source, resulting in growth of degraders. Before growth linked degradation can take place, there is generally an initial lag phase while enzymes are synthesised and degrading populations proliferate (**Fig. 1.3.a**). The chemical can be mineralised and degrading communities will continue to increase as long as the pesticide is present in the environment for them to utilise (Alexander, 1981). With co-metabolism, a pesticide is degraded by non-specific enzymes and is not used as an energy source by degrading communities, meaning the degradation kinetics are continuous and occur at a steady state (**Fig. 1.3.b**). This means that degradation is not always complete and secondary metabolites can accumulate; generally, metabolites are less toxic than the original parent compound, but sometimes they can be more toxic (Alexander, 1981, Guengerich and Liebler, 1985, Macherey and Dansette, 2015).

Microbes can be influenced by multiple factors within the environment, which can in turn influence their metabolic functions. Microbes can be influenced by climatic and

edaphic variables, such as temperature, pH, soil moisture content, organic matter content, and nutrient concentrations. Furthermore, increasing temperature can also decrease soil sorption, as well as increasing microbial activity. Lastly, deeper water or soil depths might contain fewer microbes, so metabolism will be slower in these cases (Bansal, 2012). The pesticide and its structure will influence how easily it can be degraded. For instance, pesticide motility and how polar and water soluble a pesticide is can influence its bioavailability: microbes can move more freely in water, so degradation will occur quicker. The bioaccessibility and bioavailability of a compound determines whether microbial populations can degrade a pesticide in the environment. For instance, pesticide sorption and formation of NER have been shown to reduce bioavailability and bioaccessibility to microbial communities (Barriuso *et al.*, 2008, Gaultier *et al.*, 2008, Kästner *et al.*, 1999, Semple *et al.*, 2004). The following definitions are provided by Semple *et al.* (2004):

Bioaccessible compound – *"That which is available to cross an organism's cellular membrane from the environment, if the organism has access to the chemical. However, the chemical may be either physically removed from the organism or only bioavailable after a period of time."*

Bioavailable compound – *"That which is freely available to cross an organism's cellular membrane from the medium the organism inhabits at a given time. Once transfer across the membrane has occurred, storage, transformation, assimilation, or degradation can take place within the organism."*

1.3 MODERN REGULATION OF PESTICIDE ENVIRONMENTAL FATE IN THE EUROPEAN UNION

1.3.1 Silent Spring

In the early 1960s, Rachel Carson published her ground-breaking book, *Silent Spring*. It highlighted the ecological impacts of recently developed synthetic chemicals, despite their benefits to agriculture. Carson realised that DDT and other chlorinated hydrocarbons persisted in the environment and, although this helped contribute to their effectiveness, it meant that they had the potential to reach many different environmental compartments, including groundwater or freshwater bodies (Arias-Estévez *et al.*, 2008, Stoate *et al.*, 2001, Younes and Galal-Gorchev, 2000). Pesticides may eventually bioaccumulate (Coat *et al.*, 2011) in the fatty tissues of higher vertebrates (Bernanke and Köhler, 2008, Carson, 1962), invertebrates (Canty *et al.*, 2007), and microorganisms (DeLorenzo *et al.*, 2001, Xin-Yu *et al.*, 2010). This can prove to be hazardous to entire ecosystems, especially if biomagnification along the food web occurs (Borgå *et al.*, 2001, Gray, 2002). Humans were also not left unharmed, as many pesticides are carcinogenic or cause embryonic defects (Dich *et al.*, 1997, Dikshith, 1991, Garry *et al.*, 2002, Winchester *et al.*, 2009). Furthermore, the environmental impacts could cause economic problems if a food source was affected or tourist area polluted (Carson, 1962, Pimentel, 2005). Carson further outlined the problems of pests becoming resistant to pesticides and the mixing of pesticide residues in the environment (Carson, 1962).

Carson's publication was greatly criticised by the pesticide industry, but by 1970 the Environmental Protection Agency (EPA) was formed in the United States. This saw changes in the laws associated with regulating the environment and human health, with DDT being banned in the United States in 1972, and other chemical restrictions following in the 1980s (Fishel, 2009). Although there were many problems with the early synthetic pesticides, Carson was a forerunner of the environmental movement and influenced social policy worldwide, shaping how the general public perceives pesticides (afterword by Lear, L. in Carson, 1962, Hickman, 2012). Because of the implementation of environmental regulations, modern pesticides do not pose the same risks as those outlined in her book. Nevertheless, the fact that some recent innovative pesticides may pose environmental hazards (e.g.

neonicotinoids and concerns of their impacts on pollinators (Stokstad, 2013)) suggests that her legacy lives on and her work remains in the minds of the science community and the general public to this day.

1.3.2 Pesticide registration within the European Union

Pesticides usually contain at least one active ingredient (AI). Before AIs can be registered within the European Union (EU), the effect of an AI against its target has to be evaluated, and it has to be proven that there are no adverse effects on human and animal health or the environment (European Commission, 2013a). New AIs need an extensive dossier to address all requirements in Commission Regulation (EU) No 283/2013 (for active substances) and Commission Regulation (EU) No 284/2013 (for plant protection products). The dossier must determine a detailed risk assessment of the AI, including toxicology and metabolism, residues, environmental fate and behaviour, and ecotoxicology studies (European Commission, 2013b, European Commission, 2013c). Once requirements are met, the Directive 2009/128/EC (European Commission, 2009a) sets out rules for sustainable pesticide use, according to Good Agricultural Practice. Additionally, the Organisation for Economic Cooperation and Development (OECD) provide guidelines on a number of tests to evaluate new AIs (OECD, 2005). AIs are usually approved for up to 15 years within the EU, before a renewal of approval is needed (European Commission, 2009b).

1.3.3 Organisation for Economic Cooperation and Development

The *OECD Guidelines for the Testing of Chemicals* are internationally agreed test guidelines used by government, industry, and independent laboratories in order to determine the safety of the chemicals being developed for use (Pagga, 1997). Three groups of tests are defined within the guidelines to assess environmental fate; ready biodegradability, inherent biodegradability, and simulation (Lapertot and Pulgarin, 2006, OECD, 2005). Ready biodegradability tests are carried out under aerobic conditions and act as a screening method to determine whether a chemical is rapidly degradable under natural conditions (Kowalczyk *et al.*, 2015). There is limited opportunity for biodegradation or inoculum (e.g. activated sludge, sewage effluent, water, soil) acclimation to occur in these studies and tests are carried out for only 28 days using high concentrations of the test

chemical (2 to 100 mg/L) (Comber and Holt, 2010, OECD, 2005, Reuschenbach *et al.*, 2003). A positive result in these tests has to occur within 10 days and there has to be either a 70 % reduction in dissolved organic carbon, or a 60 % reduction in theoretical O_2 demand or theoretical CO_2 evolution (Kowalczyk *et al.*, 2015). Degradation rates are often underestimated and there can be a large number of false negatives (e.g. insufficient degradation due to test design rather than lack of biodegradation) and therefore the next testing level has to be considered (Kowalczyk *et al.*, 2015, Lapertot and Pulgarin, 2006).

Inherent biodegradability tests are carried out aerobically under conditions more favourable for degradation to take place than in screening tests. This includes prior exposure of inoculum to the test compound, use of inoculum with high microbial biomass (usually activated sludge) and lower ratios of the test chemical to inoculum biomass (OECD, 2005). Therefore, insufficient degradation in these tests suggests that the test chemical has the potential to persist in the environment (Comber and Holt, 2010).

An increase in environmental realism is gained from the higher tier simulation tests, which can be carried out under both aerobic and anaerobic conditions. These tests aim to mimic a specific environment using a relevant environmental inoculum (OECD, 2008a). Low concentrations of the test chemical are used (1 µg/L < 100 µg/L) to ensure that biodegradation kinetics reflect those in the environment, and tests are devised based on the environment they simulate (Comber and Holt, 2010, OECD, 2005). Examples include test 307, which determines aerobic and anaerobic transformation in the soil, test 308, which evaluates the aerobic and anaerobic transformation in aquatic sediment systems, and test 309, which assesses aerobic mineralisation in surface water (OECD, 2002a, OECD, 2002b, OECD, 2004).

1.4 PESTICIDE FATE ASSESSMENTS

1.4.1 OECD regulatory laboratory studies

The *OECD Guidelines for the Testing of Chemicals* provides 22 tests to assess the degradation and accumulation properties of a pesticide. This thesis focuses on the fate and transformation of pesticides in flowing water systems and tests 308 and 309 provide guidance on this. OECD 308 assesses the aerobic and anaerobic transformation in aquatic sediment systems and OECD 309 assesses the aerobic mineralisation in surface waters (OECD, 2002b, OECD, 2004). These methods are used to evaluate the rate and route of test chemical transformation and its transformation products, and where these are partitioned within the system.

In OECD 308 guidelines (**Fig. 1.4.a**), water and associated sediment samples are collected from an appropriate sample site. Usually environmental samples from two different locations are used to cover different sediment organic carbon contents and textures, so as to represent different ecoregions. Water and sediment are set up in microcosms using a ratio between 3:1 and 4:1, ensuring the sediment layer is 2.5 cm and there is a minimum of 50 g dry weight. Water is treated with [^{14}C]-labelled pesticide, and microcosms are incubated under dark conditions in flow-through systems to allow air and nitrogen exchange and to ensure the trapping of volatile products. Laboratory temperature conditions are controlled between 10 and 30 ˚C, although 20 ± 2 ˚C is deemed acceptable. The concentration of the pesticide used needs to ensure that the route of transformation and the formation and decline of transformation products is characterised. Tests usually do not exceed 100 days and at least 6 destructive harvests (including time zero) are carried out. Water and sediment samples are assessed separately, using solvent to extract chemical from the sediment fraction. The concentration of the test chemical and transformation products are assessed using chromatography. Gas and volatiles are trapped (using NaOH or KOH) to assess the total amount of pesticide mineralised to $^{14}CO_2$, and NERs in the sediment fraction are quantified by combustion, then a mass balance calculated. The time taken for 50 % (DegT50) or 90 % (DegT90) of the pesticide to degrade is calculated using appropriate degradation models, which comply with the Forum for the Coordination of pesticide fate models and their Use (FOCUS) guidelines (FOCUS, 2006, OECD, 2002b).

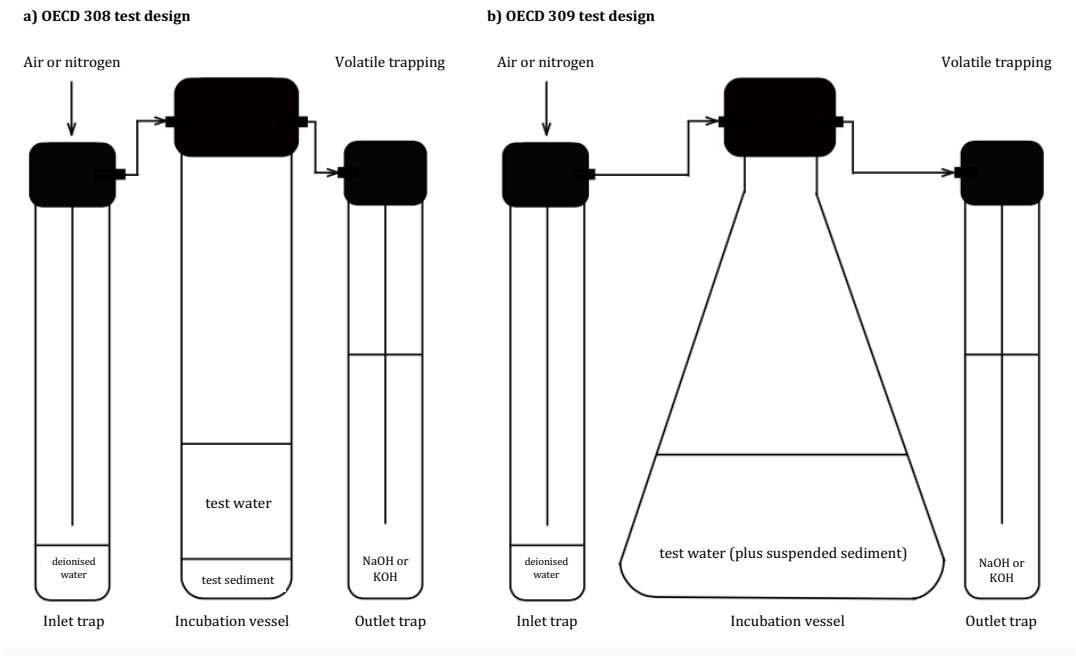

Figure 1.4: Test design for (a) OECD 308 and (b) OECD 309 test systems. Both systems can use a flow-through system, using either NaOH or KOH, to capture any volatiles (e.g. $^{14}CO_2$). Diagram created using site.youidraw.com (YouiDraw, 2016)

OECD 309 tests (**Fig. 1.4.b**) can be carried out with water only (pelagic test) or water amended with suspended sediment (suspended sediment test). The environmental inoculum is collected from a sample site appropriate to the test. These are set up in shake flasks, with water filling at least a third of the flask volume (with a minimum volume of 100 mL). If used, suspended sediment should be added at between 0.01 to 1 g/L dry weight. [^{14}C]-labelled pesticide is preferred and two concentrations of test chemical are used. These concentrations are low so as to ensure the biodegradation kinetics reflect those expected in the environment, and are usually between 1 and 100 µg/L. Laboratory temperature conditions can be standardised between 20 and 25 ˚C ± 2 ˚C, although it is also noted that the average environmental temperature from the sample site can also be used. It is preferred that studies are carried out in the dark, however, there is the option to use diffuse light. There should be gentle agitation of the systems by either stirring or shaking, yet systems should be kept homogenous. Tests do not usually exceed 60 days, with either subsamples taken (e.g. 5 mL) or destructive harvests at a minimum of five intervals along the time course. The extent of degradation should preferentially exceed 50 % of the applied concentration of test compound and a mass balance is calculated from each assessed fraction. Water is analysed using chromatography to determine the concentration of the test

chemical and transformation products. If suspended sediments are used these can either be analysed by scintillation counting or combustion. Mineralised $^{14}CO_2$ can be determined directly by acidifying the systems and collecting with an external absorber (e.g. NaOH), however, a flow-through system similar to that used in OECD 308 can also be used (OECD, 2004).

1.4.2 Environmental realism of OECD tests

Tests are standardised so that comparisons can be made across a range of different inoculum locations and pesticides. Additionally, by keeping variables which would fluctuate in the environment constant, it allows the tests to be reproducible. Despite this, in order to reliably predict degradation rates, these small-scale studies should try to mimic the real environment as much as possible. This is one reason there is such a large number of standardised tests, to ensure the most relevant can be used for a specific purpose. Nevertheless, considering these processes will all be interconnected in the real environment, it poses the question on how relevant to the real environment the fate and degradation results obtained are (Kowalczyk *et al.*, 2015, Pagga, 1997). The results of these regulatory tests will be dependent on the conditions used, and this will mean transferability of these results to the real environment will be difficult (Gartiser *et al.*, 2017).

In this thesis the addition of non-UV light (Chapters 2 and 4), temporal variation (Chapter 2), sediment addition (Chapter 2), test system scale (Chapters 3 and 4), and flowing water (Chapter 4) are assessed in the experimental chapters. These will be described in more detail in the introduction for each individual chapter, however, a brief overview is given here.

In the environment, light can have negative and positive impacts on microbial populations (Alonso-Sáez *et al.*, 2006, Jørgensen and Nielsen, 1960, Lindell *et al.*, 1996); however, there is a high diversity of phototrophic microorganisms which utilise natural sunlight as an energy source (Alonso-Sáez *et al.*, 2006, Overmann and Garcia-Pichel, 2006). Biodegradation by phototrophic communities could be an important transformation pathway in the environment and multiple studies have described their metabolic potential (Davies *et al.*, 2013a, Hand and Oliver, 2010, Lima *et al.*, 2003, Thomas and Hand, 2011,

Thomas and Hand, 2012). Additionally, these communities can aid other communities by forming synergistic relationships (Borde *et al.*, 2003). Despite this, both OECD 308 and 309 tests are carried out under dark conditions. OECD 309 tests do include the option to include diffuse light, but dark conditions are preferable. OECD 308 guidelines particularly state that dark conditions are used to avoid algal blooms (OECD, 2002b, OECD, 2004), so these phototrophic communities, which could play an important role in biodegradation in nature, are excluded from these tests. Non-UV light (i.e. Photosynthetically Active Radiation (PAR)) has been used in this thesis to minimise the impact of photolysis, yet include transformation carried out by phototrophic communities.

Microbes are influenced by environmental conditions and these can cause communities in nature to vary both spatially and temporally (Horner-Devine *et al.*, 2004, Palmisano *et al.*, 1991, Smoot and Findley, 2001). Considering microorganisms are key for pesticide degradation, changes in these communities can cause variation in their metabolic potential (Böckelmann *et al.*, 2000, Chénier *et al.*, 2003). The OECD test guidelines do not prescribe the time and place for collection of environmental inoculum (OECD, 2002b, OECD, 2004). Studies have suggested that microbial diversity could be better controlled in regulatory studies, as variations in inoculum are one of the main reasons for variation between tests (Mezzanotte *et al.*, 2005, Thouand *et al.*, 1995). In this thesis, environmental inoculum collected throughout the year was tested in order to assess how the community metabolic potential changes over time, and thus determine whether regulatory test results may differ depending on time of sample collection. Additionally, it should be noted that the addition of isopyrazam to test systems will cause a selection pressure for degraders, so the community under laboratory conditions is unlikely to exactly mimic the environmental community. Effort should be made, however, to ensure that the starting community represents that seen in nature as well as possible.

Sediment can also act as a diverse platform for microbial biofilm development, and higher sediment depths have been shown to increase primary production and respiration compared to lower depths (Uzarski *et al.*, 2004). OECD 308 studies include the addition of sediment (OECD, 2002b) and are therefore more relevant to small, shallow water bodies, whereas OECD 309 studies are intended to mimic deeper water bodies, where the influence of the sediment bed is less significant (OECD, 2004). In this thesis, a comparison between

water-sediment and water-only microcosms was carried out to determine the impact of sediment substratum on biodegradation and to evaluate whether the role of non-UV light still has an impact in ecosystems where the sediment bed, and therefore, biofilm, may not play as large a role.

OECD tests are also carried out on a small microcosm scale. OECD 308 tests state that a 2.5 cm layer of sediment should contain at least 50 g dry weight of sediment, and that the water and sediment should be in a volume ratio between 3:1 to 4:1, meaning a minimum of 150 mL water is acceptable (OECD, 2002b). OECD 309 tests, too, state that at least 100 mL of water should be used (OECD, 2004). These small volumes and unrealistic ratios might not reflect those in nature, including the diversity of microorganisms, particularly rare ones, and their metabolic capabilities (Gartiser *et al.*, 2017, Kowalczyk *et al.*, 2015, Sturman *et al.*, 1995). This thesis addresses this concern by comparing degradation between different sized microcosms and also assessing dissipation in more realistic microflume systems.

Lastly, although OECD 309 guidelines state that systems should have gentle agitation (OECD, 2004), OECD 308 tests are generally carried out statically (OECD, 2008a). Considering these systems could be representing water taken from flowing waterbodies, such as rivers and streams, this might not reflect natural conditions, such as water velocity and sediment dynamics (Gartiser *et al.*, 2017). Higher mixing in flowing systems could increase the probability that microbial degraders come into contact with the environmental pollutant, or nutrients and electron donors and acceptors, which might aid in microbial growth (Sánchez-Pérez *et al.*, 2013). The differences in pesticide dissipation between static and flowing water systems was therefore assessed in microflume systems.

Microcosm studies have been shown to not accurately predict the fate and transformation of pesticides in the field (Beulke *et al.*, 2000). Whether degradation rates are over- or under- estimated will depend on the environmental degradation process of a pesticide and whether these are represented on the small scale. For instance, studies by Davies *et al.* (2013a) incubated eight different pesticides in soil microcosm studies under both non-UV light and dark conditions. The light treatments only had an impact on transformation for five out of the eight pesticides tested, showing that degradation mechanisms are compound specific. Hence, it is difficult to predict environmental fate and

transformation in the laboratory without an understanding of all possible degradation routes present in the field and how they impact specific organisms.

1.5 ISOPYRAZAM AS A TEST CHEMICAL

Throughout this thesis, isopyrazam has been used as a test chemical (**Fig. 1.5**) and physical-chemical properties can be found in **Table 1.1**. Isopyrazam is a carboxamide fungicide, produced by Syngenta, and its main uses are to control fungal diseases of fruit trees, such as bananas, and cereals, such as barley and wheat (Blanc *et al.*, 2012, EPA, 2011, PPDB, 2017). It is a succinate dehydrogenase inhibitor and it is highly attracted to the high lipid content of fungal mitochondrial membranes, where it can shut down energy production (Syngenta, 2017a). Carboxamides have a pyrazole ring, which gives them a wide use of applications; however, isopyrazam additionally has a benzonorbornene ring, which is exclusive to its structure. This ring allows a double binding effect leading to stronger binding to fungal mitochondria, and also a stronger affinity for cuticular wax on crop leaves (Syngenta, 2017b).

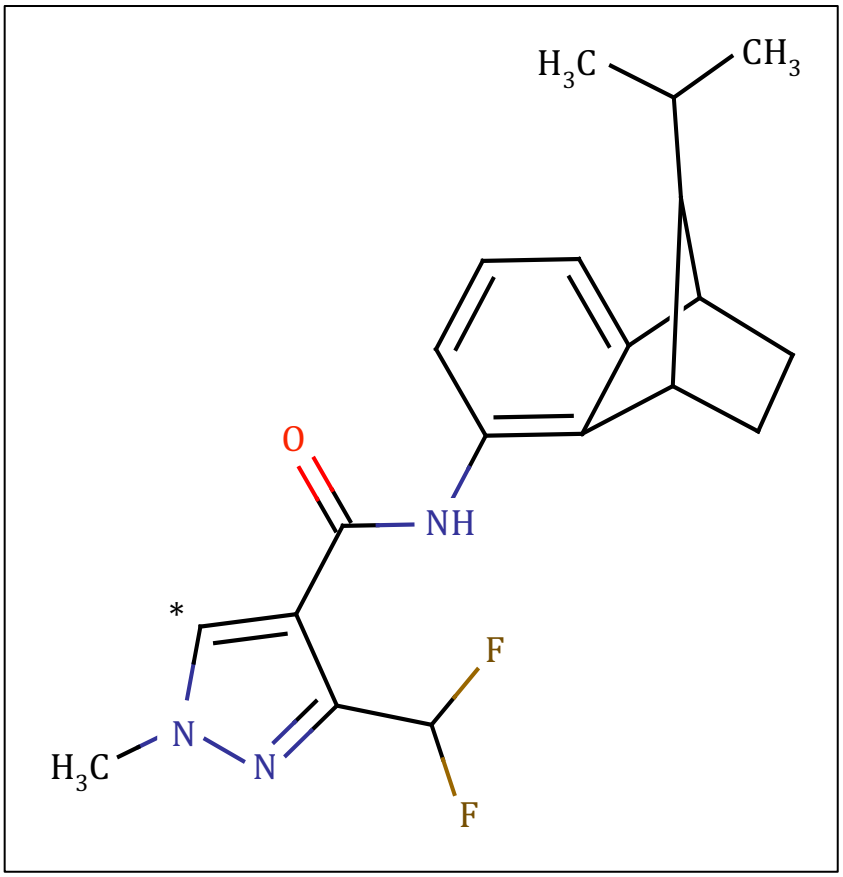

Figure 1.5: Structure of isopyrazam. The * denotes the position of the radiolabelling and the mixture was made up of 89.7 % *syn*-epimer and 9.7 % *anti*-epimer. Created using ChemDraw (PerkinElmer, US).

The DegT50 of isopyrazam depends on the conditions used. The worst case scenario in the field was given as 629 days (EFSA, 2012). In laboratory studies using light conditions, however, DegT50 was only 65 to 72 days, with no degradation in the dark (EFSA, 2012). Studies by Hand and Moreland (2014) showed that in water systems in the presence of phototrophic organisms, DegT50 was under 50 days. Isopyrazam was therefore used as a test chemical due to the relatively short DegT50, which allowed laboratory experiments to be carried out quickly, and the usual lack of degradation in the dark meaning a comparison between illuminated and dark treatments could be easily made.

Table 1.1: Physical-chemical properties of isopyrazam. Data taken from PPDB (2017), Abad-Fuentes *et al.* (2015), and Dæhli *et al.* (2012).

Isopyrazam physical-chemical properties	
Chemical formula	$C_{20}H_{23}F_2N_3O$
Molecular weight	359.40 g/mol
Melting point	137 °C
Boiling point	257 °C
Water solubility (25 °C, pH 7)	0.55 mg/L
Log K_{ow} (20 °C, pH 7)	4.25
K_{oc}	1732 – 2491 mL/g
Vapour pressure (20 °C)	2.2×10^{-8} Pa
Henry's Law constant	3.7×10^{-5} Pa m^3/mol
pK_a	No dissociation

1.6 THESIS AIMS AND OBJECTIVES

The overall aims and objectives of this thesis are to determine how the addition of environmental realism to regulatory-type tests impacts isopyrazam biodegradation. In particular by determining:

1. The role of non-UV light and its influence on isopyrazam biodegradation by the phototrophic community or heterotrophic communities also enhanced by the light treatment (Chapters 2 and 4).
2. If temporal variation in environmental inoculum from the sample site causes variation in isopyrazam biodegradation under laboratory conditions (Chapter 2).
3. Whether the addition of sediment (e.g. OECD 308 tests) impacts isopyrazam fate and degradation compared to water-only microcosms (e.g. OECD 309 tests) (Chapter 2).
4. If an increase in test system size changes the microbial community and isopyrazam biodegradation using both increasing sized microcosms and more realistic microflume systems (Chapters 3 and 4).
5. The differences in isopyrazam dissipation between systems with static and flowing water (Chapter 4).

This thesis is divided into five sections, with the general introduction (Chapter 1), preceding three self-contained experimental chapters (Chapters 2 to 4), each comprising of their own introduction, materials and methods, results, and discussion and conclusions sections. Experimental aims and objectives for each experimental chapter are detailed in the introduction sections. Lastly, these will be followed by a general discussion (Chapter 5).

CHAPTER 2 – THE IMPACTS OF LIGHT AND SEASON ON ISOPYRAZAM DEGRADATION IN RIVER MICROCOSMS

2.1 INTRODUCTION

2.1.1 Organisation for Economic Cooperation and Development: tests 308 and 309

Although agrochemicals have been, and continue to be, beneficial for the agricultural industry (Hazell, 2002, Taylor *et al.*, 2007), they also have the scope to cause detrimental effects on both the environment and human health, should transportation to environmental compartments other than their application site occur (Carter, 2000). To ensure newly developed chemicals are as safe as possible, the agrochemical industry is responsible for carrying out regulatory tests to give insight into chemical fate and transformation in the environment (Davies *et al.*, 2013a, OECD, 2005). These tests were developed by the OECD and include tests such as 308, which determines the aerobic and anaerobic transformation of a chemical in aquatic sediment systems (OECD, 2002b), and test 309, which is a simulation biodegradation test that details the aerobic mineralisation of a chemical in surface water (OECD, 2004).

Simulation tests, such as tests 308 and 309, provide additional context to preliminary ready biodegradability tests, which are carried out as a screening method (Kowalczyk *et al.*, 2015). The higher tier tests are more complex and try to increase environmental realism. Despite this, there are still limitations in the designs, and OECD tests fail to take into consideration several factors which could further increase environmental realism, and impact chemical fate and transformation (Kowalczyk *et al.*, 2015, Pagga, 1997). Both tests 308 and 309 are carried out under dark conditions. Although under test 309 there is the option for using diffuse light, the guidelines state that dark conditions are preferred and, in test 308, guidelines specifically state that dark conditions should be used to avoid algal blooms (OECD, 2002b, OECD, 2004). Tests are generally carried out under a constant temperature between 10 and 30 °C, although 20 °C is usually deemed appropriate (OECD, 2002b). There are also ambiguities on when and where sampling from the environmental source should take place, with the test guidelines stating that the site should be "selected in accordance with the purpose of the test in any given situation" (OECD, 2002b, OECD, 2004).

Chemical transformation and persistence in the environment can be heavily impacted by microbial biodegradation (Copley, 2009) and, although the OECD tests specify that there should be an active microbial population (OECD, 2004), there is little consideration of the diversity and types of community present. If laboratory conditions used for OECD tests are not an accurate representation of the conditions in the environment, the tests may not always give an accurate view of the chemical fate and transformation seen in nature.

2.1.2 Impacts of light on microbial communities and chemical degradation

In the environment, light can have both negative and positive impacts on the microbial population. Although it depends on the bacterial species and their resistance mechanisms, negative effects are usually associated with UV light (Alonso-Sáez *et al.*, 2006). This can include a reduction in metabolism and primary production with increased UV exposure, less amino acid uptake, and an inhibition of protein and DNA synthesis (Alonso-Sáez *et al.*, 2006, Jørgensen and Nielsen, 1960, Lindell *et al.*, 1996). In some circumstances, photolysis of materials may generate substances which can be utilised by microbial communities for growth. For example, photochemical transformation of dissolved organic matter can result in increased bacterial growth and cell volumes, and this could counteract any inhibitive effects of light (Lindell *et al.*, 1996). Furthermore, there is a high diversity of phototrophic microorganisms in aquatic systems, which can use natural sunlight as an energy source, converting it into chemical energy for use in cell growth and maintenance (Alonso-Sáez *et al.*, 2006, Overmann and Garcia-Pichel, 2006). In nature, these communities can reach high population levels, contributing to productivity (van Gemerden and Beeftink, 1983).

These communities are also metabolically capable of chemical biodegradation. Lima *et al.* (2003) showed that two species of microalgae, *Chlorella vulgaris* and *Coenochloris pyrenoidosa*, could degrade *p*-nitrophenol both in pure culture and when in a mixed microalgal culture containing both species. Additionally, Roldán *et al.* (1998) showed that *Rhodobacter capsulatus*, a phototrophic bacterium, could use *p*-nitrophenol as a carbon source under light conditions, with no *R. capsulatus* growth or *p*-nitrophenol degradation occurring under dark conditions.

Biodegradation by phototrophs could represent an important transformation pathway in the environment and, currently, this is excluded from the OECD test guidelines (OECD, 2002b). This has thus stimulated interest in examining the way in which inclusion of phototrophic biodegradation pathways would influence the outcome of regulatory tests. Hand and Oliver (2010) carried out modified OECD 308 type water-sediment studies, in which isopyrazam DegT50 was shorter in systems incubated under non-UV light-dark cycles (containing algal and macrophyte communities) compared to those in the dark. Biodegradation, however, is dependent on the phototrophic community present. For instance, Lima *et al.* (2003) found that *C. pyrenoidosa* was better adapted to *p*-nitrophenol degradation than *C. vulgaris*, and Thomas and Hand (2011) showed that macrophyte-dominated systems were marginally faster than algal-dominated ones. Macrophyte communities, in particular, support periphyton biofilm, and chemical can partition to this biofilm instead of to the actual macrophyte leaves. This suggests that periphyton biofilms can play a direct role in the degradation process (Thomas and Hand, 2012).

Although these previous experiments show that phototrophs could contribute to chemical degradation, it is likely that these effects are compound specific. Davies *et al.* (2013a) compared degradation of eight crop protection products in OECD 307 type soil studies incubated in the dark and under non-UV light. Under the light treatment, transformation rate was increased in five out of the eight compounds tested, with the reverse effect noted for one compound. Furthermore, the amount of NER produced increased under the light treatment for the majority of the compounds tested. Generally, phototrophs proliferated in the systems, yet there was no correlation between chlorophyll *a* abundance and degradation, suggesting that biodegradation resulted from a combination of both phototrophic and heterotrophic degraders (Davies *et al.*, 2013a). Indeed, other studies using systems containing a mix of phototrophic and heterotrophic communities saw faster degradation compared to systems containing exclusively phototrophic communities, which suggests that phototrophs, or a more inclusive and complex community structure, could enhance the overall metabolic potential of the community (Thomas and Hand, 2012). Borde *et al.* (2003) also showed that synergistic relationships between algae and bacteria promoted the biodegradation of the aromatic pollutants, salicylate, phenol, and phenanthrene. In this case, bacteria could have used O_2 from algal photosynthesis as an

electron acceptor, whereas algal species used the extra CO_2 produced from pollutant mineralisation.

Regardless of whether the role of phototrophic communities is direct or indirect, these communities are an integral part of the real environment. Exclusion of light from regulatory studies eliminates a potentially important biodegradation pathway and thus decreases environmental realism.

2.1.3 Impacts of temporal variation on microbial communities and chemical degradation

OECD test guidelines are vague regarding the time and place sampling should take place for collection of environmental substrates. Depending on the pesticide used, its mechanism, the target organism, and when a crop is planted, a chemical could potentially be used several times during a cropping season (for example, Caspell *et al.* (2006) and Okonya and Kroschel (2015)) and this could result in environmental exposures at several different times of year. Furthermore, although pesticides will not necessarily be applied outside of a cropping season, chemicals have the potential to move to different environmental compartments, so may be present in the environment outside of the application time. For instance, in Greece, occurrence of pollutant residues in watercourses has been shown to be the result of transboundary transport from other countries (Vryzas *et al.*, 2009). In the Shinano River region in Japan, there was month to month variation of residues in the watercourse, with higher amounts in May when application was at its highest (Tanabe *et al.*, 2001). Pesticide residues in the environment will also differ by location. For instance, there will be a higher chance that residues are transported from agricultural land to the aquatic environment in areas prone to flooding (Death *et al.*, 2015, Milliman, 2009, Tejerine-Garro *et al.*, 2005).

Microbial activities can be influenced by temperature, light, dissolved O_2, organic matter availability, and nutrient quality and quantity (Febria *et al.*, 2010, Feris *et al.*, 2003, Hullar *et al.*, 2006, Lyautey *et al.*, 2005). Exposure of microbial communities to changes in such environmental conditions can vary on spatial and temporal scales (Horner-Devine *et al.*, 2004, Palmisano *et al.*, 1991, Smoot and Findley, 2001). Changes may be driven by natural processes, such as nutrient exchanges with the surrounding environment (Crump *et al.*,

2009, Feris *et al.*, 2003, Hullar *et al.*, 2006), local climate and weather pattern changes (Crump *et al.*, 2009), and changes in water flow (Hullar *et al.*, 2006). Anthropogenic effects on environmental parameters include agricultural practices, especially fertiliser and chemical application (Horner-Devine *et al.*, 2004). These factors will increase selection pressures based on species fitness and cause diversification of communities. Additionally, the microbial community assemblage is influenced by stochastic changes in abundance causing species drift, and transport through habitats via water, soil, or attachment to macrobes; such changes in the community structure over time will alter its metabolic potential (Nemergut *et al.*, 2013, Vellend, 2010).

It has been suggested that distinct microbial communities can often be present at different times of year (Smoot and Findley, 2001). Feris *et al.* (2003) sequenced riverine communities and saw similarities between sediment populations at certain times of year; for example, summer and autumn communities were different to spring and winter communities. The factors causing community shifts depended on time of year, with temperature, NO_3^- concentration, and dissolved organic carbon influencing communities in summer, spring, and autumn, respectively. Some studies have shown that community population shifts are predictable on an annual basis. Crump *et al.* (2009) determined that although there were differences in riverine bacterioplankton shifts between season, there was high similarity in the same season between years. Communities were studied over three periods – winter, spring, and summer/autumn – with spring and winter having the highest and the lowest taxonomic diversity, respectively. Some bacterial populations were specific and dominant in certain seasons, yet plummeted and became rare at other times of year, and these fluctuations were strongly linked to climate and biogeochemical cycling (Crump *et al.*, 2009).

Phototrophic communities, in particular, have recurring seasonal patterns. This was shown in a four year study by Hullar *et al.* (2006), where there was seasonal variation in microbial communities. Phototrophic biofilm (cyanobacteria, diatoms, and chloroplasts) dominated in the summer, and cyanobacterium in autumn and spring. Breuer *et al.* (2016) analysed suspended (in the water phase) and attached (to substratum) algal species in lotic water systems over two years, and the former was present in March to October and the latter in March to November, with decreases in communities over the winter months. This

seasonal variation was closely related to temperature, dissolved organic carbon and, perhaps unsurprisingly, light availability (Hullar *et al.*, 2006, Smoot and Findley, 2001).

Microbial communities are key degraders of environmental contaminants, and changes over time in the community could impact the community metabolic potential and stress threshold (Böckelmann *et al.*, 2000, Chénier *et al.*, 2003). The way in which a pesticide is metabolised will influence its degradation kinetics. In order for a microbial community to utilise a pesticide as a carbon source, an adaptation phase is necessary, involving a lag phase between substance addition and the degradation of that substance (Bergström and Stenström, 1998). Repeated application of a pesticide over a short period of time, therefore, can lead to an enhancement of the degrading communities present (Anderson and Coats, 2002, Watson, 1977), resulting in more rapid degradation upon pesticide application (Torstensson, 1980). Additionally, co-metabolism, when a compound is degraded but not utilised as a substrate for growth, will lead to an exponential decline of the pollutant (Torstensson, 1980). The relative importance of growth-linked and co-metabolic biodegradation of a pesticide can vary spatially, both at the local scale (e.g. within a field) and at the landscape scale (Bending *et al.*, 2006, Parkin and Shelton, 1991, Rodríguez-Cruz *et al.*, 2006, Watson, 1977). Environmental parameters, for instance soil pH, have been shown to control degrader activity (Bending *et al.*, 2003, Walker *et al.*, 2001); however, it has been noted that in nature a variety of factors will interact and influence degradation rates (Rodríguez-Cruz *et al.*, 2006).

Degradation rates have been shown to vary temporally. Generally, increased degradation is associated with summer (Palmisano *et al.*, 1991, Parkin and Shelton, 1991); however, this can be variable and some studies have shown slower degradation in summer months (Chénier *et al.*, 2003). Higher microbial biomass is not always correlated with increased degradation rates. For instance, Kowalczyk *et al.* (2016) found that although biofilm biomass varied in space and time, there was no link with DegT50. *P*-nitrophenol degradation did vary over time; however, it was suggested that competition between microbes could have impacted the degradation outcome (Kowalczyk *et al.*, 2016). Other environmental factors which impact degrader communities could lead to differences in degradation rates. This includes soil water content (Parkin and Shelton, 1991, Rodríguez-Cruz *et al.*, 2008) or flooding events; this can increase degradation in rivers due to elevated

concentrations of suspended sediment, which may contain degrader communities (Watson, 1977).

2.1.4 Impact of microbial diversity on chemical degradation

Microbial community composition has major influences on ecosystem function (Abbasian *et al.*, 2016, Gavrilescu, 2005, Ramakrishnan, 2012) and the loss of some microbial species in an ecosystem can lead to loss of ecosystem function and tolerance. For instance, Philippot *et al.* (2013) showed that a reduction in denitrifiers significantly lowered denitrification activity. In the case of biodegradation, this could decrease overall degradative ability in an ecosystem (Ramakrishnan, 2012). Communities with a high functional and genetic diversity are more likely to adapt to stresses and evolve quicker (Ramakrishnan, 2012, Szabó *et al.*, 2007) and species can also exchange genetic elements through horizontal gene transfer (Donlan, 2002, Elias and Banin, 2012, Schwartz *et al.*, 2003). In the environment, bacteria are more likely to reside in a multispecies community (Elias and Banin, 2012, Sørensen *et al.*, 2002). Biofilms, in particular, are made up of several taxonomic kingdoms and possess many different metabolic pathways and functions (Sabater *et al.*, 2007, Schwartz *et al.*, 2003, Singh *et al.*, 2006).

Microbe-microbe interactions can be extremely intricate and this can influence their degradative ability (Gavrilescu, 2005, Ramakrishnan, 2012). Interactions between microbes can be both synergistic and antagonistic, with a network of both direct and indirect interactions within and between species, especially in more complex biofilm communities (Arif *et al.*, 2012, Elias and Banin, 2012, McGenity *et al.*, 2012). This could range from competition for resources between species (Arif *et al.*, 2012, Elias and Banin, 2012, McGenity *et al.*, 2012) or co-operative behaviour, such as nutrient cycling and syntrophy, where bacteria interact with each other by using cell products and biomass from other bacteria as energy sources (Bending *et al.*, 2003, Borde *et al.*, 2003, Donlan, 2002, McGenity *et al.*, 2012). This could impact degradation if the degraders are outcompeted (Kowalczyk *et al.*, 2016, McGenity *et al.*, 2012) or if they are dependent on growth factors or nutrients from other species (Sørensen *et al.*, 2002).

It has been suggested that a higher bacterial density and diversity will influence degradation as these factors increase the probability that degraders, especially rare ones, are present in an inoculum (Kool, 1984, Thouand *et al.*, 2011, Thouand *et al.*, 1995). Degradation is dependent on microbial biomass concentration, enzymatic activity, and diversity of the population (Boopathy, 2000). Several studies have shown that complete degradation of a compound is not always possible by a single species (Arif *et al.*, 2012, Hoskeri *et al.*, 2014, Levanon, 1993, McGenity *et al.*, 2012, Sørensen *et al.*, 2002, Thomas and Hand, 2012). Biodegradation is thus dependent on the quality and quantity of the microbial consortia, and the biotic and abiotic interactions which shape the community (Courtes *et al.*, 1995, Elias and Banin, 2012). Although microbial diversity is not properly controlled in regulatory tests (Thouand *et al.*, 1995), studies have proposed that negative results in these tests may be due to variations in inoculum (Mezzanotte *et al.*, 2005), and that a difference in the abundance and composition of bacterial biomass could lead to differences in biodegradation kinetics (Courtes *et al.*, 1995). In particular, given the intricate and complex relationships between groups within the microbial consortia, it is unsurprising that incubation in the dark could lead to an unrealistic degradation rate, both by removing the potential for direct phototrophic metabolism (Lima *et al.*, 2003, Roldán *et al.*, 1998) and also by impacting the interactions between phototrophic and heterotrophic communities (Borde *et al.*, 2003). Although several studies have carried out similar work on these processes in a regulatory context (Davies *et al.*, 2013a, Hand and Oliver, 2010), this is an area that still needs further investigation.

2.1.5 Experimental overview

OECD-type tests were carried out using water-sediment and water-only systems to explore the impacts of non-UV light (PAR in order to minimise photolysis yet include transformation by phototrophic communities) and temporal variation on the biodegradative capabilities of inoculum (water and sediment) collected from a river system. All other variables that could change temporally in the environment were kept constant in the laboratory (e.g. incubation temperature) in order to assess the reproducibility of the tests.

2.1.6 Experimental aims and objectives

The aims and objectives of this experiment were as follows:

1. To determine the effects of non-UV light on isopyrazam degradation when used in OECD regulatory-type tests.
2. To determine whether collecting inoculum (water and sediment) from the environment at different times of year shows variability in the fate and degradation of isopyrazam.
3. To establish whether microcosm sediment addition impacts isopyrazam fate and degradation compared to water-only microcosms.
4. To determine whether microbial community diversity is impacted by non-UV light and temporal variation in environmental inoculum samples and whether this subsequently has a role in isopyrazam degradation.

2.2 MATERIALS AND METHODS

2.2.1 Sample collection and processing

River water and sediment samples were collected at approximately three-monthly intervals for two years starting in June 2014. Sample collection was carried out eight times in total and these will be henceforth referred to as "collection times". Samples were obtained from the River Dene (**Fig. 2.1**) at Wellesbourne, United Kingdom at 52°12'02.5"*N* and 1°36'30.4"*W* (**Fig. 2.2**, Google (2016)), which is downstream of a Wastewater Treatment Plant (WWTP, **Fig. 2.2**). It is a small lowland river, which has a predominately agricultural catchment area (NRFA, 2016). According to the Environment Agency, the chemical quality of the water is described as "very good" (ammonia concentration) and "good" (dissolved oxygen), and the biology as "fairly good" overall, using their General Quality Assessment Scheme (Environment Agency, 2009, Naura, 2014). The mean flow rate of the River Dene is 0.64 m^3/s, with typical depths between 0.09 and 0.36 m (Environment Agency, 2017a, NRFA, 2016), and there is an average annual rainfall of 614.8 mm (Met Office, 2017b).

Samples were taken in triplicate across the river at the midpoint between each side of the riverbank, and at the 25th and 75th quartiles (**Fig. 2.3**). Sediment was sandy loam in texture and was sampled within the top 5 to 10 cm of the riverbed using a trowel and kept moist with river water. Water was sampled by submerging containers at each collection point facing upstream. Samples were not mixed and water and sediment from each collection point constituted individual replicates within the experiment at each time point. Additionally, at the site, water temperature was measured using a Total Immersion thermometer (Fisher Scientific, UK), light intensity measured using an RS-105 light meter (RS Components Ltd., UK), and water depth and velocity measured using an 801 EM flow meter (Valeport, UK). Water pH was tested in the laboratory using an Accumet basic AB15 pH meter (Fisher Scientific, UK). Individual river water samples were filtered through a 106 µm sieve (Fischer Scientific, UK) in order to remove particulates and large protozoa, as detailed in OECD 309 regulatory guidelines (OECD, 2004). Sediment was wet-sieved through a 2.36 mm sieve (Endecotts Ltd., UK) to homogenize each individual sample in accordance to OECD 308 regulatory testing (OECD, 2002b). Samples were refrigerated at 4 °C until used – this was no longer than 24 hours.

Figure 2.1: River Dene, Wellesbourne, United Kingdom in Autumn 2014 (a) and Winter 2016 (b). The river varied throughout the year in multiple parameters, e.g. water depth and flow rate.

Figure 2.2: Map showing the River Dene, Wellesbourne, United Kingdom. The red square denotes location of sample site downstream of the WWTP effluent discharge point, which is shown by the green square (Google, 2016).

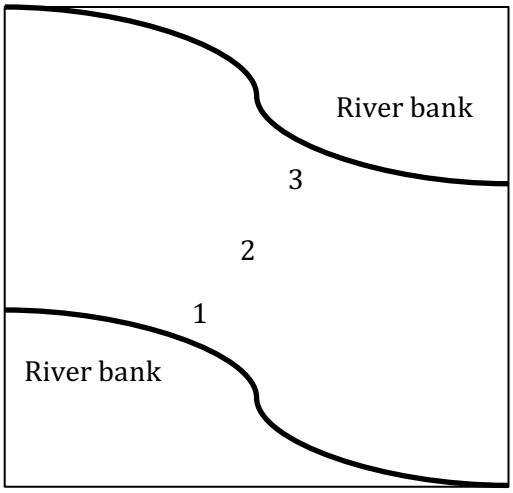

Figure 2.3: Sample collection points along the river. *1* denotes 25th quartile, *2* the 50th quartile and *3* the 75th quartile. Created using Microsoft® PowerPoint for Mac.

2.2.2 Test chemical

Studies were performed using [^{14}C]-radiolabelled chemical supplied by Syngenta, Jealott's Hill International Research Centre, United Kingdom. The compound used was [pyrazole-5-^{14}C]-isopyrazam (specific activity 4.736 MBq/mg and 98.6 % purity) (**Fig. 1.5**). The rationale for choosing isopyrazam in this study is outlined in section 1.5.

2.2.3 Experimental set up

Duran Schott 250 mL clear and amber glass bottles (Scientific Laboratory Supplies, UK) were washed and autoclaved twice at 121 °C to ensure that they were sterile prior to sample addition. Amber bottles were further wrapped in foil so that no light could penetrate and the clear and amber bottles were used as illuminated and dark treatments, respectively. The following treatments were set up in triplicate; dark water-only, illuminated water-only, dark water-sediment, illuminated water-sediment. The wet to dry weight ratio of sediment was analysed by weighing wet sediment before and after heating to dryness. In the water-sediment microcosms, 80 mL water and 20 g dry weight equivalent of sediment were added to ensure a 4:1 ratio of water to dry mass sediment. In water-only microcosms, 80 mL of water was added. The lids of each bottle were fitted with a crocodile clip. 20 mL scintillation vials were attached to the clip so that they were suspended inside the bottle. 1 mL NaOH was added to these vials in order to capture any volatiles from isopyrazam degradation (**Fig. 2.4**).

Bottles were randomly distributed on a Lab Companion SK-71 bench top rotary shaker (Jeio Tech Co., South Korea) under constant motion at 50 rpm at the School of Life Sciences, University of Warwick, United Kingdom (**Fig. 2.5**). The shaker was in a controlled environment room at 20 ± 2 °C with a sixteen-hour light and eight-hour dark cycle. Fluorescent 70 W daylight blubs (F70W/865 T8 6 ft, Fusion Lamps, UK) were used with LEE226 filters (Transformation Tubes, UK), which inhibited UV light output so that there was a transmission of less than 50 % radiation at a wavelength of 410 nm. This ensured that degradation due to photolysis was limited.

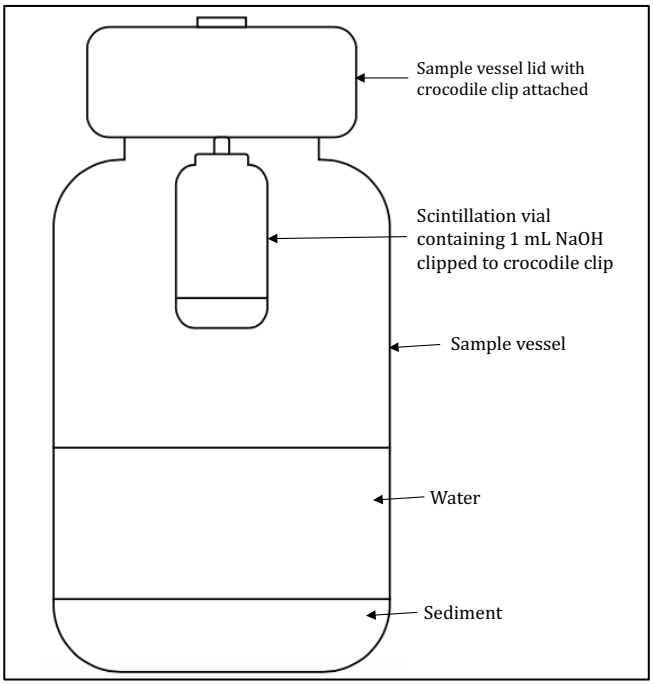

Figure 2.4: Diagram of sample vessel with attached NaOH trap. Sample vessel lids (in this case a water-sediment vessel) were fitted with a crocodile clip in order to suspend a 20 mL scintillation vial inside the vessel. This vial contained 1 mL NaOH so that any volatiles from isopyrazam degradation could be captured. Diagram created using site.youidraw.com (YouiDraw, 2016).

Water-sediment microcosms were incubated for nine days prior to chemical addition so that sedimentary communities had time to equilibrate to the laboratory conditions. After nine days, fresh water was collected from the sample site and spiked with [^{14}C]-isopyrazam to a concentration of 0.1 mg/L (0.474 MBq/L). Although conservative and likely a worst-case scenario, this is classed as an environmentally relevant concentration, ensuring that the biodegradation kinetics reflect those expected in the environment (OECD, 2004). Microcosms were then incubated for up to 36 days. Environmental realism of the test conditions are outlined in Appendix I.1.

Figure 2.5: Experimental set up at School of Life Sciences, University of Warwick, United Kingdom. Microcosms were placed on a rotary shaker at 50 rpm under fluorescent daylight bulbs covered in a LEE226 filters to inhibit UV light output.

2.2.4 Destructive harvesting

Destructive harvesting took place at 0, 9, 18, 27, and 36 days after treatment (DAT). At each time point, triplicate microcosms for each treatment were destructively harvested. Both chemical and microbial analysis was carried out at each time point, except at 0 DAT, where no chemical analysis was carried out and a nominal 0 DAT value was used, assuming that 100 % of the applied chemical was in the water fraction. 0.474 MBq/L was added to each microcosm and the percentage of radioactivity recovered from each fraction – water, sediment extract, NER in the sediment, and NaOH traps - was summed together for the mass balance. Example mass balance can be seen in Appendix I.2.

2.2.5 Chemical analysis

2.2.5.i Residual isopyrazam and ^{14}C in the water fraction

The water fraction from each microcosm was poured into a separate storage bottle gently, so as not to disturb the sediment fraction. As isopyrazam can adsorb to glassware,

microcosms were washed after removal of water and sediment with 8 mL acetonitrile (HPLC grade, Fischer Scientific, UK) and the wash collected. Duplicate samples of both water and acetonitrile from each microcosm were weighed into scintillation vials, and 10 mL of Ecoscint A scintillation cocktail (National Diagnostics, UK) was added. ^{14}C content was determined using a Tri-Carb 2800TR scintillation counter (PerkinElmer, US) with a five-minute count time. Water fraction ^{14}C content was determined by summing radioactivity determined in the water and acetonitrile wash fractions.

The acetonitrile wash remaining after scintillation counting was added to the water fraction and samples were sonicated for 3 minutes using a U300H ultrasonic bath (Ultrawave, UK) in order to lyse any radioactivity sorbed to algal cells. Water was then concentrated by solid phase extraction (SPE) to ensure that there was approximately 1500 Bq/mL after concentration. SPE was performed using a Whatman 12 port SPE vacuum manifold (GE Healthcare, UK) attached to an N 035.3 AN.18 diaphragm pump (KNF Neuberger, UK) and the SPE protocol, supplied by Syngenta, is described in Appendix I.3. Methanol was used to elute the samples and nitrogen, with a Dri-Block DB-3 (Techne, UK) attached to a SC-3 sample concentrator (Techne, UK), was used to evaporate the samples before resuspension. Examples of the concentration calculations can be seen in Appendix I.4.

Samples were then analysed for isopyrazam by High-Performance Liquid Chromatography (HPLC), using a protocol supplied by Syngenta (Appendix I.5). A LiChrospher RP-18e 5 µm column (4.0 x 250 mm, Agilent Technologies, US), ProFlow G+ scintillation cocktail (Meridian Biotechnologies Ltd., UK), and a HPLC system consisting of a AS-2055i Plus Intelligent Inert Sampler, PU-1580 Intelligent HPLC Pump, CO-2067 Plus Intelligent Column Oven (Jasco, UK), connected to a β-RAM radio-HPLC detector (LabLogic, UK) was used in conjunction with Laura software (version 4, LabLogic, UK). Confirmation of the isopyrazam peak and example chromatograms can be found in Appendix I.5.

2.2.5.ii Residual isopyrazam and ^{14}C in the sediment fraction

The sediment fraction was mixed well and 10 g dry weight equivalent of sediment from each microcosm was removed. 30 mL 80 % acetonitrile (HPLC grade, Fischer Scientific,

UK) was added to the sediment to extract the chemical mixture. Samples were shaken for 1 hour at 300 rpm, before being centrifuged for 10 minutes at 228 x *g*. The supernatant was removed and the pellet subject to two further extractions as detailed above. Duplicate samples of the combined supernatants were weighed into scintillation vials and 10 mL of Ecoscint A scintillation cocktail (National Diagnostics, UK) was added. ^{14}C was analysed using a Tri-Carb 2800TR scintillation counter (PerkinElmer, US) with a five-minute count time.

The sediment extracts were concentrated to ensure the final re-suspension would contain approximately 1500 Bq/mL. Example concentration calculations can be found in Appendix I.4. The extracts were weighed into glass vials and samples were evaporated to dryness under nitrogen using a Dri-Block DB-3 (Techne, UK) attached to an SC-3 sample concentrator (Techne, UK). Samples were then re-suspended in 1:1 acetonitrile (HPLC grade, Fischer Scientific, UK) and water (HPLC grade, VWR Chemicals, UK) and analysed by HPLC in the same way used for the water fraction samples in section 2.2.5.i. Example chromatograms can be found in Appendix I.5.

Solid sediment remaining after extraction was dried and then a combustion step was carried out with duplicate weighed amounts of sediment to quantify any NER. This was carried out using an OX500 Biological Oxidizer (R.J. Harvey Instrument Corporation, US), which burns the samples in an atmosphere of oxygen for 1.5 minutes, giving $^{14}CO_2$ as a product. This product was trapped in Oxysolve-C-400 scintillation cocktail (Zinsser Analytic, Germany) and samples were then analysed using a Tri-Carb 2800TR scintillation counter (PerkinElmer, US) with a count time of five minutes.

2.2.5.iii Gaseous fraction

All microcosms were fitted with traps consisting of a 20 mL scintillation vial containing 1 mL of a 1 M NaOH (Fischer Scientific, UK) solution attached to a crocodile clip inside the lid of the microcosm. These intended to capture any $^{14}CO_2$ that had been mineralised, and were removed every five days of the experiment and replaced with fresh ones. 10 mL Ecoscint A scintillation cocktail (National Diagnostics, UK) was added to the

vials and analysed using a Tri-Carb 2800 TR scintillation counter (PerkinElmer, US) with a count time of five minutes.

2.2.6 Water chemistry and sediment property analysis

2.2.6.i Macronutrient analysis

NO_3- concentration in the water was analysed using a NO_3- test kit (Hach, UK, 0 to 40 mg/L range). 5 mL of the water fraction was put into a colour viewing tube and a NitraVer® 6 Nitrate Reagent Powder Pillow (Hach, UK) was added and shaken for three minutes. The sample was then left for 30 seconds to allow un-oxidized particles of cadmium metal to settle before pouring the rest of the sample into another colour viewing tube. A NitriVer® 3 Nitrite Reagent Powder Pillow (Hach, UK) was added to the sample, shaken for 30 seconds, and left for at least 10 minutes so that a red colour could develop if NO_3- was present.

PO_4 concentration in the water was analysed using a PO-14 PO_4 test kit (Hach, UK, 0 to 44 mg/L range). 5 mL of sample water was put into a colour viewing tube, four drops of $(NH_4)_6Mo_7O_{24}$ (Hach, UK) added, and the tube shaken to mix. A Phosphate 2 Reagent Powder Pillow (Hach, UK) was then added and the tube inverted until the powder had dissolved. The tube was left no longer than 15 minutes for a blue colour to develop if PO_4 was present.

Treated samples were compared to untreated samples on the colour wheels provided in the respective kits to determine the respective macronutrient concentrations. The instruction manuals also gave details on multiplying factors for if a higher concentration range test needed to be carried out.

2.2.6.ii Sediment property analysis

Physico-chemical properties of sediment collected from each location at the sample site at each collection time were determined. Textural class analysis (percentages of sand, silt, and clay), pH, and percentage of organic carbon were measured. Analysis was carried out by Lancrop Laboratories, Wellington Road, The Industrial Estate, Pocklington, York, United Kingdom.

For textural class analysis, sediment was dried in a recirculating drying oven at a temperature of 35 ± 5 °C for 8 hours. The sample was weighed, manually rolled, and passed through a 2 mm mesh. The proportion retained by the mesh was weighed and, from this, the percentage stone fraction calculated. A subsample was taken from the < 2 mm fraction and suspended in a $(NaPO_3)_6$ solution to ensure complete particle dispersion. This was then presented for sand, silt, and clay fraction analysis. This was performed by a Low Angle Laser Light Scattering technique using a Mastersizer 2000 optical bench (Malvern, UK), with recirculating wet cell enhancement and a Hydro 2000MU sample introduction unit (Malvern, UK). Briefly, sand was defined as particle sizes between 2 mm to 63 μm, silt between 63 μm to 2 μm, and clay particles under 2 μm. For the pH analysis, a 1:2.5 sediment and deionised water suspension (10 and 25 mL) was placed on an orbital shaker at 250 spm for 15 minutes as described in Agricultural Development and Advisory Service (1986). Analysis was then carried out using a AS3000Q Multi Electrode pH Robot (Labfit, Australia). Lastly, sediment was dried at 105 °C for one hour, and 0.8 g of dried sediment was used. Samples were pre-treated with acid to remove any inorganic carbon in the form of carbonate inclusions and then analysis was carried out using a TruMac® CN combustion analyser (LECO Corporation, USA).

2.2.7 Microbial analysis

2.2.7.i Chlorophyll a *analysis*

Chlorophyll *a* was extracted from both the water and sediment fractions to determine the abundance of phototrophic organisms. Water samples were filtered using a Whatman GF/C 47 mm diameter glass microfiber filter paper (GE Healthcare, UK), as described in Sartory (1982). A modified version of a method described by Ritchie (2006) was used to extract the chlorophyll *a*. In separate tubes, sediment from each microcosm and the microfiber filters from the water fraction were combined with 20 mL of 90 % acetone (Fischer Scientific, UK). Tubes were wrapped in foil to prevent chlorophyll photolysis and were shaken at 200 rpm for 5 hours. For both the water and the sediment fraction, the absorbance of the solvent extract was measured at 664 nm and 750 nm using an Ultrospec 1100 pro UV/Visible spectrophotometer (GE Healthcare, UK). Samples were then acidified by the addition of 200 μL of 3 M HCl (Fischer Scientific, UK) so that the chlorophyll *a* was

converted to pheophytin. Samples were left for 30 seconds and then the absorbance was measured again, but at 665 nm and 750 nm. Absorbance readings at 750 nm were deducted from their respective absorbances at 664 nm and 665 nm. Chlorophyll *a* was calculated using the formula given in American Public Health Association (1995).

2.2.7.ii Viable plate counts

A serial dilution of water from each microcosm was set up (10^{0} - 10^{-5}) and 20 µL of each dilution was spread onto a quarter of a 9 cm R2A agar (Oxoid, UK) Petri dish. Plates were incubated for 2 days at 29 °C and colonies were counted to determine the number of bacterial colony forming units (CFU) per µL of water.

2.2.7.iii DNA isolation and quantification

DNA isolation and quantification was carried out as described in Appendix IV. Water (on filters) and sediment samples were frozen at -80 °C and processed after all eight collection times had taken place. DNA was isolated from the fresh water and sediment taken from the sample site and water and sediment from the microcosms at 36 DAT. Library preparation and sequencing of 16S rRNA and 23S rRNA genes to investigate bacterial and phototrophic community structure and diversity was carried out as described in Appendix IV. Sequencing was carried out by the Genomics Facility at the University of Warwick, Coventry, United Kingdom in July 2016 and raw data was returned for further analysis.

2.2.8 Statistical analyses

Significance of differences between treatments for isopyrazam dissipation, metabolite formation, mineralisation, sediment partitioning, NER, water chemistry analysis, water fraction bacteria concentration, and total microcosm chlorophyll *a* concentration was determined using a two-way ANOVA (with microcosm type and collection time). Ordinary one-way ANOVA (with collection time) was performed on sample site variation data and sediment property data. The Tukey method (Haynes, 2013) was used to correct for multiple comparison tests. Statistical analyses and figures were performed and created using Prism (version 7, GraphPad Software, Inc., US).

Isopyrazam degradation kinetics (DegT50) were estimated using Computer Aided Kinetic Evaluation (CAKE) (version 3.2, Tessella Ltd., UK), which is a modelling program that conforms to the FOCUS requirements (FOCUS, 2006). Single first-order (SFO) kinetics was used for assessing the degradation of isopyrazam. SFO works from an exponential equation in which the rate of compound decline is proportional to the concentration in the system. There are a number of acceptance requirements which need to be met before the fit of the model can be accepted; goodness of fit ($\chi^2 < 15$ %), assessment of whether the degradation rate constant differs from zero (t-test, probability ≤ 0.05), and correlation between the observed and the expected values ($r^2 \geq 0.7$).

A number of R packages were used to assess the microbial community data, and data generation was carried out in RStudio (version 0, RStudio Inc., US). Alpha (α) diversity of the bioinformatics analysis was analysed using Fisher's method in the phyloseq package in R (McMurdie and Holmes, 2013) using the Operational Taxonomic Unit (OTU) table before rarefaction. One-way ANOVA and figures were then generated as above in Prism (version 7, GraphPad Software, Inc., US). Rarefied data (see IV.3.8) was then used to analyse beta (β) diversity, and this was evaluated with PERMANOVA using the vegan package in R (Oksanen *et al.*, 2017). A modified script was used to analyse pairwise comparisons (Arbizu, 2015). PERMANOVA was used to determine the level of dissimilarity between groups (R^2) and the level of significance (p). R values ranged between -1 and +1, with higher R values being associated with higher levels of dissimilarity. Bray Curtis similarity matrices with non-metric multidimensional scaling (NMDS) and cluster analysis was used to visualise β diversity with charts being generated in Primer software (version 6, Primer-E Ltd., UK). Two-way ANOVA (with taxa and collection time or microcosm type, depending on the comparison) was carried out and figures created as above in Prism (version 7, GraphPad Software, Inc., US) to evaluate the relative abundance of communities. Pearson correlation coefficients were also calculated using Prism (version 7, GraphPad Software, Inc., US) to determine any links between the variables tested throughout the experiment and both DegT50 and mineralisation data. Quantitative Insights Into Microbial Ecology (QIIME) was used to determine any OTUs showing significant correlation to DegT50 and mineralisation data. This was carried out using the Kruskal-Wallis test and Bonferroni correction was used to reduce type I error from

performing multiple tests. This was implemented as in the group_significance.py script (Caporaso *et al.*, 2010).

2.3 RESULTS

2.3.1 Sample site temporal characteristics

Water pH at the sample site (**Fig. 2.6.a**) was significantly impacted by collection time ($p \leq 0.0001$) with pH at summer 2014, winter 2015, spring 2015, and spring 2016 ranging between pH 8.0 and 8.2, which was significantly higher than at the other collection times. Comparing between collection times at the same time of year, summer 2014 had a significantly higher ($p \leq 0.05$) pH to summer 2015 (8.0 and 7.6, respectively) and winter 2015 had a significantly higher pH ($p \leq 0.001$) compared to winter 2016 (8.1 and 7.5, respectively).

Water temperature at the sampling site (**Fig. 2.6.b**) in summer and autumn was generally warmer than the other collection times ($p \leq 0.0001$) ranging between 13.0 and 16.0 °C. Compared to summer and autumn, spring collection times showed an intermediate temperature (10.5 °C both years) and winter collection times were significantly colder ($p \leq 0.0001$, 6.5 and 7.5 °C). Although winter collection times were colder than other collection times, winter 2016 was significantly ($p \leq 0.05$) warmer (7.5 °C) compared to winter 2015 (6.5 °C). There were no significant differences in temperature between summer, autumn, and spring collection times between the two collection years.

Sample site water depth (**Fig 2.6.c**) was significantly impacted by collection time ($p \leq 0.0001$); in winter 2016, the water depth was significantly deeper than the other collection times, measuring at 43.5 cm. This was most notable ($p \leq 0.0001$) compared to summer 2015 (20.0 cm) and autumn 2015 (20.5 cm). There was also a significant impact ($p \leq 0.0001$) of collection time on light intensity (**Fig. 2.6.d**). Summer 2014 and autumn 2014 had significantly higher ($p \leq 0.01$) light intensities compared to other collection times, measuring at 2.0×10^5 lux. Spring 2015 had a light intensity of 1.6×10^5 lux and this was significantly higher ($p \leq 0.05$) than winter 2015 (3.1×10^3 lux), autumn 2015 (3.0×10^4 lux), winter 2016 (1.5×10^4 lux), and spring 2016 (6.4×10^4 lux).

Although summer 2014 had a higher average concentration of bacteria in the water compared to all other collection times (2.1×10^7 CFU/µL), there was higher variance

between replicate samples which skewed the analysis. Thus, there was no significant difference ($p \leq 0.6235$) between collection times (**Fig. 2.6.e**). This only took into account bacteria that could be cultured using the media and incubation conditions outlined in section 2.2.7.ii. DNA sequencing data, outlined in section 2.3.4, gave more insight on temporal shifts at the sample site.

River velocity at the sample site (**Fig. 2.6.f**) was significantly impacted by collection time ($p \leq 0.0001$). In particular, winter 2016 and spring 2016 both had significantly higher water velocities (0.47 and 0.52 m/s, respectively) compared to summer 2015 and autumn 2015 ($p \leq 0.0001$, 0.17 and 0.24 m/s, respectively). In addition, winter 2015 had a velocity of 0.41 m/s and this was significantly faster ($p \leq 0.0001$) than summer 2015. Generally, a quicker water velocity was associated with deeper water depths.

Table 2.1: Sediment characteristics from the sample site across different collection times. The mean and standard deviation of the sample site sediment characteristics across different collection times. Analysis included silt, clay, and sand content, organic carbon content, and pH, and was carried out by Lancrop Laboratories, York, United Kingdom. *SD* denotes *standard deviation*.

Collection time/year	Descriptive statistic	Silt (%)	Clay (%)	Sand (%)	Organic carbon (%)	pH
Summer '14	Mean	10.5	5.4	84.0	1.3	7.6
	SD	3.9	2.4	6.3	0.1	0.1
Autumn '14	Mean	7.9	3.8	88.3	1.2	7.7
	SD	3.2	2.0	5.1	0.3	0.1
Winter '15	Mean	13.7	7.0	79.3	1.3	7.8
	SD	2.5	1.4	3.9	0.1	0.1
Spring '15	Mean	13.6	6.6	79.8	1.0	7.7
	SD	3.3	1.5	4.7	0.1	0.1
Summer '15	Mean	6.3	2.8	90.8	1.7	7.8
	SD	0.5	0.2	0.6	0.1	0.2
Autumn '15	Mean	7.8	4.3	87.9	1.3	7.9
	SD	2.2	1.3	3.5	0.4	0.2
Winter '16	Mean	12.2	6.1	81.7	1.3	7.9
	SD	7.8	4.4	12.2	0.3	0.2
Spring '16	Mean	18.0	9.2	72.8	1.6	8.0
	SD	7.0	3.5	10.6	0.2	0.0

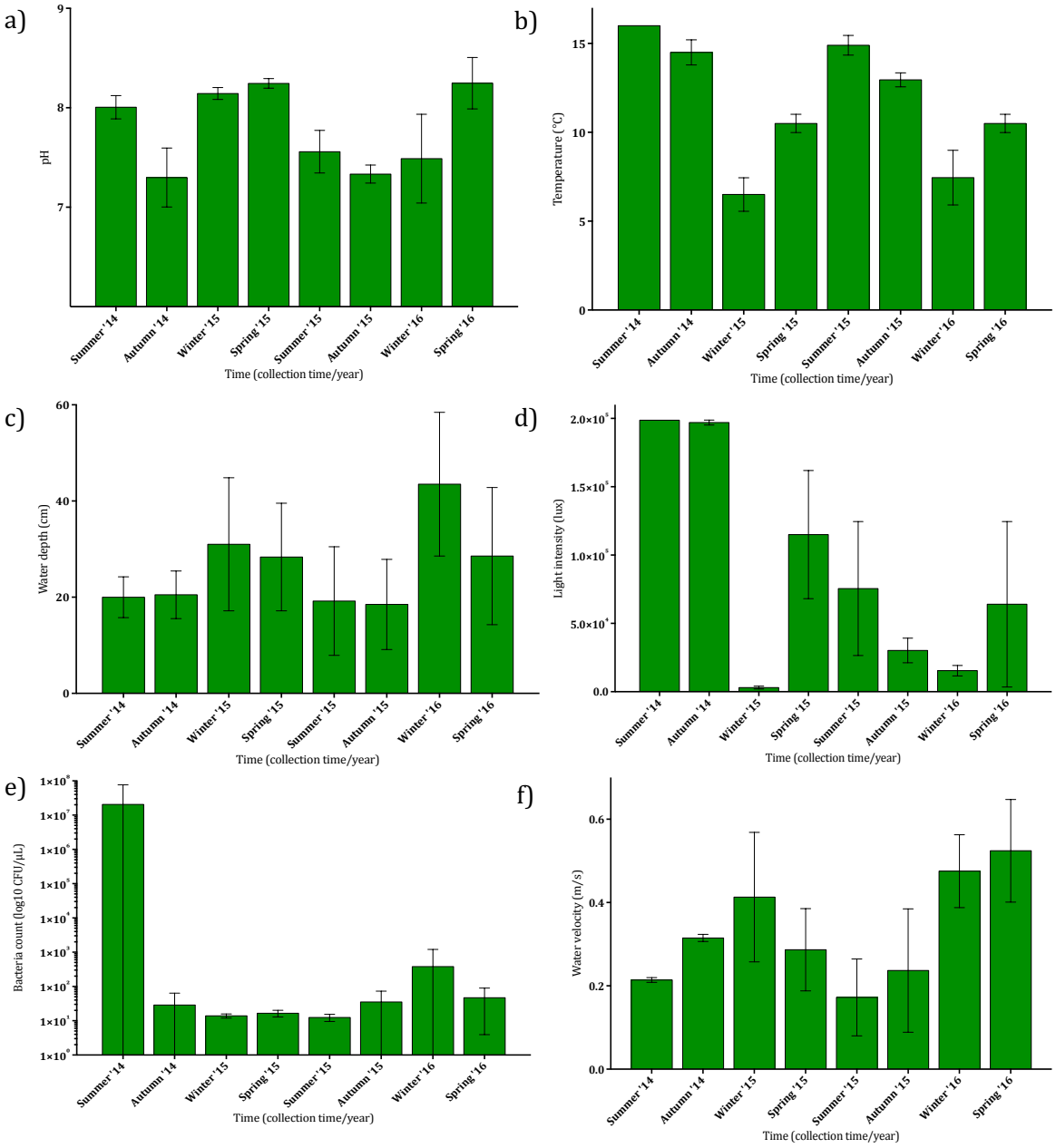

Figure 2.6: Variation in conditions at the sample site over time between collection times. Variation at the sample site of pH (a), water temperature (b), water depth (c), light intensity (d), water bacteria plate count (e), and water velocity (f). Error bars show ± standard deviation.

NO_3- and PO_4 concentrations in the water are presented in Appendix I.6. Water NO_3- concentration (**Fig. I.9**) was significantly impacted by collection time ($p \leq 0.0001$) with significantly higher ($p \leq 0.0001$) NO_3- concentrations in summer 2014 (33.9 mg/L) compared to all other collection times, where concentrations ranged between 10.6 and 18.6

mg/L. PO_4 concentrations (**Fig. I.10**) ranged between 1.0 and 3.0 mg/L and there were significant differences between collection times ($p \leq 0.0001$). Summer 2014 had a significantly higher PO_4 concentration ($p \leq 0.05$, 2.4 mg/L) compared to winter collection times and spring 2016, while spring 2015 ($p \leq 0.05$, 4.3 mg/L) had significantly higher PO_4 concentrations compared to all collection times except summer 2014 and autumn 2015.

Analysis of the sediment at the sample site (**Table 2.1**) provided composition of silt, clay, and sand content, organic carbon content, and pH. The sediment was predominately sandy and, in all analyses, there was not a significant change in sediment characteristics between collection times. Silt content ranged between 6.3 and 18 % ($p \leq 0.2556$), clay content between 2.8 and 9.2 % ($p \leq 0.2779$), and sand content between 72.8 and 90.8 % ($p \leq 0.2632$). Organic carbon content of the sediment ranged between 1.0 and 1.6 % ($p \leq 0.4362$) and the pH between 7.6 and 8.0 ($p \leq 0.3593$).

2.3.2 Chemical analysis results

2.3.2.i Isopyrazam decline

One illuminated water-only replicate was lost during the course of the experiment (18 DAT in spring 2015). Other than this, all replicates were used and generally mass balance reached above 90 %. In illuminated water-only microcosms in autumn 2014 (9 DAT) and dark water-only microcosms in summer 2014 (27 and 36 DAT) and autumn 2014 (18 and 36 DAT), the average mass balance was between 84.0 and 89.9 %. These replicates, however, were still included as they continued to follow the general trend of the results.

There was a significant effect of both treatment and collection time on the rate of isopyrazam degradation ($p \leq 0.0001$). In illuminated water-sediment systems (**Fig. 2.7**), between 12.6 and 65.0 % of the applied radioactivity remained as isopyrazam at 36 DAT, whereas in dark water-sediment systems (**Fig. 2.7**), isopyrazam remaining at 36 DAT varied between 82.6 and 91.0 %.

The variation in illuminated water-only systems (**Fig. 2.8**) was between 56.0 and 88.4 % and in dark water-only systems (**Fig. 2.8**) between 84.2 and 101.0 %. Within each

collection time, isopyrazam degradation varied between microcosm treatment; however, a temporal variation in isopyrazam degradation was only seen in microcosms incubated under illuminated conditions.

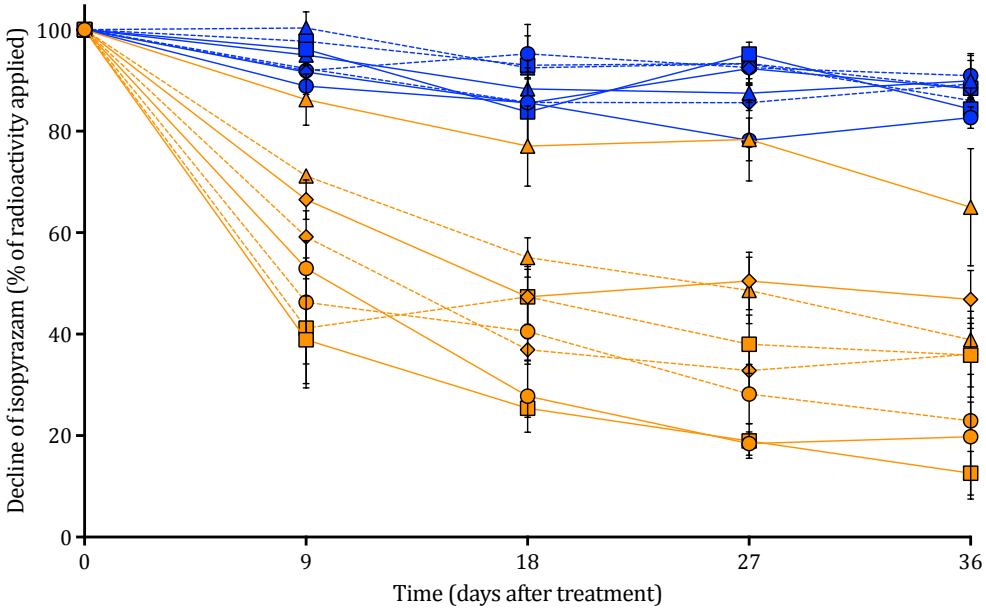

Figure 2.7: Degradation of isopyrazam in water-sediment microcosms as a percentage of the radioactivity originally applied. Degradation of isopyrazam in illuminated (orange) and dark (blue) water-sediment microcosms over 36 days in summer (circles), autumn (squares), winter (triangles), and spring (diamonds). The first year of each collection time was denoted by a solid line and the second year by a dashed line. Error bars show ± standard deviation.

The addition of non-UV light to the experiments had a significant impact on degradation. At all collection times, degradation in illuminated water-sediment systems was significantly faster compared to dark water-sediment, illuminated water-only, and dark water-only treatments. This was generally highly significant ($p \leq 0.0001$) although there was some variance within winter 2015, when degradation was slower compared to other illuminated water-sediment microcosms.

In illuminated water-only systems, the impact of light treatment was less pronounced than in water-sediment systems. At some collection times, there was no significant difference in degradation between illuminated and dark systems (winter 2015, spring 2015, and winter 2016). In summer, autumn, and spring 2016, however, there was significantly faster degradation in illuminated water-only compared to dark water-only microcosms ($p \leq 0.05$). There was no significant difference in degradation between dark

water-sediment and dark water-only treatments, regardless of sediment addition. This highlights that the addition of sediment in the systems had an impact only in the illuminated treatments.

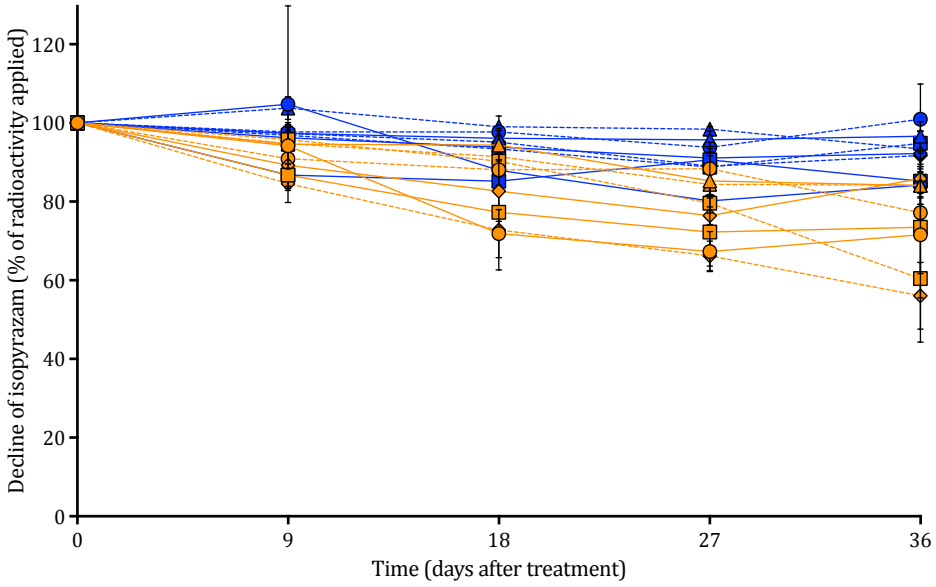

Figure 2.8: Degradation of isopyrazam in water-only microcosms as a percentage of the radioactivity originally applied. Degradation of isopyrazam in illuminated (orange) and dark (blue) water-only microcosms over 36 days in summer (circles), autumn (squares), winter (triangles), and spring (diamonds). The first year of each collection time was denoted by a solid line and the second year by a dashed line. Error bars show ± standard deviation.

Although there was increased degradation in illuminated water-sediment microcosms compared to other treatments, there was variation between collection times within this treatment of 12.6 and 65.0 % isopyrazam remaining by 36 DAT (**Fig. 2.7**). There was no significant difference in degradation between the two summer collection times (19.8 and 22.9 %, respectively), however, in autumn ($p \leq 0.0001$), winter ($p \leq 0.0001$), and spring ($p \leq 0.05$) there was a significant difference in degradation between the two collection years. This suggests that although there were temporal changes in the degradation rate of isopyrazam, it was not predictable at specific times of year. Summer and autumn 2014 (19.8 and 12.6 % degradation by 36 DAT) collection times had a significantly ($p \leq 0.001$) quicker isopyrazam decline compared to winter and spring collection times. Winter 2015, on the other hand, had a significantly slower degradation rate ($p \leq 0.0001$) when compared to all other collection times, with 65.0 % isopyrazam remaining in the microcosm by 36 DAT. Summer and autumn 2015 and spring 2016 reached 22.9, 35.9, and 36.0 % isopyrazam

remaining by 36 DAT and these collection times were not significantly different to each other. Isopyrazam decline reached 46.9 and 36.0 % in spring 2015 and winter 2016 and these collection times were not significantly different to each other. These five collection times showed more intermediate degradation rates between the faster declines in summer 2014 and autumn 2014 and the slower decline in winter 2015; significant differences varied depending on the collection times compared.

In illuminated water-only systems (**Fig. 2.8**), there was no significant difference in isopyrazam decline between the two years in summer, autumn, or winter collection times. There was significantly ($p \leq 0.0001$) more isopyrazam degradation in spring 2016 than spring 2015, with 56.1 % and 88.4 % isopyrazam remaining by 36 DAT, respectively. When comparing degradation rates between different collection times, spring 2016 was also significantly different ($p \leq 0.05$) to all collection times apart from summer 2014 and autumn 2014. There was also significantly more ($p \leq 0.05$) degradation in summer 2014 and autumn 2014 (60.5 and 77.2 % of isopyrazam remaining by 36 DAT, respectively) when compared to winter collection times (84.1 and 84.2 % remaining by 36 DAT in respective years).

In dark water-sediment microcosms (**Fig. 2.7**) there was no significant difference between different years of the same collection time or between different collection times. In general, this was also the same for dark water-only microcosms (**Fig. 2.8**); however, autumn 2014 had 85.2 % of isopyrazam remaining by 36 DAT which was significantly different ($p \leq 0.05$) to summer 2015 and winter 2016 (101.0 and 93.4 % remaining, respectively).

Charts showing isopyrazam decline by collection time, which more clearly show the differences in degradation between the microcosm treatments within each collection time, can be found in Appendix I.6. DegT50 and rate constant estimates from CAKE can additionally be found in Appendix I.6. DegT50 data were only used for illuminated water-sediment microcosms in further analyses. For dark water-sediment, illuminated water-only, and dark water-only treatments, DegT50 estimates were beyond the duration of the study and key acceptance criteria (see section 2.2.8) were not met. This meant it was difficult to extrapolate from the results and, therefore, DegT50 estimates from these treatments were not used in further analyses.

2.3.2.ii Total metabolite generation

Metabolite generation was calculated by summing together the percentages of any non-isopyrazam peaks from the HPLC chromatograms. There was a significant impact of both microcosm treatment and collection time on the rate of metabolite generation ($p \leq 0.0001$). As with the isopyrazam decline, there were differences between microcosm treatments at each collection time, as well as temporal changes between collection times for illuminated treatment microcosms. Percentage of metabolites at 36 DAT varied between 24.9 and 80.8 % in illuminated water-sediment microcosms and, generally, there were significantly higher amounts ($p \leq 0.0001$) of metabolites produced in these systems (**Fig. 2.9**) compared to dark water-sediment, illuminated water-only, and dark water-only treatments. This was the case for all collection times except in winter 2015. Metabolite generation in the illuminated water-sediment microcosms were lower in winter 2015 (24.9 %) and there were no significant differences in metabolite generation compared to illuminated water-only microcosms (10.0 %) at the same collection time.

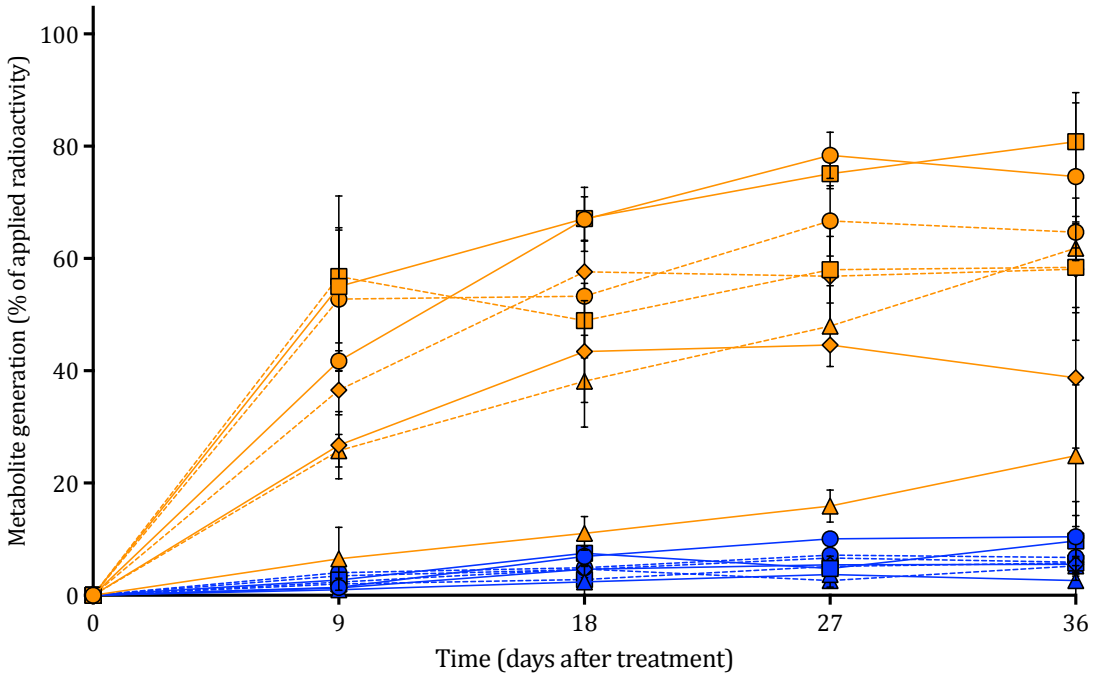

Figure 2.9: Generation of metabolites in water-sediment microcosms as a percentage of the radioactivity originally applied. Generation of metabolites in illuminated (orange) and dark (blue) water-sediment microcosms over 36 days in summer (circles), autumn (squares), winter (triangles), and spring (diamonds). The first year of each collection time was denoted by a solid line and the second year by a dashed line. Error bars show ± standard deviation.

As with isopyrazam decline, metabolite generation in illuminated water-only microcosms (**Fig. 2.10**) was very variable and ranged between 9.8 and 38.7 % of the applied radioactivity, whereas in dark water-sediment (**Fig. 2.9**) and dark water-only (**Fig. 2.10**) microcosms, percentage of metabolite formation ranged between 2.6 and 10.4 %, and 0.6 and 4.8 %, respectively. In winter and spring 2015, metabolite generation was low and there was no significant difference between dark water-sediment, illuminated water-only, and dark water-only treatments. At all other collection times, there was a significant difference in metabolite formation between illuminated water-only and dark water-only microcosms ($p \leq 0.05$). There was only a significant difference between illuminated water-only and dark water-sediment microcosms in summer and autumn 2014 ($p \leq 0.05$) and spring 2016 ($p \leq 0.0001$). There was no significant difference in metabolite generation between dark treatments at any collection time, again showing that the addition of sediment to the systems only impacted the illuminated microcosms.

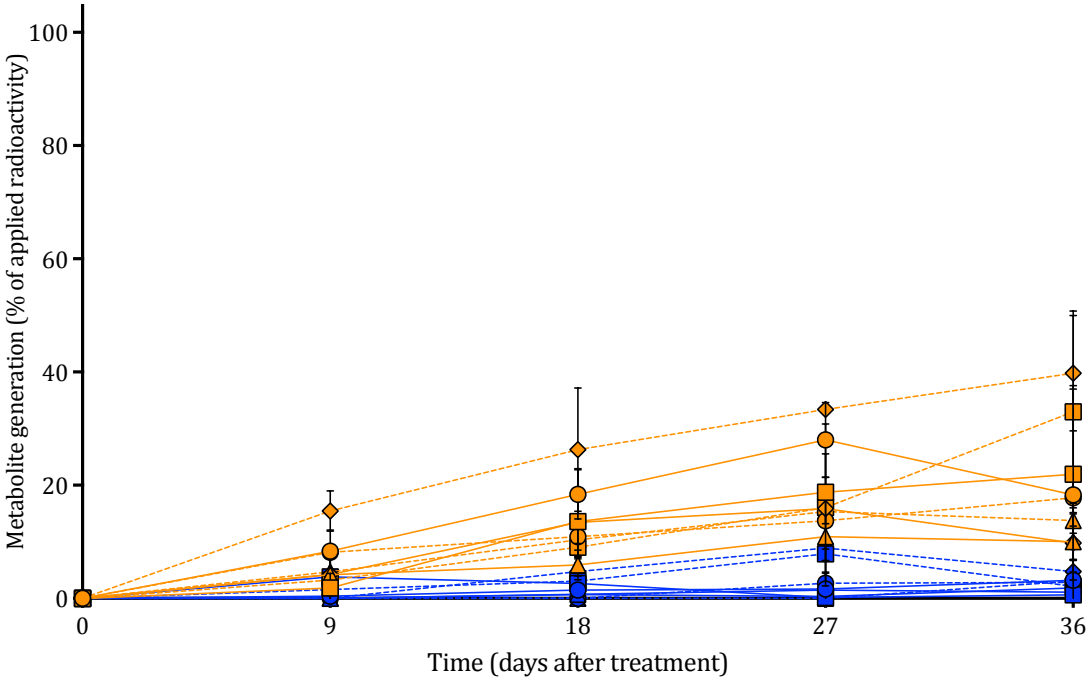

Figure 2.10: Generation of metabolites in water-only microcosms as a percentage of the radioactivity originally applied. Generation of metabolites in illuminated (orange) and dark (blue) water-only microcosms over 36 days in summer (circles), autumn (squares), winter (triangles), and spring (diamonds). The first year of each collection time was denoted by a solid line and the second year by a dashed line. Error bars show ± standard deviation.

Differences in metabolite generation between collection times mirrored the isopyrazam decline data, with no significant difference between summer collection times in illuminated water-sediment microcosms (13.3 and 17.8 %), but significant differences between collection times in autumn ($p \leq 0.001$), winter ($p \leq 0.0001$), and spring ($p \leq 0.001$) collection times. By 36 DAT, there were higher levels of metabolites in summer and autumn 2014 (74.6 and 80.8 %, $p \leq 0.0001$) and significantly lower levels of metabolites in winter 2015 ($p \leq 0.0001$, 24.9 %). Metabolite generation in all other collection times was intermediate to the summer and autumn 2014 and the winter 2015 levels.

Generally, there were no significant differences in metabolite generation between collection times in illuminated water-only microcosms. In spring 2016, however, there were significantly higher amounts (39.8 %) of metabolites compared to all other collection times (generally $p \leq 0.0001$). In both dark water-sediment and dark water-only systems, there was no impact of collection time on the total percentage of metabolites, regardless of sediment addition.

2.3.2.iii Sediment partitioning of total radioactivity

In water-sediment microcosms there was a significant impact ($p \leq 0.0001$) of microcosm treatment on the amount of total radioactivity that partitioned to the sediment fraction (**Fig. 2.11**). In illuminated microcosms, this ranged between 41.6 and 60.4 %, whereas in dark treatment microcosms it was between 69.4 and 73.8 %. In both the illuminated and dark treatments, there were no significant differences in the amounts of radioactivity partitioned to the sediment between collection times within the separate light treatments. Between illuminated and dark treatments within each individual collection time, however, there was significantly less radioactivity partitioned to the sediment in both illuminated summer and autumn collection times compared to their respective dark treatments. In summer, there was 46.4 and 45.9 % radioactivity partitioned to the sediment in illuminated systems, whereas in the dark, 71.1 and 74.0 % was partitioned to the sediment ($p \leq 0.01$ and $p \leq 0.0001$ in consecutive years). 41.6 and 50.1 % of the radioactivity partitioned to the sediment in autumn 2014 and 2015, respectively, but in dark treatments there were 73.8 and 70.3 % in the respective years ($p \leq 0.0001$ and $p \leq 0.05$ in the consecutive years). There were, however, no significant differences in isopyrazam sediment

partitioning between the two light treatments when comparing samples conducted in winter or comparing samples conducted in spring.

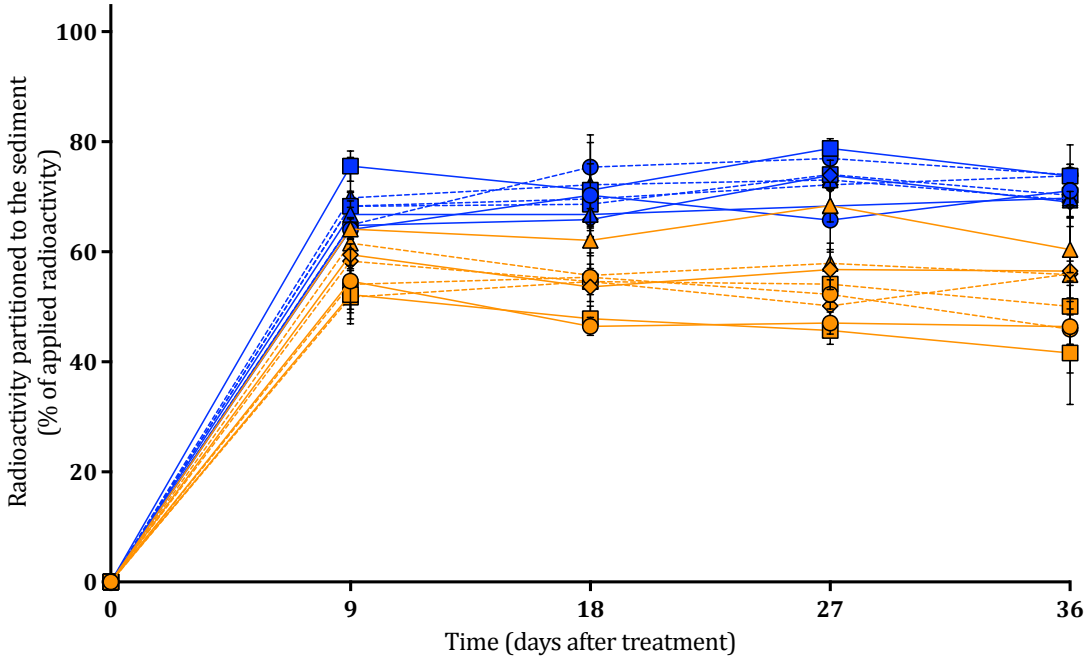

Figure 2.11: Partitioning of radioactivity to the sediment fraction as a percentage of the total applied radioactivity. Sediment partitioning of radioactivity in illuminated (orange) and dark (blue) water-sediment microcosms over 36 days in summer (circles), autumn (squares), winter (triangles), and spring (diamonds). The first year of each collection time was denoted by a solid line and the second year by a dashed line. Error bars show ± standard deviation.

2.3.2.iv Sediment fraction non-extractable residues

In general, only small amounts of radioactivity were present as NER in the sediment after extraction (**Fig. 2.12**). In illuminated treatments, this ranged between 2.1 and 7.4 % of the radioactivity present as NER and in dark treatment microcosms this ranged between 1.3 and 6.2 %. Although there were slightly higher levels of NER in 2016 collection times, a two-way ANOVA showed there was no significant difference between any microcosm treatment, regardless of either collection time or light treatment ($p \leq 0.1326$).

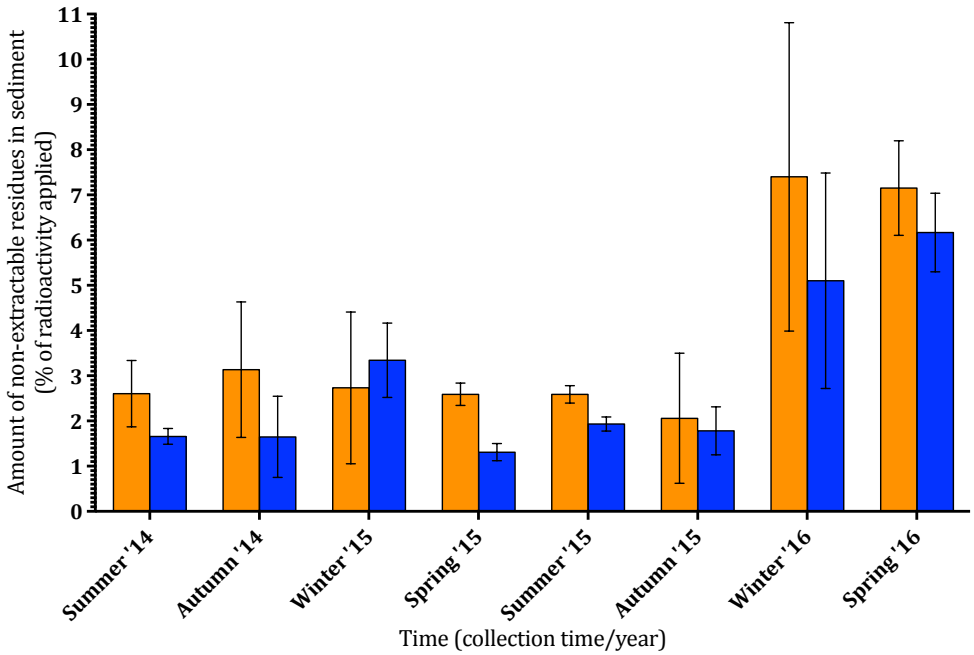

Figure 2.12: Amount of NER remaining in the sediment at 32 DAT as a percentage of the total applied radioactivity. NER in the sediment fraction were analysed using a combustion step with sediment from illuminated water-sediment (solid orange) and dark water-sediment (solid blue) microcosms at 36 DAT over different collection times. Error bars show ± standard deviation.

2.3.2.v Isopyrazam mineralisation

The cumulative amount of isopyrazam which was completely degraded and mineralised to $^{14}CO_2$ throughout each collection time is shown in **Figure 2.13**. Mineralisation was very variable, ranging from just 0.03 % isopyrazam mineralised in dark water-only microcosms in spring 2016 to 5.4 % in illuminated water-sediment microcosms in summer 2014. A two-way ANOVA showed there was a significant ($p \leq 0.0001$) impact of microcosm treatment on the amount mineralised. A Tukey multiple comparison test showed that it was only in summer 2014 that illuminated water-sediment systems had a significantly higher mineralisation when compared to the dark water-sediment, illuminated water-only, and dark water-only microcosms ($p \leq 0.0001$). In summer 2014, 5.4 % of the isopyrazam was mineralised in illuminated water-sediment microcosms, whereas 2.1, 2.7, and 2.4 % was mineralised in dark water-sediment, illuminated water-only, and dark water-only microcosms, respectively. At all other collection times, there was no impact of microcosm treatment on the amount of isopyrazam mineralised.

Across all microcosm treatments, collection time had a significant impact on total mineralisation ($p \leq 0.0001$). In summer 2014, total mineralisation ranged between 2.1 and 5.4 % of the total radioactivity applied to the systems, and there was significantly more mineralisation at this collection time when compared to all other collection times ($p \leq 0.0001$). In winter 2015, total mineralisation ranged between 0.9 and 1.5 % of the total radioactivity applied to the systems. This was also significantly higher (generally $p \leq 0.0001$) compared to mineralisation in all other collection times, except summer 2014, despite the lower degradation rate of isopyrazam itself. At all other collection times, the total mineralisation was low, below 0.5 % of the total applied radioactivity.

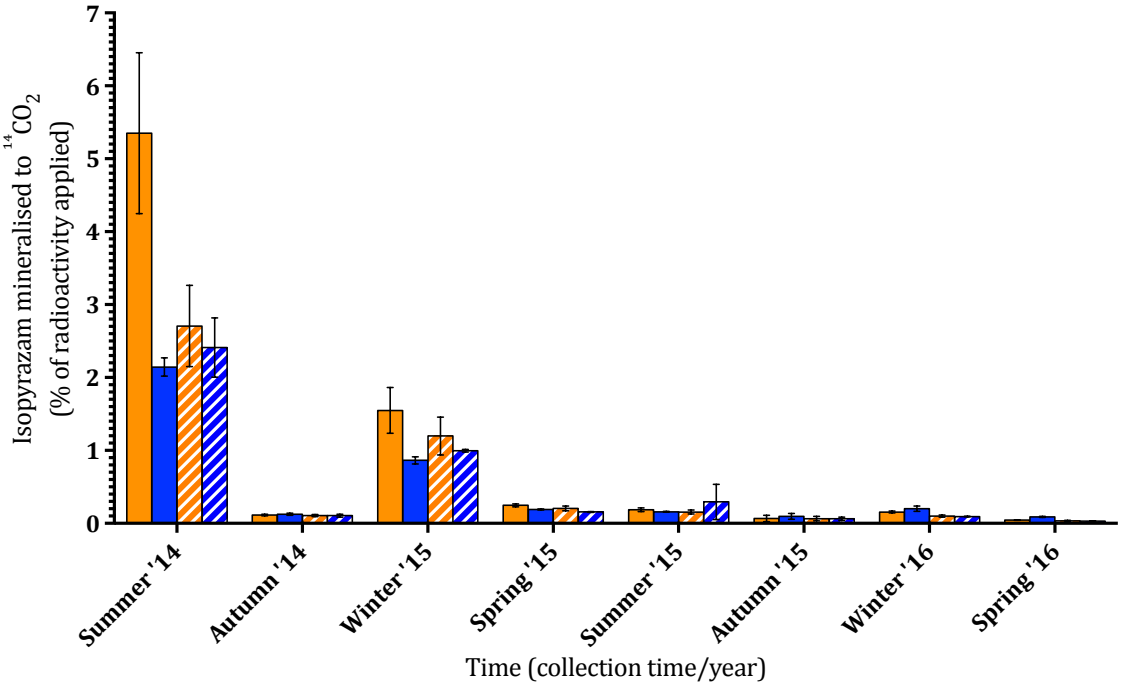

Figure 2.13: Cumulative amount of isopyrazam mineralised to $^{14}CO_2$ as a percentage of the total applied radioactivity. Mineralised $^{14}CO_2$ was captured in NaOH traps throughout the experiment in illuminated water-sediment (solid orange), dark water-sediment (solid blue), illuminated water-only (dashed orange), and dark water-only (dashed blue) microcosms over 36 days at each collection time. Error bars show ± standard deviation.

2.3.3 Water chemistry analysis results

Water NO_3- and PO_4 concentration was measured at each experimental time point and this is outlined in Appendix I.6. Concentrations in the fresh water samples have already been discussed in section 2.3.1. For NO_3- concentration, generally dark water-sediment microcosms contained significantly higher levels compared to fresh samples and the other

treatments. Apart from some exceptions, overall PO_4 concentration was not significantly different between microcosm treatments; however, levels did decrease from the fresh river sample during incubation. This is discussed in more detail in Appendix I.6.

2.3.4 Microbial analysis results

2.3.4.i Chlorophyll a *concentration*

There was a significant impact ($p \leq 0.0001$) of microcosm treatment on the concentration of chlorophyll *a* (**Fig. 2.14** and **2.15**). There was substantial variation in chlorophyll *a* concentration in illuminated systems. In those containing sediment, peak chlorophyll *a* concentrations were between 10.3 and 31.4 µg/L depending on the collection time, whereas in dark water-sediment microcosms, peak concentrations were between 3.8 and 6.6 µg/L. In illuminated water-only systems, chlorophyll *a* concentrations were lower than illuminated water-sediment systems, with peak concentrations between 0.4 and 3.6 µg/L. Similarly, dark water-only microcosms had lower chlorophyll *a* concentrations than dark water-sediment microcosms, with peak concentrations between 0.04 and 0.6 µg/L depending on the collection time.

At all collection times, there was significantly more ($p \leq 0.0001$) chlorophyll *a* present in illuminated water-sediment systems (**Fig. 2.14**) when compared to the dark water-sediment, illuminated water-only, and dark water-only microcosms. At some collection times, illuminated water-only microcosms (**Fig. 2.15**) had significantly more chlorophyll *a* compared to dark water-sediment systems (spring 2015 ($p \leq 0.001$) and summer 2015 ($p \leq 0.0001$)). Despite this, in general illuminated water-only microcosms were not significantly different to the dark water-sediment and dark water-only microcosms.

There was also a significant impact of collection time on the amount of chlorophyll *a* present in the microcosm treatments ($p \leq 0.0001$). A Tukey multiple comparisons test showed that in dark water-sediment, illuminated water-only, and dark water-only microcosms there was not a significant difference in chlorophyll *a* concentration between collection times. In illuminated water-sediment microcosms, however, there was

significantly more chlorophyll *a* in summer and autumn 2014 ($p \leq 0.0001$) than at the other collection times. In summer 2014 and 2015, chlorophyll *a* reached highs of 25.3 and 14.5 µg/L, respectively, and in autumn 2014 and 2015 between 31.4 and 16.4 µg/L, respectively. Other collection times were more variable, but there was also significantly more chlorophyll *a* in summer and autumn 2015 when compared to spring 2016 ($p \leq 0.01$), in which chlorophyll *a* peaked at only 11.4 µg/L during the time course. There was no effect of either light or sediment addition on water bacteria concentration and details can be found in Appendix I.6.

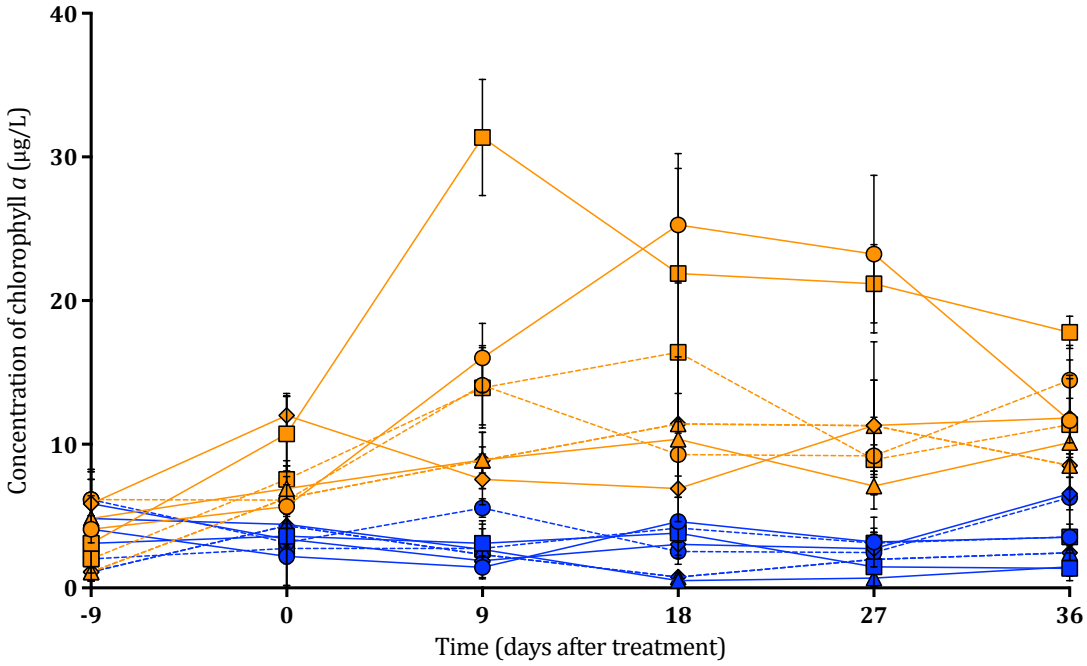

Figure 2.14: Concentration of chlorophyll *a* in the water and sediment in water-sediment microcosms. Chlorophyll *a* was extracted from both the water and the sediment using acetone and then the totals summed together in illuminated water-sediment (orange) and dark water-sediment (blue) microcosms over 36 days in summer (circles), autumn (squares), winter (triangles), and spring (diamonds). The first year of each collection time was denoted by a solid line and the second year by a dashed line. Error bars show ± standard deviation.

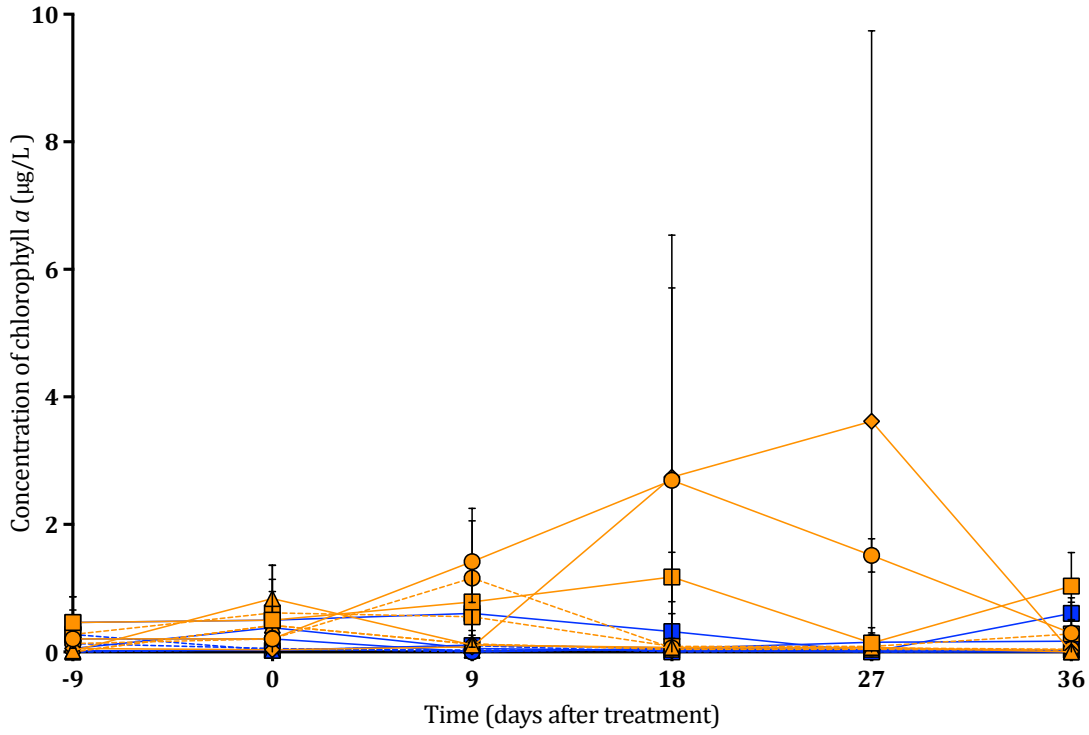

Figure 2.15: Concentration of chlorophyll *a* in the water in water-only microcosms. Chlorophyll *a* was extracted from the water using acetone in illuminated (orange) and dark (blue) water-only microcosms over 36 days in summer (circles), autumn (squares), winter (triangles), and spring (diamonds). The first year of each collection time was denoted by a solid line and the second year by a dashed line. Error bars show ± standard deviation.

2.3.4.ii Microbial community rarefaction

Microbial community data were rarefied before analysis (**Table 2.2**, see section IV.3.8 for details). Bacterial community data were rarefied at 6000 sequences. For the phototroph community data, rarefaction was carried out at 7000 sequences and relative abundance of total OTUs attributed to phototrophs was determined. Non-phototrophs were then removed from the unrarefied data set, leaving 261 samples and 848 OTUs with an average of 5768 sequences per sample; this data was then rarefied at 200 sequences to leave 258 samples and 530 OTUs.

Table 2.2: OTU table summaries for bacterial and phototrophic analysis. Data were rarefied and numbers in italics show the summary post-rarefaction. Phototroph data was rarefied before and after non-phototroph communities were discarded and these are separated by a forward-slash.

OTU table summary	16S rRNA (bacterial)	23S rRNA (phototrophic)
Sample count	267, *264*	267, *265/258*
Number of OTUs across all samples	18,256, *15,800*	6066, *5744/530*
Average sequences/sample	20,786	15996
Rarefaction level	6000	7000/200

2.3.4.iii Bacterial community composition

Alpha diversity (mean species diversity at a local site (Whittaker, 1972)) of the bacterial community was tested at the sample site and in each microcosm at 36 DAT. Although there were some differences in α diversity between collection times (full breakdown of results is shown in Appendix I.6), the general trend from pooled data is shown in **Figure 2.16**. Fresh water samples had a significantly higher α diversity (748.0) compared to water in the microcosms at 36 DAT ($p \leq 0.0001$, except $p \leq 0.01$ for dark water-sediment microcosms). The fresh sediment, however, only had a significantly higher α diversity (924.5) compared to the sediment in illuminated systems at 36 DAT ($p \leq 0.0001$, 463,1), and there was no significant difference compared to the dark microcosms (780.3).

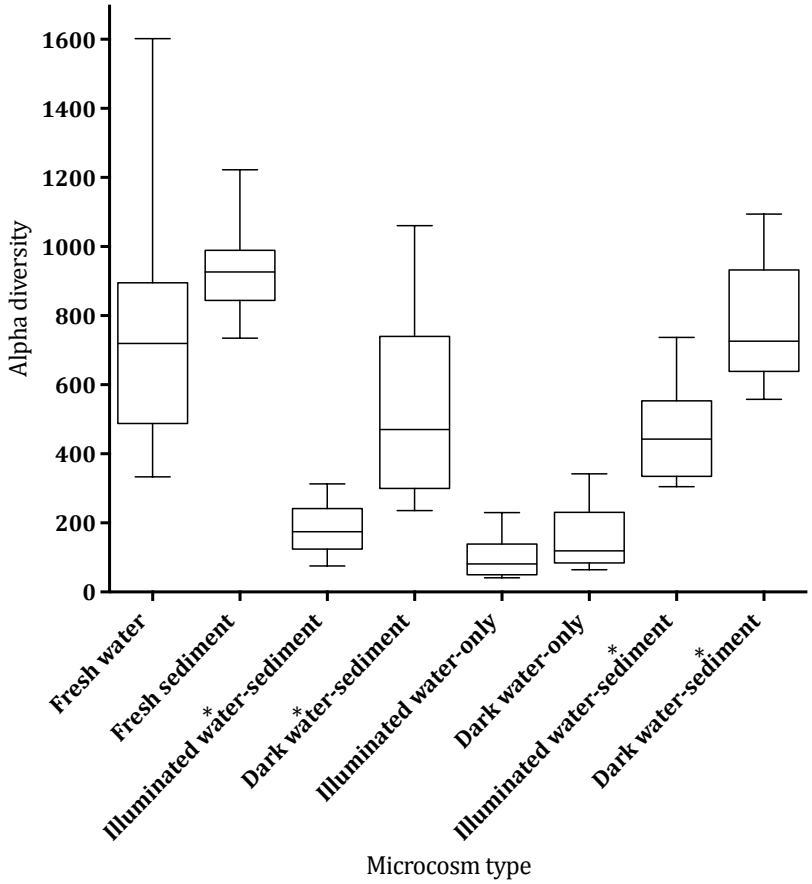

Figure 2.16: Alpha diversity of bacterial communities in the different microcosm treatments. Fisher's α index was calculated from the observed bacterial species in fresh water and sediment, illuminated water-sediment, dark water-sediment, illuminated water-only, and dark water-only microcosms. Whiskers show the minimum and maximum values, middle lines the median values, and * over *water* or *sediment* in the water-sediment systems indicates the sample type.

In both the water and the sediment fractions at 36 DAT, dark water-sediment microcosms had a significantly higher α diversity (541.5 and 1094.4 in the water and sediment, respectively) compared to illuminated water-sediment, illuminated water-only, and dark water-only microcosms ($p \leq 0.0001$). In the water fraction, illuminated water-sediment, illuminated water-only, and dark water-only microcosms were not significantly different to each other. The sediment α diversities in the illuminated and dark water-sediment microcosms were also significantly higher ($p \leq 0.0001$, 734.0 and 1094.4, respectively) compared to the illuminated and dark water-only microcosm water fractions (104.1 and 162.3, respectively).

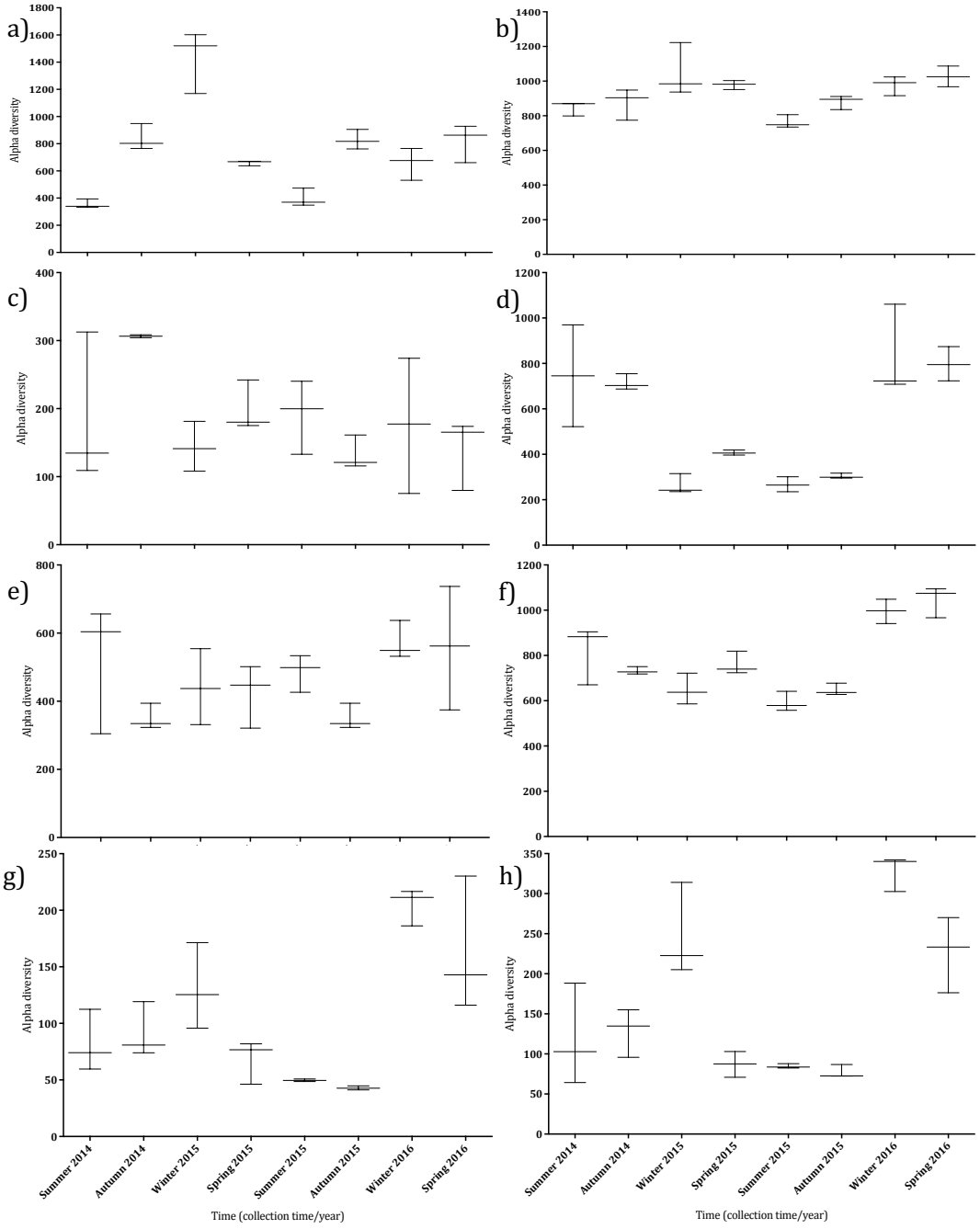

Figure 2.17: Alpha diversity of bacterial communities between collection times at the sample site and at 36 DAT. Fisher's α index was calculated from the observed bacterial species in fresh water (a), fresh sediment (b), the water in illuminated water-sediment (c) and dark water-sediment (d) microcosms, the sediment in illuminated water-sediment (e) and dark water-sediment (f) microcosms, and in illuminated water-only (g) and dark water-only (h) microcosms. Whiskers show minimum and maximum values and middle lines the median values.

There was a significant impact of collection time on α diversity in both the fresh water ($p \leq 0.0001$) and sediment ($p \leq 0.0027$) at the sample site. This was more variable in the water samples than in the sediment samples (**Fig. 2.17.a** and **2.17.b**). In the water, winter 2015 had an α diversity of 1430.6 and this was significantly higher compared to all other collection times ($p \leq 0.001$). In addition, summer 2014 and 2015 had α diversities of 255.7 and 397.1, respectively, and these were significantly lower when compared to autumn 2014, autumn 2015, and spring 2016 ($p \leq 0.01$). In the sediment, although collection time had a significant impact on the α diversity, a Tukey multiple comparisons test showed that only summer 2015 had a significantly lower α diversity compared to winter and spring collection times ($p \leq 0.05$).

In illuminated water-sediment systems at 36 DAT (**Fig. 2.17.c** and **2.17.e**), there was no significant difference in α diversity in either the water ($p \leq 0.0722$) or the sediment ($p \leq 0.1535$) between collection times. Alpha diversity ranged between 132.6 and 306.4 in the water and 350.6 and 572.9 in the sediment. In the dark water-sediment microcosms at 36 DAT (**Fig. 2.17.d** and **2.17.f**), there was a significant impact of collection time ($p \leq 0.0001$) on α diversity in both the water and the sediment. In the water, summer and autumn 2014 and winter and spring 2016 α diversities were not significantly different to each other, ranging between 715.0 and 830.8. Generally, α diversities at these collection times were significantly higher than the remaining collection times ($p \leq 0.001$), which ranged between 264.2 and 407.3. In the sediment, α diversities ranged between 579.1 and 1094.3 and winter 2016 and spring 2016 had significantly higher α diversities ($p \leq 0.01$, 941.2 and 1094.4) compared to all other collection times, except summer 2014. Additionally, summer 2014 had a significantly higher ($p \leq 0.05$, 904.7) α diversity when compared to summer 2015 (579.1).

In illuminated water-only microcosms at 36 DAT (**Fig. 2.17.g**), there was a significant impact ($p \leq 0.0001$) of collection time on α diversity. Winter 2016 had the highest α diversity (204.7) and this was significantly higher ($p \leq 0.001$) compared to summer and autumn collection times and spring 2015, which ranged between 42.9 and 91.4. Alpha diversity in Winter 2015 (130.9) and spring 2016 (163.1) was significantly higher compared to a number of other collection times, most notably autumn 2015 ($p \leq 0.05$, 42.9). Finally, α diversity was also significantly impacted ($p \leq 0.0001$) by collection time in dark water-only microcosms at 36 DAT (**Fig. 3.17.h**). Winter 2015 (247.3), winter 2016 (328.3), and spring

2016 (226.6) had the highest α diversities, and α diversity in the winter collection times was significantly higher ($p \leq 0.05$) compared to the remaining collection times. Alpha diversity in Spring 2016 was only significantly higher compared to spring 2015, summer 2015, and autumn 2015 ($p \leq 0.05$).

Beta diversity (difference in species diversity between sites (Whittaker, 1972)) of the bacterial community was compared across collection times and microcosm treatments at 36 DAT. There were some differences in β diversity between collection times (full breakdown of results is shown in Appendix I.6); however, the general trend from pooled data is shown in **Figure 2.18** – each point in an NMDS ordination plot is a sample and the closer two samples are the more similar the diversities. These trends are not always clear in the data shown in Appendix I.6, as the effect is not as obvious with only three replicates. This means that although the overall PERMANOVA stated significance, pairwise tests did not.

There was a significant effect of microcosm treatment on β diversity ($p \leq 0.001$). R^2 values, however, were low (< 0.5), which showed low dissimilarity overall. In the water fraction (**Fig. 2.18.a**), fresh samples (orange) clustered closely, suggesting that the samples were similar regardless of collection time. At 36 DAT, samples clustered depending on treatment, especially the respective light treatments (red and green for illuminated and blue and pink for dark). This shows that samples were similar within treatments. Pairwise tests showed significant differences ($p \leq 0.028$) in β diversity between treatments, except between the illuminated water-sediment (red) and illuminated water-only (green) microcosm water fractions ($p \leq 0.056$); this is evident from **Figure 2.18.a** in which these samples cluster closely. Pairwise tests show significant differences in β diversity between microcosm treatments in the sediment fraction ($p \leq 0.028$). In particular, there was less divergence of the dark samples (blue) and the fresh samples (orange) compared to the illuminated samples (red) (**Fig. 2.18.b**), suggesting dark treatment samples were more similar to the fresh samples.

In fresh samples (**Fig. 2.19**), there were significant differences in β diversity ($p \leq 0.001$) between collection times and R^2 values were high (0.88 and 0.74 in water and sediment, respectively) showing high dissimilarity between collection times. Pairwise tests showed no significant differences in β diversity between individual collection time

comparisons (mainly $p \leq 0.1$). Beta diversity in the water (triangles) was more variable than the sediment (circles) (R^2 generally > 0.7 in the water, yet < 0.5 in the sediment); this is evident from the sediment samples clustering more closely together and the water samples having a bigger spread (**Fig. 2.19**). Although there was clear distinction between the water (triangles) and sediment (circles) samples, samples were 50 % similar within the two compartments despite being sampled at different times of year.

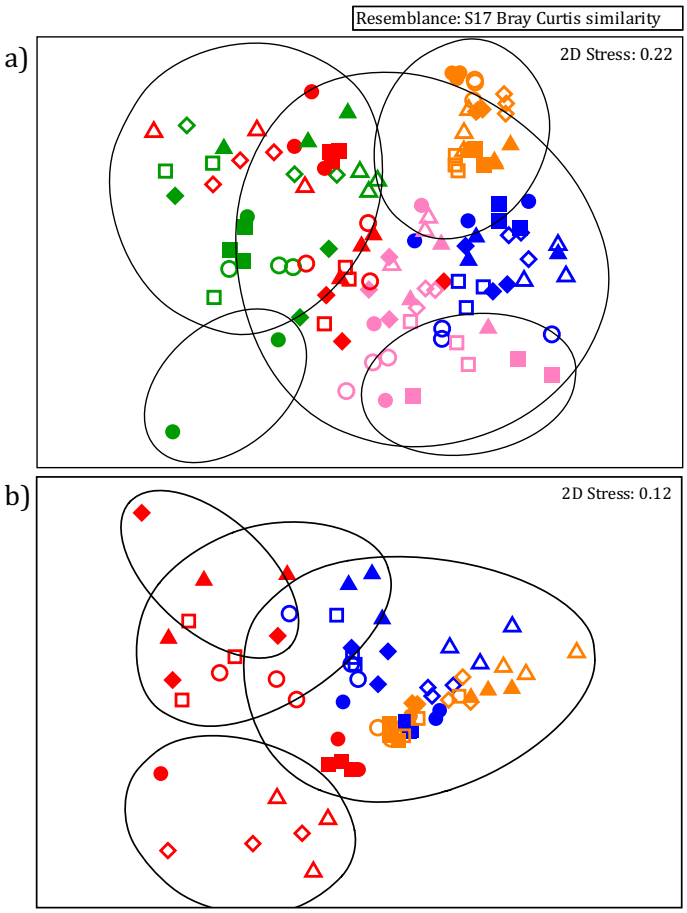

Figure 2.18: Ordination plots from NMDS scaling analysis of Bray Curtis similarities for bacterial communities between treatments. Water (a) and sediment (b) were analysed and comparisons made between fresh samples (orange), and samples from illuminated water-sediment (red), dark water-sediment (blue), illuminated water-only (green), and dark water-only (pink) microcosms. Samples were taken in summer (circles), autumn (squares), winter (triangles), and spring (diamonds), with the first year of each collection time denoted by closed symbols and the second year by open symbols. Black lines show 25 % similarity in (a) or 50 % similarity in (b).

In the microcosms at 36 DAT, PERMANOVA showed significant differences between collection times in all treatments ($p \leq 0.001$, **Fig. 2.20**) with higher R^2 values (> 0.68) in water-sediment microcosms than in water-only microcosms (< 0.6), showing the former had higher dissimilarity between collection times. For all treatments, pairwise tests showed no significant differences between any comparison ($p \geq 0.1$) and, apart from a few individual comparisons in water-sediment treatments, R^2 values were generally low. In water-sediment microcosms (**Fig. 2.20.a** and **2.20.b**), sediment (circles) samples tended to cluster more closely and were less variable than the water samples (triangles), showing that sediment samples were similar regardless of collection time. In water microcosms (**Fig. 2.20.c** and **2.20.d**), generally summer (red) and autumn (blue) samples clustered together and winter (green) and spring (pink) samples together, suggesting that diversity was similar in these respective collection times.

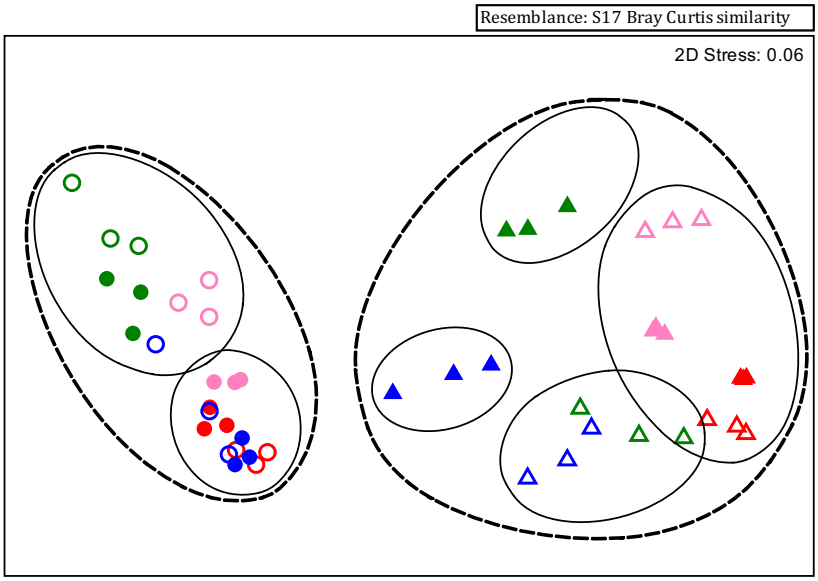

Figure 2.19: Ordination plots from NMDS scaling analysis of Bray Curtis similarities for fresh sample site bacterial communities between collection times. Water (triangles) and sediment (circles) were analysed and comparisons made between summer (red), autumn (blue), winter (green), and spring (pink), with the first year of each collection time denoted by closed symbols and the second year by open symbols. Solid black lines show 60 % similarity and dashed black lines show 50 % similarity.

Relative abundance of bacterial phyla at the sample site and in each treatment at 36 DAT was analysed. Pooled data for each treatment is shown in **Figure 2.21**; however, there were some differences between collection times and the full breakdown of results is shown in Appendix I.6. There was a significant difference in bacterial phyla between treatments ($p \leq 0.0001$). The majority of the relative abundance consisted of Proteobacteria

across all samples. Apart from the two water-sediment microcosms (61.9 and 65.2 % in illuminated and dark, respectively), Proteobacteria relative abundance was significantly different between all treatments ($p \leq 0.0001$) ranging between 33.9 and 65.2 %. Compared to microcosms at 36 DAT, fresh samples had a significantly higher ($p \leq 0.0001$) relative abundance of Actinobacteria in both the water (28.0 %) and the sediment (16.9 %) and of Bacteroidetes in the water (16.0 %)

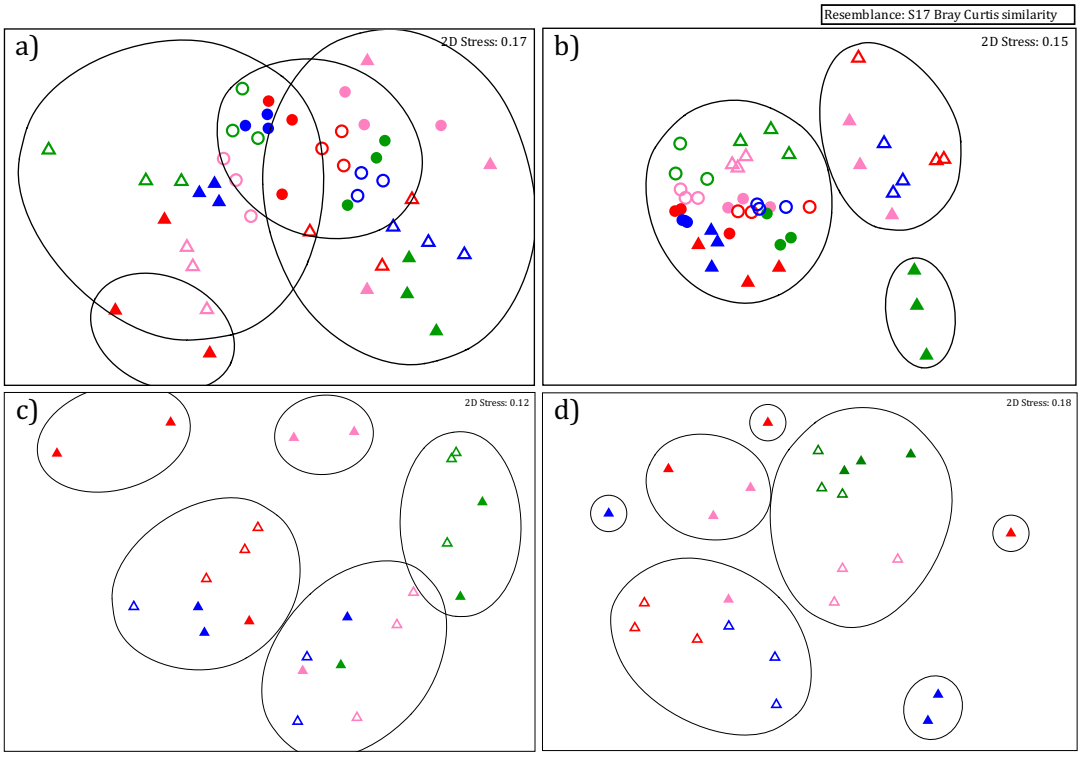

Figure 2.20: Ordination plots from NMDS scaling analysis of Bray Curtis similarities for microcosm bacterial communities at 36 DAT. Water (triangles) and sediment (circles) were analysed in illuminated water-sediment (a), dark water-sediment (b), illuminated water-only (c), and dark water-only (d) microcosms, and comparisons made between summer (red), autumn (blue), winter (green), and spring (pink). The first year of each collection time is denoted by closed symbols and the second year by open symbols. Black lines show 30 % similarity in (a) or 40 % similarity in (b), (c), and (d).

Dark microcosms had significantly higher relative abundances ($p \leq 0.001$) of Actinobacteria in the water fraction (13.2 and 16.0 % in water-sediment and water-only microcosms, respectively) compared to the illuminated microcosms (8.2 and 7.2 % in water-sediment and water-only microcosms, respectively). Additionally, in the sediment fraction, dark microcosms had significantly higher ($p \leq 0.0001$) relative abundances of both Actinobacteria and Chloroflexi (15.0 and 9.8 %, respectively) compared to illuminated systems (11.5 and 6.0 %, respectively). Illuminated microcosms had significantly higher (p

≤ 0.0001) relative abundances of Cyanobacteria in the water (22.0 and 17.8 % in water-sediment and water-only microcosms, respectively) and the sediment (14.0 %) compared to both fresh samples and dark microcosm samples.

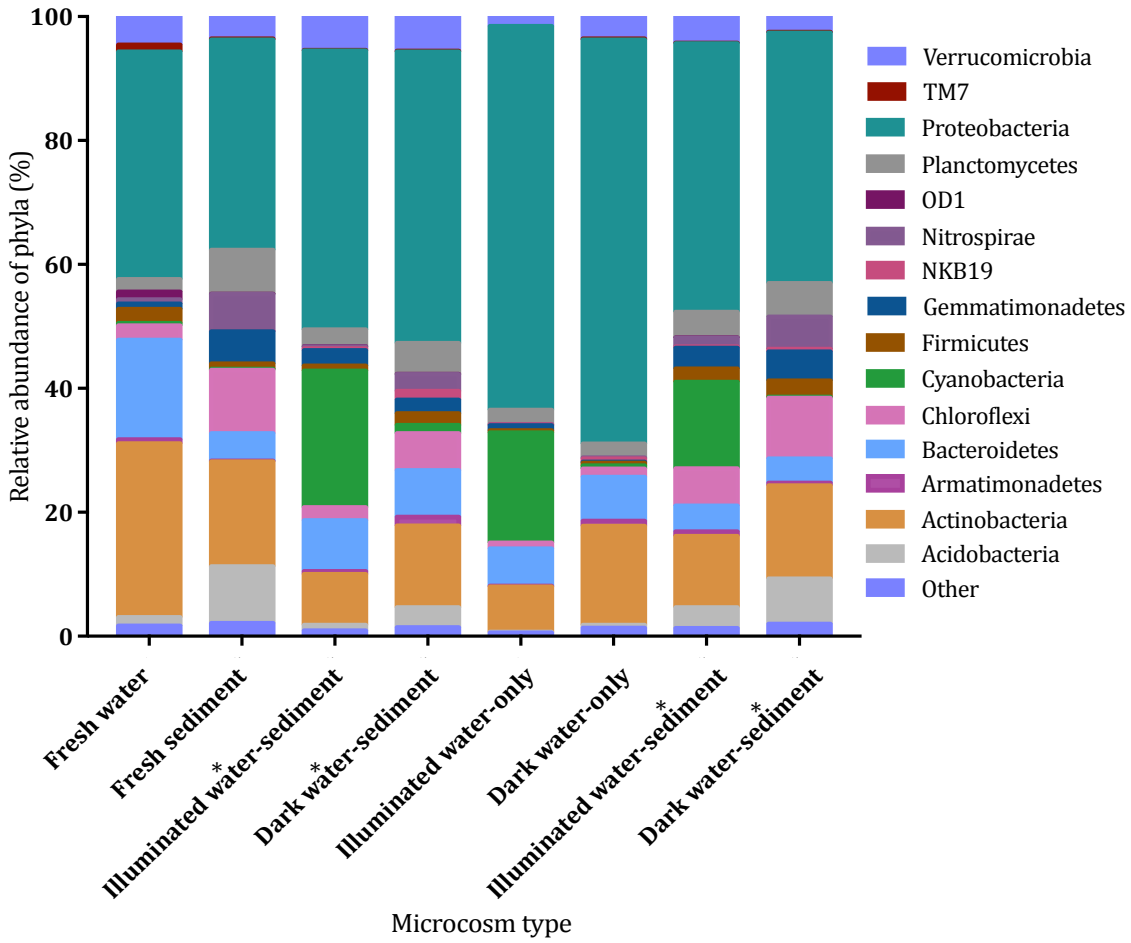

Figure 2.21: Relative abundance of bacterial phyla between fresh samples and different microcosm treatments in water and sediment. Different bacterial phyla are denoted by different colours and phyla making up < 1 % of the relative abundance are listed under *other*. Analysis was carried out on fresh river samples and at 36 DAT on both water and sediment samples. * over *water* or *sediment* in the water-sediment systems indicates the sample type.

In the dark, water from water-sediment microcosms (2.2 %) had higher relative abundances ($p \leq 0.05$) of Gemmatimonadetes compared to water microcosms (0.2 %). In the illuminated treatments, however, water-sediment microcosms (22.0 %) had significantly higher ($p \leq 0.001$) relative abundances of Cyanobacteria in the water compared to water-only microcosms (17.8 %). Overall, water-only microcosms had lower relative abundances ($p \leq 0.05$) of Firmicutes (0.4 %) compared to the fresh river water (2.3 %). Illuminated water-only microcosms (1.6 %) had a lower relative abundance of Verrucomicrobia

compared to water-sediment ($p \leq 0.0001$) and dark water-only microcosms ($p \leq 0.05$). Dark water-sediment microcosms had a wider range of phyla making up larger proportions of the bacterial relative abundance in the water fraction compared to illuminated water-sediment, illuminated water-only, and dark water-only microcosms at 36 DAT. In the water fraction, dark water-sediment microcosms had higher relative abundances of Nitrospirae ($p \leq 0.05$, 2.3 %), Planctomycetes ($p \leq 0.0001$, 5.0 %), and Chloroflexi ($p \leq 0.0001$, 6.0 %) compared to other treatments and, in the sediment, higher relative abundances of Nitrospirae ($p \leq 0.0001$, 5.2 %) compared to illuminated water-sediment microcosms (1.4 %).

For each microcosm treatment, there was a significant effect of collection time on the relative abundance of bacterial phyla for both the water and the sediment ($p \leq 0.0001$). Generally, there was more variation in illuminated microcosms than in the dark (**Fig. 2.22**). In the fresh samples from the river, although there was significant variation over time ($p \leq 0.0001$), generally, in terms of the phyla present, the community was stable. The fresh water samples (**Fig. 2.22.a**) were more variable than the sediment (**Fig. 2.22.b**), and Proteobacteria, Bacteroidetes, and Actinobacteria dominated the relative abundance. Except for a few individual comparisons, relative abundance of these three phyla were significantly different between collection times ($p \leq 0.0001$). There was additionally significant ($p \leq 0.05$) variation between Chloroflexi (0.5 to 4.8 %), Planctomycetes (0.5 to 4.8 %), and Verrucomicrobia (2.6 to 12.7 %) between collection times.

In autumn 2014 fresh water (**Fig. 2.22.a**), Acidobacteria, Gemmatimonadetes, and Nitrospirae reached 5.0, 2.6, and 2.3 %, respectively, and these relative abundances were significantly higher than all other collection times ($p \leq 0.0001$). Armatimonadetes reached 3.7 % in summer 2015 and this was significantly higher compared to other collection times ($p \leq 0.05$). Lastly, TM7 relative abundance was significantly higher in winter 2015 and spring 2016 (2.7 and 3.3 %, respectively) than the other collection times ($p \leq 0.0001$). The sediment fraction (**Fig. 2.22.b**) was a lot less variable over time and relative abundance was dominated by Proteobacteria (29.9 to 37.9 %) and a number of other phyla making up smaller percentages of the relative abundance, such as, Actinobacteria (12.0 to 26.3 %), Acidobacteria (8.0 to 10.7 %), Chloroflexi (7.6 to 15.3 %), Nitrospirae (4.0 to 8.2 %), Planctomycetes (5.6 to 9.5 %), and Bacteroidetes (1.7 to 5.7). Between collection times, these phyla were very variable, but most of the comparisons across sampling times revealed

significant differences in relative abundances ($p \leq 0.0001$). In particular, relative to other collection times, Gemmatimonadetes had a significantly lower relative abundance in spring 2016 ($p \leq 0.0001$, 4.0 %), Firmicutes were significantly higher in winter 2015 ($p \leq 0.0001$, 2.0 %), and Verrucomicrobia significantly higher in spring 2015 ($p \leq 0.01$, 5.7 %).

In illuminated water-sediment microcosms (**Fig. 2.22.c** and **Fig. 2.22.e**), Proteobacteria dominated in both the water ($p \leq 0.01$, 31.4 to 54.8 %) and the sediment ($p \leq 0.0001$, 32.2 to 55.3 %) fractions and this significantly varied between the majority of collection times. Cyanobacteria proliferated in a number of collection times, but this was variable and significantly ($p \leq 0.0001$) different between collection times in both water (0.04 to 42.6 %) and sediment (0.06 to 32.6 %). In particular, relative abundance in the water and the sediment fraction in winter 2015 (0.04 and 0.07 %), summer 2015 (7.9 and 2.8 %), and autumn 2015 (2.1 and 0.06 %) were low.

In the water fraction (**Fig. 2.22.c**), Actinobacteria relative abundance varied (6.5 to 11.3 %) and was significantly higher ($p \leq 0.05$) in summer 2014 (10.7 %) and winter 2015 (11.3 %) compared to winter 2016 (6.6 %). Bacteroidetes relative abundance also varied (2.1 to 17.4 %) and was significantly higher ($p \leq 0.001$) in winter 2015 (17.4 %) and autumn 2015 (15.7 %) and significantly lower in winter 2016 (2.1 %) compared to the majority of other collection times. Furthermore, compared to other collection times, Chloroflexi relative abundance was higher in autumn 2015 ($p \leq 0.05$, 5.6 %), Verrucomicrobia relative abundance higher ($p \leq 0.0001$) in winter 2015 (10.7 %) and autumn 2015 (10.7 %), and Planctomycetes relative abundance higher in autumn 2014 ($p \leq 0.01$, 9.1 %). In the sediment fraction (**Fig. 2.22.e**), Actinobacteria (7.4 to 14.4 %), Bacteroidetes (1.8 to 6.7 %), and Chloroflexi (4.5 to 10.5 %) significantly ($p \leq 0.05$) varied between collection times, as did Gemmatimonadetes (1.8 to 5.1 %), Nitrospirae (0.3 to 4.4 %), and Verrucomicrobia (2.0 to 7.5 %). In particular, relative to other collection times, Planctomycetes relative abundance was significantly higher ($p \leq 0.0001$) in summer and autumn 2014 (6.2 and 8.9 %, respectively) and Firmicutes relative abundance significantly higher ($p \leq 0.05$) in winter 2015 (5.9 %).

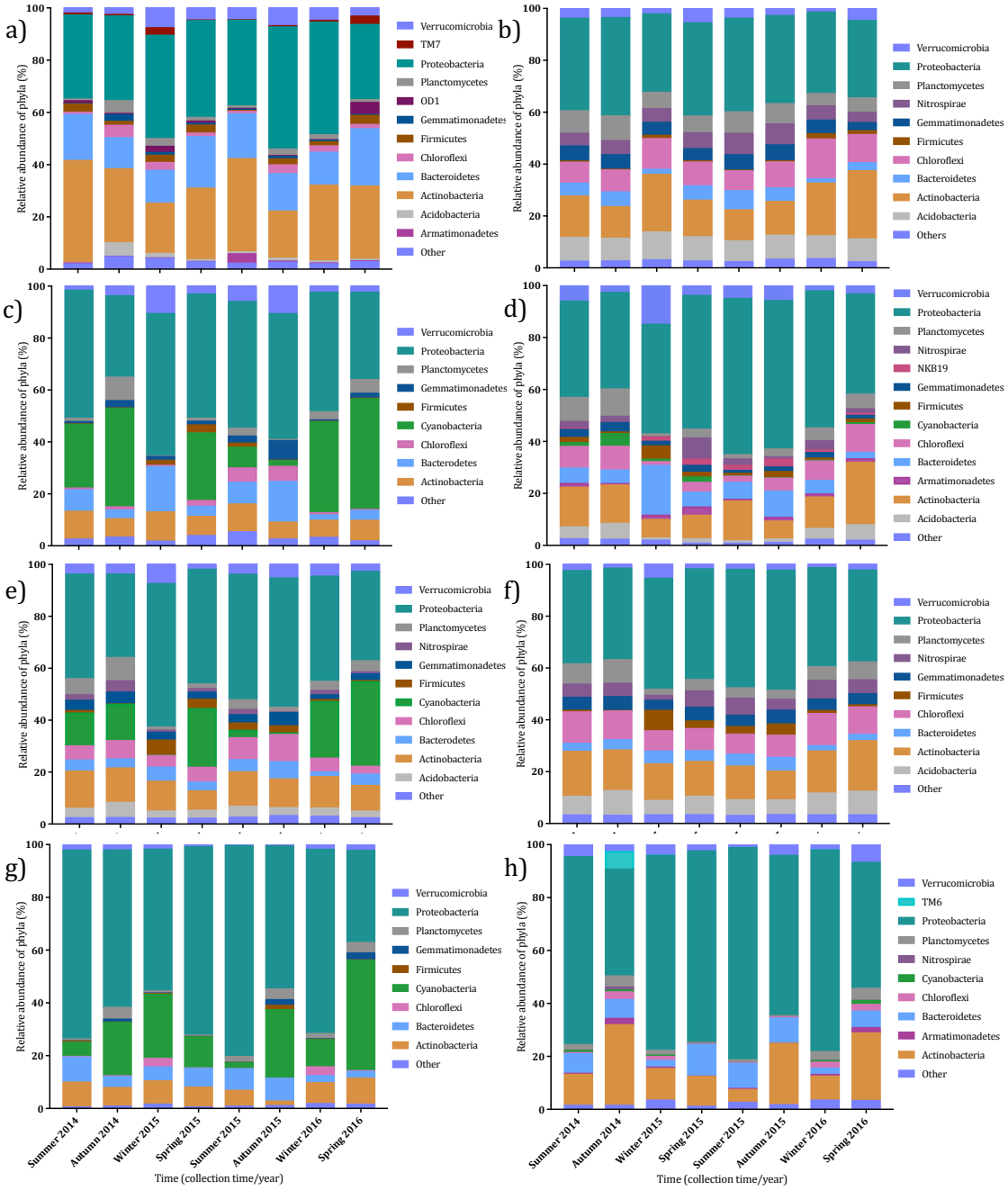

Figure 2.22: Relative abundance of bacterial phyla between collection times at the sample site and at 36 DAT. Different bacterial phyla are denoted by different colours and phyla making up < 1 % of the relative abundance are listed under *other*. Analysis was carried out at the sample site and at 36 DAT on fresh water (a) and sediment (b), water in illuminated (c) and dark (d) water-sediment microcosms, sediment in illuminated (e) and dark (f) water-sediment microcosms, and water in illuminated (g) and dark (h) water-only microcosms.

In the dark water-sediment microcosms (**Fig. 2.22.d** and **2.22.f**), there was less variation between collection times, especially in the sediment fraction. Although there was variation in bacterial community relative abundance over time, generally, similar phyla were present regardless of collection time. Proteobacteria dominated the relative abundance in both the water (35.3 to 46.4 %) and the sediment (37.0 to 60.1 %) fractions, although relative abundance varied significantly ($p \leq 0.0001$) between collection times. In the water fraction (**Fig. 2.22.d**), Actinobacteria relative abundance (7.0 to 24.0 %) was highly significantly different ($p \leq 0.0001$) between collection times. Relative abundances of Acidobacteria (0.9 to 6.1 %), Chloroflexi (1.5 to 10.7 %), and Planctomycetes (1.7 to 10.5 %) also significantly varied between collection times ($p \leq 0.05$). Compared to other collection times, relative abundance of Bacteroidetes was significantly higher in winter 2015 ($p \leq 0.001$, 19.1 %) and autumn 2015 ($p \leq 0.01$, 10.1 %), Firmicutes ($p \leq 0.05$, 5.1 %) and Verrucomicrobia ($p \leq 0.001$, 15.0 %) significantly higher in winter 2015, Nitrospirae significantly higher in spring 2015 ($p \leq 0.0001$, 8.2 %), and Cyanobacteria significantly higher in autumn 2014 ($p \leq 0.05$, 4.9 %). In the sediment fraction (**Fig. 2.22.f**), Actinobacteria (11.1 to 19.5 %), Acidobacteria (5.5 to 9.5 %), Chloroflexi (7.7 to 12.4 %), and Firmicutes (0.2 to 7.9 %) varied significantly ($p \leq 0.05$) between collection times. Compared to other collection times, Bacteroidetes relative abundance was significantly lower ($p \leq 0.05$) in winter 2016 (2.0 %) and spring 2016 (2.4 %), Nitrospirae significantly lower ($p \leq 0.01$) in winter 2015 (1.9 %), and Verrucomicrobia relative abundance significantly higher ($p \leq 0.0001$) in winter 2015 (5.5 %).

Water-only microcosms (**Fig. 2.22.g** and **2.22.h**) supported a lower number of phyla present at relative abundances > 1 %. Proteobacteria dominated the systems in both illuminated and dark treatments and varied significantly ($p \leq 0.0001$) between collection times (35.0 to 79.9 % and 40.4 to 80.2 % in illuminated and dark, respectively). In the illuminated microcosms (**Fig. 2.22.g**), relative abundance of Cyanobacteria varied significantly ($p \leq 0.0001$) between collection times (2.3 to 41.8 %), as did Bacteroidetes (2.6 to 9.5 %) and Actinobacteria (1.7 to 9.9 %) relative abundances ($p \leq 0.05$). In dark water-only microcosms (**Fig. 2.22.h**), Actinobacteria relative abundance (4.9 to 30.5 %) varied significantly ($p \leq 0.0001$) between collection times, as did Bacteroidetes (2.5 to 12.0 %), Verrucomicrobia (1.2 to 6.9 %), and Planctomycetes (0.4 to 4.6 %) relative abundances ($p \leq$

0.05). Lastly, TM6 relative abundance was significantly higher ($p \leq 0.0001$) in autumn 2014 (6.6 %) compared to other collection times (< 1 %).

2.3.4.iv Phototrophic community composition

Alpha diversity of the phototrophic communities was compared across the collection times and in each microcosm at 36 DAT. Phototrophic communities were more variable than the bacterial communities and the full breakdown of data can be found in Appendix I.6; however, the pooled data for the different microcosm treatments is shown in **Figure 2.23**. Fresh water samples had a significantly higher ($p \leq 0.0001$, 38.7) α diversity compared to the water in the microcosms at 36 DAT (12.3 to 18.9). Fresh sediment, on the other hand, only had a significantly higher ($p \leq 0.0001$, 26.9) α diversity compared to sediment from illuminated water-sediment microcosms at 36 DAT (15.9), and there was no significant difference in α diversity compared to dark water-sediment microcosms (21.4). At 36 DAT, water in dark water-sediment microcosm had a significantly higher α diversity ($p \leq 0.05$, 18.9) compared to water in illuminated water-sediment microcosms (12.3), but there was no significant difference compared to the water-only microcosms (13.3 and 13.1 in illuminated and dark water-only microcosms, respectively). It should be noted, that the phototrophic communities in the dark treatments will likely be dormant (e.g. low chlorophyll *a* concentration in **Fig. 2.14** and **2.15**). There was also no significant difference in sediment α diversity at 36 DAT between illuminated (15.9) or dark (21.4) water-sediment microcosms.

Within treatments, there was a significant difference in α diversity between collection times in both the water ($p \leq 0.0001$) and the sediment ($p \leq 0.0065$). Fresh water from the sample site (**Fig. 2.24.a**) had a significantly (mainly $p \leq 0.01$) higher α diversity in winter 2015 (55.9), autumn 2015 (47.3), and winter 2016 (49.5) compared to all other collection times (27.1 to 34.5). Fresh sediment at the sample site (**Fig. 2.24.b**) had significantly lower ($p \leq 0.05$) α diversities in winter 2015 (20.6), spring 2015 (24.5), and winter 2016 (23.4) compared to summer 2014 (34.5).

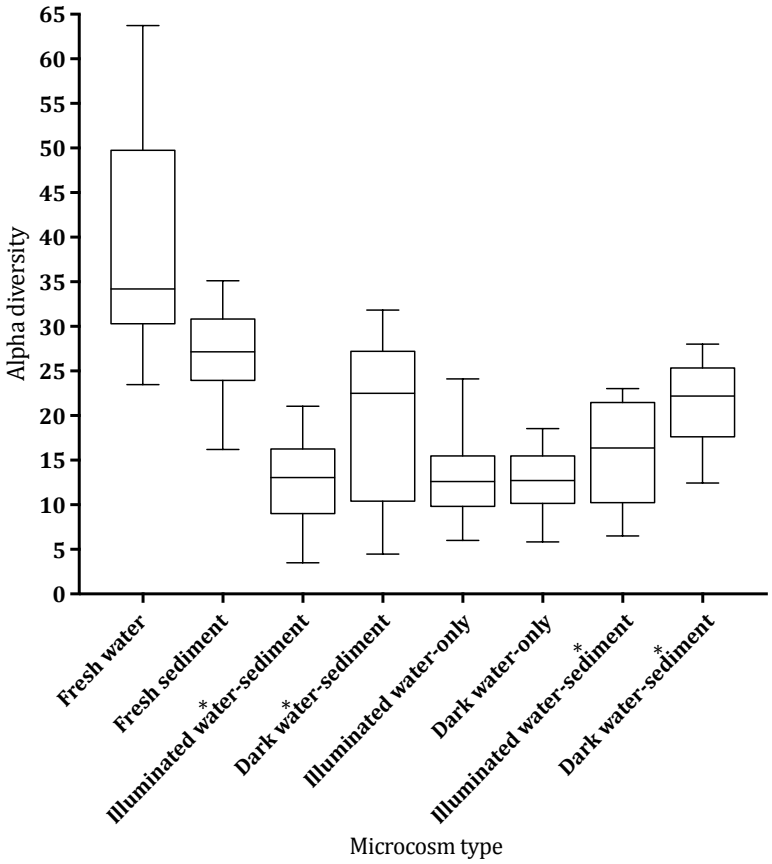

Figure 2.23: Alpha diversity of phototrophic communities in the different microcosm treatments. Fisher's α index was calculated from the observed phototrophic species in fresh water and sediment, illuminated water-sediment, dark water-sediment, illuminated water-only, and dark water-only microcosms. Whiskers show the minimum and maximum values, middle lines the median values, and * over *water* or *sediment* in the water-sediment systems indicates the sample type.

Alpha diversities in illuminated water-sediment microcosms were significantly different between collection times in both the water ($p \leq 0.0061$) and the sediment ($p \leq 0.0001$) fractions at 36 DAT. In the water (**Fig. 2.24.c**), autumn 2014 (17.6) and winter 2016 (16.3) had significantly higher α diversities ($p \leq 0.05$) compared to winter 2015 (3.5) and autumn 2015 (6.1), which had the lowest values. In the sediment (**Fig. 2.24.e**), autumn 2015 (22.1) had a significantly higher α diversity ($p \leq 0.05$) compared to winter 2015 (8.8), spring 2015 (11.6), and autumn 2015 (8.3), with winter 2015 and autumn 2015 having significantly lower ($p \leq 0.05$) α diversities to the majority of other collection times.

In dark water-sediment microcosms, the α diversity in the sediment ranged between 15.8 and 27.3 and there were no significant differences between collection times ($p \leq 0.0601$). In the water, however, there were significant differences in α diversity between collection times ($p \leq 0.0001$, **Fig. 2.24.c**). In the water fraction, winter 2015 had a significantly lower α diversity ($p \leq 0.01$, 6.4) compared to the majority of other collection times. Autumn 2014 (26.6), spring 2016 (28.9), and winter 2015 (25.5) also had significantly higher α diversities ($p \leq 0.05$) compared to spring 2015 (14.3) and autumn 2015 (10.1).

In illuminated water-only microcosms (**Fig. 2.24.g)**, α diversities ranged between 8.3 and 23.8 and there was a significant difference between collection times ($p \leq 0.0031$), with winter 2016 (28.8) having a significantly higher α diversity ($p \leq 0.05$) relative to the majority of other collection times. In dark water-only microcosms (**Fig. 2.24.h**), however, α diversities ranged between 10.8 and 16.0, and there were no significant differences between collection times ($p \leq 0.8309$).

Beta diversity of the phototrophic community was compared for fresh samples at the sample site and between each microcosm treatment at 36 DAT. Full breakdown of the results can be found in Appendix I.6; however, the general trend from pooled data is shown in **Figure 2.25**. There was a significant effect of microcosm treatment on β diversity ($p \leq 0.001$); however, R^2 values were low even between individual comparisons (< 0.29), showing low overall dissimilarity. In both the water (**Fig. 2.25.a**) and the sediment (**Fig. 2.25.b**), fresh samples (orange) had a significantly different β diversity compared to the samples at 36 DAT ($p \leq 0.028$); this suggests divergence in diversity after incubation in the laboratory. In the water at 36 DAT, there was no significant difference between water-sediment and water-only microcosms in both the illuminated ($p \leq 0.056$, red and green) and the dark ($p \leq 0.112$, blue and pink) treatments, showing similarity between samples based on light treatment. There were, however, significant differences ($p \leq 0.028$) in β diversity between water in dark water-only microcosms (pink) and both illuminated treatments (red and green) and between ($p \leq 0.028$) water in dark water-sediment microcosms (blue) and illuminated water-only microcosms (green). Although there were no significant differences in β diversity between the water in the two water-sediment microcosms ($p \leq 0.140$), there were significant differences in β diversity in the sediment fraction ($p \leq 0.028$).

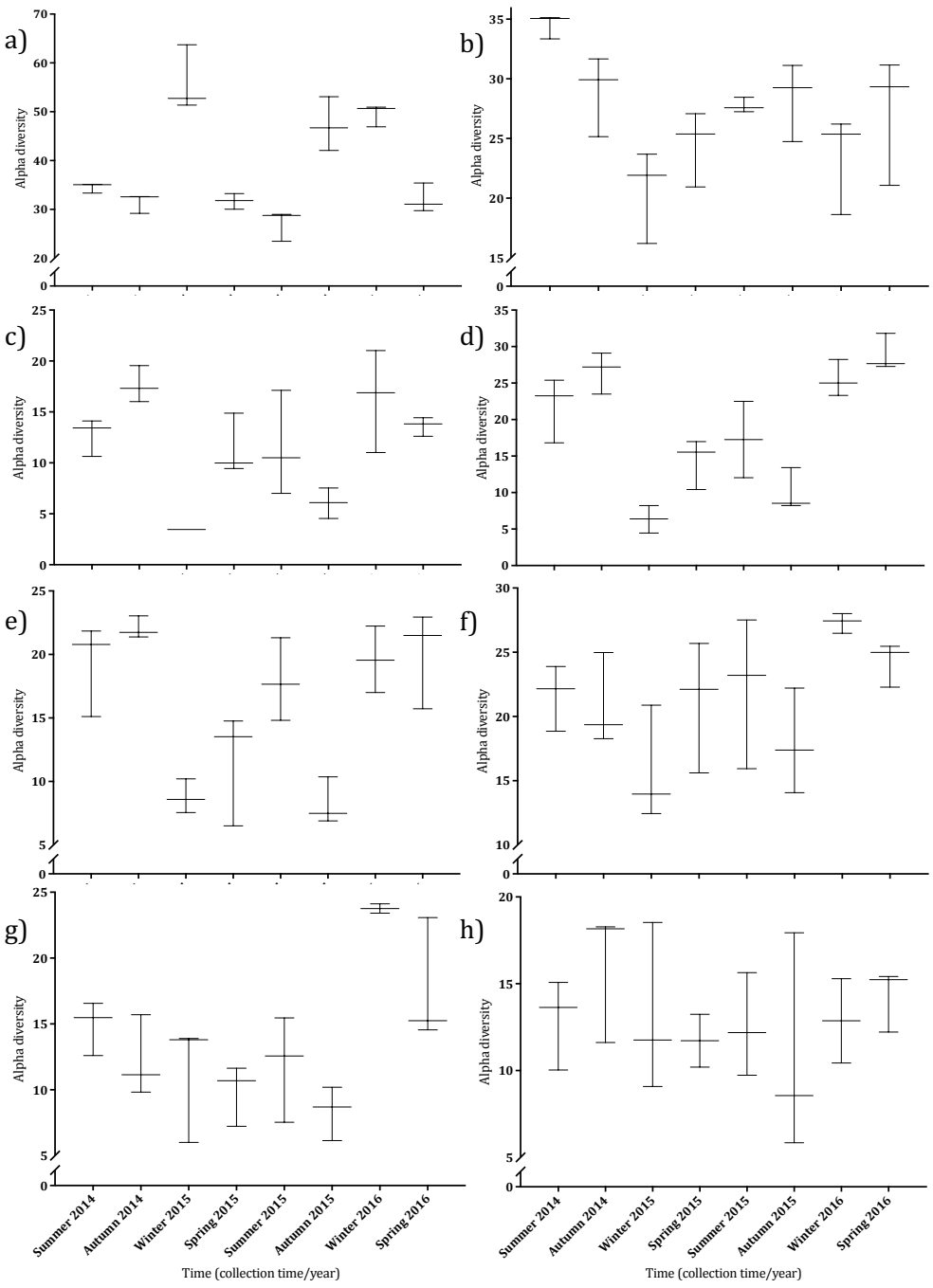

Figure 2.24: Alpha diversity of phototrophic communities between collection times at the sample site and at 36 DAT. Fisher's α index was calculated from the observed phototrophic species in fresh water (a), fresh sediment (b), the water in illuminated water-sediment (c) and dark water-sediment (d) microcosms, the sediment in illuminated water-sediment (e) and dark water sediment (f) microcosms, and in illuminated water-only (g) and dark water-only (h) microcosms. Whiskers show minimum and maximum values and middle lines the median values.

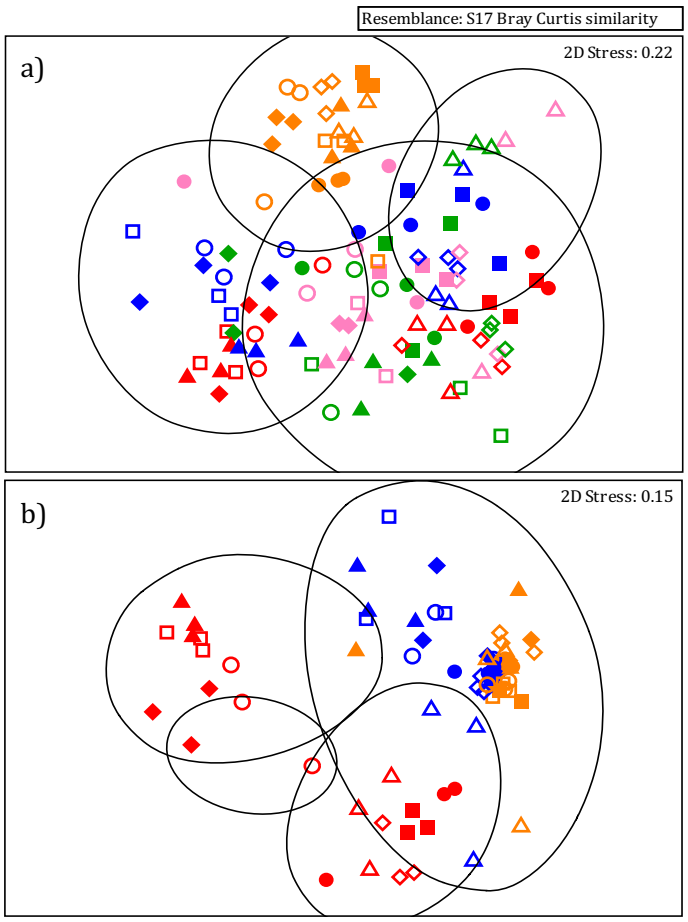

Figure 2.25: Ordination plots from NMDS scaling analysis of Bray Curtis similarities for phototrophic communities between treatments. Water (a) and sediment (b) were analysed and comparisons made between fresh samples (orange), and samples from illuminated water-sediment (red), dark water-sediment (blue), illuminated water-only (green), and dark water-only (pink) microcosms. Samples were taken in summer (circles), autumn (squares), winter (triangles), and spring (diamonds), with the first year of each collection time denoted by closed symbols and the second year by open symbols. Black lines show 10 % similarity in (a) or 15 % similarity in (b).

In fresh samples (**Fig. 2.26**), there was a significant difference in β diversity ($p \leq 0.001$) between collection times and R^2 values were higher in the water fraction (0.76, triangles) but low in the sediment samples (0.48, circles), showing that the water samples were more variable. Pairwise tests, however, showed no significant differences between collection times (mainly $p \leq 0.1$). In the water fraction, R^2 values vary and, in particular, winter 2016 (pink open triangles) had a higher R^2 value (> 0.7) compared to the majority of the other collection times, showing it was more dissimilar. R^2 values in the sediment fraction, however, were lower (generally < 0.5). This is clear from **Figure 2.26**, as sediment samples

cluster closely together with little divergence and with a distinct community compared to the water fraction. This suggests that sediment samples were similar at the sample site regardless of collection time, yet water samples diverged more over time.

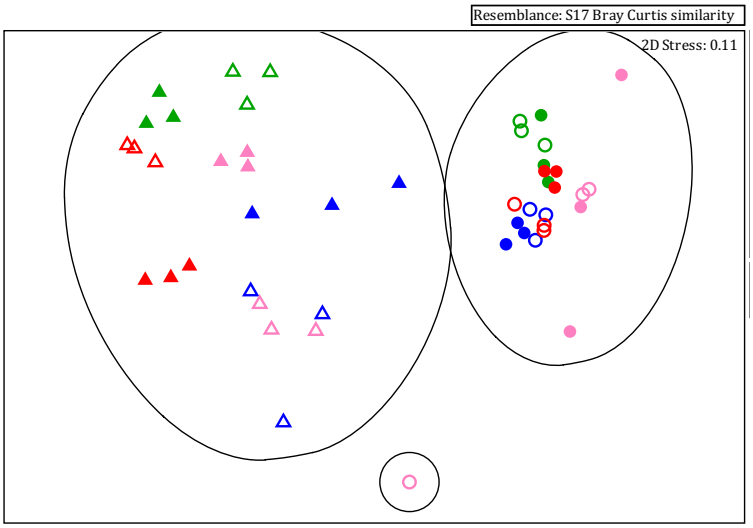

Figure 2.26: Ordination plots from NMDS scaling analysis of Bray Curtis similarities for fresh sample site phototrophic communities between collection times. Water (triangles) and sediment (circles) were analysed and comparisons made between summer (red), autumn (blue), winter (green), and spring (pink), with the first year of each collection time denoted by closed symbols and the second year by open symbols. Solid black lines show 20 % similarity.

In each microcosm at 36 DAT, there was a significant difference ($p \leq 0.001$) in β diversity between collection times. In the water-sediment microcosms, R^2 values were high (> 0.7) suggesting there was high dissimilarly between collection times. In water-only microcosms, however, R^2 values were lower (< 0.6) so there was less variance between collection times. Despite this, in all pairwise tests, there were no significant differences in β diversity between any individual comparisons (mainly $p \leq 0.1$). In illuminated water-sediment microcosms, there were large divergences between collection times (**Fig. 2.27.a**). R^2 values for a number of comparisons were high in the water (> 0.9) and the sediment (> 0.7) fractions, showing dissimilarity between collection times. In dark water-sediment microcosms (**Fig. 2.27.b**), there was higher dissimilarly (> 0.7) when comparing winter 2015 (green closed) to the majority of other collection times and, especially in the sediment, winter 2015 diverges from the other collection times. In both illuminated (**Fig. 2.27.c**) and dark (**Fig. 2.27.d**) water-only microcosms, R^2 values were lower (< 0.5) except for some comparisons for dark water-only microcosms. Additionally, there was more clustering

between summer (red) and autumn (blue) collection times and between winter (green) and spring (pink) collection times; this suggests there was similarity in diversity between these respective collection times.

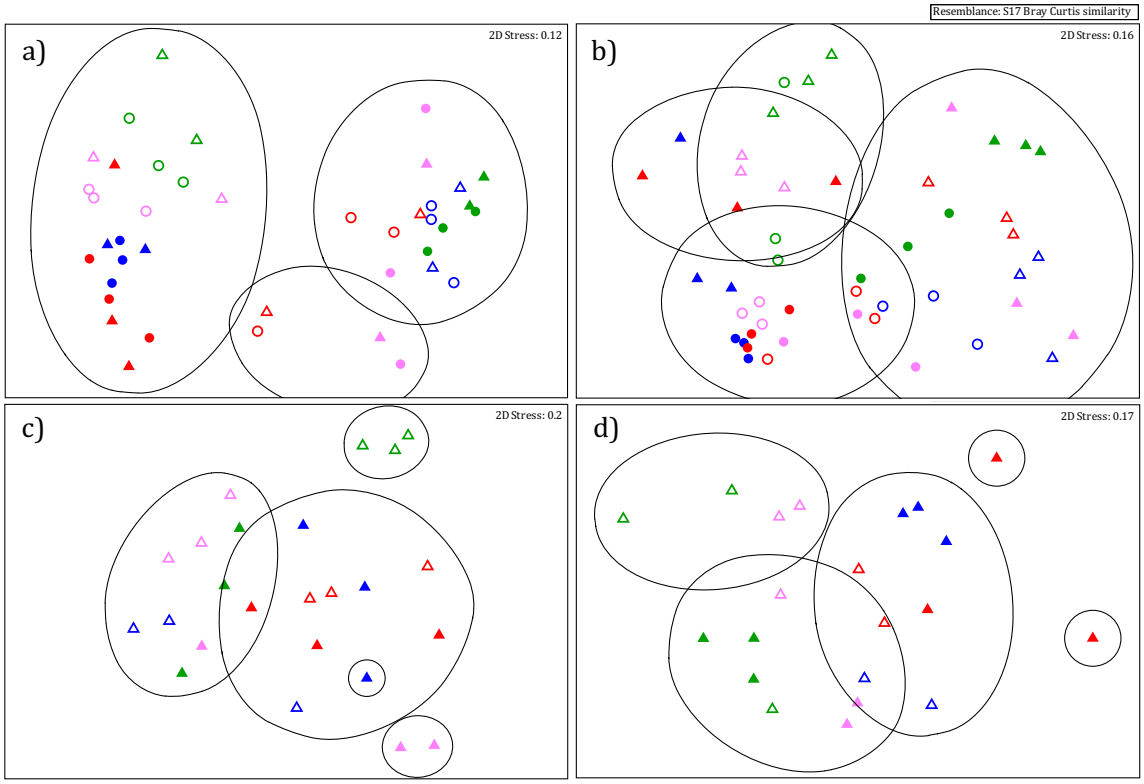

Figure 2.27: Ordination plots from NMDS scaling analysis of Bray Curtis similarities for microcosm phototrophic communities at 36 DAT. Water (triangles) and sediment (circles) were analysed in illuminated water-sediment (a), dark water-sediment (b), illuminated water-only (c), and dark water-only (d) microcosms, and comparisons made between summer (red), autumn (blue), winter (green), and spring (pink). The first year of each collection time is denoted by closed symbols and the second year by open symbols. Black lines show 20 % similarity.

The 23S rRNA gene amplified both non-phototrophic and phototrophic OTUs. The percentages of these in each treatment at each collection time can be found in Appendix I.6. Non-phototrophic OTUs were then discarded and the relative abundance of phototrophic communities assessed. Pooled data for each treatment is shown in **Figure 2.28** and, regardless of treatment, similar taxa were present. The relative abundances of these individual taxa, however, were variable and full breakdown of the data can be found in Appendix I.6. It should also be noted that in dark treatment microcosms phototrophic taxa may be dormant.

There were significant differences between phototrophic taxa between treatments ($p \leq 0.0001$). The majority of the relative abundance consisted of Chlorophyta, Diatoms, and Cyanobacteria. Fresh river water and water from dark water-sediment microcosms were similar and these both had significantly higher ($p \leq 0.0001$) relative abundances of Diatoms (37.4 and 40.7 %, respectively) compared to the water in illuminated water-sediment, illuminated water-only, and dark water-only microcosm treatments (ranging between 2.6 and 14.1 %). Additionally, water from dark water-sediment microcosms had significantly higher ($p \leq 0.001$, 15.3 %) relative abundances of Cryptophyta compared to illuminated water-sediment (0.06 %), illuminated water-only (0.02 %), and dark water-only (0.0 %) microcosm treatments.

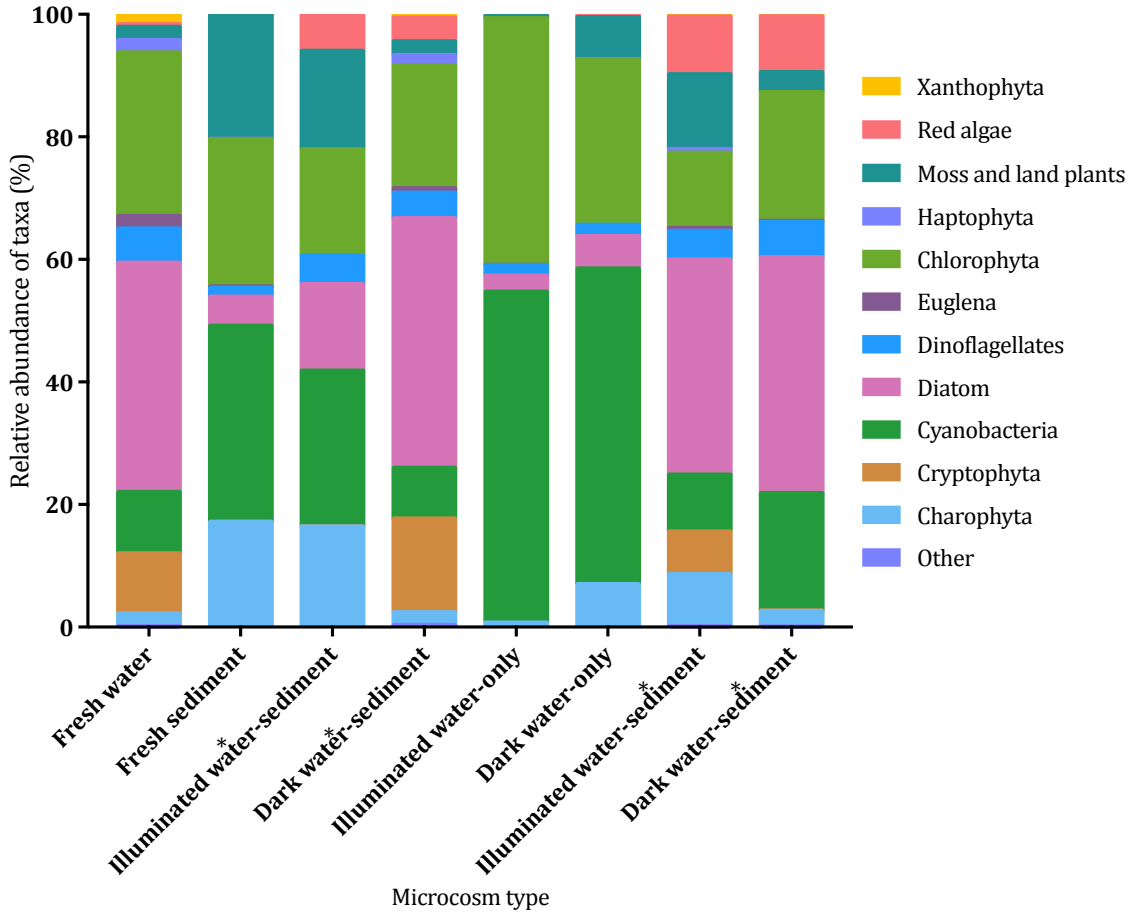

Figure 2.28: Relative abundance of phototrophic taxa in fresh samples and different microcosm treatments at 36 DAT in water and sediment. Different phototrophic taxa are denoted by different colours and taxa making up < 1 % of the relative abundance are listed under *other*. Analysis was carried out on fresh river samples and at 36 DAT on both water and sediment samples. * over *water* or *sediment* in the water-sediment systems indicates the sample type.

Water from illuminated water-sediment microcosms had significantly higher ($p \leq 0.01$) relative abundances of Charophyta (16.4 %) and Moss and Land Plants (16.1 %) compared to fresh water and water from dark water-sediment and illuminated water-only microcosm treatments (ranging between 2.1 and 0.7 % for Charophyta and 2.2 and 0.4 % for Moss and Land Plants). Additionally, water from illuminated water-sediment microcosms had significantly higher ($p \leq 0.001$) relative abundances of Cyanobacteria (25.4 %) compared to fresh water (10.0 %) and water from dark water-sediment microcosms (8.3 %). Water-only microcosms, however, had significantly higher ($p \leq 0.01$) relative abundances of Cyanobacteria (54.0 and 51.5 % in illuminated and dark treatments, respectively) compared to fresh water (10.0 %) and water in both water-sediment microcosms (25.4 and 8.3 % in illuminated and dark treatments, respectively). Illuminated water-only microcosms additionally had significantly higher ($p \leq 0.01$) relative abundances of Chlorophyta (40.3 %) compared to fresh water (26.7 %) and water in both illuminated and dark water-sediment microcosms (17.3 and 20.0 %, respectively).

For the sediment fraction, fresh sediment had a significantly lower ($p \leq 0.0001$) relative abundance of Diatoms (4.8 %) compared to sediment from water-sediment microcosms at 36 DAT (25.1 and 38.5 % in illuminated and dark treatments, respectively). Fresh sediment also had a significantly higher ($p \leq 0.001$) relative abundance of Charophyta (17.1 %) and Moss and Land Plants (20.2 %) compared to dark water-sediment microcosms (2.5 and 3.4 %, respectively), as well as a significantly higher ($p \leq 0.05$) relative abundance of Chlorophyta (24.1 %) compared to illuminated water-sediment microcosms (12.3 %). Lastly, fresh sediment had a significantly higher ($p \leq 0.01$) relative abundance of Cyanobacteria (32.0 %) compared to sediment in both water-sediment microcosms (9.3 and 19.2 % in illuminated and dark treatments, respectively).

Similarly, there were differences in the relative abundance of phototrophic taxa between collection times (**Fig. 2.29**). In fresh water samples (**Fig. 2.29.a**), there was a significant difference between the relative abundances of phototrophic taxa between collection times ($p \leq 0.0001$). Cryptophyta relative abundance was significantly higher ($p \leq 0.001$) in autumn 2014 (21.5 %) compared to spring 2015 (6.8 %), autumn 2015 (4.3 %), and winter 2016 (6.0 %); however, in summer 2014, no Cryptophyta were present and this was significantly lower compared to autumn 2014, winter 2015, summer 2015, and spring

2016 (12.7 to 21.5 %). Cyanobacteria relative abundance was very variable (0.7 to 24.5 %) and summer 2014 (23.3 %), autumn 2015 (24.5 %), and winter 2016 (18.5 %) had significantly higher relative abundances ($p \leq 0.0001$) compared to all other collection times (0.7 to 4.5 %). Diatom relative abundance was significantly lower ($p \leq 0.0001$) in summer 2014 (0.8 %) compared to all other collection times (24.2 to 57.3 %). The other collection times varied in significance ($p \leq 0.01$), with a lower Diatom relative abundance in autumn 2015 and winter 2016 (24.2 to 27.2 %), intermediate amounts in autumn 2014 and winter 2015 (39.5 to 42.0 %), and higher amounts in spring 2015, summer 2015, and spring 2016 (51.7 to 56.7 %). Winter 2015 (15.0 %) had a significantly ($p \leq 0.05$) higher relative abundance of Dinoflagellates compared to summer 2014, winter 2015, spring 2015, summer 2015, and spring 2016 (0.5 to 3.7 %) and summer 2014 (74.8 %) had a significantly ($p \leq 0.0001$) higher relative abundance of Chlorophyta compared to all other collection times (11.7 to 29.0 %). Additionally, spring 2015 (29.0 %) and summer 2015 (23.8 %) had significantly higher ($p \leq 0.05$) relative abundances of Chlorophyta compared to winter 2016 (13.2 %) and spring 2016 (11.7 %).

In fresh sediment samples (**Fig. 2.29.b**), there was a significant difference between the relative abundances of phototrophic taxa between collection times ($p \leq 0.0001$). Charophyta relative abundance was significantly higher ($p \leq 0.01$) in summer 2014 (42.2 %) compared to autumn 2014 (0.2 %) and spring 2015 (2.0 %). Spring 2015 had a significantly ($p \leq 0.001$) higher relative abundance of Cyanobacteria (64.7 %) compared to both collection times in summer and winter and to autumn 2015 (17.3 to 23.0 %). Winter 2016 had a significantly lower ($p \leq 0.05$) relative abundance of Chlorophyta (3.2 %) compared to autumn 2014 (35.0 %) and autumn 2015 (39.8 %); autumn 2015 additionally had a significantly higher relative abundance compared to spring 2016 ($p \leq 0.05$, 8.2 %). Lastly, Moss and Land Plant relative abundance was very variable across collection times. Winter 2016 (63.0 %) had a significantly ($p \leq 0.001$) higher relative abundance compared to all collection times except spring 2016 (0.0 to 18.2 %) and spring 2016 had a significantly ($p \leq 0.05$) higher relative abundance (35.8 %) compared to summer 2014 (2.7 %), autumn 2014 (0.0 %), and spring 2015 (1.8 %).

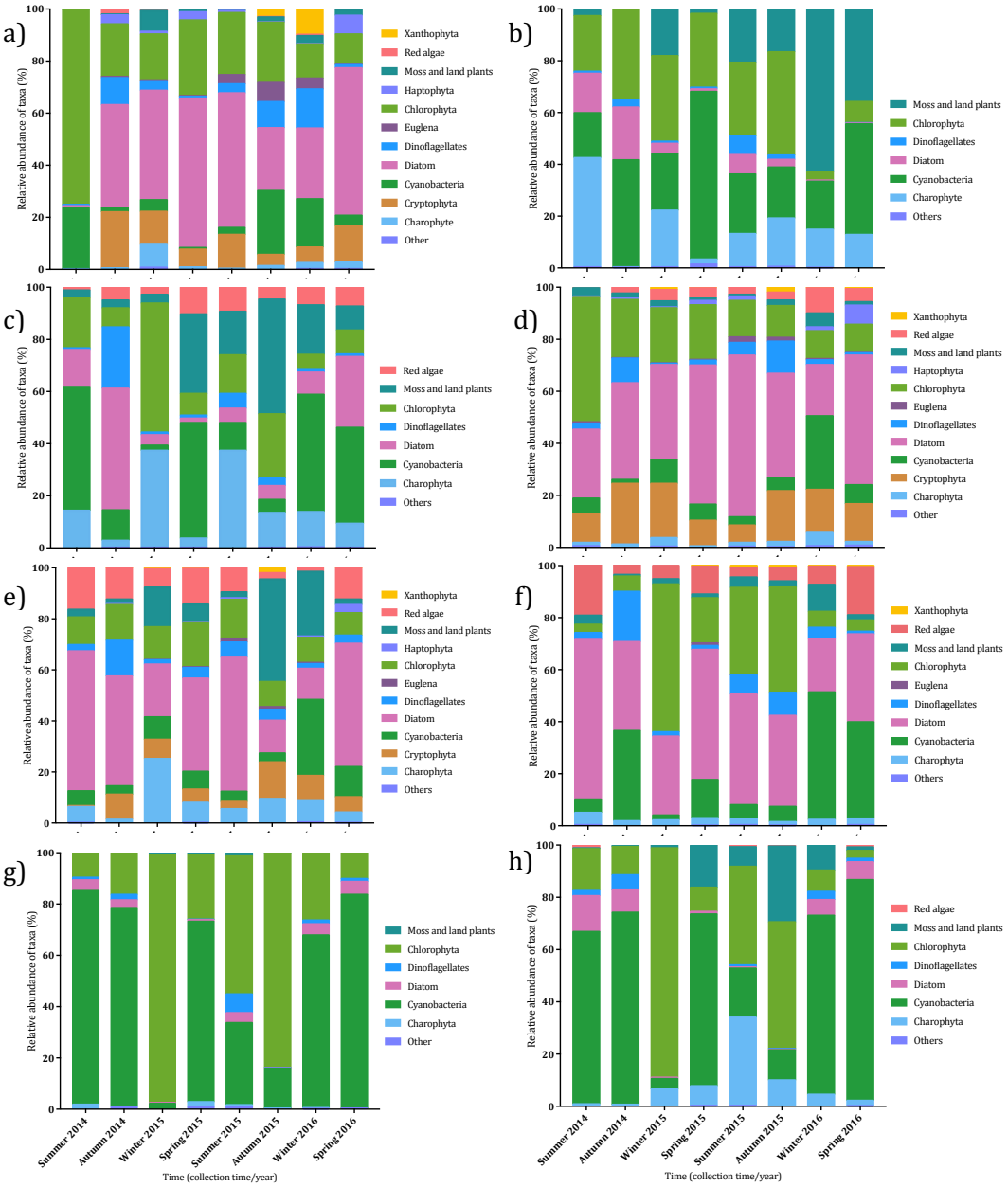

Figure 2.29: Relative abundance of phototrophic taxa between collection times in fresh samples and each microcosm treatment at 36 DAT. Different phototrophic taxa are denoted by different colours and taxa making up < 1 % of the relative abundance are listed under *other*. Analysis was carried out on fresh water (a) and sediment (b), water in illuminated (c) and dark (d) water-sediment microcosms, sediment in illuminated (e) and dark (f) water-sediment microcosms, and in illuminated (g) and dark (h) water-only microcosms at 36 DAT.

In all microcosm treatments at 36 DAT, there was a significant difference between collection time and phototrophic taxa ($p \leq 0.0001$), except in the sediment in dark water-sediment microcosms ($p \leq 0.3435$). In the illuminated water-sediment microcosm water fraction (**Fig. 2.29.c**), relative abundances of Charophyta were significantly higher ($p \leq 0.05$) in winter 2015 (37.2 %) and spring 2015 (37.3 %) compared to autumn 2014 (2.7 %), spring 2015 (3.5 %), and spring 2016 (9.2 %). Diatom relative abundance was significantly higher ($p \leq 0.01$) in autumn 2014 (46.7 %) compared to all collection times except spring 2016 (1.7 to 14.2 %). Additionally, spring 2016 had a significantly higher ($p \leq 0.05$) Diatom relative abundance (27.2 %) compared to spring 2015 (1.7 %). Chlorophyta relative abundance was significantly higher ($p \leq 0.01$) in winter 2015 (49.5 %) compared to all collection times except autumn 2015 (5.5 to 19.3 %). Spring 2015 and autumn 2015 had significantly higher ($p \leq 0.05$) relative abundances of Moss and Land Plants (30.5 and 44.0 %, respectively) compared to summer 2014 (2.8 %), autumn 2014 (3.0 %), and winter 2015 (3.3 %); autumn 2015 additionally had a significantly higher ($p \leq 0.05$) relative abundance when compared to spring 2015 (16.7 %) and spring 2016 (9.2 %). Lastly, Cyanobacteria relative abundance was significantly higher ($p \leq 0.05$) in summer 2014 (47.5 %), spring 2015 (44.3 %), winter 2016 (45.0 %), and spring 2016 (36.8 %) when compared to autumn 2014 (11.7 %), winter 2015 (2.0 %), summer 2015 (10.7 %), and autumn 2015 (5.0 %).

In the sediment fraction in illuminated water-sediment microcosms (**Fig. 2.29.e**) Charophyta relative abundance was significantly higher ($p \leq 0.05$) in winter 2015 (25.7 %) compared to autumn 2014 (1.3 %) and Cyanobacteria relative abundance was significantly higher ($p \leq 0.05$) in winter 2016 (29.8 %) compared to all collection times except winter 2015 and spring 2016 (3.3 to 7.0 %). Autumn 2015 had a significantly higher ($p \leq 0.05$) relative abundance of Moss and Land Plants (40.2 %) compared to all collection times except winter 2016 (1.8 to 15.5 %); winter 2016 similarly had a significantly higher ($p \leq 0.05$) relative abundance compared to summer 2014 (3.0 %), autumn 2014 (1.8 %), summer 2015 (2.3 %), and spring 2016 (2.2 %). Lastly, Diatom relative abundance was significantly higher ($p \leq 0.05$) in summer 2014, autumn 2014, spring 2015, summer 2015, and spring 2016 (36.5 to 54.8 %) compared to winter 2015, autumn 2015, and winter 2016 (12.2 to 20.7 %).

In dark water-sediment microcosm water (**Fig. 2.29.d**), the relative abundance of Cyanobacteria was significantly higher ($p \leq 0.05$) in winter 2016 (28.3 %) compared to all

other collection times (1.5 to 9.2 %). Diatom relative abundance was highest in summer 2015 (62.2 %) and this was significantly higher ($p \leq 0.01$) compared to all collection times except spring 2015 and spring 2016 (19.2 to 40.2 %). Winter 2016 (19.2 %) also had a significantly lower relative abundance compared to the autumn and spring collection times (37.2 to 53.5 %), and summer 2014 (26.5 %) a significantly lower relative abundance compared to the spring collection times (53.5 and 29.8 % in the respective years). Lastly, Chlorophyta relative abundance was significantly higher in summer 2014 (48.2 %) compared to all other collection times (10.6 to 22.3 %). Although there was no overall significant difference ($p \leq 0.3435$) between collection times in the sediment fraction in dark water-sediment microcosms (**Fig. 2.29.f**), Cyanobacteria relative abundance was higher in winter 2016 (49.0 %) and lower in summer 2014, winter 2015, summer 2015, and autumn 2015 (1.8 to 5.8 %), and Chlorophyta relative abundance was highest in winter 2015 (56.8 %) and lower in summer 2014, autumn 2014, spring 2015, winter 2016, and spring 2016 (3.2 to 17.3 %).

In illuminated water-only microcosms (**Fig. 2.29.g**), Cyanobacteria relative abundance was significantly lower (mainly $p \leq 0.0001$) in winter 2015 (2.6 %) compared to all other collection times (15.5 to 83.7 %). The remaining collection times varied in Cyanobacteria relative abundance with summer 2014, autumn 2014, spring 2015, and spring 2016 having higher amounts (70.3 to 83.7 %), summer 2015 and winter 2016 having intermediate amounts (32.0 and 67.5 %, respectively), and autumn 2015 having lower amounts (15.5 %); these varied in significance depending on the comparison (mainly $p \leq 0.01$). Winter 2015 had a significantly higher ($p \leq 0.05$) relative abundance of Chlorophyta (96.7 %) compared to all other collection times (9.7 to 83.7 %); however, the other collection times were also variable. These ranged between higher amounts in summer 2015 and autumn 2015 (53.8 and 83.7 %, respectively), intermediate amounts in spring 2015 and winter 2016 (25.3 and 26.3 %, respectively), and lower amounts in summer 2014, autumn 2014, and spring 2016 (9.7, 16.3, and 10.7 %, respectively); these varied in significance depending on the comparison (mainly $p \leq 0.01$).

In dark water-only microcosms (**Fig, 2.29.h**), Charophyta relative abundance was significantly higher ($p \leq 0.05$) in summer 2015 (33.8 %) compared to all other collection times except autumn 2015 (0.7 to 7.5 %). Cyanobacteria relative abundance was

significantly lower ($p \leq 0.0001$) in winter 2015 (4.0 %), summer 2015 (18.8 %), and autumn 2015 (11.5 %) compared to autumn 2014, spring 2015, winter 2016, and spring 2016 (65.8 to 84.5 %). Moss and Land Plant relative abundance was significantly higher ($p \leq 0.01$) in autumn 2015 (29.0 %) compared to summer 2014, autumn 2014, winter 2015, and spring 2016 (0.3 to 9.7 %). Lastly, Chlorophyta relative abundance was significantly higher ($p \leq 0.0001$) in winter 2015 (87.8 %) compared to all other collection times (3.0 to 48.5 %) and autumn 2015 and summer 2015 (48.5 to 37.8 %) had significantly higher ($p \leq 0.01$) relative abundances compared to the remaining collection times (3.0 to 15.7 %).

2.3.5 Relationship between isopyrazam fate versus environmental characteristics and microbial community composition at the sample site

The relationship between DegT50 and total mineralisation data compared to sample site environmental characteristics and microbial community composition were determined using correlation analysis. DegT50 data was unreliable for dark microcosms and illuminated water-only microcosms because DegT50 estimates extended beyond the duration of the study. Therefore, only correlations for total mineralisation were tested in these microcosm treatments. Additionally, a number of correlations (e.g. sample site water NO_3- concentration verses mineralisation at 36 DAT or sedimentary Charophyta relative abundance at 36 DAT verses illuminated water-sediment DegT50) gave significant results but proved to be skewed by either the higher mineralisation rates in summer 2014 or the longer DegT50 in winter 2015. These analyses were carried out again without the outlier (summer 2014 or winter 2015) to determine whether the correlation was still significant. If there was no correlation when the outlier was removed, the original analyses were not classed as significantly correlated.

2.3.5.i Correlation between isopyrazam DegT50 and mineralisation versus sample site characteristics

Water temperature at the time of sampling was significantly negatively correlated (**Fig. 2.30**) with the DegT50 data for the illuminated water-sediment microcosms ($r = -0.80$, $p \leq 0.0179$) and when water temperature was warmer DegT50 values were lower, showing quicker degradation.

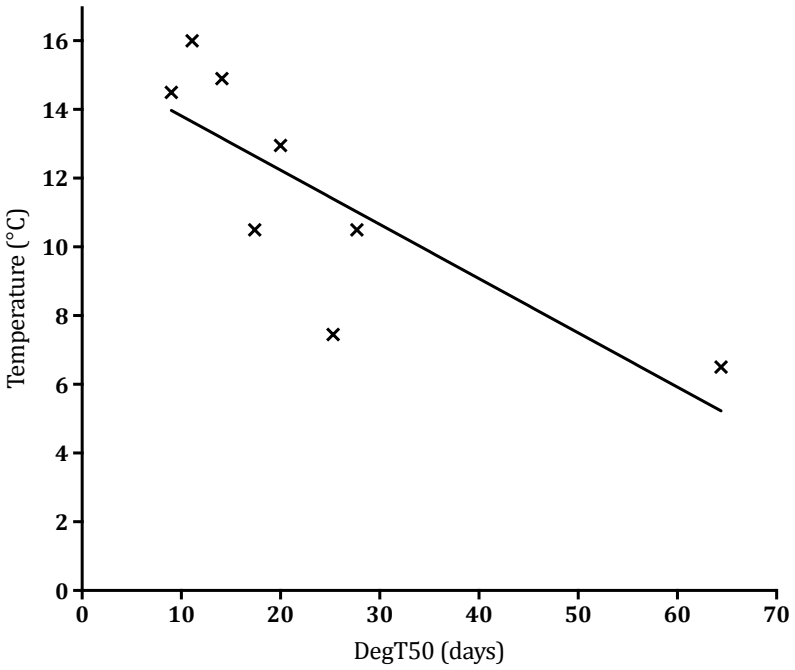

Figure 2.30: Correlation between illuminated water-sediment microcosm DegT50 values and water temperature at the sample site. Correlation was negative with longer DegT50 values when water temperature was colder. Data points show average DegT50 values from each collection time.

2.3.5.ii Relationships between bacterial and phototrophic OTUs versus DegT50

DegT50 in the illuminated water-sediment microcosms was split into fast (9.0 to 11.0 days, summer and autumn 2014), medium (14.0 to 20.0 days, summer 2015, autumn 2015, and spring 2016), medium-slow (20.0 to 30.0 days, spring 2015 and winter 2016), and slow (30.1 + days, winter 2015) rates of decline. In fresh sediment, there were only two bacterial OTUs which were significantly associated with a specific DegT50 rate, and these were in the family 0319-6A21 from the phyla Nitrospirae (6966, $p \leq 0.0227$) and the class S085 from the phyla Chloroflexi (17572, $p \leq 0.0232$). They had a significantly higher relative abundance in collection times with slow DegT50 (0.02 and 0.03 %, respectively) and were not present at all in other collection times. There was no link between DegT50 and any phototrophic OTUs in the fresh water and sediment.

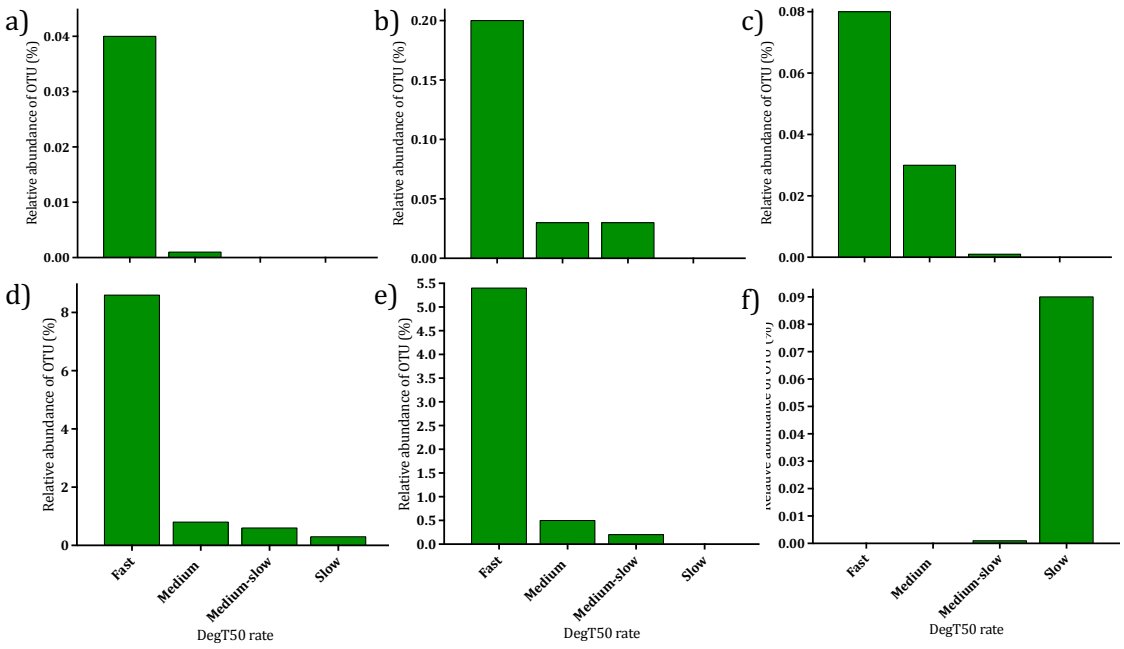

Figure 2.31: Relative abundance of OTUs present at 36 DAT in illuminated water-sediment microcosms with different DegT50 rates. OTU relative abundance of 2427 (a, Proteobacteria), 370 (b, Proteobacteria), 345 (c, Planctomycetes), 15 (d, Cyanobacteria), 1530 (e, Cyanobacteria), and 9316 (f, Proteobacteria). DegT50 rates are described as; *fast* (9.0 to 11.0 days), *medium* (14.0 to 20.0 days), *medium-slow* (20.0 to 30.0 days), and *slow* (30.1 + days).

At the end of the experiment, bacterial OTUs from the phyla Proteobacteria, Cyanobacteria, Actinobacteria, Planctomycetes, Chlamydiae, Acidobacteria, and TM7 and phototrophic OTUs from the taxa Cyanobacteria and Viridiplantae were higher when there was a fast DegT50. Twenty-four OTUs had a significant relationship with DegT50 ($p \leq 0.0485$) and many of these OTUs were not present at all in collection times with slow DegT50s. Several OTUs (345, 15, 6064, and 1530) decreased in relative abundance as DegT50 increased. Only four OTUs had significantly higher ($p \leq 0.0447$) relative abundances when DegT50 was slow and these consisted of Proteobacteria, Bacteroidetes, and Viridiplantae. Full breakdown of relative abundances, significance, and taxonomy is shown in Appendix I.6, with examples shown in **Figure 2.31**.

2.3.5.iii Relationship between bacterial and phototrophic OTUs versus higher mineralisation rates

When data were split between high mineralisation (summer 2014 and winter 2015) and low mineralisation (all other collection times), there were no specific OTUs common to both summer 2014 and winter 2015. Data were then compared separately between both of these collection times with high mineralisation and the other collection times (grouped as low mineralisation) to determine whether there were OTUs specific to either summer 2014 and winter 2015. In fresh samples, no bacterial OTUs were specific to summer 2014, however, the same OTUs as in section 2.3.5.ii (6955 and 17572) were significantly linked to winter 2015. No phototrophic OTUs in the fresh sample were linked to mineralisation at any collection time.

In summer 2014 at 36 DAT, eleven OTUs classified as Proteobacteria, Cyanobacteria, Bacteroidetes, and Viridiplantae had significantly higher relative abundances compared to collection times with low mineralisation ($p \leq 0.0007$). In winter 2015 at 36 DAT, thirteen OTUs classified as Proteobacteria, Bacteroidetes, Actinobacteria, Verrucomicrobia, Firmicutes, and Viridiplantae had significantly higher relative abundances compared to collection times with low mineralisation ($p \leq 0.0407$). Full breakdown of relative abundances, significance, and taxonomy is shown in Appendix I.6, with examples shown in **Figure 2.32**.

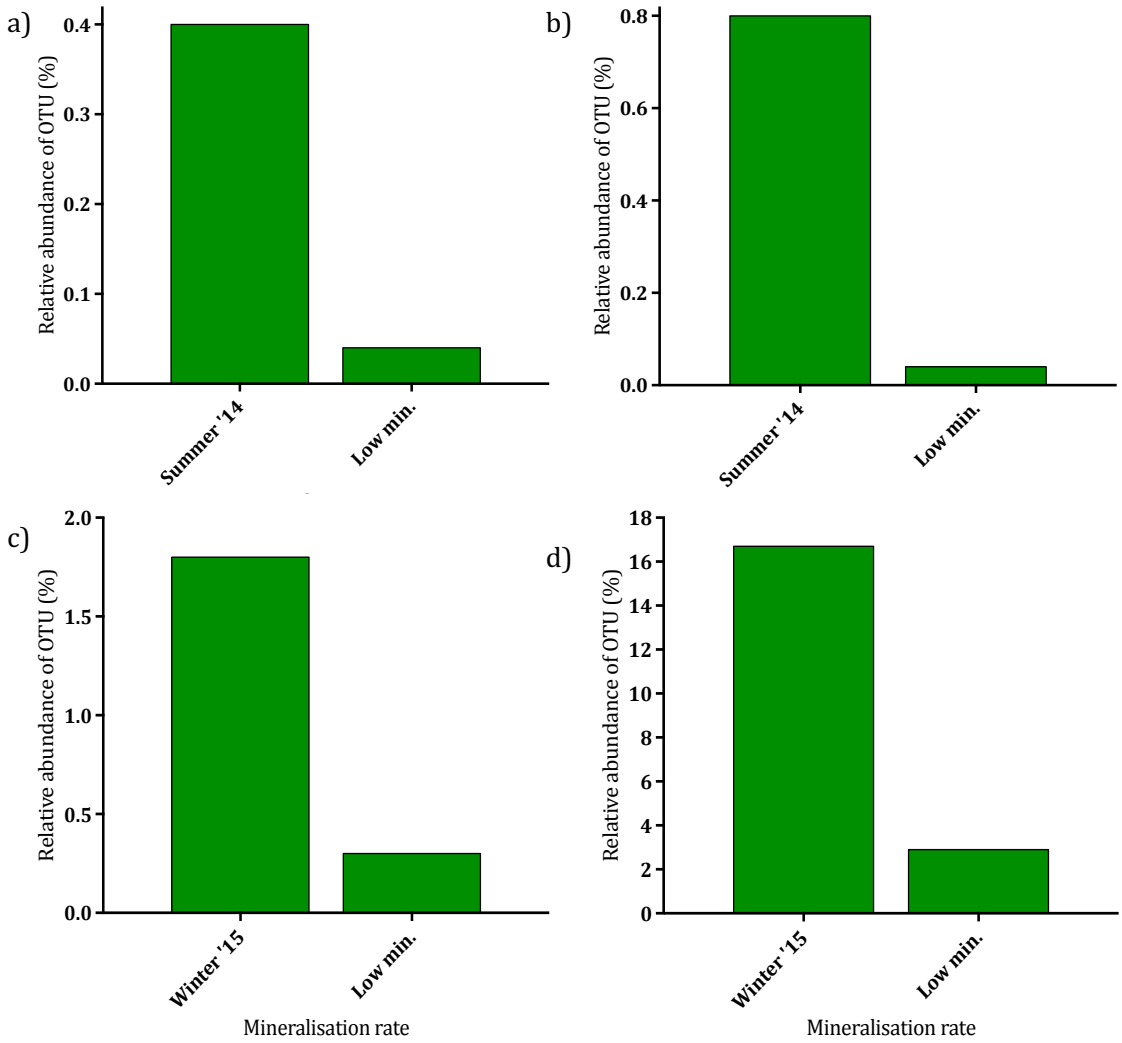

Figure 2.32: Relative abundance of OTUs present at 36 DAT in collection times with high mineralisation (summer 2014 or winter 2015) and low mineralisation. OTU relative abundance of 395 (a, Proteobacteria), 115 (b, Viridiplantae), 5014 (c, Viridiplantae), and 12 (d, Viridiplantae).

2.4 DISCUSSION AND CONCLUSIONS

This study found that non-UV light increased isopyrazam degradation in river microcosms compared to dark treatments, in which there was little degradation. This was more pronounced in illuminated microcosms containing sediment, whereas sediment addition did not significantly impact degradation in the dark. Generally, a similar trend was seen for illuminated water-only microcosms although to a lesser extent; at some collection times, there were no significant differences to the dark microcosms. Temporal variation in isopyrazam degradation was only seen in illuminated microcosms; however, this was not predictable as degradation did not follow a seasonal pattern. Mineralisation of isopyrazam varied temporally with time of inoculum collection, but similar rates were usually seen in all microcosm treatments within a collection time, regardless of non-UV light treatment or sediment addition. This was particularly interesting in the treatments or collection times with low isopyrazam decline, as it suggests that there was variation in the effectiveness of different parts of the metabolic pathway.

Microbial community diversity and structure varied temporally, yet there was no clear link between any microbial phylum and isopyrazam degradation or mineralisation rates. At the OTU level, particular OTUs were specific or present in higher relative abundances in collection times with high or low degradation and mineralisation rates. In the illuminated treatments, when degradation was highest, phototrophic communities were more abundant. Dark treatment microcosms, however, also showed high levels of mineralisation in some collection times, suggesting that heterotrophic communities may also play a role in the degradation process. Lastly, DegT50 was negatively correlated with water temperature at the sampling site at the time of inoculum collection, suggesting that this influences the metabolic potential of the microbial community present in the river at this time and which subsequently developed in the river microcosms.

2.4.1 Impacts of non-UV light on isopyrazam degradation and microbial communities

Contaminants have been shown to sorb to algal cells, including pesticides (Crum *et al.*, 1999, Friesen-Pankratz *et al.*, 2003), heavy metals (Holan and Volesky, 1992, Holan *et al.*, 1992, Mehta and Gaur, 2008, Rajfur and Klos, 2013, Rajfur *et al.*, 2013, Sandau *et al.*, 1996),

and hydrocarbons (Headley *et al.*, 2008). In particular, Brown Algae have been shown to have higher sorption capabilities than other types of algae (Holan and Volesky, 1992, Holan *et al.*, 1992, Romera *et al.*, 2006), although there is substantial species and strain variation in the degree of sorption (O'Kelley and Deason, 1976, Rajfur and Klos, 2013). In illuminated microcosms, phototrophic communities likely played a role in the increased degradation of isopyrazam, as has been described in multiple studies with a range of chemicals (Davies *et al.*, 2013, Lima *et al.*, 2003, Roldán *et al.*, 1998, Thomas and Hand, 2011), including specifically isopyrazam transformation (Hand and Moreland, 2014, Hand and Oliver, 2010).

Partitioning of total radioactivity to the sediment was lower in illuminated microcosms in summer and autumn compared to dark microcosms, and this may have been due to sorption to phototrophic organisms within the water fraction. Sorption can be dependent on multiple factors, such as, morphology and surface area, pH, geography, and season (Holan and Volesky, 1992, Holan *et al.*, 1992, Mehta and Gaur, 2008, Rajfur and Klos, 2013, Sandau *et al.*, 1996), and environmental conditions or the microbial communities present may have influenced sorption at these collection times. A range of factors could have reduced sorption into the sediment in illuminated microcosms. Potentially, isopyrazam was sorbed to algal cells within the water fraction where it was subsequently degraded. Additionally, isopyrazam could have sorbed to the biofilm on top of the sediment (Flemming, 1995, Makris *et al.*, 2014) where it was degraded and metabolites then released back into the water fraction. Biofilm can additionally act as a physical barrier by clogging pores (Battin and Sengschmitt, 1999), which could have reduced exchange of isopyrazam between the sediment and the water column, thereby reducing contact and associated sorption of isopyrazam to the sediment. This suggests that the majority of isopyrazam recovered from the sediment fraction may not have reached the sediment bed itself.

2.4.2 Impact of temporal variation on isopyrazam degradation and microbial communities

There was substantial temporal variation of isopyrazam decline in illuminated microcosms. In the dark treatments, where there was little variation in isopyrazam decline between collection times, communities were less variable than they were in the illuminated microcosms. Although mineralisation of isopyrazam varied over time, there was little difference between treatments within a collection time.

Despite no clear links between degradation and mineralisation and the microbial taxa present, several OTUs were more abundant at certain DegT50 and mineralisation rates. Multiple studies have highlighted the importance of utilizing more microbially inclusive systems to assess pollutant biodegradation, since microbial consortia and co-metabolism rather than a single species are typically responsible for transformation (De Schrijver and De Mot, 1999, Lima *et al.*, 2003, Takagi *et al.*, 2012, Thomas and Hand, 2012). In particular, some OTUs which were significantly associated with degradation were only present at very low levels, suggesting rare taxa may contribute to degradation. Biodegradation in biofilms may be associated with a range of synergistic relationships between community members (Borde *et al.*, 2003). While some components may play a direct role in metabolism, their activities may be supported by other members which have an indirect contribution, such as provision of nutrients (Flemming, 1993, Writer *et al.*, 2011).

There was a broad range of species specific to collection times with fast DegT50 (summer and autumn 2014, **Fig. 2.31** and **Tables I.6** and **I.7**), including Gammaproteobacteria, Halomonadaceae, Sphingomonadaceae, Piscirickettsiaceae, Cyanobacteria, Synechococcaceae, Actinomycetales, Parachlamydiaceae, and Sphaeropleales, isolates of which have all been shown to degrade a range of pesticides (Bansal, 2012, Batisson *et al.*, 2010, Cáceres *et al.*, 2008, De Schrijver and De Mot, 1999, Fang *et al.*, 2014, Lew *et al.*, 2013, Lin *et al.*, 2016, Maltseva *et al.*, 1996, Megharaj *et al.*, 1994, Ning *et al.*, 2010, Sun *et al.*, 2015, Wipa and Fa-Aroonsawat, 2008, Ye *et al.*, 2004), hydrocarbons (Brakstad *et al.*, 2017, Chen *et al.*, 2016a, Ferguson *et al.*, 2017, Jung *et al.*, 2016, Mishamandani *et al.*, 2014, von der Weid *et al.*, 2007, Yang *et al.*, 2014), and other environmental contaminants (Kumar *et al.*, 2017, Takagi *et al.*, 2012). TM7, Pirellulaceae, and Holophagales have all been found in environments polluted with pesticides (De Schrijver and De Mot, 1999, Lima *et al.*, 2003), hydrocarbons (Bargiela *et al.*, 2015), pharmaceuticals (Llorens-Blanch *et al.*, 2015), and other contaminants (Lebrero *et al.*, 2016, Takagi *et al.*, 2012), and TM7 in particular are resilient to harsh environments, including those contaminated with chemicals (Hamamura *et al.*, 2006, Winsley *et al.*, 2014).

In collection times with slow DegT50 (winter 2015, **Fig. 2.31** and **Tables I.6** and **I.7**), a different range of taxa were significantly associated with degradation, such as Rhodospirillaceae, BD7-3, and Chlorellaceae, isolates of which have been shown to degrade

hydrocarbons (Antoniou *et al.*, 2015, Cui *et al.*, 2008, Galitskaya *et al.*, 2016, Thompson *et al.*, 2017), detergents (Bassey, 2010), and pesticides (Thomas and Hand, 2012). Degradation did still occur, albeit at a slower rate, so although these taxa may have the potential to degrade isopyrazam, it could be that they are not as effective as communities within high DegT50 samples, or that degradation was limited by microbe-microbe interactions within the community, e.g. competition (Fredrickson and Stephanopoulos, 1981). Degradation of chemicals has been shown to vary across time (Chénier *et al.*, 2003, Kowalczyk *et al.*, 2016, Palmisano *et al.*, 1991, Parkin and Shelton, 1991) and species changes associated with environmental conditions could contribute to this (Smoot and Findley, 2001), since taxa can vary considerably in the functional traits they possess (Ramakrishnan, 2012).

The highest rates of mineralisation were in summer 2014 and winter 2015 and, although there were no specific OTUs associated with degradation which were common to both collection times (**Fig. 2.32** and **Tables I.8** and **I.9**), they each contained certain OTUs which were distinctive to other collection times with less mineralisation. In summer 2014, Sphingomonadaceae, Xanthomonadaceae, Synechococcus, and Chlamydomonadaceae all had significantly higher relative abundances compared to other collection times, isolates of which have all been shown to degrade pesticides (Bansal, 2012, Cáceres *et al.*, 2008, Lin *et al.*, 2016, Talwar and Ninnekar, 2015, Wipa and Fa-Aroonsawat, 2008, Ye *et al.*, 2004, Zhang *et al.*, 2011). In addition, Chromatiaceae has been shown to be pollutant tolerant (Riser-Roberts, 1992) and Cyclobacteriaceae has been found at sites contaminated with hydrocarbons, although with no direct evidence of degradation (Bell *et al.*, 2013, Ferrera-Rodrígues *et al.*, 2012, Kohli *et al.*, 2016).

In winter 2015, Saprospiraceae, Chitinophagaceae, Firmicutes, Alphaproteobacteria, Caulobacteraceae, and Chlorellales had significantly higher relative abundances than other collection times, and these taxa have been shown to aid in the degradation of hydrocarbons (Alonso-Gutiérrez *et al.*, 2009, Bell *et al.*, 2013, Brakstad *et al.*, 2015, Ghosal *et al.*, 2016, Kostka *et al.*, 2011, Lamendella *et al.*, 2014, Nakamura *et al.*, 2014, Rodgers-Vieira *et al.*, 2015, Viñas *et al.*, 2005, Wang *et al.*, 2016, Yang *et al.*, 2016, Yang *et al.*, 2014), pesticides (Chaussonnerie *et al.*, 2016, Fang *et al.*, 2014, Storck, 2016, Thomas and Hand, 2012), and other environmental pollutants (Cortés-Lorenzo *et al.*, 2013, Debroas *et al.*, 2011, Du *et al.*, 2017). In addition, Verrucomicrobiaceae has been shown to be enriched in hydrocarbon

contaminated sites (Akbari, 2014, Patel *et al.*, 2016), although with no direct evidence that it contributes to degradation. Although DegT50 rate was slower in winter 2015 relative to other collection times, complete mineralisation to CO_2 occurred at a higher rate than at other collection times, suggesting that the microbial community present was better adapted to carrying out the later metabolic steps of degradation.

The confines of this study do not allow a clear identification of microbial species responsible for isopyrazam degradation; however, it is clear that a multitude of species are present in the systems, and that the nature of the communities varied over time, as did degradation rates. Non-UV light and phototrophic community metabolism are important agents of degradation; additionally, although UV light and thus indirect photolysis was limited in this study, phototrophs have the potential to cause indirect pollutant degradation if free radicals are formed during oxygenic photosynthesis (Roeselers *et al.*, 2008). Nevertheless, there is probably a key role in degradation for the heterotrophic community present in the microcosms. Non-phototroph OTUs were linked to fast DegT50 and mineralisation rates, and high mineralisation rates were not exclusive to illuminated microcosm treatments. Heterotrophs have been shown to be important contributors to degradation in several studies in which phototrophic degradation has been detected (Davies *et al.*, 2013, Sánchez-Pérez *et al.*, 2013) and perhaps the addition of light and the associated communities enhances the overall community in diversity, richness, and activity. For instance, bacteria utilising O_2 from algal photosynthesis (Borde *et al.*, 2003) or macrophytes providing an increased surface area for microbial biofilms (Thomas and Hand, 2011, Thomas and Hand, 2012).

Although there were fluctuations in the environmental parameters at the sample site, there was only correlation between the DegT50 in illuminated water-sediment microcosms and the water temperature at the sample site at the time of collection, with quicker degradation at higher water temperatures. Although the environment is heterogeneous, it is thought that species are adapted to the environment in which they originate from with different microbial taxa dominating at different times of year (Beales, 2004, Crump *et al.*, 2009, Hall and Cotner, 2007, Hall *et al.*, 2010, Hottes *et al.*, 2013, Kuffner *et al.*, 2012, Pettersson and Bååth, 2003, Rutter and Nedwell, 1994). Although the process can be slow, species are able to acclimatise to new environments and, in this case, transfer

from the environment to laboratory conditions would have required an acclimatisation period (Bárcenas-Moreno *et al.*, 2009, Birgander *et al.*, 2014, Pettersson and Bååth, 2003, Pires *et al.*, 2014, Walker, 2006).

Acclimatisation can include phenotypic and genotypic changes, as well as species sorting to those which are better adapted to the conditions they are exposed to (Bárcenas-Moreno *et al.*, 2009, Díaz-Raviña and Bååth, 1996, Hottes *et al.*, 2013). Physiological changes include alterations in the cell membrane composition or protein synthesis and shifts in nutrient and energy use, which can cause disruptions in cell division – changes may affect fitness and populations may not be able to compete under the new conditions (Barria *et al.*, 2013, Beales, 2004, Hall and Cotner, 2007, Pettersson and Bååth, 2003). There is also evidence that environments may have subpopulations with different temperature preferences, meaning that at different times of year certain populations will dominate and outside the optimum the population will be inactive (Ranneklev and Bååth, 2001, Simon and Wünsch, 1998).

The alteration of the microcosm community during acclimatisation will depend on the extent of the temperature shift and whether it is within the historical range of the environment – small scale shifts are unlikely to cause a big impact; however, there will be greater community sensitivity if the change is not a regular occurrence (Beales, 2004, Kuffner *et al.*, 2012, Waldrop and Firestone, 2006). Data collected by the Environment Agency (2017b) between 2010 and 2017 show that water temperature of the River Dene ranges from 1.0 °C (January 2010) to 18.6 °C (July 2013), indicating that the 20 °C temperature used in the laboratory is not within the usual environmental parameters. In summer 2014, water temperatures were only 4 °C higher in the laboratory; however, in winter 2015 laboratory conditions were 13.5 °C higher than they were in the environment at the time of collection. It is likely that at cold environmental temperatures there would have been a selection pressure for species adapted to that environment. When these were moved to the warmer laboratory conditions, the selection pressure would have changed (Ranneklev and Bååth, 2001), involving an adaptation phase and altering the isopyrazam degradation function. Potentially, the community metabolic potential may have been different had they encountered the same concentrations of isopyrazam in an environment they were already adapted to. Additionally, temperature can regulate growth in the

environment, especially of some algal communities, and this will determine community interactions by regulating nutrient competition between communities (Rier and Stevenson, 2002, White *et al.*, 1991). Changes in temperature may therefore change community dynamics. Perhaps utilising temperatures which are true to the real environment is a more robust approach for degradation studies.

2.4.3 Impact of sediment on isopyrazam degradation and microbial communities

Although there was no impact of the addition of sediment on isopyrazam degradation in dark microcosms, in illuminated water-sediment microcosms there was greater isopyrazam degradation compared to the illuminated water-only microcosms. This finding was similarly noted for *p*-nitrophenol degradation studies conducted by Spain *et al.* (1984).

Studies have shown that higher amounts of sediment can increase primary productivity and respiration compared to lower sediment depths (Uzarski *et al.*, 2004), and sediment could additionally act as a diverse, nutrient rich platform for biofilm development. Indeed, illuminated water–sediment microcosms had an increased concentration of chlorophyll *a* relative to water microcosms, with the majority of this coming from the sediment fraction. The hyporheic zone between the water and the sediment is an important zone of biogeochemical activity (Fang *et al.*, 2017, Sánchez-Pérez *et al.*, 2013), and there is also evidence for transformation and sorption of organic pollutants, such as pesticides, within this transitional zone (Sánchez-Pérez *et al.*, 2013). Sedimentary microbes play a major role in nutrient and energy transport within aquatic ecosystems and these communities can be enhanced by the presence of phototrophs, which provide carbon from photosynthesis (Smoot and Findley, 2001). Furthermore, biofilms can offer a substratum for heterotroph colonisation so that cells can be localised in close proximity to each other, offering protection for other communities (e.g. from predation or environmental stresses) (Hall-Stoodley *et al.*, 2004, Pesce *et al.*, 2010, Rier and Stevenson, 2002). The inclusion of sediment within microcosms increased the abundance of phototrophic communities. Although these have been shown to aid in isopyrazam transformation (Hand and Moreland, 2014, Hand and Oliver, 2010), sediment provides a complex system which also supports heterotrophic degraders.

Several phyla were present in the sediment in much higher relative abundances than in the water. These included Chloroflexi, Gemmatimonadetes, Acidobacteria, and, in the dark water-sediment microcosms, Nitrospirae. Although the water fraction was variable in terms of community composition, both at the sample site and at the end of the experiment, the sediment fraction was usually more constant across collection times. The sediment fraction also had a higher α diversity than the water fraction, suggesting there was a wider range of species present. Despite this, sediment addition only had an effect in the illuminated systems, and only Acidobacteria OTUs were linked to DegT50 and mineralisation. Therefore, it is more probable that phototrophic biofilms associated with the sediment benefitted isopyrazam degradation in illuminated microcosms.

2.4.4 Implications of the study

Dark treatment microcosms carried out in this study, which most closely represent OECD tests, saw little isopyrazam degradation. When variables which helped increase realism were added to the study design, isopyrazam degradation significantly increased. This suggests that OECD regulatory tests may be conservative and, in the case of isopyrazam, degradation rates are underestimated. This study was only carried out with one compound and it is likely that not all compounds will be influenced by non-UV light to the same extent, as has previously been shown by Davies *et al.* (2013). Regardless of whether light treatment has a positive or negative effect on degradation, the addition of light into OECD tests could provide a more accurate transformation rate with greater relevance to the real environment. Phototrophic communities are actively excluded from the test guidelines (OECD, 2002b). This work highlights the impact that phototrophic communities can have on the degradation process, including their influences on non-phototrophic microorganisms. Despite this, there would be additional benefits from carrying out studies in natural light conditions (including the UV spectrum). This would reflect the real environment further and include more of the degradation pathways seen in nature, which would usually not be isolated processes.

Temporal variation has additionally been shown to vary under light conditions, and this was linked to water temperature at the sample site. Additional studies would need to be carried out to confirm the impact of acclimatising inoculum to the laboratory conditions prior to the commencement of the study. It may also be beneficial to carry out tests at

conditions similar to those in the environment at the time of sampling. Regardless, this data suggests that it would be useful for OECD tests to be amended, especially in terms of controlling microbial consortia present which, as has been suggested by other studies, is the main driver of inconsistencies in biotransformation rates (Thouand *et al.*, 1995). Diversity within the microcosms will additionally be enhanced by increased environmental realism. The diversity of genes present in the community and the overall community structure can influence the community metabolic potential and the processes that it can carry out (Wang *et al.*, 2017). As the species diversity increases in the microcosms, it increases the chances that degraders are present within the systems (Kool, 1984, Thouand *et al.*, 2011, Thouand *et al.*, 1995); this could be further impacted by light, temporal variation, and sediment addition.

For instance, addition of light causes phototroph proliferation and, although algae can be important for contaminant sorption, some algae may only have binding sites for particular compounds (O'Kelley and Deason, 1976). This means an increase in diversity will increase the chance that species which can sorb a given environmental pollutant are present. With temporal variation, certain species may only be present at certain times of year. For instance, α diversity in winter 2015 was high in the water for both bacteria and phototrophs at the sample site (**Fig. 2.17** and **2.24**). The high diversity of microbes in the starting inoculum suggests that there was a higher probability that communities able to mineralise isopyrazam were present. Nevertheless, diversity does not guarantee degradation will occur, as in winter 2015, communities able to initially degrade isopyrazam were clearly not as abundant. Similarly, α diversity was generally higher in the sediment fraction, which will mean there was a more diverse range of phyla present compared to the water-only microcosms. This only impacted isopyrazam degradation in the illuminated microcosms, as the main degrading communities were not able to proliferate in the dark treatments. This suggests both diversity and beneficial environmental conditions are key for degradation to occur. In particular, with high diversity comes increased competition for resources (Jousset *et al.*, 2016), meaning degrading communities may be outcompeted.

2.4.5 Conclusions

This work has determined that non-UV light impacts isopyrazam degradation at all times of year, especially in more complex and realistic systems also containing sediment. Phototrophic communities, especially sedimentary biofilm, undoubtedly play a role in the transformation process; however, it also seems likely heterotrophs are involved. Light treatment provides a more inclusive community, which would not be able to proliferate under the dark conditions used in the OECD test guidelines.

Although complete mineralisation of isopyrazam to CO_2 varied temporally in all systems, isopyrazam decline only varied across collection times in illuminated microcosms. This suggests that throughout the year, different species are present with different metabolic functions, which changes the degradation process and the overall community function. Collection times with fast DegT50s had a broader range of OTUs associated with the transformation process, suggesting that higher diversities of species facilitate increased degradation. Nevertheless, high diversity does not guarantee degradation will occur, suggesting that the quality of the consortium and the species present is also vital for biodegradation to occur. Lastly, temperature at the sample site was linked to the community function in the laboratory, suggesting species take time to acclimatise to new conditions. Mimicking the environmental conditions at the time of sampling in the laboratory may aid in community adaption.

CHAPTER 3 – THE IMPACTS OF MICROCOSM SCALE ON ISOPYRAZAM DEGRADATION IN RIVER MICROCOSMS

3.1 INTRODUCTION

3.1.1 Scale in regulatory testing: OECD test 308

Pesticides are vital to control agricultural pests and this, in turn, helps increase crop yields (Hazell, 2002, Taylor *et al.*, 2007). Despite this, there are concerns that these chemicals can enter other environmental compartments, where they can cause harm to both the environment and human health. To ensure products are safe, regulatory tests need to be carried out by the agrochemical industry to determine the environmental fate and transformation of these chemicals (Carter, 2000, Davies *et al.*, 2013a, OECD, 2005).

OECD test 308 determines the aerobic and anaerobic transformation of a chemical in aquatic sediment systems (OECD, 2002b). In terms of scale, the test guidelines state that water and sediment should be between a 3:1 and a 4:1 ratio, and that there should be at least 50 g of dry weight sediment comprising a 2.5 cm layer (OECD, 2008a). Taking into account these ratios, it suggests that a test using 150 mL of water and 50 g of sediment is acceptable, even though the volume of water and sediment encountered in the environment by a given pesticide will often be much higher than this. Pesticide fate and transformation is controlled by a wide range of abiotic and biotic environmental factors (Gao *et al.*, 2012), and studies as small-scale as OECD test 308 may not reflect the diversity seen in nature (Kowalczyk *et al.*, 2015). This poses the question of whether these studies are sufficiently environmentally realistic.

For biodegradation studies, field experiments acknowledge real-time environmental variation, which could impact fate. They are, however, expensive, laborious, and difficult to control. This leads to uncertainty on the exact causes and limitations of degradation, as only a single space and time is represented (Aichberger *et al.*, 2005, Spain *et al.*, 1984, Sturman *et al.*, 1995, Wang *et al.*, 2008). Because of this, small-scale tests, which are cheaper and easier to execute and control, are essential to determine the mechanisms controlling pesticide fate and transformation, despite compromising on environmental realism

(Aichberger *et al.*, 2005, EPA, 2000, Khan and Zytner, 2011, Spain *et al.*, 1984). It is therefore useful to understand what factors impact biodegradation at different scales. These scale-up factors should then be considered before directly applying results from small-scale studies to the field-scale (Khan and Zytner, 2013).

3.1.2 Factors influenced by scale in the environment

There is no single regulatory testing process which can represent a variety of sites, making biodegradation very hard to predict (Davis *et al.*, 2003, Khan *et al.*, 2015). Indeed comparisons by Beulke *et al.* (2000), who assessed 178 mathematical pesticide persistence models, found that generally there was an overestimation of DegT50 values when comparing small-scale regulatory tests to data generated in the field. In the environment, there are complex interactions between biological, chemical, and physical processes. Abiotic stresses in the natural environment will be different to the laboratory studies, but there will also be biotic heterogeneities leading to patches of optimal areas for degradation to occur (Brockman and Murray, 1997, Goldstein *et al.*, 1985, Sturman *et al.*, 1995).

There are multiple different phenomena interacting at the field scale which will impact pesticide kinetics and partitioning, and these are not always represented at the microscale (Sturman *et al.*, 1995). Soil and sediment properties such as pH, organic matter content, and soil texture and morphology, are heterogeneous within and between sites, depending on site history and geology (Aichberger *et al.*, 2005, Davis *et al.*, 2003, Khan and Zytner, 2011, Khan and Zytner, 2013, Khan *et al.*, 2015, Sturman *et al.*, 1995). These properties can result in different permeability within the matrix and can also impact water and air flow (Cort *et al.*, 2001, Davies *et al.*, 2013b, Khan and Zytner, 2011, Khan and Zytner, 2013). Differences in soil and sediment properties can result in physical and biological processes which can lead to different interactions with chemical pollutants, influencing fate and dissipation (Huang *et al.*, 2003). If only a small environmental sample is used in regulatory laboratory studies these heterogeneities might be ignored, giving an inaccurate representation of what might occur at the field-scale.

Mass transport, and processes such as electron acceptor availability or pollutant and microbial degrader movement, can be limiting in the environment or on a large scale, due to

contact occurring over long spatial distances. This is likely to be minimised in small-scale studies, which could directly increase biodegradation, for instance if pollutants are more accessible for degraders, leading to unrealistic degradation rates (Aichberger *et al.*, 2005, Davies *et al.*, 2013b, Khan and Zytner, 2011, Khan and Zytner, 2013, Sturman *et al.*, 1995). Biodegradation is dependent on access and uptake of oxygen to microbial degraders and, if oxygen levels are low, the biodegradation rate is likely to decrease (Cort *et al.*, 2001, Hutchins, 1991, Khan and Zytner, 2011, Khan and Zytner, 2013, Sturman *et al.*, 1995). If oxygen supply is limited, biodegradation can occur with different electron acceptors, such as nitrate, but at a slower rate (Hutchins, 1991). Oxygen supply is less likely to be limited in small-scale studies, so there is a lower probability that microbes will utilise alternative electron acceptor sources. This means biodegradation rates will be more efficient, but not necessarily realistic of the environment.

Degrading microbial populations are obviously essential for degradation to occur; however, simply the presence of a community with metabolic potential is not sufficient and environmental conditions also need to be favourable for metabolism to occur (Goldstein *et al.*, 1985, Khan *et al.*, 2015). Conditions are likely to be heterogeneous in the real environment, including nutrient and substrate availability, and the presence of microorganisms which might outcompete degrading populations (Aichberger *et al.*, 2005, Davis *et al.*, 2003, Goldstein *et al.*, 1985, Khan and Zytner, 2011, Khan and Zytner, 2013, Ko *et al.*, 2007). Microbial hotspots, which are made up of areas of high diversity or degradative ability, may only occur in small compact areas in-between inactive ones (Davis *et al.*, 2003, Sjøholm *et al.*, 2010, Sturman *et al.*, 1995). Biodegradation is likely to be due to microbial consortia rather than a single species and, as well as soil characteristics, microbes will also be diverse and vary through space and time (EPA, 2000, Ko *et al.*, 2007, Sturman *et al.*, 1995).

The quantity of environmental inoculum used under laboratory conditions is small compared to the real environment. Assuming that microorganisms are not uniformly distributed through time and space, small sample volumes may not reflect the metabolic potential and abundance of degrading microbes actually present in the environment (Aichberger *et al.*, 2005, Hoyle and Arthur, 2000). Because of this, there could be differing abundances of degrading communities between samples, and this could cause ambiguous biodegradation outcomes despite being carried out under controlled laboratory conditions

(Aichberger *et al.*, 2005, Brockman and Murray, 1997). This suggests that the inoculum volume for laboratory tests should be carefully considered to accurately reflect the abundance of specific microorganisms in the environment and the processes which might impact them (Dechesne *et al.*, 2014).

3.1.3 The impacts of test system scale on biodegradation

Although the literature is limited, several studies have been carried out to determine the impacts of scale on biodegradation rates (Aichberger *et al.*, 2005, Davis *et al.*, 2003, Douglas *et al.*, 2012, Khan and Zytner, 2013, Khan *et al.*, 2015, Khan *et al.*, 2002, Spain *et al.*, 1984, Wang *et al.*, 2008). The results from these experiments, however, are conflicting. This is likely due to certain factors mentioned above holding more weight in any given test, which will depend on the factor contributing the most to the degradation of a particular compound. There are advantages and disadvantages to reducing study scale, yet the extent to which small scale tests reflect the degradation seen at the field scale is likely to include a trade-off between factors that could make degradation slower in the field, and those that could make it faster. For instance, biodegradation could be enhanced in small-scale tests relative to field situations due to increased mass transport, yet if the degraders are not present due to small inoculum size, then degradation will be diminished. Similarly, if laboratory conditions closely mimic the real environment, the results may be more representative.

Some studies suggest degradation rate increases as the test system size increases. Khan *et al.* (2015) carried out work on hydrocarbon bioventing and suggested that mesoscale reactor studies (17.8 cm height, 7.95 cm radius, containing 4 kg soil) better represented the processes that would occur in the field than smaller scale reactors. This was because an increased volume of soil and a higher surface area were more beneficial for microbial activity. This was mainly attributed to there being larger pore sizes in the mesoscale studies, which meant better availability of oxygen for aerobic microbial activities. This was linked to soil type, with a higher clay content negatively impacting degradation and higher sand content having a positive impact. Clay traps microbes causing a decrease in access to the hydrocarbon; however, higher sand content leads to better air flow and easier microbe movement due to larger pore sizes.

Other studies (Khan and Zytner, 2011, Khan and Zytner, 2013) have also shown differences in degradation kinetics between microscale respirometers (1 L with 150 g soil) and the same mesoscale reactors described above. Microcosm studies showed SFO kinetics, whereas the mesoscale studies had two stages of degradation, which was initially fast but slowed after eight days. The slower second degradation rate in the mesocosm experiment was similar to the overall degradation rate seen at the microscale, so it was assumed that the microscale reflected the long-term degradation after the initial fast decline. A more realistic environment for microorganisms, with better airflow and carbon and nitrogen access, aided in the overall faster degradation seen at the mesoscale. Small hydrocarbon molecules, which were more readily accessible, were preferentially degraded in the larger system, hence the initial faster degradation, which slowed once these smaller molecules were utilised.

In contrast, some studies have suggested that an increase in system scale can have a negative impact on biodegradation rate. Davis *et al.* (2003) carried out several different sized column experiments (10, 50, and 120 cm in height) and also work in a larger-scale tank (245 x 122 x 8 cm). Degradation rate was quicker in small-scale studies and this did not accurately reflect what would occur at the field-scale. Oxygen consumption decreased with an increase in system size, and more efficient substrate and electron acceptor diffusion rates enhanced degradation at the small-scale. Similarly, Wang *et al.* (2008) also suggested that limitation of oxygen in large-scale tests was key to the slower degradation.

Aichberger *et al.* (2005) suggested that small-scale studies overestimated what would occur at the field-level. Soil was set up in flasks (0.01 kg), columns (90 kg), and lysimeters (1500 kg) and compared to a full-scale bioventing site. Degradation rates from the site, however, were five times lower than even the lowest value acquired from the laboratory studies and, as scale increased, degradation rates decreased. This was due to optimum laboratory conditions which favoured degradation and, at larger scales, although degradation was slower, the microbial and structural heterogeneities made the conditions more realistic to the field.

Finally, Spain *et al.* (1984) determined that laboratory tests using water and sediment (500 mL flasks and 3 L microcosms) were a good predictor of what would occur in

the field and could be used to directly compare the two. The major trends of *p*-nitrophenol degradation were accurately predicted in terms of lag period, microbial population changes, and presence of specific bacteria, and these factors all correlated well with biodegradation rates in the field. Douglas *et al.* (2012) also determined that petroleum degradation in the laboratory (40 mL vials) was similar to that occurring in the field; however, there were differences in which petroleum component microbes degraded first, with hopane degrading to a higher extent in the laboratory. It was hypothesised that this was because optimal laboratory conditions caused microbes to be less selective over their energy source. In the field, where factors are limiting, microbes tend to degrade the components which yield the most energy. The route of chemical degradation is compound specific due to differing structures and degradation pathways (ECETOC, 2003, Javaid *et al.*, 2016). Although the degradation of some compounds in the field can be effectively predicted using laboratory tests, it seems to depend on whether the main degradation route and environmental controlling factors are adequately reflected in the laboratory tests.

Furthermore, some of the previous investigations of the effect of scale on biodegradation do not directly compare scales in parallel. A number of the studies (Khan and Zytner, 2011, Khan and Zytner, 2013, Khan *et al.*, 2015) compared the larger scale tests to previously completed microscale experiments. Additionally, although Davis *et al.* (2003) and Wang *et al.* (2008) carried out tests in parallel using various sized columns and bioreactors, respectively, they also compared these to larger scale studies carried out beforehand. Bearing in mind the spatial and temporal variation in environmental samples, it is problematic to directly compare data carried out at different times. The work by Aichberger *et al.* (2005) also did not treat environmental samples in the same way between vessels. For instance, soil in the flasks was sieved to < 2 mm, yet the other vessels had soil sieved to < 50 mm. Sieving has been shown to impact communities, such as fungi (Petersen and Klug, 1994), and samples should still be treated in exactly the same way between vessels to enable robust comparison. Without control over factors other than scale in the experimental design, it is difficult to determine whether any differences between varying sized vessels is due to scale or another variable.

3.1.4 Experimental overview

OECD 308-type tests were carried out to explore the impacts of microcosm scale on the degradation of isopyrazam in water-sediment microcosms. The only variable that changed was the vessel and environmental inoculum quantities, with microcosm sample volume increased 200-fold between small (3.2 mL water and 0.8 g sediment), medium (80 mL water and 20 g sediment), and large (640 mL and 160 g sediment) sized vessels. The role of microcosm size in shaping the microbial communities and subsequently isopyrazam degradation was assessed. Differences in degradation rate associated with scale could give insight into factors which should be considered before results from small-scale tests regarding pesticide fate are implemented in the field. Alternatively, if there is little difference between scales, it could pave the way for smaller, cheaper, high-throughput regulatory testing.

3.1.5 Experimental aims and objectives

The experimental aims and objectives of this experiment were as follows;

1. To evaluate whether microcosm scale has an effect on chemical degradation, microbiology, and water chemistry.
2. To understand the mechanisms underlying any differences in degradation rates associated with scale.
3. To determine the scope for downscaling OECD tests and the implications for regulatory testing.

3.2 MATERIALS AND METHODS

3.2.1 Sample collection and processing

River water and sediment samples were collected from the River Dene at Wellesbourne at the same location detailed in section 2.2.1. Sampling took place in mid-January 2017. Water and sediment samples were taken at three different sections of the river to ensure that there were three replicates – sampling technique is explained in section 2.2.1.

At the sampling site, water temperature was measured with a Total Immersion thermometer (Fischer Scientific, UK), light intensity measured with an RS-105 light meter (RS Components Ltd., UK), and water depth and velocity measured with an 801 EM flow meter (Valeport, UK). Water pH was analysed using an Orion Star™ AR11 Benchtop Meter (Thermo Scientific, US). The river water was filtered through a 106 µm sieve (Fischer Scientific, UK) in order to remove particulates and large protozoa (OECD, 2004), and sediment was wet-sieved through a 2.36 mm sieve (Endecotts Ltd, UK) to homogenize the sample in accordance to OECD 308 regulatory testing (OECD, 2002b). Samples were refrigerated at 4 °C prior to use.

3.2.2 Test chemical

Studies were performed using [^{14}C]-radiolabelled chemical supplied by Syngenta, Jealott's Hill International Research Centre, United Kingdom. The compound used was [pyrazole-5-^{14}C]-isopyrazam (specific activity 6.42 MBq/mg and 98.2 % purity) (**Fig. 1.5**). The rationale for choosing isopyrazam is outlined in section 1.5.

3.2.3 Experimental set up

Three scales of microcosm were employed in this experiment: (1) Duran Schott 2 L clear glass bottles (Scientific Laboratory Supplies, UK), (2) Duran Schott 250 mL clear glass bottles (Scientific Laboratory Supplies, UK), and (3) 40 mL clear Class 100 Chromacol® vials (Thermo Scientific, US). The following illuminated treatments were set up in triplicate

containing sample prepared using the OECD 308 method as in chapter 2; small, medium, and large sized microcosms, which corresponded to the different volumes above.

Figure 3.1: Large, medium, and small (from left to right) microcosm vessels (a) and experimental set up at Syngenta, Jealott's Hill International Research Centre, United Kingdom (b). Different sized microcosms were placed on an orbital shaker at 50 rpm under fluorescent lights which had a PAR light intensity, to ensure that degradation due to photolysis was kept to a minimum.

The wet to dry weight ratio of sediment was analysed by the same method detailed in section 2.2.3. A 4:1 mass ratio of water to dry weight sediment was used in all bottles, with 3.2, 80, and 640 mL water and 0.8, 20, and 160 g dry weight equivalent of sediment in small, medium, and large microcosms, respectively. This equated to approximately 1.2, 4.9, and 5.5 cm water depth, 0.2, 0.9, and 2.1 cm sediment depth, and 8.1, 8.5, and 19.0 cm air space in small, medium, and large microcosms, respectively. Bottles were randomly distributed on an orbital shaker under constant motion at 50 rpm at Syngenta, Jealott's Hill International Research Centre, United Kingdom (**Fig. 3.1**). The shaker was in a controlled environment room at 20 ± 2 °C with a 16-hour light and 8-hour dark cycle using a Sanyo M9536 Bench (Sanyo Electrical Company Ltd., Japan), fitted with six Phillips TLD 58W/840 fluorescent lights (Phillips, Netherlands). Microcosms were incubated under a light intensity of 1.6×10^4 lux, under PAR (400 – 700 nm) to ensure any degradation due to photolysis was limited. Light intensities were measured using an RS-105 light meter (RS Components Ltd., UK). Laboratory conditions were the same as in Chapter 2 and the environmental realism of these are discussed in Appendix I.1.

Microcosms were incubated for nine days prior to chemical addition so that communities had time to equilibrate. After nine days, fresh water was collected from the sample site and spiked with [^{14}C]-isopyrazam to a concentration of 0.1 mg/L (0.642 MBq/L). Although conservative, this is classed as an environmentally relevant concentration, as it is low enough to ensure that the biodegradation kinetics reflect those typical of the environment (OECD, 2004). Microcosms were then incubated for up to 43 days.

3.2.4 Destructive harvesting

Triplicate microcosms for each treatment were destructively harvested at 0, 9, 17, 27, 35, and 43 DAT. Both chemical and microbial analysis was carried out at each time point, except at 0 DAT, where no chemical analysis was carried out and a nominal 0 DAT value was used, assuming 100 % of the applied chemical was in the water fraction. 0.642 MBq/L was added to each microcosm and the percentage of radioactivity recovered from each fraction – water, sediment extract, NER in the sediment, and mineralised $^{14}CO_2$ captured in the NaOH traps – was summed together for a mass balance at each destructive harvest. Example mass balance calculations can be found in Appendix II.1.

3.2.5 Chemical analysis

3.2.5.i Residual isopyrazam and ^{14}C in the water fraction

The water sample from each microcosm was removed to a separate storage bottle. As isopyrazam adsorbs to glassware, the small, medium, and large microcosms were washed after sample removal with 3, 8, and 50 mL acetonitrile (HPLC grade, Fischer Scientific, UK), respectively, and the wash collected. Samples of water and acetonitrile from each microcosm were weighed into scintillation vials. 20 mL Hionic-Fluor™ liquid scintillation cocktail (PerkinElmer, US) was added to the water samples and 5 mL of ScintiSafe Gel liquid scintillation cocktail (Fischer Scientific, UK) to the acetonitrile samples. ^{14}C content was analysed using a Tri-Carb 2910 TR scintillation counter (PerkinElmer, US) with a five-minute count time. The combined results from the water and the acetonitrile determined total radioactivity recovered from the water fraction.

A proportion of the water fraction (water plus a proportionate amount of acetonitrile) was kept aside for Thin-Layer Chromatography (TLC) analysis to determine the percentage of parent and non-parent compound within the fraction. Normal phase TLC was conducted using silica gel 60 F254 plates (20 cm x 20 cm, 0.25 mm thickness, Merck, Germany). winCATS Planar Chromatography Manager software (CAMAG, Switzerland) was used to set up a chromatography method. It was ensured that 5 Bq of sample was added to each sample track on the plate using an Automatic TLC Sampler 4 (CAMAG, Switzerland). A non-radiolabelled isopyrazam standard was run alongside the samples in order to determine which band corresponded to isopyrazam – this was visualised under UV-light after elution. A Latch-Lid Chromototank (General Glassblowing Co. Inc., US) was lined with TLC saturation pads (Sigma-Aldrich, US) and plates were eluted in saturated vapour conditions using 100 mL of a 6:3:1 ratio of chloroform (Rathburn Chemicals Ltd., UK) to acetonitrile (HPLC grade, Fischer Scientific, UK) to concentrated formic acid (Fischer Scientific, UK). Following chromatography, plates were left in a lead box with an imaging plate (20 x 40, Fujifilm, Japan) for five days. Radioluminograms of the plates were obtained using a FLA-5000 phosphor imager (Fujifilm, Japan) and Image Reader FLA-5000 software (version 3, Fujifilm, Japan). Chromatograms were evaluated from the radioluminograms using Advanced Image Data Analyzer (AIDA) software (Raytest, Germany). This allowed

quantitative analysis based on the intensity of the respective bands and each band could therefore be given a percentage based on the total band intensity. Confirmation of the isopyrazam band can be found in Appendix II.2 and example TLC chromatogram analysis in Appendix II.3.

3.2.5.ii Residual isopyrazam and ^{14}C in the sediment fraction

Sediment from each microcosm was sampled and the chemical was extracted using 80 % acetonitrile (HPLC grade, Fischer Scientific, UK). 5 mL, 30 mL, and 160 mL were added to small, medium, and large microcosm samples, respectively. This was a similar methodology used in Chapter 2, however, was scaled up or down accordingly for the small and large microcosms. Samples were shaken for 1 hour at 300 rpm, centrifuged at 1000 rpm for 10 minutes, and then the extract collected. This was carried out three times in total and the extracts combined. An aliquot was taken from each sample extract and 5 mL of ScintiSafe Gel liquid scintillation cocktail (Fischer Scientific, UK) was added before analysis using a Tri-Carb 2910 TR scintillation counter (PerkinElmer, US), with a five-minute count time. This determined the amount of applied radioactivity present in the sediment fraction which was extractable. Sediment extract was then analysed by TLC in the same way as described for the water fraction in 3.2.5.i.

Solid sediment remaining after extraction was dried in a fume hood and then ground using a pestle and mortar. Combustion was carried out with duplicate weighed amounts of sediment to analyse NER. Samples were weighed into Combusto Cones (Perkin Elmer, US) and covered in a Combusto Pad (Perkin Elmer, US). Three drops of Combustaid™ (Perkin Elmer, US) was added on top of the pad. Combustion was carried out using a Model 307 Sample Oxidiser (Perkin Elmer, US) with 20 mL of Carbo-Sorb® E (Perkin Elmer, US) and Permafluor® E+ (Perkin Elmer, US) in a 1:1 ratio as a scintillation cocktail. Samples were burned in the presence of oxygen for 1.5 minutes. This gave $^{14}CO_2$ as a product, which was then trapped in the scintillation cocktail. Samples were analysed using a Tri-Carb 2910 TR scintillation counter (PerkinElmer, US) with a count time of five minutes.

3.2.5.iii Gaseous fraction

All microcosms were fitted with traps (**Fig. 2.4**) consisting of a 2 mL HPLC vial (in small microcosms) or a 20 mL scintillation vial (in medium and large microcosms) to capture any $^{14}CO_2$ that had been mineralised. These were filled with 1 mL, 7 mL, and 14 mL of 2 M NaOH (laboratory solution, Fischer Scientific, UK) for small, medium, and large microcosms, respectively. For large microcosms, these were removed at every time point and replaced with fresh ones to ensure maximum trapping. Traps in small and medium microcosms contained enough NaOH to allow trapping of $^{14}CO_2$ for the duration of the experiment, and remained in place until destructive harvesting. 20 mL of Hionic-Fluor™ liquid scintillation cocktail (PerkinElmer, US) was added to the vials and analysis was carried out with a Tri-Carb 2910 TR scintillation counter (PerkinElmer, US) and a count time of five minutes.

3.2.6 Water chemistry analysis

3.2.6.i pH analysis

The pH of the water fraction was analysed at each time point using an Orion Star™ AR11 Benchtop Meter (Thermo Scientific, US).

3.2.6.ii Macronutrient analysis

NO_3- and PO_4 concentrations in the water fraction were analysed at each time point using the methods as described in section 2.2.6.i.

3.2.7 Microbial analysis

3.2.7.i Chlorophyll a *analysis*

Chlorophyll *a* was extracted from both the water and sediment fraction to estimate phototrophic biomass at each time point. The same method as described in section 2.2.7.i was used; however, samples were analysed using a NanoDrop 2000c spectrophotometer (Thermo Scientific, US).

3.2.7.ii DNA isolation and quantification

DNA isolation and quantification was carried out as described in Appendix IV. DNA was isolated from the fresh water and sediment taken from the sample site and water and sediment samples from the microcosms at 43 DAT. Library preparation and sequencing of 16S rRNA and 23S rRNA genes to investigate bacterial and phototrophic community structure and diversity was carried out as described in Appendix IV. Sequencing was carried out by the Genomics Facility at the University of Warwick, Coventry, United Kingdom in June 2017.

3.2.8 Statistical analyses

Significance of differences between treatments for isopyrazam dissipation, metabolite formation, mineralisation, water and sediment partitioning, NER, water chemistry analysis, and microcosm chlorophyll *a* concentration was determined using a repeated measures two-way ANOVA (with microcosm size and time point). The Tukey method was used to correct for multiple comparison tests. Statistical analyses were performed using Prism (version 7, GraphPad Software, Inc., US).

Isopyrazam degradation kinetics (DegT50) were estimated in the same way as in section 2.2.8. Analysis of α diversity, β diversity, and relative abundance (two-way ANOVA with taxa and microcosm size) was carried out as described in section 2.2.8. Determination of OTUs which were significantly linked to microcosm treatments were tested using QIIME as in 2.2.8 (Caporaso *et al.*, 2010).

3.3 RESULTS

3.3.1 Sample site characteristics

Characteristics were analysed at the sample site (**Table 3.1**). Water temperature, water depth, and water velocity measurements were typical for sampling in January (Chapter 2). Additionally, water pH and light intensity were measured.

Table 3.1: Sample site characteristics at the River Dene, Wellesbourne, United Kingdom in January 2017. Mean and standard deviation of water temperature, light intensity, water depth, water velocity, and water pH taken at the sample site at the time of sampling.

Characteristic	Mean	Standard deviation
Water temperature	4.9 °C	1.2
Light intensity	1.6×10^4 lux	2.9×10^3
Water depth	0.53 m	0.16
Water velocity	0.4 m/s	0.1
Water pH	8.1	0.1

3.3.2 Chemical analysis results

3.3.2.i Isopyrazam decline

Average mass balance for all treatments was above 90 % throughout the experiment, showing that methods were robust. Isopyrazam decline was similar between microcosms and there was no statistically significant difference between the microcosm types ($p \leq 0.2382$). Decline ranged from 31 to 39 % remaining by 43 DAT (**Fig. 3.2**).

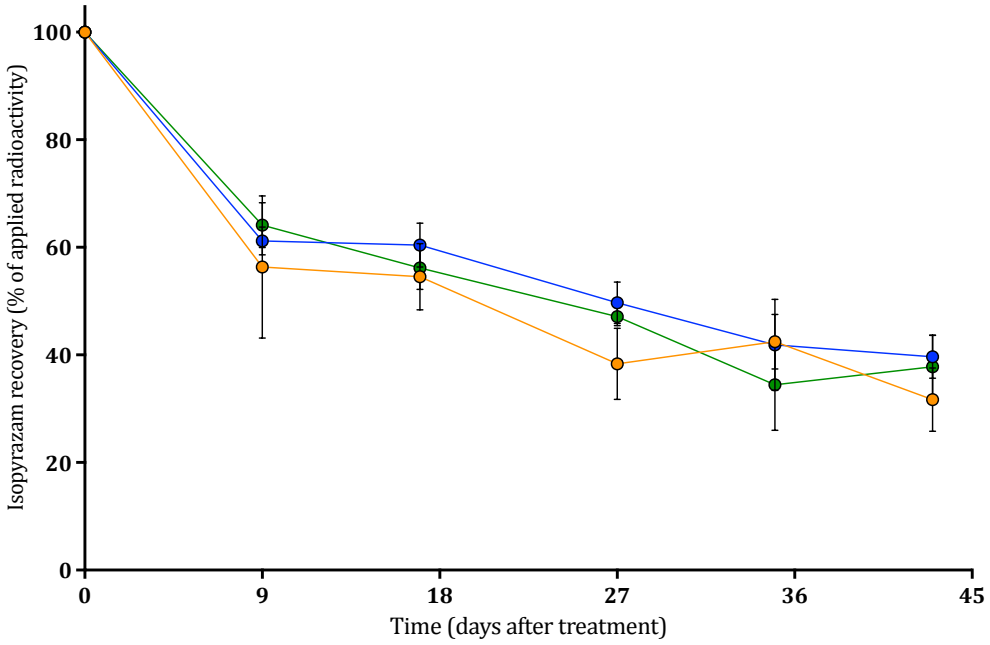

Figure 3.2: Decline of isopyrazam in different sized water-sediment microcosms as a percentage of the radioactivity originally applied. Degradation of isopyrazam in small (orange), medium (blue), and large (green) microcosms over 43 days. Error bars show ± standard deviation.

The DegT50 and rate constant estimates (**Table 3.2**) met the acceptance requirements outlined in section 2.2.8 for SFO kinetic models (see Appendix II.4). This showed that the estimates were robust and they followed a similar trend to the isopyrazam decline curves. Estimates ranged between 24.7 days for small microcosms and 30.3 days for medium microcosms.

Table 3.2: DegT50 and rate constant estimates from CAKE. SFO kinetic models were used for all data and 95 % confidence intervals calculated for the rate constant. k_1 denotes the first-order kinetics rate constant and *CI* denotes *confidence interval*.

Microcosm scale	DegT50 (days)	k_1	Lower 95 % CI	Upper 95 % CI
Small	24.7	0.028	0.020	0.036
Medium	30.3	0.023	0.018	0.028
Large	26.3	0.027	0.022	0.031

3.3.2.ii Metabolite generation

There was a significant impact of microcosm type on metabolite generation ($p \leq 0.0042$) with significantly higher levels of metabolites present in large systems (58.8 %) compared to both small ($p \leq 0.05$, 50.1 %) and medium ($p \leq 0.01$, 43.4 %) microcosms (**Fig. 3.3**). There was no significant difference in metabolite generation between small and medium microcosms.

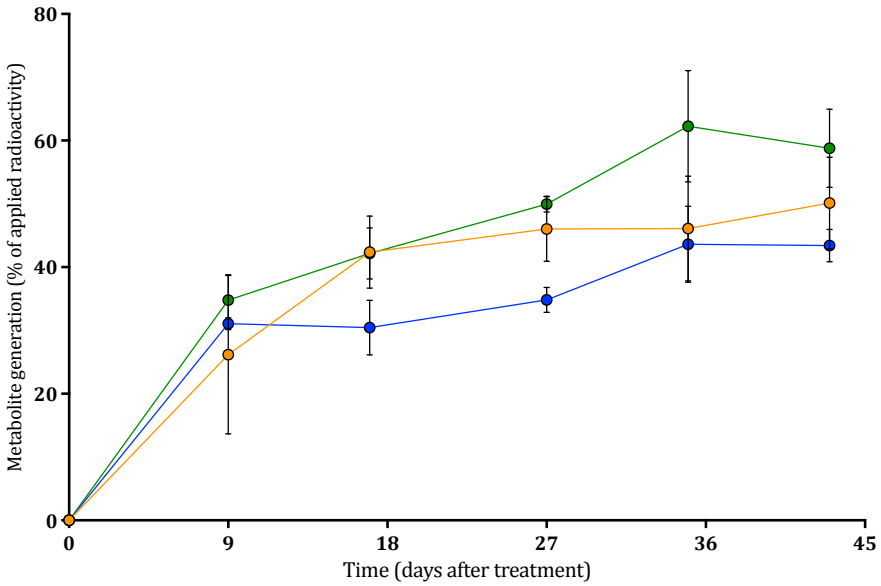

Figure 3.3: Generation of metabolites in different sized water-sediment microcosms as a percentage of the radioactivity originally applied.
Generation of metabolites in small (orange), medium (blue), and large (green) microcosms over 43 days. Error bars show ± standard deviation.

3.3.2.iii Water and sediment partitioning of isopyrazam and metabolites

Although isopyrazam decline had a similar trend between different sized microcosms, the dynamics of the partitioning of radioactivity between the water and sediment fractions were dissimilar (**Fig. 3.4**). In the water fraction, there was a significant impact of microcosm type on partitioning of radioactivity ($p \leq 0.0002$, **Fig. 3.4.a**), with a significantly higher percentage remaining in the water column in the large microcosms (42.3 %, $p \leq 0.001$) compared to the small (37.2 %) and medium (33.1 %) microcosms. There was, however, no significant impact of microcosm type on partitioning of radioactivity to the

sediment ($p \leq 0.1280$, **Fig. 3.4.b**. Nevertheless, there was higher fluctuation in the amount of radioactivity partitioned to the sediment in the small microcosms. In particular, partitioning to the sediment in the small microcosms was higher at 17 DAT (66.1 %), and this subsequently decreased suggesting degradation in the sediment was occurring.

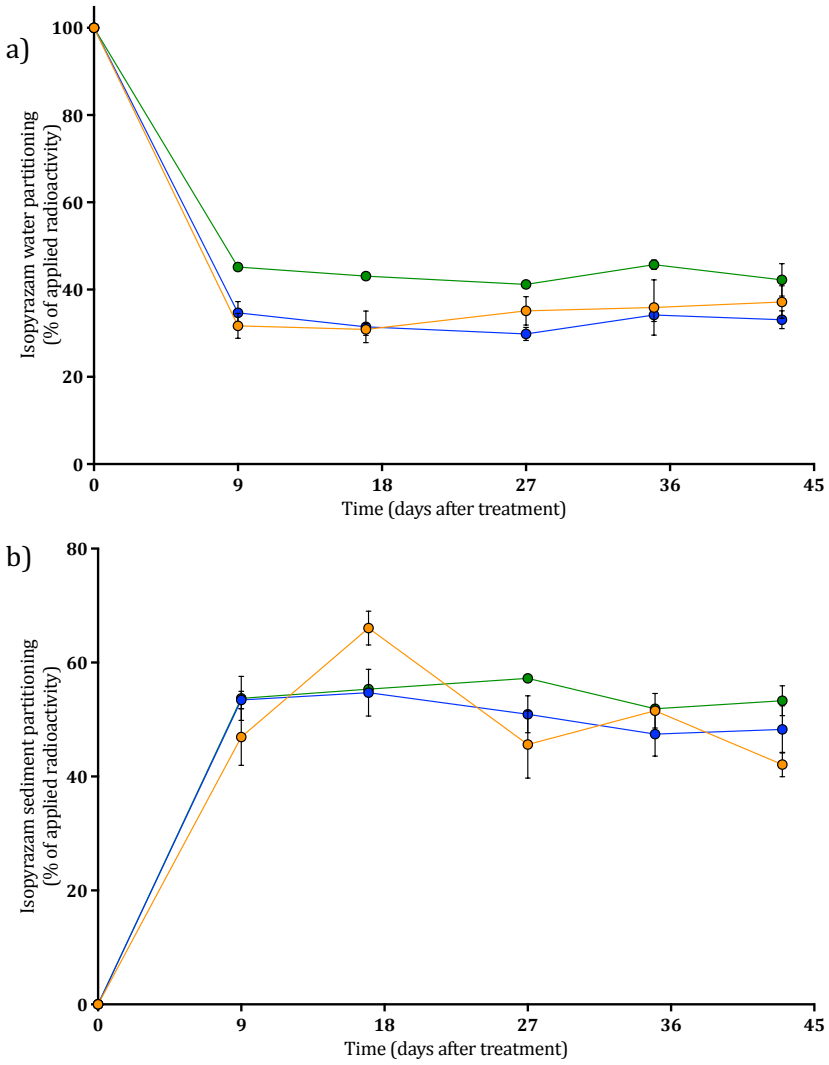

Figure 3.4: Partitioning of total radioactivity to the water fraction (a) and the sediment fraction (b) as a percentage of the total applied radioactivity.
Partitioning of radioactivity in small (orange), medium (blue), and large (green) microcosms over 43 days. Error bars show ± standard deviation.

3.3.2.iv Sediment fraction non-extractable residues

There was a significant difference between microcosms in the amount of radioactivity which was non-extractable from the sediment ($p \leq 0.0001$, **Fig. 3.5**). NER

represented 17.6 and 15.1 % of the total amount of applied radioactivity in small and medium microcosms, respectively. In the larger systems, NER was only 3.2 % of the applied radioactivity and this was significantly less ($p \leq 0.0001$) compared to small and medium microcosms.

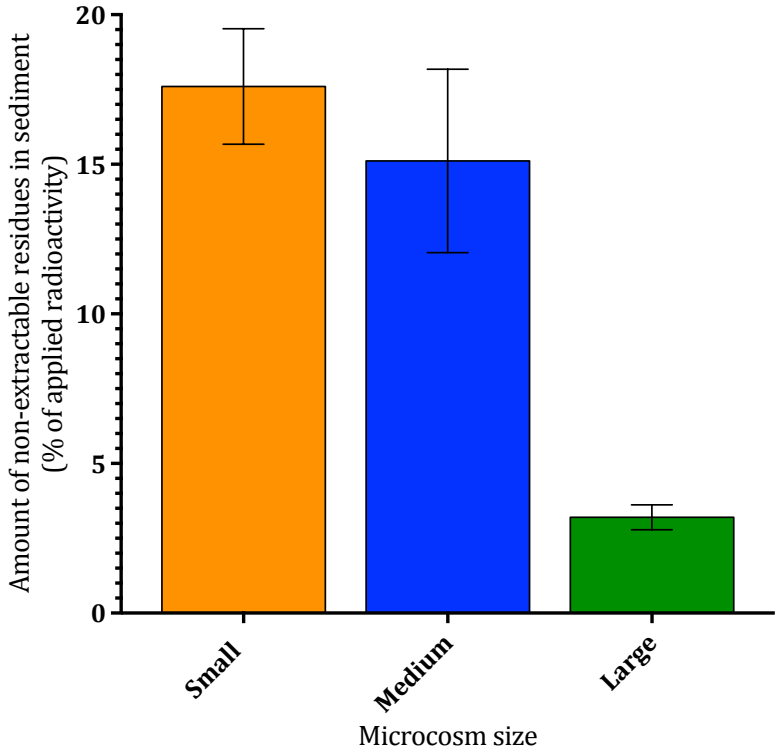

Figure 3.5: Amount of NER remaining in the sediment at the end of the experiment as a percentage of the total applied radioactivity. Amount of NER in the sediment at 43 DAT in small (orange), medium (blue), and large (green) microcosms over 43 days. Error bars show ± standard deviation.

3.3.2.v Isopyrazam mineralisation

There was a significant difference between microcosm type when assessing the cumulative amount of isopyrazam mineralised to $^{14}CO_2$ by 43 DAT ($p \leq 0.0167$, **Fig. 3.6**). The percentage mineralised was low in all microcosms; however, the amount increased slightly with a decrease in microcosm scale and small microcosms (0.05 %) had significantly more ($p \leq 0.05$) mineralisation compared to large microcosms (0.01 %). Small microcosms showed increased variation, evident by the large standard deviation, so although the average amount mineralised was higher than the other microcosms, the range between replicates was within the range of the other systems.

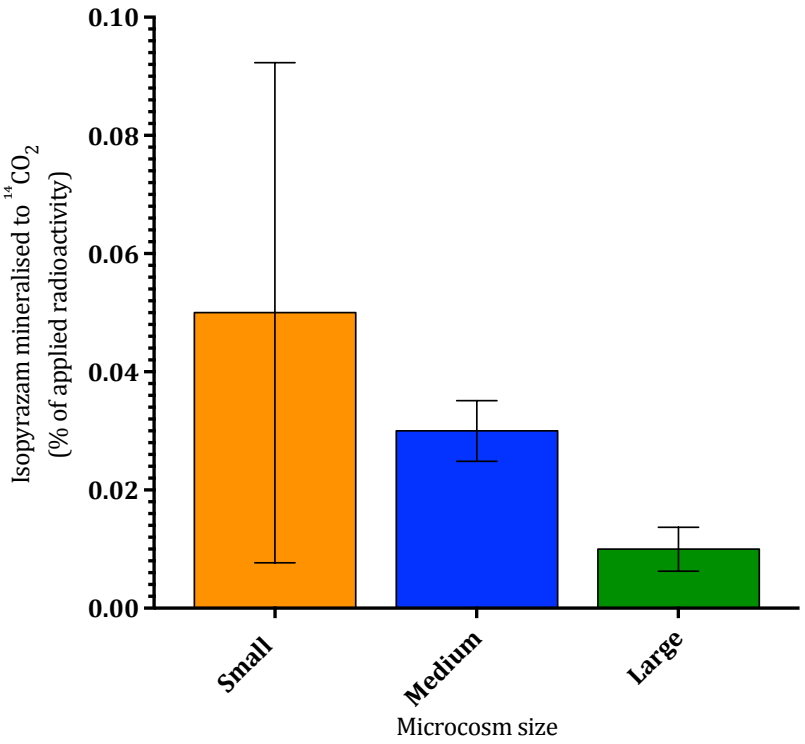

Figure 3.6: Cumulative amount of isopyrazam mineralised to $^{14}CO_2$ as a percentage of the total applied radioactivity. Mineralisation of isopyrazam in small (orange), medium (blue), and large (green) microcosms over 43 days. Error bars show ± standard deviation.

3.3.3 Water chemistry analysis results

3.3.3.i Water pH

Generally, the trend of pH in the water was similar between treatments with an increase in all microcosms from the start of the experiment (8.1). Nevertheless, there was a significant impact of microcosm type on water pH ($p \leq 0.0001$, **Fig. 3.7**) with small microcosms having a significantly lower pH ($p \leq 0.001$) overall compared to medium and large microcosms. By the end of the experiment, pH in the small microcosms was 9.3; however, in the medium and the large microcosms it was 9.7 and 10.1, respectively.

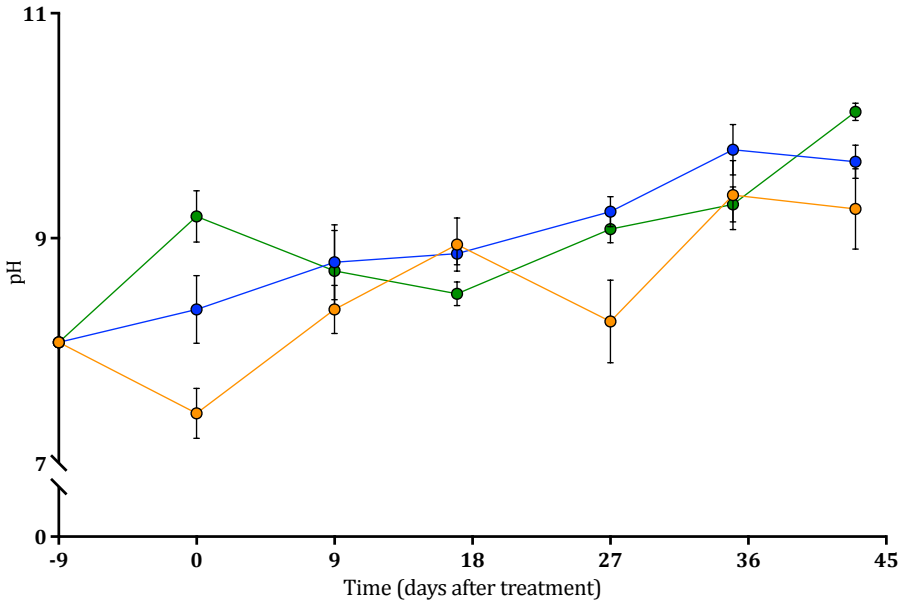

Figure 3.7: pH of the water in different sized microcosms. pH of the water in small (orange), medium (blue), and large (green) microcosms over 43 days. Error bars show ± standard deviation.

3.3.3.ii Water macronutrient concentration

There was no significant difference between microcosms for water NO_3- concentration ($p \leq 0.1511$, **Fig. 3.8**). There were significant fluctuations over time ($p \leq 0.0001$), yet these remained similar regardless of microcosm size. When sampled from the river, NO_3- concentration was at 26.4 mg/L, and this decreased in all systems to between 3.5 and 14.6 mg/L by 9 DAT. By 27 DAT the concentration had risen to between 30.2 and 33.7 mg/L, and this increase continued until 35 DAT.

There was a significant impact of microcosm size and the PO_4 concentration in the water ($p \leq 0.01$, **Fig. 3.9**). Small microcosms had a spike at 0 DAT, prior to isopyrazam addition, amounting to 1.9 mg/L and, although levels were similar by the end of the experiment, across the time course these systems had significantly higher concentrations compared to medium ($p \leq 0.05$) and large ($p \leq 0.01$) microcosms. Samples from the river contained 0.9 mg/L of PO_4 and overall there was a decrease in all systems to between 0.2 and 0.4 mg/L by 43 DAT.

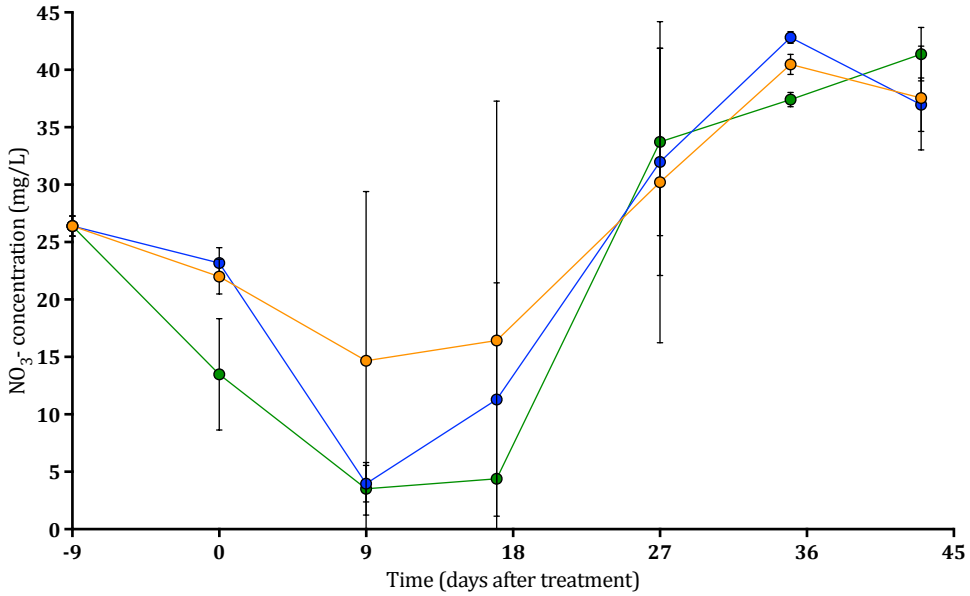

Figure 3.8: NO_3- concentration of the water in different sized microcosms. NO_3- concentration of the water in small (orange), medium (blue), and large (green) microcosms over 43 days. Error bars show ± standard deviation.

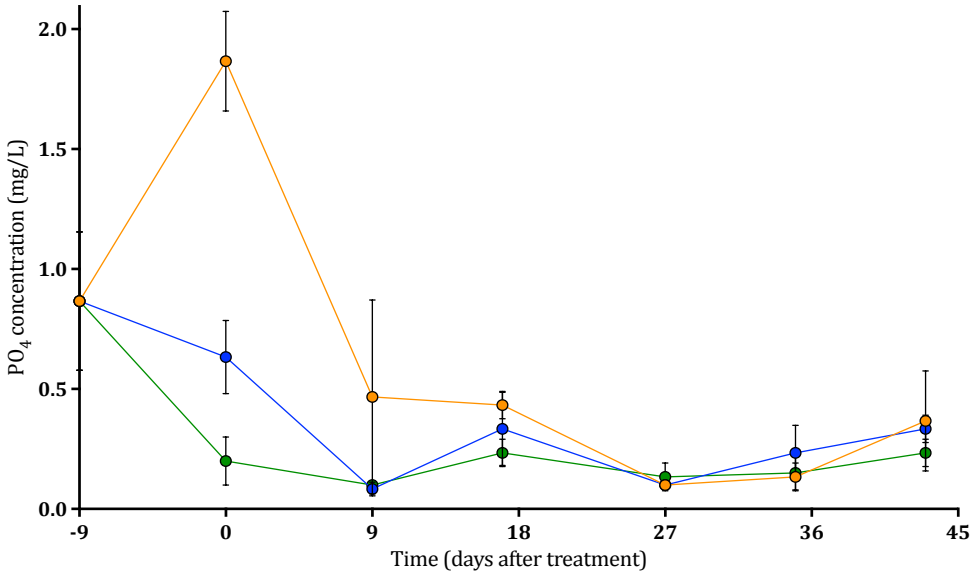

Figure 3.9: PO_4 concentration of the water in different sized microcosms. PO_4 concentration of the water in small (orange), medium (blue), and large (green) microcosms over 43 days. Error bars show ± standard deviation.

3.3.4 Microbial analysis results

3.3.4.i Chlorophyll a *concentration*

The concentration of chlorophyll *a* in both the water and the sediment was summed together but there were no significant differences ($p \leq 0.0607$) between the microcosm sizes and their impact on the concentration within the systems across the time course (**Fig. 3.10**). There was an increase in concentration along the time course in all systems; however, small microcosms also had some large spikes in abundance (e.g. 10.8 mg/m^3 at 9 DAT). By the end of the experiment there was 6.1, 4.0, and 4.5 mg/m^3 of chlorophyll *a* in small, medium, and large sized microcosms, respectively.

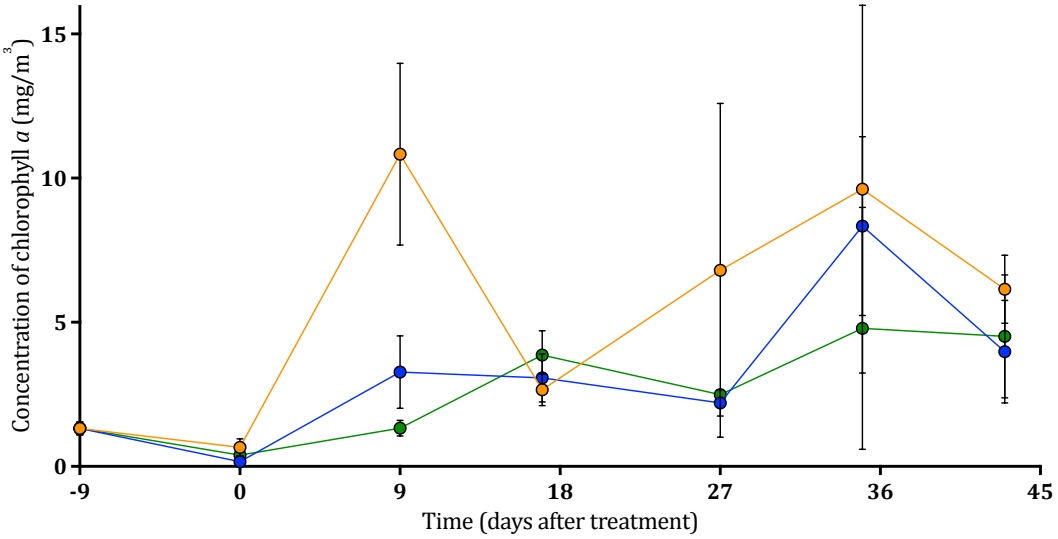

Figure 3.10: Chlorophyll *a* concentration in the water and sediment in different sized microcosms. Chlorophyll *a* concentration of the water and sediment in small (orange), medium (blue), and large (green) microcosms over 43 days. Error bars show ± standard deviation.

3.3.4.ii Microbial community rarefaction

Bacterial community data was rarefied at 2000 sequences leaving 4353 OTUs (**Table 3.3,** see section IV.3.8 for details). Phototrophs were initially rarefied to 10,000 sequences. Non-phototrophs were then removed from the original phototroph sequences, leaving 70 samples with an average of 9101 sequences per sample; this data was then rarefied at 1200 sequences to leave 69 samples and 543 OTUs (**Table 3.3**).

Table 3.3: OTU table summaries for bacterial and phototrophic analysis. Data was rarefied and numbers in italics show the summary post-rarefaction. Phototroph data was rarefied before and after non-phototroph communities were discarded and these are separated by a forward-slash.

OTU table summary	16S rRNA (bacterial)	23S rRNA (phototrophic)
Sample count	74, *64*	70, *66/69*
Number of OTUs across all samples	4709, *4353*	5841, *5306/543*
Average sequences/sample	3941	25,563
Rarefaction level	2000	10,000/1200

3.3.4.iii Bacterial community composition of the microcosm systems

Fresh water and sediment from the river were analysed as well as water and sediment samples from the microcosms at 43 DAT. The α diversity of the bacterial community was calculated using Fischer's α index in both the water (**Fig. 4.11.a**) and sediment (**Fig. 4.11.b**) fractions. In the water, there was a significant impact ($p \leq 0.0139$) of treatment on α diversity. Fresh samples had a significantly higher ($p \leq 0.05$, 111.2) α diversity compared to all microcosms at the end of the experiment, which showed no significant difference, regardless of size. There was also a significant impact ($p \leq 0.0001$) of treatment on α diversity in the sediment. All treatments were significantly different to each other ($p \leq 0.0001$, except $p \leq 0.01$ between medium and large microcosms) with fresh samples having the highest α diversity (593.1). At the end of the experiment, α diversity decreased with microcosm size, with higher diversity in large microcosms (309.4) and lower diversity in small microcosms (80.3). This suggests that as sample inoculum size increased, diversity in the microcosms was more similar to the diversity in the fresh river sample.

PERMANOVA determined a significant impact of microcosm treatment on β diversity in both the water ($p \leq 0.005$) and the sediment ($p \leq 0.002$) fractions, although R^2 values were midrange (0.53 and 0.56, respectively) showing there were not high levels of dissimilarity between samples. Pairwise tests, however, showed that there were no significant differences in β diversity between the separate treatments ($p \leq 0.6$ or $p \leq 1.0$). Despite this, R^2 values give some insight into which samples differed the most from each other. In both water and

sediment pairwise tests, R^2 values were higher when comparing microcosm treatments at the end of the experiment to the fresh samples from the river (0.54 to 0.69). Nevertheless, when comparing between microcosms, R^2 values were low (under 0.39). This showed that although microcosms were similar to each other by 43 DAT, when fresh sample was incubated under laboratory conditions β diversity of the community changed; this can be seen clearly in **Figure 3.12** with microcosm samples (orange, blue, and green) clustering further away from fresh samples (red).

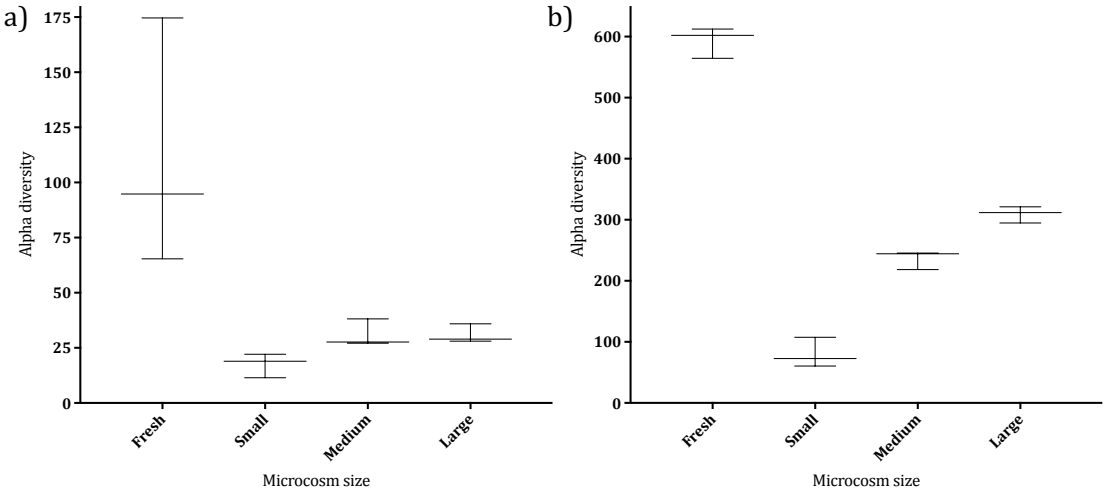

Figure 3.11: Alpha diversity of bacterial communities between microcosm systems in the water (a) and the sediment (b). Fisher's α index was calculated from the observed bacterial species at the sample site and from each microcosm at the end of the experiment, with the whiskers showing the minimum and maximum values and the middle lines showing the median values.

Bacteria phyla relative abundance was analysed for both the water and the sediment and there was a significant difference ($p \leq 0.0001$) between treatment and phyla in both the water (**Fig. 3.13.a**) and the sediment (**Fig. 3.13.b**) fractions. In the water, fresh samples had significantly higher levels of Actinobacteria ($p \leq 0.0001$, 14.3 %), Bacteroidetes ($p \leq 0.001$, 25.8 %), and Proteobacteria ($p \leq 0.0001$, except $p \leq 0.05$ compared to small microcosms, 49.4 %), but significantly less Cyanobacteria ($p \leq 0.0001$, 0.4 %) compared to the microcosms at the end of the experiment. Medium and large microcosms had similar relative abundances across all phyla; however, small microcosms had a significantly higher relative abundance of Bacteroidetes ($p \leq 0.01$, 14.8 %) and Proteobacteria ($p \leq 0.0001$, 41.0 %), and significantly lower levels of Cyanobacteria ($p \leq 0.0001$, 25.7 %) compared to the other treatments at 43 DAT.

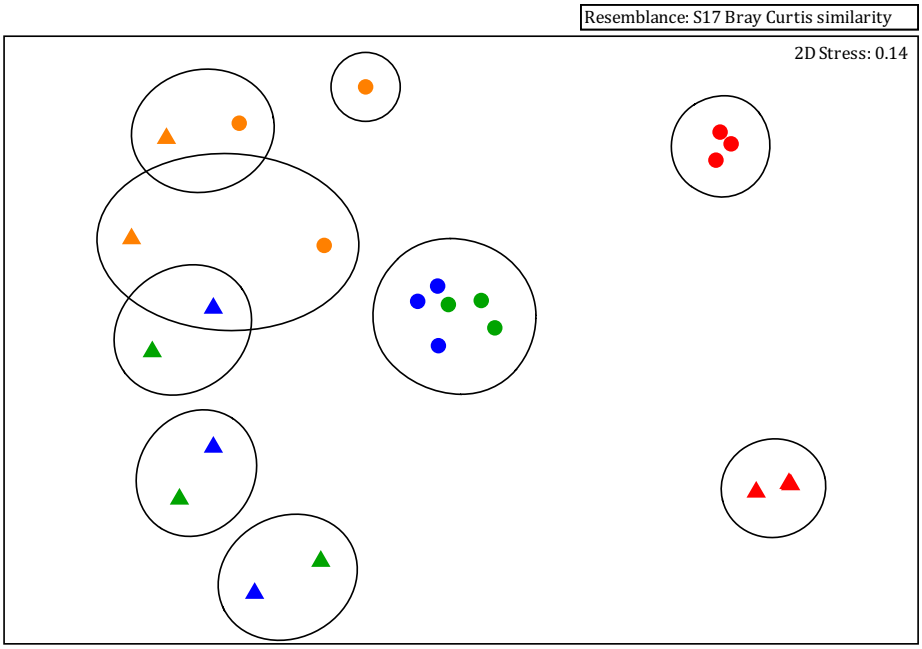

Figure 3.12: Ordination plots from NMDS scaling analysis of Bray Curtis similarities between bacteria in microcosm treatments. Water (triangles) and sediment (circles) were analysed at the start of the experiment (red) and at 43 DAT in small (orange), medium (blue), and large (green) microcosms. Black lines represent a similarity threshold of 30 %.

In the sediment fraction, fresh samples had significantly higher levels of Acidobacteria ($p \leq 0.0001$, 9.6 %), Actinobacteria ($p \leq 0.0001$, 12.2 %), Chloroflexi ($p \leq 0.0001$, 15.0 %), and Nitrospirae ($p \leq 0.05$, 4.6 %), but lower levels of Cyanobacteria ($p \leq 0.0001$, 0.03 %) and Proteobacteria ($p \leq 0.0001$, 31.5 %) compared to the microcosm samples at the end of the experiment. Comparing just the systems at the end of the experiment, small microcosms had higher levels of Gemmatimonadetes ($p \leq 0.05$, 4.5 %), but lower levels of Acidobacteria ($p \leq 0.05$, 0.6 %) and Chloroflexi ($p \leq 0.0001$, 3.0 %) compared to medium and large microcosms, whereas large microcosms has significantly less Cyanobacteria ($p \leq 0.0001$, 25.5 %) compared to small (31.3 %) and medium (28.7 %) microcosms. Lastly, both fresh and small microcosm samples had significantly higher levels of Planctomycetes ($p \leq 0.05$, 4.7 % for both) compared to medium microcosms (1.5 %) and large microcosms (1.9 %). No OTUs were significantly different between microcosm treatments.

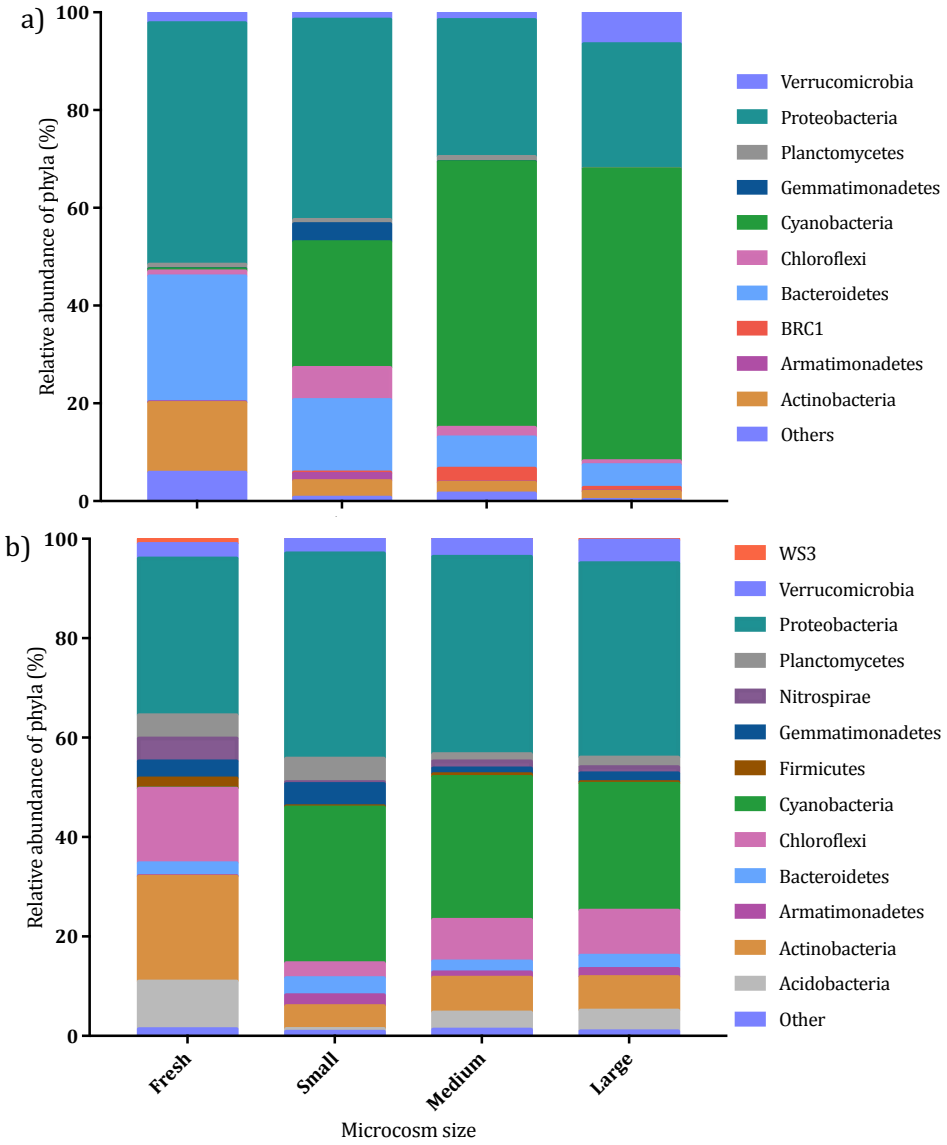

Figure 3.13: Relative abundance of bacterial phyla between microcosm treatments in the water (a) and the sediment (b). Different bacterial phyla are denoted by different colours and phyla making up < 1 % of the relative abundance are listed under *other*. Analysis was carried out on water and sediment at the beginning of the experiment and at 43 DAT.

3.3.4.iv Phototrophic community composition of the microcosm systems

There was no significant difference in the α diversity between different systems in the water fraction ($p \leq 0.3448$, **Fig. 3.14.a**), which ranged between 6.5 and 8.4. In the sediment fraction (**Fig. 3.14.b**), however, microcosm treatments had significantly different α diversities ($p \leq 0.0001$). Fresh samples had a higher α diversity ($p \leq 0.0001$, 33.9)

compared to the microcosm samples at 43 DAT. Furthermore, large microcosms (17.8) had a significantly higher α diversity ($p \leq 0.05$) compared to the small microcosms (11.4). There was no significant difference between the medium size microcosms and either the small or large microcosms.

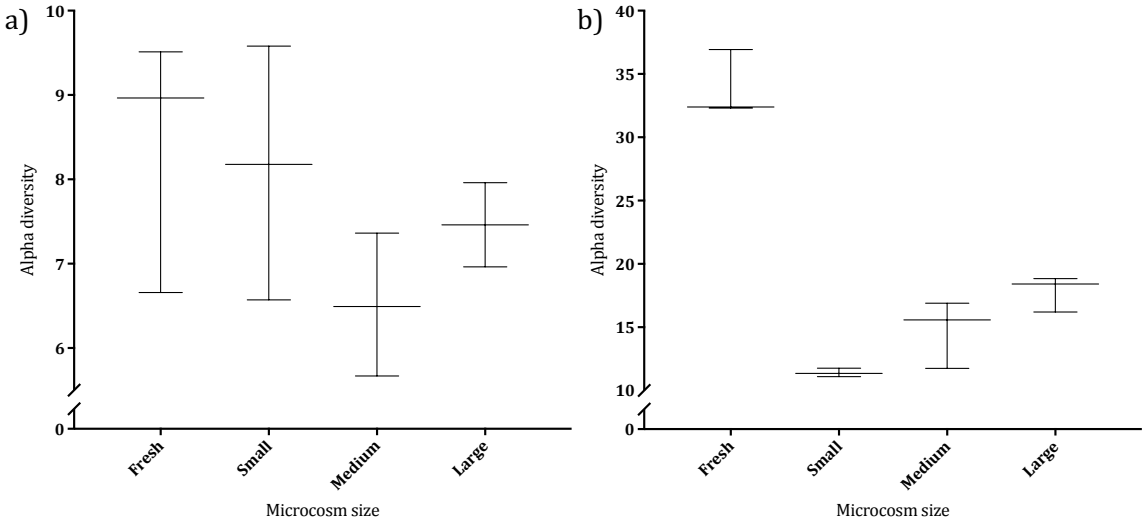

Figure 3.14: Alpha diversity of phototrophic communities between microcosm treatments in the water (a) and the sediment (b) fractions. Fisher's α index was calculated from the observed phototrophic species at the sample site and from each microcosm treatment at the end of the experiment, with the whiskers showing the minimum and maximum values and the middle lines showing the median values.

PERMANOVA analysis ascertained that β diversity of phototrophic communities was significantly impacted by microcosm treatment in both the water ($p \leq 0.03$) and the sediment ($p \leq 0.002$) fractions, although R^2 values were midrange (0.52 and 0.59, respectively) suggesting that dissimilarity between samples was not high. Pairwise tests, however, showed no significant difference between separate treatments ($p \leq 0.6$ or $p \leq 1.0$). R^2 values can give insight into which samples differed the most from each other, and values were higher in fresh river samples relative to microcosm samples at the end of the experiment (0.59 to 0.64 in the water and 0.61 to 0.71 in the sediment). When comparing just between microcosm treatments, however, R^2 values were low (under 0.34). This showed that microcosm samples were similar despite incubation in different vessels, yet these samples were more dissimilar to fresh river samples. This divergence can be seen in **Figure 3.15**, with fresh samples (red) clustering away from microcosm samples (orange, blue, and green).

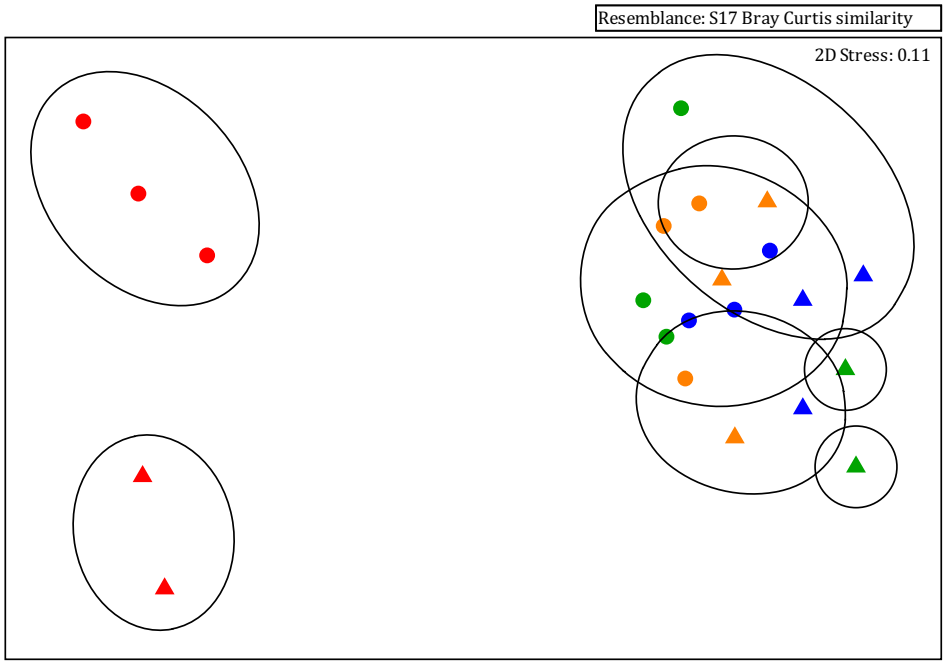

Figure 3.15: Ordination plots from NMDS scaling analysis of Bray Curtis similarities between phototrophic communities in microcosm treatments. Water (triangles) and sediment (circles) were analysed at the start of the experiment (red) and at 43 DAT in small (orange), medium (blue), and large (green) microcosms. Black lines represent a similarity threshold of 30 %.

Abundance of phototrophic OTUs amplified using the 23S rRNA gene can be found in Appendix II.4. There was a significant difference between phototrophic taxa and microcosm treatment in both the water and the sediment fractions ($p \leq 0.0001$). After incubation under laboratory conditions, the phototrophic community diversity reduced significantly ($p \leq 0.0001$) in terms of taxa present at higher relative abundances (> 1 %), and systems became dominated by Cyanobacteria (between 83.1 and 98.2 %). Fresh samples had a significantly lower Cyanobacteria relative abundance compared to the microcosms in both the water (1.9 %) and the sediment (4.6 %) fractions. In the water fraction (**Fig. 3.16.a**), fresh samples had significantly higher relative abundances of Cryptophyta ($p \leq 0.05$, 10.5 %), Diatoms ($p \leq 0.0001$, 15.0 %), Golden Algae ($p \leq 0.0001$, 34.3 %), and Haptophyta ($p \leq 0.0001$, 17.8 %) compared to the microcosms at 43 DAT. Both fresh samples and samples from small microcosms had a higher relative abundance ($p \leq 0.01$) of Chlorophyta (11.7 and 12.1 %, respectively) compared to medium (1.6 %) and large (0.6 %) microcosms and,

additionally, small microcosms also had a lower relative abundance of Cyanobacteria ($p \leq 0.0001$, 83.1 %) compared to medium and large microcosms (97.9 and 98.2 %).

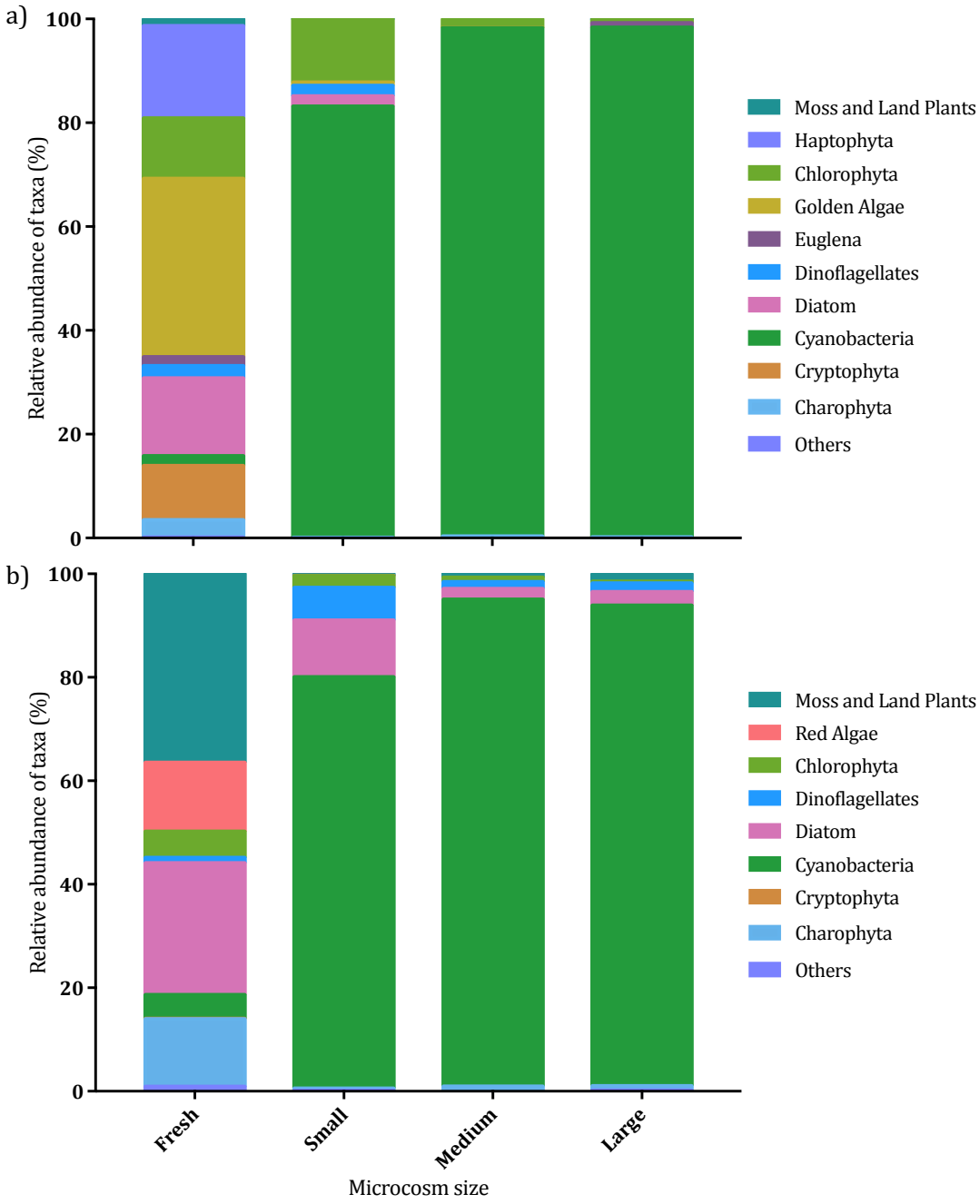

Figure 3.16: Relative abundance of phototrophic taxa between microcosm treatments in the water (a) and the sediment (b). Different phototrophic taxa are denoted by different colours and taxa making up < 1 % of the relative abundance are listed under *other*. Analysis was carried out on water and sediment at the beginning of the experiment and at 43 DAT.

In the sediment fraction (**Fig. 3.16.b**), fresh samples had significantly higher relative abundances ($p \leq 0.0001$) of Charophyta (13.1 %), Diatoms (25.5 %), Moss and Land Plants (e.g. seeds, roots from river, etc., 36.5 %), and Red Algae (13.3 %) compared to the microcosm samples at the end of the experiment. In addition, relative abundance of Cyanobacteria was significantly lower ($p \leq 0.0001$) in the small microcosms (79.5 %) compared to the medium (94.1 %) and large (92.6 %) microcosms. In contrast, Diatoms were significantly higher ($p \leq 0.001$, 11.0 %) in small microcosms relative to medium and large microcosms (2.1 and 2.6 %, respectively). No OTUs were significantly different between microcosm treatments.

3.4 DISCUSSION AND CONCLUSIONS

There were no statistically significant differences in isopyrazam degradation rate between the three microcosm sizes. There were, however, differences in the formation of metabolites between the systems and the percentage of NER in the sediment fraction. NER increased with decreasing microcosm size; however, although metabolite generation was highest in large systems, it did not progressively decrease with microcosm size. Microbial community structure was generally similar between microcosms, although there was a significant reduction in the diversity of bacterial and phototrophic sediment communities with decreasing microcosm size.

Despite similarity in microbial community structure between microcosms, all systems diverged from the fresh sample from the river. Notably, the majority of phototrophic taxa diminished once incubated under laboratory conditions so that one phylum (Cyanobacteria) dominated the phototrophic relative abundance; this is likely the reason for the NO_3- fluxes in the water, as Cyanobacteria have been shown to be important for nitrification and denitrification processes (Chen *et al.*, 2016b). Despite some small significant differences in isopyrazam fate, the overall DegT50 was similar between microcosms, suggesting that there could be scope for smaller scale tests to be used for some purposes (e.g. high-throughput testing of a large number of compounds). Further work would be required to develop this methodology, including the testing of more compounds, particularly those that are primarily degraded by heterotrophic organisms rather than phototrophic communities, which are most associated with isopyrazam degradation.

3.4.1 Variation of kinetic processes between microcosm sizes

Several studies have shown that an increase in test system size can increase degradation rate (Khan and Zytner, 2011, Khan and Zytner, 2013, Khan *et al.*, 2015). In this experiment, however, although large microcosms had a higher percentage of radioactivity comprising metabolites compared to small or medium microcosms, the DegT50s between the systems were similar. In this experiment, the large microcosms had a higher percentage of radioactivity partitioned to the water fraction compared to the small and medium microcosms. This could suggest that isopyrazam had greater bioavailability in the large

microcosms and thus greater accessibility for degrading communities present within the water column (e.g. planktonic algae). The higher percentage of NER in small and medium microcosms could suggest that less compound was available for degradation within the water column of these microcosms, although biofilm on the sediment surface could have had a more significant role in these systems.

Large microcosms had a larger depth and volume of water compared to the other microcosms. This can cause compounds to have a longer residence time within the water fraction where biodegradation could have occurred prior to sediment biofilm sorption (Särkkä *et al.*, 1996). Higher water depths increase the distance molecules need to travel to reach the sediment, thus decreasing sorption rates and settlement within the sediment. Whereas in shallow water there is a shorter distance to travel, leading to an increase in sorption to the sediment and an increased binding potential (Calvert and Pedersen, 2010, Gaullier *et al.*, 2017, Lange *et al.*, 2011). Phototrophic microbes have been shown to be metabolically capable of degrading isopyrazam (Hand and Oliver, 2010) and deeper water has also been shown to have the potential to increase the amount of suspended algae (Bouwer and Rice, 1989), although there is little evidence to support an increase of water column phototrophs in large systems in this data. Nevertheless, phototrophic biofilm on the sediment surface has degradative capabilities should isopyrazam subsequently reach the sediment surface (Thomas and Hand, 2012).

In the environment, microbes are not uniformly distributed and so the number of degraders present in an inoculum will increase with sample volume (Aichberger *et al.*, 2005, Hoyle and Arthur, 2000). Higher bacterial diversity can contribute to degradation due to a higher probability that degraders are present in the inoculum, and this can change biodegradation kinetics between or within experiments (Courtes *et al.*, 1995, Kool, 1984, Thouand *et al.*, 2011, Thouand *et al.*, 1995). Biofilms in particular can have high diversity, meaning that there is a greater chance that rare species are present, and a vast metabolic function with the potential for genetic exchange between organisms (Sabater *et al.*, 2007, Schwartz *et al.*, 2003, Singh *et al.*, 2006, Thouand *et al.*, 2011, Thouand *et al.*, 1995). Biofilms additionally have the potential to sorb and degrade pollutants, and subsequently release metabolites (Flemming, 1993, Flemming, 1995, Sánchez-Pérez *et al.*, 2013, Thomas and Hand, 2012, Writer *et al.*, 2011). Biodegradation is dependent on the quality and quantity of

consortia and degradation is unlikely to occur via a single species (Arif *et al.*, 2012, Courtes *et al.*, 1995, Elias and Banin, 2012, Levanon, 1993, McGenity *et al.*, 2012). This could include synergistic relationships between algae and bacteria (Borde *et al.*, 2003, McGenity *et al.*, 2012), suggesting that even if an increase in diversity doesn't directly impact degrader community abundance, other communities may indirectly play a role in their proliferation.

There were differences in bacterial and phototroph α diversity associated with the sediment fraction of the different microcosms, with higher diversities in the large systems. This could suggest that the biofilm communities on top of the sediment layer were more diverse and productive in the large microcosms. Indeed, Uzarski *et al.* (2004) determined that systems containing higher amounts of sediment (20 cm) had an increased primary productivity and respiration compared to those with lower depths (5 cm), due to higher substrate availability for heterotrophic colonisation and metabolism. In large systems, the high diversity associated with the sediment could have aided in the increased percentage of metabolites in the water fraction. Metabolites are generally more polar and less hydrophobic than the parent compound (Schüle *et al.*, 2008, Singh, 2012) and this was evident from the shorter metabolite retention time during TLC analysis (Appendix II.3). If metabolites were released back into the water fraction, it explains the higher radioactivity in this compartment.

In small and medium microcosms, however, there was higher NER formation. The proportion of NER in the sediment can be controlled by multiple factors, such as pesticide and substrate properties, biological activity, and environmental conditions e.g. temperature (Barriuso *et al.*, 2008). Considering that laboratory conditions and sediment inoculum were controlled in this experiment, differences in microbial communities within the different sized systems could additionally have played a role in the formation of a higher percentage of NER in small and medium microcosms. Some studies propose that a higher proportion of NER is associated with an inhibition of metabolism or low metabolic capabilities of the microbial community (Barriuso *et al.*, 2008, Kästner *et al.*, 1999). Small and medium microcosms did have a lower α diversity in the sediment compared to large microcosms, so potentially there was a lower chance that degrading communities were present in these systems (Kool, 1984, Thouand *et al.*, 2011, Thouand *et al.*, 1995).

Nevertheless, NER can be comprised of both parent compound and metabolites (Kästner *et al.*, 1999), so formation of NER does not necessarily mean that a pesticide has not been degraded. Additionally, NER can be biogenic in nature if degraders incorporate carbon (in this case ^{14}C) from pesticides into cellular components (Nowak *et al.*, 2013, Nowak *et al.*, 2011). Biogenic NER formation is usually associated with higher mineralisation rates (Nowak *et al.*, 2014) and there was significantly higher mineralisation in small compared to large microcosms. Regardless, as systems contained phototrophs the extent of any mineralisation will be difficult to determine due to associated CO_2 fixation (Madigan *et al.*, 2009). Further analysis would need to be carried out; however, if the NER in the small and medium microcosms were biogenic, it could suggest that the metabolic capabilities were actually similar between microcosm sizes, but there were differences in how the metabolites were compartmentalised in the systems e.g. water fraction in large systems and, possibly biogenic, NER in the small and medium systems.

There is evidence of better mixing between the water and sediment at lower water depths (Chandler *et al.*, 2016) and this may influence contact between dissolved chemicals and the sediment, influencing sorption. Biofilm on top of the sediment bed, however, could act as a barrier to mixing, decreasing connectivity to the lower sediment layers (Battin and Sengschmitt, 1999). The small and medium microcosms had a lower water depth and a lower surface area to sediment volume ratio compared to the large microcosms. If isopyrazam is mainly sorbed to the top layer of biofilm, or ^{14}C is present as biogenic NER within this microbial biomass, this would result in a higher percentage of radioactivity present within the sediment fraction (including the biofilm) than in the large microcosms. Furthermore, as phototrophic microorganisms may play a key role in isopyrazam degradation (Hand and Oliver, 2010), light will be able to penetrate these lower sediment depths in the small and medium microcosms to a greater extent. This might have caused more efficient assimilation of metabolites into microbial biomass within the sediment bed and reduction of metabolite diffusion back into the water fraction; thus, explaining the higher proportion of NER in small and medium systems (Nowak *et al.*, 2011),

3.4.2 Representation of communities and biodegradation potential

Generally, the relative abundances of communities were similar between the three microcosms, however, there were some minor differences between the small microcosms compared to medium and large microcosms. Nevertheless, all microcosms deviated from the fresh sample community. This poses the question of how relevant these tests are to the environment if the microbial community is substantively changed under laboratory conditions. Environmental changes, such as when samples are moved from their natural habitat to the laboratory, can lead to new selection pressures. Microbial community diversity and relative abundance will be reassembled, causing disruption to physiological and metabolic activities, such as pesticide degradation (Epstein, 2013, Hunter-Cevera, 1998, Kertesz and Mirleau, 2004). It proves difficult for sampling to account for the diversity present in large and heterogeneous populations in nature, and only a fraction of this diversity will be represented in laboratory samples (Keith, 1991, Morris *et al.*, 2002, Stewart, 2012).

Laboratory microcosm studies can lead to ambiguous results as small subsets of environmental samples will be dynamic due to uneven distribution of microbes in nature (Aichberger *et al.*, 2005, Brockman and Murray, 1997, Hoyle and Arthur, 2000). Ideally, these tests should mimic the diversity and abundance of microbial communities in environmental compartments to provide an accurate representation of the processes which they carry out e.g. biodegradation (Dechesne *et al.*, 2014, Thornton and Wilson, 2008). This can prove difficult, especially from biases due to microbial community variation in space and time e.g. seasonal variation (Environment Agency, 2003). Laboratory tests are a useful tool to determine biodegradation as they provide a level of control over experimental variables (Aichberger *et al.*, 2005, Sturman *et al.*, 1995). Organisms, however, will most efficiently mimic their dynamics in nature when grown in conditions similar to their natural habitat, and this is often not replicated in the laboratory (Stewart, 2012). Regulatory studies would benefit from more closely mimicking the real environment to ensure communities, and degradative potential, is represented as well as possible.

3.4.3 Scope for high-throughput tests

Although there were some differences between different scaled microcosms, the DegT50s between systems were similar. The DegT50 is the most important output from the study with respect to the environmental risk assessment (OECD, 2002b). In this test, small microcosms gave a similar DegT50 to large microcosms. If the purpose, therefore, of high-throughput tests is to estimate and compare DegT50 across a range of compounds, there does appear to be potential for small microcosms to fulfil this need.

Determination of the formation and decline of transformation products is also a key output from OECD 308 studies (OECD, 2002b). In this experiment, there were differences observed in the total measured amounts of transformation products between the test systems. Additionally, in small and medium microcosms, although there was a higher percentage of NER, these residues could be assimilated metabolites which accumulated in the water in the large microcosms. If the NER mainly consist of metabolites, then the main difference between the large microcosms and the small and medium microcosms is where these metabolites are partitioned within the system. Although the metabolites in large systems could be readily available for further degradation in the water fraction, if the NER in the small and medium microcosms are bound to the sediment, the residues are assumed less bioavailable, less mobile, and less toxic (Kästner *et al.*, 1999). If NER are biogenic in nature within the biofilm, however, it suggests high levels of turnover within the microbial community, meaning biodegradation rate could be similar to large microcosms, despite dissimilar partitioning within the systems (Nowak *et al.*, 2013, Nowak *et al.*, 2011). Without further investigation into how these NER have been formed, the utility of smaller microcosms for accurately predicting transformation product formation is, therefore, less certain at this stage.

Additional work on other compounds would need to be carried out to determine that the results from this study were not compound specific. This would need to include studies within the confines of OECD 308 tests, e.g. under dark conditions (OECD, 2002b), to determine whether there is similarly little impact with microcosm scale from a regulatory point of view. These tests are unlikely to ever be entirely realistic as specific conditions influencing microorganisms, and their associated processes, may not always be represented

on a small scale, thus potentially influencing the outcome of biodegradation (McDonald and Rittmann, 1993). This experiment, however, showed that small microcosms can reflect processes seen on a larger scale to some extent (e.g. DegT50), suggesting that there is the scope for smaller tests to be used as a high-throughput method. Although tests may not fully represent the processes occurring on a larger scale (e.g. partitioning verses degradation), they could give some indication of the main degradation and fate mechanisms which can then be assessed further in larger scale systems. Small scale systems would be beneficial for use as an initial screening test, and it would be cheaper (less materials, especially radiochemical, required), permit a higher level of replication, and allow an increase in the possible number of variables assessed. (Aichberger *et al.*, 2005, Carpenter, 1996, EPA, 2000, Khan and Zytner, 2011, Spain *et al.*, 1984).

3.4.4 Conclusions

In terms of isopyrazam recovery and DegT50, there were no significant differences between microcosm sizes. Despite this, there were differences in the fate and transformation processes, with large systems having a higher proportion of metabolites available in the water fraction and small and medium microcosms having a higher proportion of NER. This could have been due to a higher water depth and volume in the large microcosms, allowing isopyrazam to have a longer residence time in the water fraction where degradation could occur. In small and medium microcosms, the water depth and volume was smaller, allowing isopyrazam to partition to the sediment fraction and form NER.

Water chemistry and microbial communities were similar within the microcosms; however, α diversity in the sediment did increase with microcosm size. In the large microcosms, this could contribute to the higher percentage of metabolites in the water fraction; however, without assessment on how the NER in the small and medium microcosms were formed, it is difficult to determine whether microbial diversity directly impacted biodegradation. Microbial communities within the microcosms also deviated from the fresh river inoculum, which poses the question on whether laboratory tests reflect the real environment. Regardless, they are a valuable resource in assessing pesticide fate and transformation and if there is little difference between DegT50 with microcosm size, it paves the way for potential smaller and high-throughput approaches to environmental fate testing.

CHAPTER 4 – THE IMPACTS OF LIGHT AND FLOW ON ISOPYRAZAM DISSIPATION IN LARGER SCALE MICROFLUME SYSTEMS

4.1 INTRODUCTION

4.1.1 Implications of using different scales for environmental experiments

Agrochemicals have huge benefits as a mechanism for pest control and improving crop yields (Hazell, 2002, Taylor *et al.*, 2007), but they are also capable of reaching a number of environmental compartments (Carter, 2000), where there is the potential to cause adverse effects on both the environment and human health. The chemical industry is responsible for carrying out tests to determine how chemicals transform in the environment, and ensuring products are safe and pose as little risk as possible (Davies *et al.*, 2013, OECD, 2005).

Biodegradation by microbes is an important factor impacting chemical transformation and persistence in the environment (Copley, 2009), and tiered tests are used to assess these processes in regulatory testing schemes. Firstly, ready biodegradability tests are carried out over 28 days as a screening method to determine if a chemical is rapidly degradable. Simulation tests provide additional context and are designed to be more realistic of a particular environmental compartment, such as OECD 308 which uses water and sediment inoculum to represent an aquatic environment (Kowalczyk *et al.*, 2015, OECD, 2002b). Although more realistic than the ready biodegradability tests, simulation tests still lack environmental realism as they are carried out on a small microcosm scale, statically, and under dark conditions (Gartiser *et al.*, 2017, OECD, 2002b). Industry can provide additional information from studies that include other variables, such as light, or are carried out on a larger scale. Nevertheless, regulators currently tend to fall back on the guideline studies due to uncertainty over how to account for potential variability in, for example, light intensity in the environment.

The real environment is difficult to simulate and natural experiments in the field are more realistic than laboratory studies as they consider real-time abiotic and biotic variation. Logistical issues in the field, however, are not easily overcome and a level of control and

replicability are usually sacrificed (Carpenter, 1996, Sturman *et al.*, 1995). Results can also lack external validity as they usually represent a single space and time. Microcosm studies, on the other hand, can support data from the field by enabling more precise control over experimental variables, and they represent a rapid and cost-effective means of generating data on biodegradation processes (Aichberger *et al.*, 2005, Carpenter, 1996, Clements and Newman, 2002, Diamond, 1986, EPA, 2000, Khan and Zytner, 2011, Spain *et al.*, 1984, Sturman *et al.*, 1995, Wang *et al.*, 2008). Although there are many benefits to microcosm studies, due to the size and duration of small-scale tests, results can be misleading as they often only represent samples taken from a subset of geographical locations. This means that phenomena seen at a larger scale, such as higher trophic level organisms, or over a longer period of time, for instance seasonal processes, are not represented at the microcosm scale. Because of this, results need to be considered at the scale they are carried out, with context from the field (Carlisle and Clements, 1999, Carpenter, 1996).

In particular, the structure and abundance of microbial communities is determined by interactions with a range of environmental abiotic and biotic factors. These are constantly changing in time and space and are hard to simulate in the laboratory, meaning small-scale laboratory tests, which are usually carried out under controlled conditions, lack realism and might not reflect the microbial densities seen in nature (Carpenter, 1996, Diamond, 1986). If microbial populations incubated under laboratory conditions do not reflect the populations seen in the environment, biodegradation rates generated from regulatory tests may not be representative.

Data generated at the microscale may, therefore, not directly translate to higher spatial scales and this could cause inaccuracies in estimations of pesticide fate and persistence in the field (Carpenter, 1996, Clements and Newman, 2002, Sturman *et al.*, 1995). The use of a range of different scales of study may prove useful for addressing specific questions relating to biotransformation of chemicals in the environment. For instance, microscale studies may give insight into factors which limit biotransformation, while larger scale studies may prove useful to understand spatial heterogeneity of biotransformation processes. Larger scale laboratory experiments are therefore considered as a good bridging tool between small-scale tests and the field (Khan and Zytner, 2011, Sturman *et al.*, 1995).

4.1.2 The impacts of light on microbial communities and chemical degradation

OECD 308 tests are usually carried out under dark conditions (OECD, 2008a). In nature, however, sunlight may be a contributing factor to environmental conditions, especially for microorganisms in the water or on the sediment surface. Sunlight can have a negative impact on microbial communities. For instance, increased UV radiation exposure can, in some cases, reduce primary production and metabolism (Alonso-Sáez *et al.*, 2006, Lindell *et al.*, 1996). Despite this, photolysis can have positive effects on microorganisms by increasing the available biological substrate pool and subsequently increasing microbial productivity (Kieber, 2000). Furthermore, phototrophic organisms can utilise natural light as an energy source for cell growth and maintenance, and these populations can proliferate in nature with higher population levels and productivity (Alonso-Sáez *et al.*, 2006, Overmann and Garcia-Pichel, 2006, van Gemerden and Beeftink, 1983). By disregarding light in OECD 308 tests, there is no consideration of its impacts on microbial communities, particularly phototrophs, and their biotransformation potential. This could be detrimental to producing data that is relevant to the environment.

Phototrophic communities have been shown to be metabolically capable of chemical biodegradation and possess biotransformation enzymes, e.g. cytochrome P450 (Stravs *et al.*, 2017). The phototrophic bacterium, *Rhodobacter capsulatus*, has been shown to utilise *p*-nitrophenol as a carbon source, with no bacterial growth or degradation occurring under dark conditions (Roldán *et al.*, 1998). Furthermore, microalgal species, *Chlorella vulgaris* and *Coenochloris pyrenoidosa*, have been shown to degrade *p*-nitrophenol; however, different species have different metabolic potentials, with *C. pyrenoidosa* having higher degradative capabilities of the two (Lima *et al.*, 2003). Although Stravs *et al.* (2017) found that three phytoplankton species could only degrade nine out of the twenty-four chemicals tested, it was noted that, in nature, microbial systems are diverse with a broad range of biotransformation properties within a community. Hand and Oliver (2010) determined that isopyrazam degraded at a faster rate in systems containing algal and macrophyte communities when incubated under non-UV light. Additional work also revealed that chemical degradation was enhanced by phototrophic communities, with macrophyte communities being marginally more competent than algal communities (Thomas and Hand,

2011), potentially due to the periphyton biofilm associated with them (Thomas and Hand, 2012).

The impact of light on chemical degradation is compound specific. Davies *et al.* (2013) showed that chemical transformation in soil was impacted by light treatment in five out of eight tested compounds. In addition to directly contributing to degradation, phototrophs may promote degradation by heterotrophs by altering environmental parameters such as pH and carbon availability (Davies *et al.*, 2013). Furthermore, synergistic relationships can occur between algae and bacteria. For instance, photosynthesis supplies O_2 which could be used as an electron acceptor for bacterial species, while algal species can utilise CO_2 generated from mineralisation (Borde *et al.*, 2003). Indeed, studies have shown that mixed systems of both phototrophs and heterotrophs significantly increase degradation rate relative to systems with exclusively phototroph or heterotroph communities. This suggests that heterotrophs are enhanced by a more complex and inclusive microbial community and phototrophs may play more of an indirect role in the degradation process (Thomas and Hand, 2012). Whether the role of phototrophs is direct or indirect, these studies show that they can have a role in chemical biotransformation and it highlights that the addition of light in regulatory tests could further increase environmental realism.

4.1.3 The impacts of water flow on microbial communities and chemical degradation

OECD 308 tests are usually carried out statically and this does not always adequately represent the conditions seen in nature, especially when considering rivers and streams, as there is no consideration for flow velocity and sediment dynamics (Gartiser *et al.*, 2017). Environmental conditions such as these can have impacts on microorganisms and biodegradation (Naudin *et al.*, 2001) and there are intrinsic differences between static and flowing water systems in nature, such as nutrient cycling processes, dissolved O_2 content, and taxonomic composition (Brabec *et al.*, 2004, Simmons and Wallschläger, 2005).

Although mixing can occur in both types of systems, in terms of water movement, static systems (e.g. ponds and lakes) are generally considered more stable than flowing systems (e.g. rivers) (Reynolds *et al.*, 1994). This results in differences in the microbial and macrophyte populations between systems. In flowing systems, water is continually moving

unidirectionally, meaning they can change physically, chemically, and biologically. Bacteria are more likely to be removed from the sediment bed causing species dispersion, which causes system homogenisation (Bornette *et al.*, 1998, Leff *et al.*, 1992, Reynolds *et al.*, 1994, Vannote *et al.*, 1980, Williams *et al.*, 2003). Mixing in static systems, on the other hand, is influenced by environmental factors, such as wind, rain, and runoff (Reynolds, 1994, Reynolds *et al.*, 1994). Static systems are more isolated so will have higher abundances of rare species through having a smaller catchment area. Studies have also shown increased heterogeneity between different site locations, depending on the surrounding environment, such as land use and geology, influencing inputs into the water source (Vincent and James, 1996, Williams *et al.*, 2003).

Although there is some overlap of taxa between static and flowing systems, there is a clear separation in the microbial populations present (Reynolds *et al.*, 1994, Rodrigues and Bicudo, 2001). Studies have shown that higher bacterial densities and diversities in static systems, and a higher probability of rare species being present, could promote biodegradation (Kool, 1984, Thouand *et al.*, 2011, Thouand *et al.*, 1995). In static and slow-flowing systems, planktonic algae will be more common as they have a longer retention time to grow in the water column. In rivers, however, algae which are attached to the sediment bed will be adapted morphologically in order to withstand turbulence (Breuer *et al.*, 2017, Reynolds *et al.*, 1994). In static systems, species do not need to depend on a high growth rate to survive as the environment is more stable, and Cryptophyta and Desmids, the latter usually associated with macrophytes, are more common in these environments (Reynolds *et al.*, 1994, Rodrigues and Bicudo, 2001). In flowing systems, Diatoms are more common as they are better adapted to more turbulent environments due to mucilage secretion and structures which allow them to fix to surfaces in high currents (Dorigo *et al.*, 2007, Reynolds *et al.*, 1994, Rodrigues and Bicudo, 2001).

Biofilm structure and function are also likely to be impacted by turbulence (Kugaorasatham *et al.*, 1992) and studies using flume systems of different velocities have shown that in the slow-flowing systems, biofilms were thicker and had better surface flexibility than in fast-flowing systems (Battin *et al.*, 2003a, Battin *et al.*, 2003b). Other studies by Wetzel (1993) also found that biofilm thickness was inversely correlated to water current and Kugaorasatham *et al.* (1992) noted that under high turbulence, biofilms showed

greater uniformity and covered the entire surface, whereas spatial variation was higher in low turbulence systems. Flow velocity and water level will impact the growth and distribution of aquatic plants and microbes which are closely associated with them (Chambers *et al.*, 1991, Rodrigues and Bicudo, 2001, Thullner *et al.*, 2002). Furthermore, flow dynamics will change throughout the year, impacting species distribution, biomass, and diversity, with lower water levels being associated with higher plant cover and biomass (Chambers *et al.*, 1991, Hudon, 1997, Loder and Reichard, 1981).

Higher mixing rates in flowing systems can increase the chance of microbes coming into contact with electron donors and acceptors, benefitting growth rates (Bauer *et al.*, 2008, Kirchman *et al.*, 1989, Naudin *et al.*, 2001, Reynolds, 1994, Thullner *et al.*, 2002). Although there is a complex relationship between flow velocity and mass transport, water movement impacts the diffusion rate of solutes and gases, concentration gradients, microbial fluxes, and nutrient levels, and there can also be areas where water flow is limited (Gantzer *et al.*, 1988, Reynolds, 1994, Wetzel, 1993). This can mean that although there might be high substrate levels within a system, across space and time system hydraulics may cause uneven dispersion of microbes and substrates. This could limit biodegradation if microbes do not come into contact with the required substrates in order to proliferate or with the pollutant they may then subsequently degrade (Mulholland *et al.*, 1994).

Mixing has been shown to aid in biodegradation as water flow and recirculation increases the probability that a chemical will come into contact with relevant degraders (Sánchez-Pérez *et al.*, 2013). Furthermore, mixing aids biodegradation processes by impacting mass transport and encouraging microbial growth (Bauer *et al.*, 2008, Chapelle *et al.*, 1996, Gantzer *et al.*, 1988, Thullner *et al.*, 2002). Spain *et al.* (1984) determined that faster mixing in large-scale systems was linked to higher degradation rates as mixing aided transportation within the system. Additionally, Oya and Valocchi (1998) concluded that degradation only occurred in mixing zones due to promotion of microbial growth.

In flowing systems, there can be an increase of suspended sediments and this can affect biodegradation rates. Some studies have shown that although suspended sediments can aid in an initial faster degradation rate, over longer periods they can lower the overall degradation rate. This may be due to impacts on contaminant bioavailability and the

relationship between desorption rates and biodegradation e.g. if desorption rate is low it may be a limiting factor on biodegradation (Flenner *et al.*, 1991, Parsons, 1992, Yang *et al.*, 2008). Suspended sediments can also impact light attenuation for phototrophic organisms. Some algal species, however, can increase their photosynthetic capabilities by increasing photosynthetic pigment amounts, and this can combat fluctuations in light intensity (Reynolds, 1994, Reynolds *et al.*, 1994). Some studies indicate that suspended sediment can increase biodegradation rates by increasing nutrient availability, and thus microbial degrader growth and population size, as well as providing a platform for growth. Suspended sediment can also play a role in increasing the probability that degraders come into contact with a pollutant, and this can be influenced by sediment properties, such as carbon content (White and Franks, 1978, Xia *et al.*, 2011, Yang *et al.*, 2008).

4.1.4 Experimental overview

Experiments were carried out to investigate the impacts of non-UV light and water flow on isopyrazam dissipation. Microflume systems were used to provide a more environmentally realistic scale than the water-sediment systems used in Chapter 2, in order to more effectively simulate field conditions. Particular attention was paid to the relative influences and interactions of light and water flow on microbial communities and its relationship with isopyrazam dissipation.

4.1.5 Experimental aims and objectives

The aims and objectives of this experiment were as follows;

1. To determine if non-UV light impacts microbial communities and isopyrazam dissipation processes in microflume systems.
2. To establish whether microbial communities and the isopyrazam dissipation processes are impacted by water being static or flowing.
3. To identify whether there is an interaction between the light and flowing treatments on microbial communities and their role in isopyrazam dissipation.

4.2 MATERIALS AND METHODS

4.2.1 Sample collection and processing

River water and sediment samples were obtained from the River Dene at Wellesbourne, United Kingdom at the same location as detailed in section 2.2.1. Sampling took place at the end of August 2016 over two days. On the first day, sediment was sampled within the top 5 to 10 cm of the riverbed using a shovel and kept moist with river water. On the second day, whilst facing upstream, water was collected in jerry cans; this took place over two sampling sessions, one in the morning and one in the afternoon.

During each sampling session, water temperature was measured using a Total Immersion thermometer (Fisher Scientific, UK), light intensity measured using an RS-105 light meter (RS Components Ltd., UK), and water depth and velocity measured using an 801 EM flow meter (Valeport, UK). Water pH was measured using an Accumet basic AB15 pH meter (Fisher Scientific, UK). Sediment was wet-sieved through a 20.00 mm sieve (Endecotts Ltd., UK) to homogenize the sample. Although OECD 308 guidelines specify a smaller sediment diameter (OECD, 2002b), as used in Chapters 2 and 3, for this experiment, a coarser sieve was used in order to complement the increase in scale, and mimic environmental sediment characteristics more closely. Aliquots of water and sediment from the sample site were taken so that microbial and water chemistry analysis could be carried out on fresh samples prior to addition to the microflumes. Samples were refrigerated at 4 °C and used within 24 hours.

4.2.2 Test chemical

Studies were performed using isopyrazam (99.4 % purity) supplied by Syngenta, Jealott's Hill International Research Centre, United Kingdom (**Fig. 1.5**). Confirmation of the isopyrazam peak by Liquid Chromatography-Mass Spectrometry (LC-MS) can be found in Appendix III.1. The rationale for choosing isopyrazam is outlined in section 1.5.

4.2.3 Experimental set up

4.2.3.i Microflume design and laboratory conditions

The microflume systems were situated in Warwick School of Engineering, University of Warwick, United Kingdom and comprised twelve rectangular microflume systems (four banks of three) – 6 of these were flowing systems with associated plumbing, which recirculated water (2.36 m length, 0.2 m height, 0.1 m width) and 6 were static systems without the plumbing (2 m length, 0.2 m height, 0.1 m width). These systems had a similar design to other continuous flow studies, such as in Finnegan *et al.* (2009). The flowing systems had a divide 0.18 m from each end of the microflume, so that the sediment bedform would not interfere with the water inlet and outlet. The glass used for the systems was 10 mm toughened glass, which was polished and arised (Thee Spires Glass Company Ltd., UK) to remove sharpness from the glass edge. This was held together by silicone sealent in an aluminium frame. The frame had adjustable legs so that the slope of the systems could be altered to adhere uniform flow. The plumbing used was 316 seamless stainless steal tubing with 150 lb 316 stainless steel BSP threaded pipe fittings (Pipestock, UK).

The slope of the flowing systems meant water could flow down a gravity chute and a Clarke TAM105 pump (Clarke International, UK) was placed at the downstream end of the systems to recirculate the water along the length of the microflume channel. Water then passed over a weir, which was used to regulate the flow depth, and re-entered the pipes, which were fitted with a water chiller and flow meter. Water could then pass through the pump again and re-enter the channel. These pumps were used as they had a large discharge range (2 to 40 L/min) and did not heat the water significantly. Along the length of the pipe work was a GPI TM Series electronic flow meter (Great Plains Industries, Inc., US) and a Haillea HC-300A aquarium chiller (Hailea Group Co., China) (**Fig. 4.1**). The systems were located in a controlled environment room at 20 ± 2 °C and the chillers on the flowing systems were similarly set at 20 °C to ensure that they stayed at the same temperature as the static systems. Temperature was monitored throughout the experiment using an NTC030WP00 temperature sensor (Carel, UK) in each middle microflume bank connected to a HY3003 DC Power supply (digimess®, UK). This was connected to a computer and monitored

throughout the experiment using National Instruments LabVIEW software (version 10, National Instruments™, UK).

a)

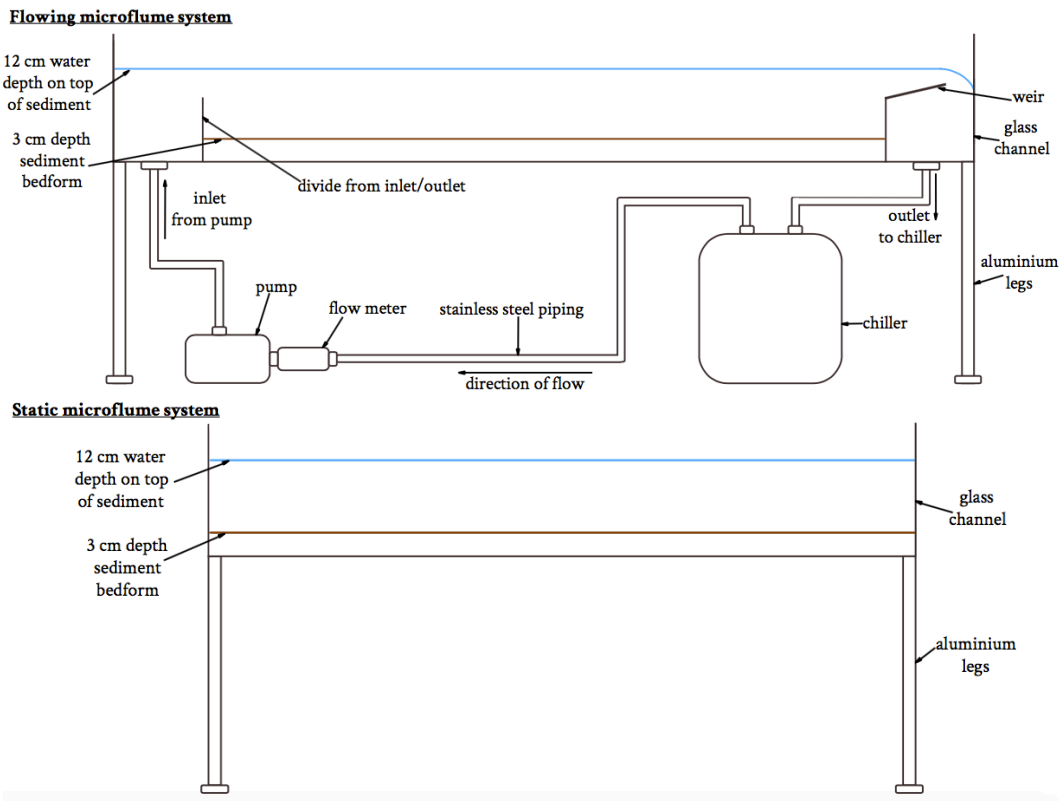

b)

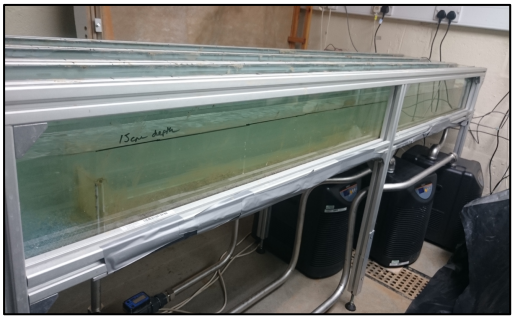

c)

Figure 4.1: (a) The flowing (top) and static (bottom) microflume systems, (b) a flowing microflume channel containing sample, and (c) plumbing of a flowing microflume. Both the microflume systems compromise a glass channel supported by an aluminum frame with legs. Additionally, the flowing microflume systems had connecting stainless steel piping, along which a pump, flow meter, and chiller are attached. Diagram created using site.youidraw.com (YouiDraw, 2016).

Each microflume was labelled from A to P on the top of the frame at 20 cm intervals along the 2 m length of the channel where the sediment bed resided. This was for allocation of random sampling sites, and 20 cm at each end was left unsampled to avoid discrepancies from turbulance at the flow inlet and outlet (see Appendix III.2).

Dark treatment microflumes were covered with DMP black damp-proof membrane 1200GA (Capital Valley Plastics, UK) so that no light could penetrate the systems. Illuminated treatment microflumes were covered with LEE226 filter (Transformation Tubes, UK) covers. These covers also aided in preventing evaporation from the systems (**Fig. 4.2**). Fluorescent 70 W daylight bulbs (F70W/865 T8 6ft, Fusion Lamps, UK) were used with LEE226 filters (Transformation Tubes, UK) on a 16-hour light and 8-hour dark cycle. The filters, which were also used for the illuminated system covers, inhibited UV light output so that there was a transmission of less than 50 % radiation at a wavelength of 410 nm and minimal transmission at wavelengths below 390 nm. This ensured that degradation due to photolysis was limited.

4.2.3.ii Environmental sample addition

Before sample addition, microflume channels were cleaned with 1 % Virkon disinfectant (Scientific Laboratory Supplies, UK) and then with 80 % absolute ethanol (VWR Chemicals, UK) before being allowed to dry.

The following treatments were set up using triplicate channels; dark static, dark flowing, illuminated static, and illuminated flowing. Prior to sediment addition, latex free stoppers obtained from 100 mL syringes (BD Plastipak™, US) (**Fig. 4.4.c**) were placed at each randomly allocated sediment sampling site (Appendix III.2). Sieved sediment was then added along the length of the channel up to the 3 cm depth, being careful not to disturb the stoppers. Sediment was leveled off with a customised tool (**Fig. 4.3**). River water was weighed into each microflume and added at the water inlet. This ensured that piping was filled first and then water gradually flowed over the divide into the microflume channel, minimising sediment disturbance as much as possible. Water was added until a 12 cm depth on top of the sediment bed was reached.

4.2.3.iii Establishment of water flow conditions

All microflumes were left static (pumps and chillers turned off) for a two-day incubation to allow sediment particulates to settle. In the flowing systems, after this static incubation, a piece of perforated metal mesh (2 mm round hole, 3 mm triangular pitch, Steel

Express, UK) was placed over the flow inlet and 400 mL of 5 mm glass beads (VWR International Ltd., UK) placed over the top to calm the flow, which was otherwise very turbulent. Uniform flow was then established in each flowing system, which meant that the flow depth was constant along the channel (Chow, 1959). Although this is rarely seen in nature (Chanson, 2004), in the case of an experimental system, it ensured that systems could be comparable. This was achieved by using a Vernier depth gauge at either end of the system and adjusting the aluminum legs until the slope allowed the water depth to be equal at both ends. Weirs were set at an angle such that the top of the weir came to the 9 cm depth mark. Pumps and chillers were then turned on in the flowing systems with an average water velocity in the flowing systems of 0.03 m/s. Each system was left in its respective light-dark or constant darkness condition for a further seven-day incubation to equilibrate prior to chemical addition. Environmental realism of the laboratory conditions are discussed in Appendix III.3.

4.2.3.iv Addition of isopyrazam

An isopyrazam stock was prepared in acetonitrile (HPLC grade, Fischer Scientific, UK) and, for each system, the appropriate mass was added to a mixture of 160 mL sterile distilled water and 40 mL acetonitrile (HPLC grade, Fischer Scientific, UK) such that, when added to each respective microflume, the concentration would be 0.1 mg/L isopyrazam. Although conservative, this is classed as an environmentally relevant concentration, as it is still low enough to ensure that the biodegradation kinetics reflect those expected in the environment (OECD, 2004) as described in 2.2.3. The actual isopyrazam amount added to the systems was determined by diluting aliquots (0.1 mL in triplicate) of each stock and then analysing the chemical content. This was carried out by LC-MS, as will be described in section 4.2.5.i and Appendix III.1. After the seven-day incubation, pumps and chillers were turned off in the flowing systems and each stock was added to the respective system along the length of the sediment bed. Pumps and chillers were left off for four days before being turned back on again. This was to allow initial sorption to the sediment rather than potentially to the plumbing if isopyrazam was in circulation. Systems were incubated for a total of 52 days after chemical addition. Although minimal, if any evaporation did occur in the systems, water was topped up with river water obtained from the original sampling trip.

4.2.4 Sampling

Samples were removed for analysis after 0, 10, 24, 34, 45, and 52 DAT. At each time point, water and sediment samples were taken from each microflume and chemical, microbial (chlorophyll *a* concentration and water bacterial counts), and water chemistry analysis was carried out. DNA extraction and quantification was only carried out on fresh river samples and at 52 DAT. At 0 DAT, samples were analysed directly from the fresh sample obtained from the river and no chemical analysis was carried out. A nominal 0 DAT value was used, assuming that 100 % of the applied chemical was in the water fraction. OECD test 307 states that for non-labelled chemicals a recovery between 70 % and 110 % should be reached (OECD, 2002a) and since no radiochemical was applied, a mass balance could not be generated. Despite this, previous tests (Appendix III.4) showed that sorption to the microflume systems (e.g. glass tank and piping) was minimal and that the majority of the isopyrazam mass originally applied was recovered. Additionally, as only a small quantity of sample was taken at each time point in relation to the size of the systems, variability was expected in the recovery rate due to potentially high heterogeneity in a large system.

Pumps and chillers were turned off while sampling took place so that sediment particulates did not go into the plumbing. Sediment sampling occurred first and particulates left to settle while the rest of the sampling was carried out. Water sampling then took place and the pumps and chillers were turned on again afterwards.

For the sediment fraction, sampling was carried out using the catheter tip body of a 100 mL syringe (BD Plastipak™, US), which had been cut down to 5 cm in height (**Fig. 4.4.a**). DMP black damp-proof membrane 1200GA (Capital Valley Plastics, UK) and duct tape was used to make a sheath, which went around the core (**Fig. 4.4.b**). At each time point, two cores from each microflume channel were taken from two separate sites (Appendix III.2) for both the isopyrazam and microbial analysis - this was carried out by bunging the core with the stopper (BD Plastipak™, US) under the sediment bed as described in 4.2.3 (**Fig. 4.4.c**). The core and stopper were then extracted from the microflume system, leaving the sheath in place. A mixture of both 5 mm and 0.5 mm glass beads (VWR International, UK) were washed and autoclaved at 121 °C. This was used to fill in the sediment core and then the sheath was removed. A diagram of the technique can be seen in **Figure 4.5**.

For the water fraction, samples were taken at the allocated site (see Appendix III.2) using a 10 mL glass pipette (Type 2, Fischer Scientific, UK), submerging it until above the sediment bed. Once the pipette was filled with water from the microflume, a finger was placed over the top to create a vacuum. This water sample was used for isopyrazam analysis and was transferred to a glass vial containing 2 mL acetonitrile (HPLC grade, Fischer Scientific, UK) to prevent any chemical sorbing to the glassware. A second sample was taken by submerging a 50 mL falcon tube at the allocated site for microbial analysis.

Figure 4.2: Microflume systems with covers in the School of Engineering, University of Warwick, United Kingdom. The microflume on the left is the dark treatment and the microflumes on the right and in the centre are the illuminated treatments.

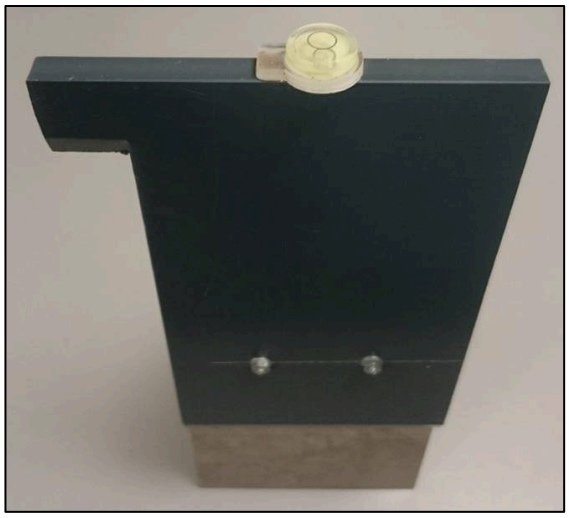

Figure 4.3: Customised level tool. The hook on the left was steadied on top of the microflume frame and the base of the tool extended down to the desired 3 cm depth needed for the sediment bed. The spirit level on top of the tool ensured that the bed was level.

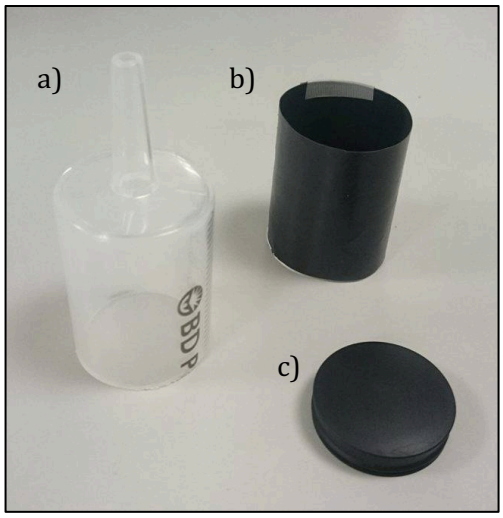

Figure 4.4: Sediment sampling equipment. The stopper (c) was placed under the sediment bed prior to sample addition. The syringe body (a) was encased in the sheath (b) and the stopper used to bung the sample in the core. The sheath was left in place until the core was filled with glass beads.

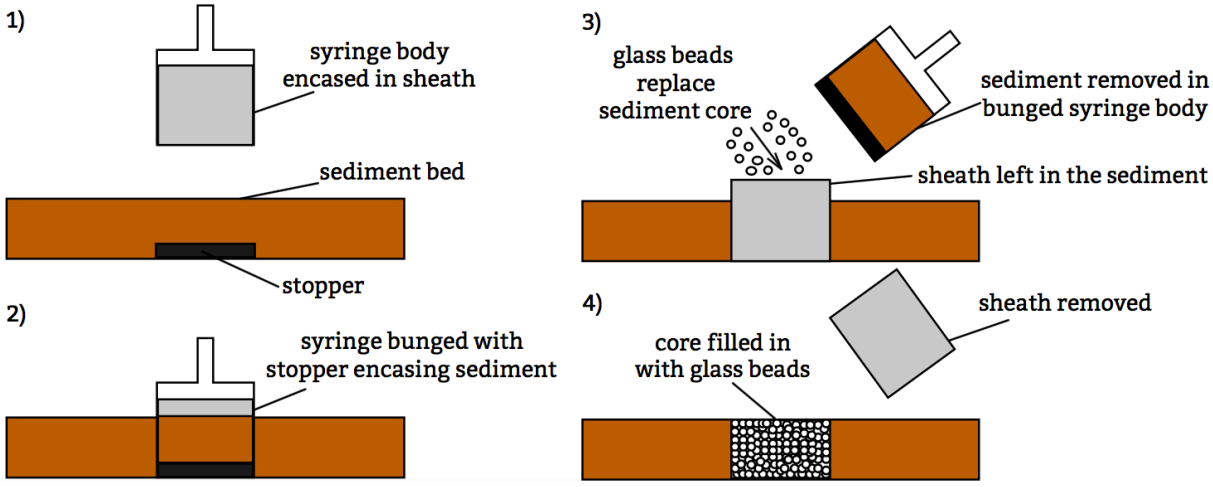

Figure 4.5: Sediment sampling technique. A syringe body encased in a sheath was pushed into the sediment bed, so that the bung underneath the bedform encased the sediment within the syringe body. The syringe body was then removed, leaving the sheath in place. The core was filled in with glass beads, then the sheath also removed. Diagram created using site.youidraw.com (YouiDraw, 2016).

4.2.5 Chemical analysis

4.2.5.i Water fraction

Glass vials containing the sample and acetonitrile mixture were sonicated for 10 minutes using an U3OOH ultrasonic bath (Ultrawave, UK). Sample was then transferred to a tube and centrifuged at 1000 rpm for 10 minutes. The supernatant was collected in the original glass vial and a further 2 mL acetonitrile (HPLC grade, Fischer Scientific, UK) was added to the pellet. This was again sonicated and centrifuged in the same way as before and the supernatants pooled. This was carried out to ensure that any chemical sorbed to particulate matter in the water fraction was accounted for.

Samples were then analysed by LC-MS using the protocol devised in Appendix III.1. A Poroshell 120 EC-C18 2.7 µm column (2.1 x 50 mm, Agilent Technologies, US) was used with an LC-MS system consisting of an Ultimate 3000 RS pump, column compartment, and autosampler (Dionex, US) and an amaZon SL ion trap (Bruker, US). This was used in conjunction with HyStar (version 3.2, Brucker, US), trapControl (version 7.2, Agilent Technologies, US), Chromeleon (version 6.8, Thermo Scientific, US), and DataAnalysis (version 4.2, Brucker, US) software. An example of a chromatogram from the water samples can be found in Appendix III.1 and examples of the recovery calculations in Appendix III.5.

4.2.5.ii Sediment fraction

Chemical was extracted from the sediment using the method outlined in section 2.2.5.ii and was analysed by LC-MS, as described in 4.2.5.i. Although a mass balance could not be generated without using radiochemical, the efficiency of this method at recovering isopyrazam in Chapters 2 and 3 served as validation for its use in this experiment. An example of a chromatogram from the sediment samples can be found in Appendix III.1 and examples of the recovery calculations in Appendix III.5.

4.2.6 Water chemistry analysis

4.2.6.i Water pH

The pH of the water was analysed using an Accumet basic AB15 pH meter (Fisher Scientific, UK).

4.2.6.ii Macronutrient analysis

NO_3- and PO_4 concentrations in the water were analysed as described in 2.2.6.i.

4.2.7 Microbial analysis

4.2.7.i Chlorophyll a *analysis*

Chlorophyll *a* analysis was carried out on both the water and the sediment fraction as described in 2.2.7.i.

4.2.7.ii Viable plate counts

Bacterial colony counts from the water fraction were analysed as described in 2.2.7.ii.

4.2.7.iii DNA extraction and quantification

DNA extraction and quantification was carried out as described in Appendix IV. DNA was extracted from the fresh water and sediment taken from the sample site, as well as water and sediment samples from the microflumes at the end of the experiment at 52 DAT. Library preparation was carried out for 16S, 23S, and 18S rRNA genes to investigate bacterial, phototrophic, and eukaryotic community structure and diversity, respectively. Sequencing was carried out by the Genomic Facility at the University of Warwick, Coventry, United Kingdom in January 2017.

4.2.8 Statistical analyses

A repeated measures two-way ANOVA (with microflume treatment and time point) was performed on isopyrazam dissipation, isopyrazam partitioning, water pH, water macronutrient concentration, microflume chlorophyll *a* concentration, and water bacteria concentration. The Tukey method was used to correct for multiple comparison tests. Statistical analyses and figures were performed and created using Prism (version 7, GraphPad Software, Inc., US).

Isopyrazam kinetics were estimated in the same way as in section 2.2.8 to determine the time it took for 50 % of isopyrazam to dissipate (DT50). As described in section 2.2.8, α diversity, β diversity, and relative abundance (two-way ANOVA with taxa and microflume treatment) were analysed. Significance of OTUs to treatments and dissipation rates were tested using QIIME as in 2.2.8 (Caporaso *et al.*, 2010).

4.3 RESULTS

4.3.1 Sample site characteristics

At the time of collection, water temperature, water depth, water velocity, water pH, and light intensity were analysed at the sample site (**Table 4.1**).

Table 4.1: Characteristics of the River Dene, Wellesbourne, United Kingdom in August 2016. Mean and standard deviation of water temperature, light intensity, water depth, water velocity, and water pH taken at the sample site at the time of sampling.

Characteristic	Mean	Standard deviation
Water temperature	16.4 °C	0.5
Light intensity	1.4×10^5 lux	5.6×10^4
Water depth	0.31 m	0.14
Water velocity	0.08 m/s	0.02
Water pH	7.5	0.1

4.3.2 Chemical analysis results

4.3.2.i Isopyrazam dissipation in the total system

Isopyrazam dissipated in all systems, yet there were significant differences between the microflume treatments ($p \leq 0.0004$, **Fig. 4.6**). In dark and illuminated flowing systems, dissipation was not significantly affected by light treatment and by 34 DAT, isopyrazam had dissipated to around 18 % of the applied amount, with no subsequent decline by 52 DAT. Despite an initially slower dissipation in the illuminated static systems, overall they were not significantly different to the dark and illuminated flowing microflumes, and by 34 DAT dissipation had reached a similar level. Dark static systems, however, showed significantly slower ($p \leq 0.001$) isopyrazam dissipation, with 48.5 % of the applied mass of isopyrazam remaining by 52 DAT.

DT50 was assessed using a SFO model, and DT50 and rate constant estimates from each microflume system (**Table 4.2**) are in accordance with the decline curves (**Fig. 4.6**). The DT50 values can, therefore, be considered as indicative of the general dissipation behavior of the different systems. DT50 was lower in flowing systems (16.8 and 15.3 days in dark and illuminated treatments, respectively), marginally slower in illuminated static systems (20.6 days), and the longest in dark static systems (47.7 days). Despite this, some of the acceptance requirements outlined in section 2.2.8 were not met (see Appendix III.6), mainly for the χ^2 values, which shows the goodness of fit, indicating that SFO is not the best fit for the data. Dark static microflumes additionally failed the r^2 criteria, which shows the correlation between observed and expected values. This was most likely due to the large variance in the dissipation at 24 DAT in these systems.

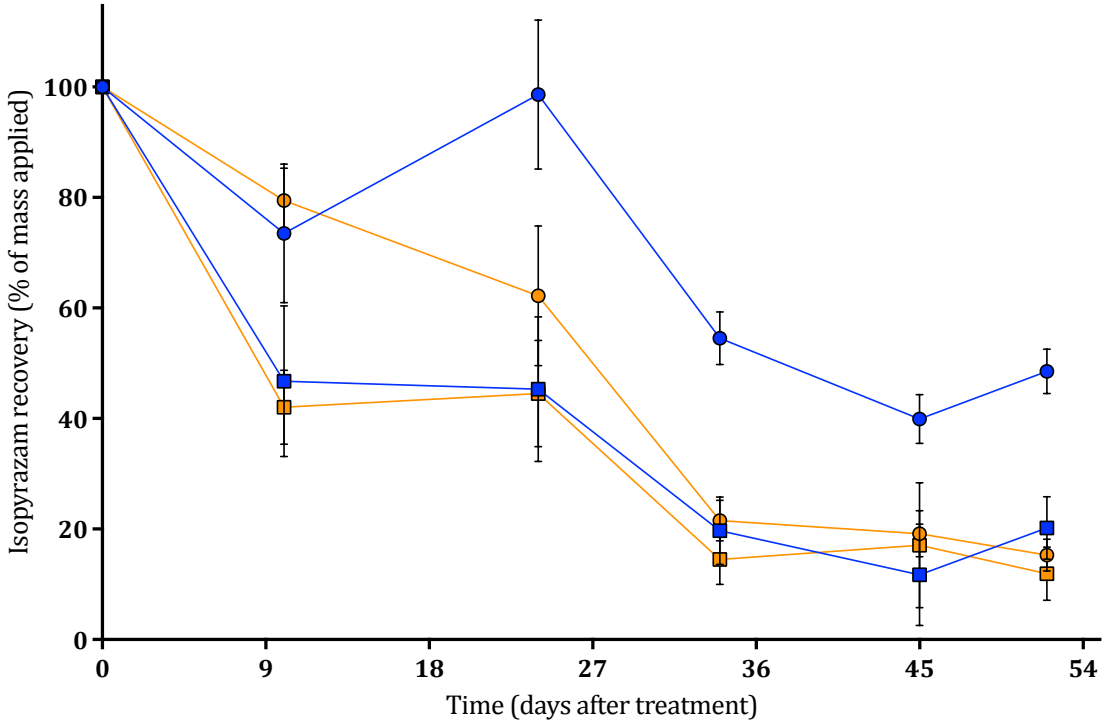

Figure 4.6: Dissipation of isopyrazam in microflume systems as a percentage of the mass originally applied. Dissipation of isopyrazam in dark static (blue circles), dark flowing (blue squares), illuminated static (orange circles), and illuminated flowing (orange squares) microflume systems. Error bars show ± standard deviation.

Table 4.2: DT50 and rate constant estimates from CAKE for the microflume treatments. SFO kinetic models were used for all data and 95 % confidence intervals calculated for the rate constant. k_1 denotes the first-order kinetics rate constant and *CI* denotes *confidence interval*.

Microflume treatment	DT50 (days)	k_1	Lower 95 % CI	Upper 95 % CI
Dark static	47.7	0.015	0.009	0.022
Dark flowing	16.8	0.041	0.030	0.053
Illuminated static	20.6	0.034	0.027	0.041
Illuminated flowing	15.3	0.045	0.033	0.058

4.3.2.ii Water and sediment partitioning of isopyrazam

There were different partitioning dynamics between the microflume systems. This resulted in differences in isopyrazam concentration in both the water ($p \leq 0.0002$, **Fig. 4.7.a**) and the sediment ($p \leq 0.0015$, **Fig. 4.7.b**) between treatments. In the water fraction, dissipation was significantly quicker ($p \leq 0.001$) in the flowing microflumes compared to dark static microflumes. At 10 DAT, 33.9 and 28.7 % of the applied isopyrazam was present in the water in the dark and illuminated flowing systems, respectively. By 34 DAT, amounts in the water had declined to 6.6 and 4.5 % in the dark and illuminated flowing systems respectively, and there was a further slow decline until 52 DAT. Illuminated static microflumes had a marginally slower dissipation from the water fraction, with 46.4 % isopyrazam remaining in the water by 24 DAT and 11.2 % by 34 DAT. This was significantly slower compared to the flowing microflumes ($p \leq 0.05$), but significantly faster compared to dark static microflumes ($p \leq 0.05$). In dark static microflumes, 67.9 % isopyrazam remained in the water at 24 DAT and 31.9 % remained by 52 DAT.

In the sediment fraction, around 14 % of the applied isopyrazam partioned to the sediment by 10 DAT, with a slow decline thereafter, in both flowing systems and the illuminated static systems; there was no significant difference between these microflumes. In the dark static systems, however, 30 % of the applied isopyrazam partitioned to the sediment by 24 DAT, significantly more ($p \leq 0.01$) than in the other systems. By 52 DAT this had declined to 16.7 % of the applied isopyrazam.

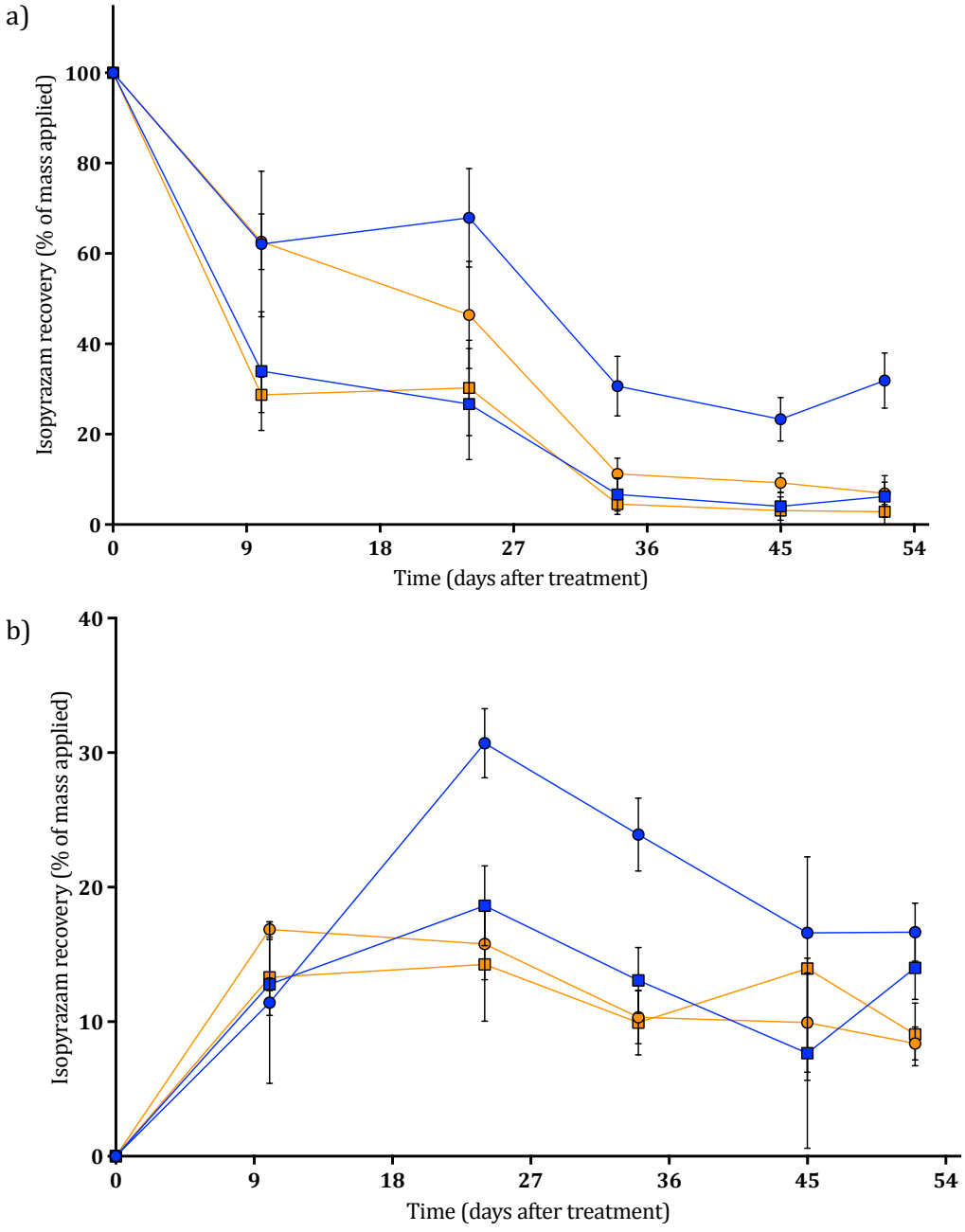

Figure 4.7: Partitioning of isopyrazam to the water (a) and the sediment (b) of the microflume systems as a percentage of the mass originally applied. Partitioning of isopyrazam in dark static (blue circles), dark flowing (blue squares), illuminated static (orange circles), and illuminated flowing (orange squares) microflume systems. Error bars show ± standard deviation.

4.3.3 NO_3- concentration in microflume water

There was a significant impact of microflume treatment on NO_3- concentration in the water ($p \leq 0.0001$, **Fig. 4.8**). Dark static microflumes had a significantly lower NO_3- concentration than the other systems ($p \leq 0.001$), remaining low at around 4.7 mg/L, although this did increase slightly nearer the end of the experiment. The flowing systems were not significantly different to one another with NO_3- concentration increasing to over 40.0 mg/L from 24 DAT to the end of the experiment. Illuminated static systems followed the same trend as the flowing systems, but with a 16 day lag period. Overall, the illuminated static microflumes had a significantly lower NO_3- concentration compared to the flowing systems ($p \leq 0.01$) over the course of the experiment. Supporting data detailing the water pH and the water PO_4 concentration in the microflumes can be found in Appendix III.6. Briefly, although dark flowing microflumes had a significantly different pH compared to dark static microflumes, there was no clear impact of microflume treatment on water pH; however, dark static microflumes had higher concentrations of PO_4 in the water.

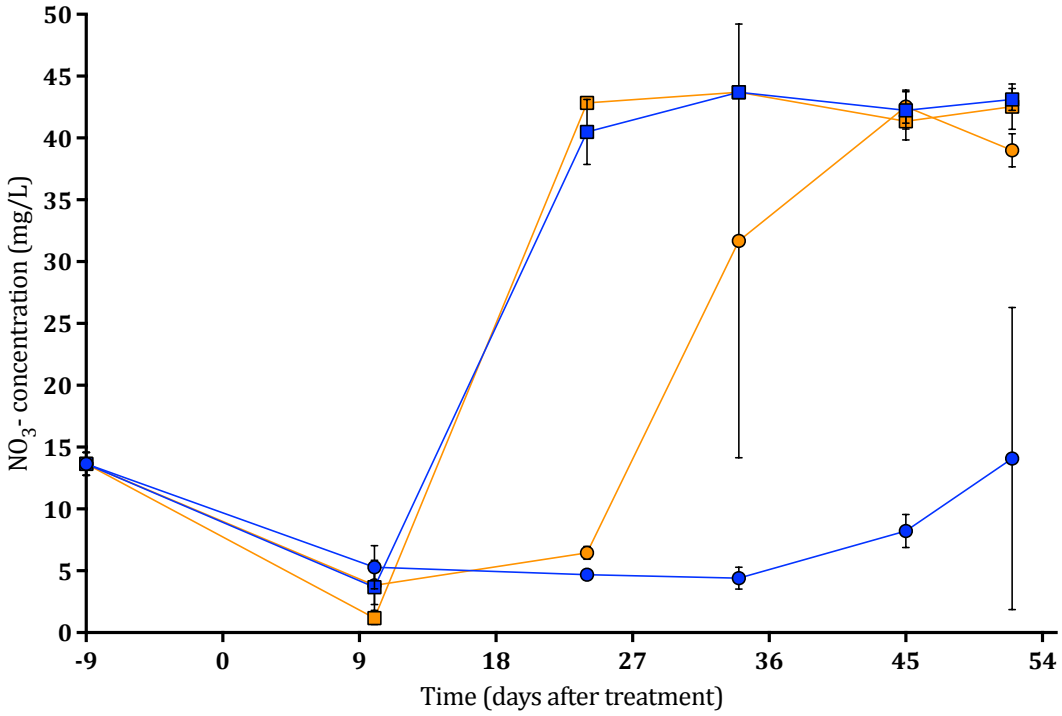

Figure 4.8: Water concentration of NO_3- in microflume systems. NO_3- concentration of the water was measured at each time point in dark static (blue circles), dark flowing (blue squares), illuminated static (orange circles), and illuminated flowing (orange squares) microflume systems. Error bars show ± standard deviation.

4.3.4 Microbial analysis results

4.3.4.i Chlorophyll a *and biofilm development*

There was a significant impact of microflume treatment on the concentration of chlorophyll *a* in the systems ($p \leq 0.0009$, **Fig. 4.9**). Illuminated static microflumes had a significantly higher chlorophyll *a* concentration than all other systems ($p \leq 0.01$), which were not significantly different to each other. In illuminated static microflumes, chlorophyll *a* concentration reached 21.33 mg/m^3 of chlorophyll *a* by 52 DAT, while in the other treatments, concentrations were less than 1 mg/m^3 of chlorophyll *a* for the majority of the time course. Generally, the majority of the chlorophyll *a* originated from the sediment fraction, with an average of 80 % of the total in the dark systems and 90 – 95 % in the illuminated systems coming from the sediment.

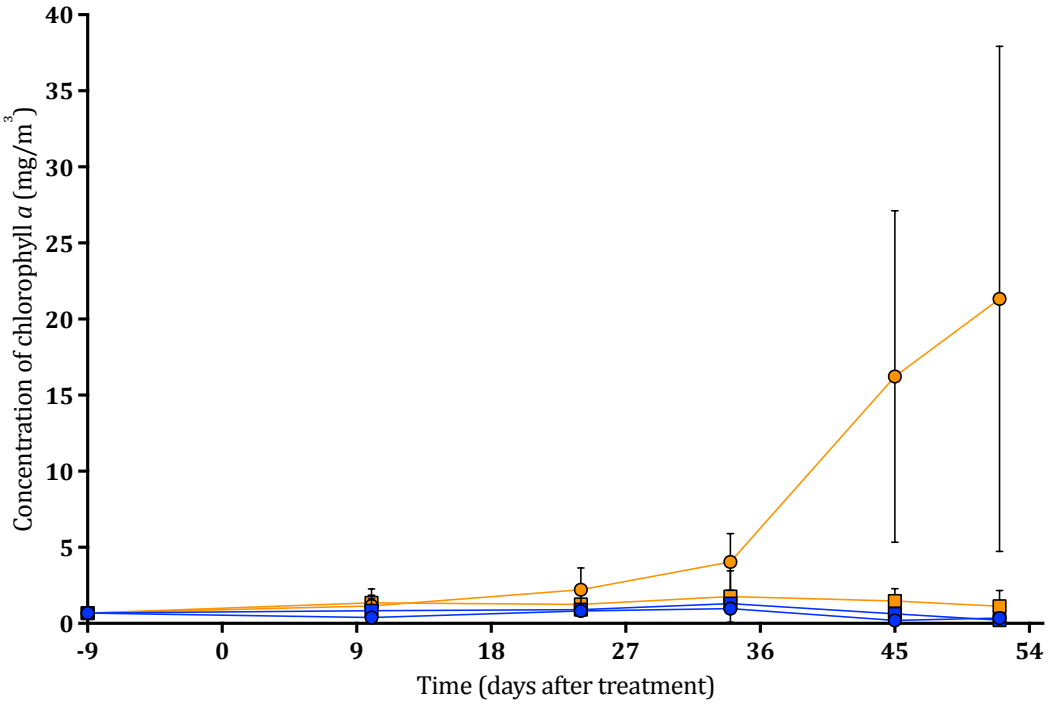

Figure 4.9: Concentration of chlorophyll *a* in water and sediment (summed) in microflume systems. Chlorophyll *a* was extracted from both the water and the sediment using acetone and then the totals summed together in dark static (blue circles), dark flowing (blue squares), illuminated static (orange circles), and illuminated flowing (orange squares) microflume systems. Error bars show ± standard deviation.

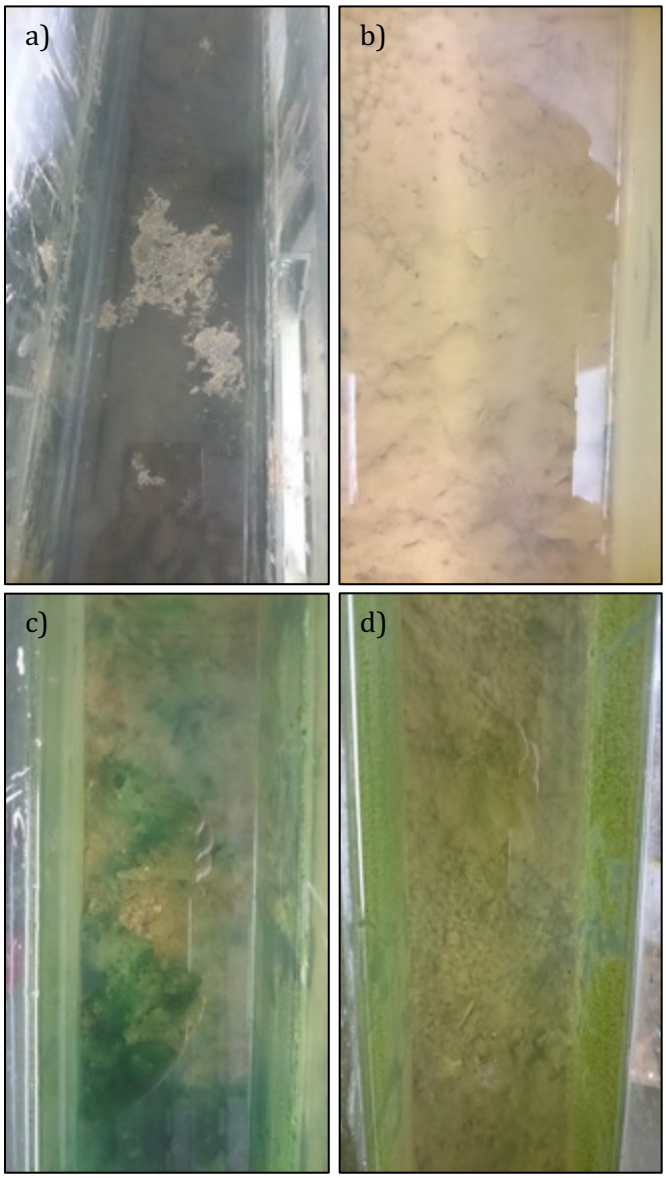

Figure 4.10: Microflume system sediment beds at 52 DAT. Photographs of the sediment bed at 52 DAT in (a) dark static, (b) dark flowing, (c) illuminated static, and (d) illuminated flowing microflume systems.

The differences in phototroph and biofilm abundance between treatments could also be seen by visual examination of the sediment bed (**Fig 4.10**). In both static systems, there was biofilm floating on the water surface, which was absent in the flowing systems. The nature of the floating biofilm differed markedly between the light treatments, with white biofilms in dark systems (**Fig. 4.10.a**) and green biofilms in illuminated systems. Although biofilm wasn't seen on the water surface in the flowing systems, illuminated flowing systems

had a build-up of green biofilm on the sediment surface, as did illuminated static systems. In flowing systems, this was more uniform along the sediment bed (**Fig. 4.10.d**). In static systems, biofilm development was more heterogeneous; in some areas there was minimal growth, but in others there was dense patches (**Fig. 4.10.c**). This likely explains the large standard deviation in measured values (**Fig. 4.9**). Dark flowing systems also had a much more uniform sediment bed, but there was minimal biofilm development (**Fig. 4.10.b**). Details of water bacteria counts can be found in Appendix III.6, and there were no significant differences between treatments.

4.3.4.ii Microbial community rarefaction

Microbial community data was rarefied before analysis (**Table 4.3**, see section IV.3.8 for details). Bacterial community data was rarefied at 4800 sequences, which did not reduce the sample count. Phototrophic community data was rarefied at 19,000 sequences. Non-phototrophs (coincidentally amplified by the selected primers) were then removed from the original data set, leaving 33 samples and 627 OTUs with an average of 16,950 sequences per sample; this data was then rarefied at 5000 sequences to leave 32 samples and 556 OTUs. Eukaryotic community data was rarefied at 6800 sequences, which reduced the sample count from 30 to 28.

Table 4.3: OTU table summaries for bacterial, phototrophic, and eukaryotic analysis. Data was rarefied and numbers in italics show the summary post-rarefaction. Phototroph data was rarefied before and after non-phototroph communities were discarded and these are separated by a forward-slash.

OTU table summary	16S rRNA (bacterial)	23S rRNA (phototrophic)	18S rRNA (eukaryotic)
Sample count	33, *33*	33, *33/32*	30, *28*
Number of OTUs across all samples	4469, *4257*	3554, *3323/556*	2695, *2176*
Average sequences/sample	10,203	51,010	26,642
Rarefaction	4800	19,000/5000	6800

4.3.4.iii Bacterial community composition of the microflume systems

There was no significant difference between the bacterial α diversity in the water between fresh river water and any of the microflume treatments ($p \leq 0.1030$, **Fig. 4.11.a**), with the average α diversities ranging between 64.6 in the dark static microflumes and 146.6 in the dark flowing microflumes. Similarly, there were no significant differences ($p \leq 0.1307$, **Fig. 4.11.b**) in the sediment fraction α diversity between fresh sediment from the river or the microflume treatments, which ranged between 540.6 in the illuminated flowing microflumes and 661.2 in the fresh samples from the river.

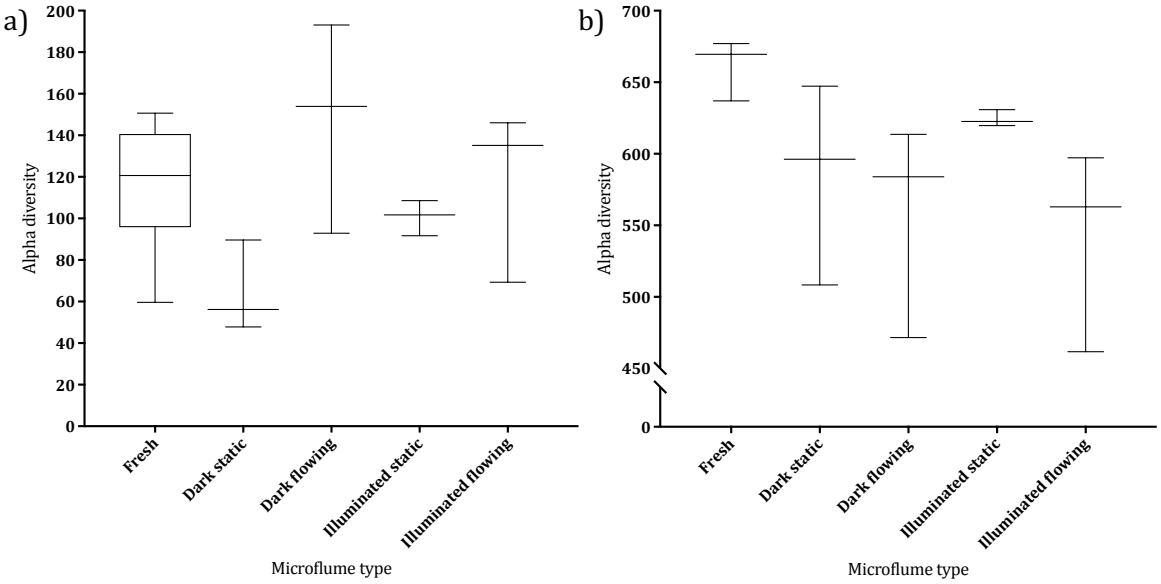

Figure 4.11: Alpha diversity of bacterial communities between microflume systems in the water (a) and the sediment (b). Fisher's α index was calculated from the observed bacterial species at the sample site and from each microflume system at 52 DAT, with the whiskers showing the minimum and maximum values and middle lines showing the median values.

There was a significant impact of microflume treatment on the bacterial community β diversity in both the water and the sediment fractions ($p \leq 0.001$). In the water fraction, pairwise tests showed that β diversity in the fresh river water sample was statistically ($p \leq 0.017$) different to water in the microflumes at 52 DAT (**Fig. 4.12**), which were not significantly different to each other ($p \leq 0.1000$, low (< 0.5) or midrange R^2 values). In particular, when comparing fresh samples to dark microflumes, R^2 values were higher (> 0.7) showing increased dissimilarity, which is especially evident by the larger divergence

between fresh water and dark static water in **Figure 4.12**. Although microflumes at 52 DAT were not statistically different to each other, **Figure 4.12** shows that flowing systems cluster closely regardless of light treatment. In static systems, however, illuminated treatments cluster closer to the fresh samples, whereas dark treatments diverge to a larger extent from all other water samples. For the sediment fraction, pairwise tests showed that there was no significant difference between any of the comparisons (mainly $p \leq 0.1000$), and R^2 values were low (generally < 0.5) showing little dissimilarity. This is clear from **Figure 4.12** where samples cluster closely with less divergence compared to the water samples.

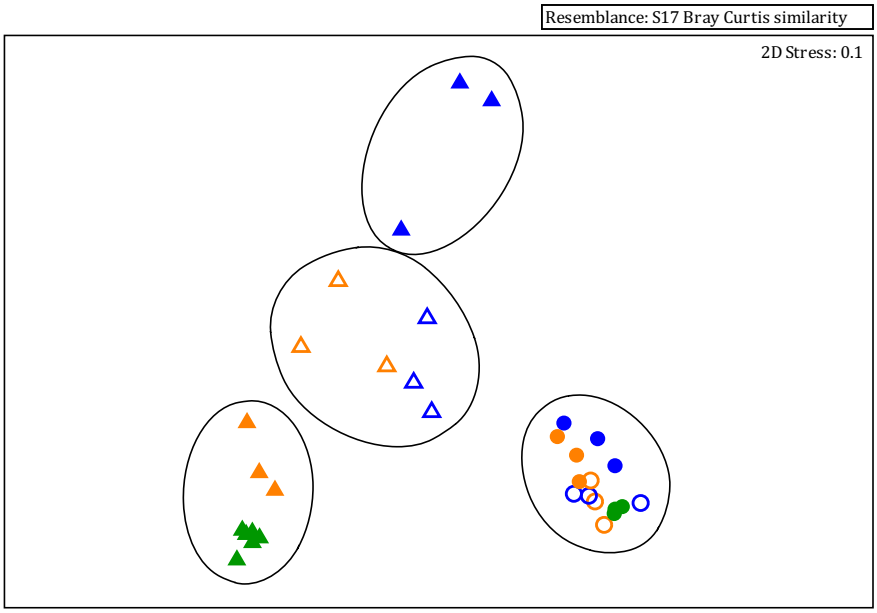

Figure 4.12: Ordination plots from NMDS scaling analysis of Bray Curtis similarities between bacteria in microflume systems. Water (triangles) and sediment (circles) were analysed at the start of the experiment (green) and at 52 DAT in dark static (blue closed), dark flowing (blue open), illuminated static (orange closed), and illuminated flowing (orange open) microflume systems. Black lines represent a similarity threshold of 30 %.

There was a significant impact of microflume treatment on the relative abundance of bacterial phyla in both the water and the sediment fractions ($p \leq 0.0001$, **Fig. 4.13**). In the water fraction, Proteobacteria relative abundance varied between all treatments ($p \leq 0.0001$, 44.7 to 75.4 %) except between the two flowing microflumes (52.9 and 54.5 % in dark and illuminated, respectively). In terms of the relative abundance of communities present, dark static microflumes diverged the most compared to the fresh samples, with the majority of the bacterial relative abundance dominated by Proteobacteria (75.4 %). Compared to all other treatments, these systems had a significantly lower ($p \leq 0.0001$, 2.0

%) relative abundance of Actinobacteria, but a significantly higher relative abundance of Firmicutes ($p \leq 0.001$, 4.7 %).

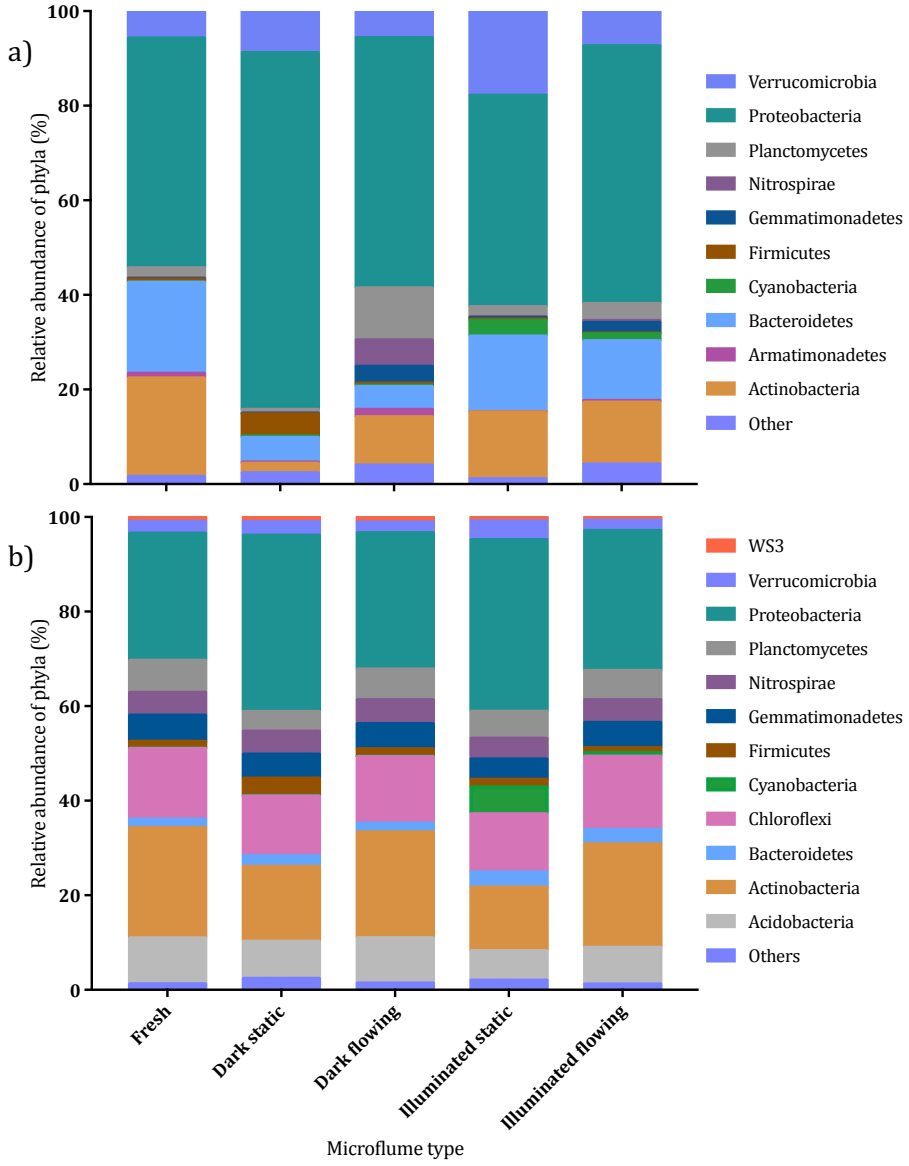

Figure 4.13: Relative abundance of bacterial phyla between microflume systems in the water (a) and the sediment (b). Different bacterial phyla are denoted by different colours and phlya making up < 1 % of the relative abundance are listed under *other*. Analysis was carried out on water and sediment at the beginning of the experiment and at 52 DAT.

Although dark flowing microflumes had a different community relative abundance to fresh samples, a wider range of phyla had higher relative abundances (> 1 %) compared to dark static microflumes. Dark flowing microflumes had a significantly higher relative

abundance of Nitrospirae ($p \leq 0.0001$, 5.6 %) and Planctomycetes ($p \leq 0.0001$, 11.0 %) compared to all other treatments and a significantly higher relative abundance of Gemmatimonadetes ($p \leq 0.01$, 3.6 %) compared to fresh and static microflume samples, with Gemmatimonadetes relative abundance generally being higher in flowing microflumes (2.3 % in illuminated flowing systems).

Generally, fresh samples were similar to the illuminated microflume samples; however, fresh samples did have significantly higher Actinobacteria ($p \leq 0.0001$, 20.8 %) and Bacteroidetes ($p \leq 0.01$, 19.2 %) relative abundances compared to microflumes at 52 DAT. Overall, both illuminated microflumes were similar to one another with illuminated treatments also having a significantly higher relative abundance of Actinobacteria ($p \leq 0.05$, 14.2 and 13.1 % in static and flowing, respectively) and Bacteroidetes ($p \leq 0.0001$, 16.0 and 12.6 in static and flowing, respectively) compared to dark treatments. Furthermore, illuminated static microflumes had significantly higher relative abundances of Verrucomicrobia ($p \leq 0.0001$, 17.9 %) compared to fresh and flowing treatments, and of Cyanobacteria ($p \leq 0.05$, 3.3 %) compared to fresh and dark treatments.

In the sediment fraction, relative abundance of phyla between treatments varied less compared to the water fraction. Nevertheless, flowing treatments were more similar to the fresh river sample in terms of relative abundance of communities present. Despite this, fresh samples did have a significantly higher relative abundance of Acidobacteria ($p \leq 0.05$, 9.7 %) compared to static and illuminated flowing microflumes. In terms of differences between microflumes at 52 DAT, microflumes with the same flowing treatment had the most similar phyla relative abundances. Proteobacteria still dominated the bacterial communities with significantly higher (mainly $p \leq 0.0001$) relative abundances in static microflumes (37.3 and 36.3 in dark and illuminated, respectively) compared to flowing microflumes (28.8 and 29.6 % in dark and illuminated, respectively). Static microflumes also had significantly lower relative abundances of Actinobacteria ($p \leq 0.0001$, 15.8 and 13.4 % in dark and illuminated, respectively) and of Chloroflexi ($p \leq 0.05$, 12.6 and 12.3 % in dark and illuminated, respectively). There was some variance between dark and illuminated static microflumes, and dark treatments had a significantly higher relative abundance of Firmicutes ($p \leq 0.05$, 3.7 %) compared to fresh and flowing treatments, and a significantly lower relative abundance of Planctomycetes ($p \leq 0.05$, 4.2 %) compared to all other treatments.

Illuminated static microflumes also had a significantly higher relative abundance of Cyanobacteria ($p \leq 0.0001$, 5.7 %) compared to all other treatments.

There were no significant differences between treatments linked to any specific OTU. Microflumes were then split by fast dissipation (flowing and illuminated static microflumes) and slow dissipation (dark static microflumes). Only two bacterial OTUs were significantly different between these groups. These were from the family GZKB119 (1013, Bacteroidetes, $p \leq 0.00936$) and the order PL-11B10 (1049, Spirochaetes, $p \leq 0.0312$). Both of these OTUs had a higher relative abundance in dark static microflumes present at 0.07 and 0.1 % of the relative abundance. The other microflumes had no 1013 present, and only illuminated static microflumes had 1049 present (0.003 %). Full breakdown of significant OTUs and their taxonomies can be found in Appendix III.6.

4.3.4.iv Phototrophic community composition of the microflume systems

Although phototrophic species in the dark are likely dormant, there was a significant difference in phototrophic α diversity between microflume treatments in both the water ($p \leq 0.0001$, **Fig. 4.14.a**) and the sediment fractions ($p \leq 0.0002$, **Fig.4.14.b**). In the water fraction, α diversity was significantly higher ($p \leq 0.0001$, except $p \leq 0.01$ for illuminated static microflumes) in the fresh samples from the river (27.7) compared to all microflume treatments at 52 DAT (between 8.1 and 15.1). In the sediment fraction, fresh samples from the river also had a significantly higher α diversity (41.2) compared to both the dark microflumes ($p \leq 0.001$, 27.4 and 25.8) and the illuminated microflumes ($p \leq 0.01$, 29.5 and 31.1) at 52 DAT. In both fractions, there were no significant differences in phototrophic α diversity between any of the microflume treatments at 52 DAT.

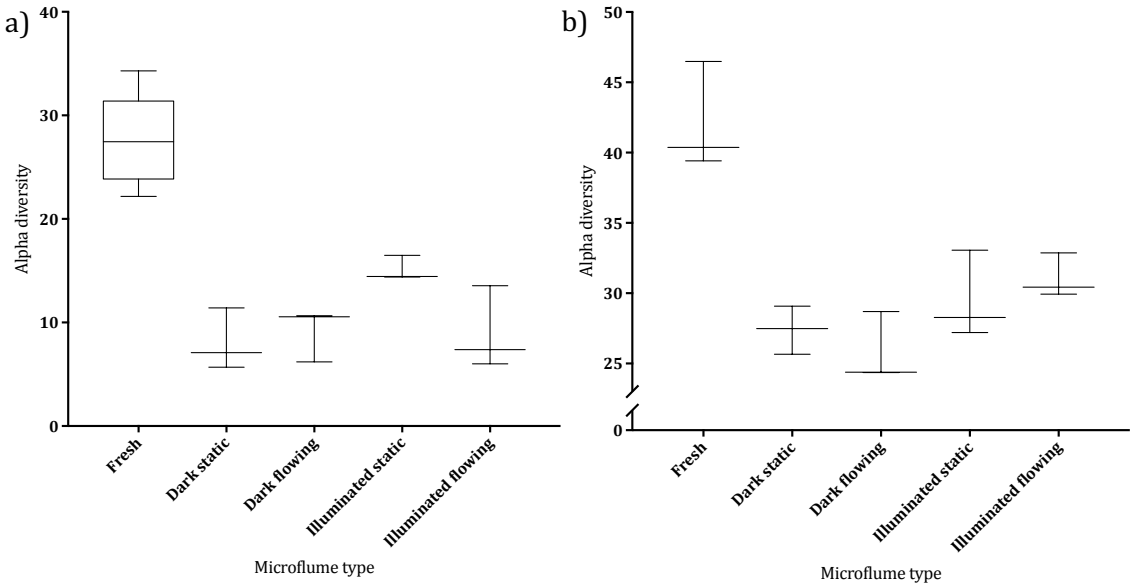

Figure 4.14: Alpha diversity of phototrophic communities between microflume systems in the water (a) and the sediment (b). Fisher's α index was calculated from the observed phototrophic species at the sample site and from each microflume system at 52 DAT, with the whiskers showing the minimum and maximum values and the middle lines showing the median values.

Microflume treatment had a significant impact on phototrophic β diversity ($p \leq 0.001$), which was variable in both the water and the sediment fractions (**Fig. 4.15**) with high R^2 values showing dissimilarity (0.72 and 0.66 in water and sediment, respectively). Pairwise tests showed a significant difference between fresh samples from the river and static and flowing microflumes in the dark ($p \leq 0.029$ and $p \leq 0.009$, respectively) and the illuminated ($p \leq 0.007$ and $p \leq 0.016$, respectively) treatments. This was also evidenced by higher R^2 values ($0.51 < 0.75$) showing dissimilarity (**Fig. 4.15**). There was also dissimilarity between the dark and illuminated static microflumes (0.75) with illuminated treatments diverging further from the original sample (**Fig. 4.15**). In the sediment fraction, pairwise tests showed no significant difference between treatments (mainly $p \leq 0.1$) and most samples did not diverge far from the fresh river samples. R^2 values were higher comparing illuminated static microflumes to the fresh sediment samples (0.75) and the dark microflume treatments at 52 DAT (0.72 for both); this suggests phototrophic communities in illuminated static microflumes were more distinct to the other treatments.

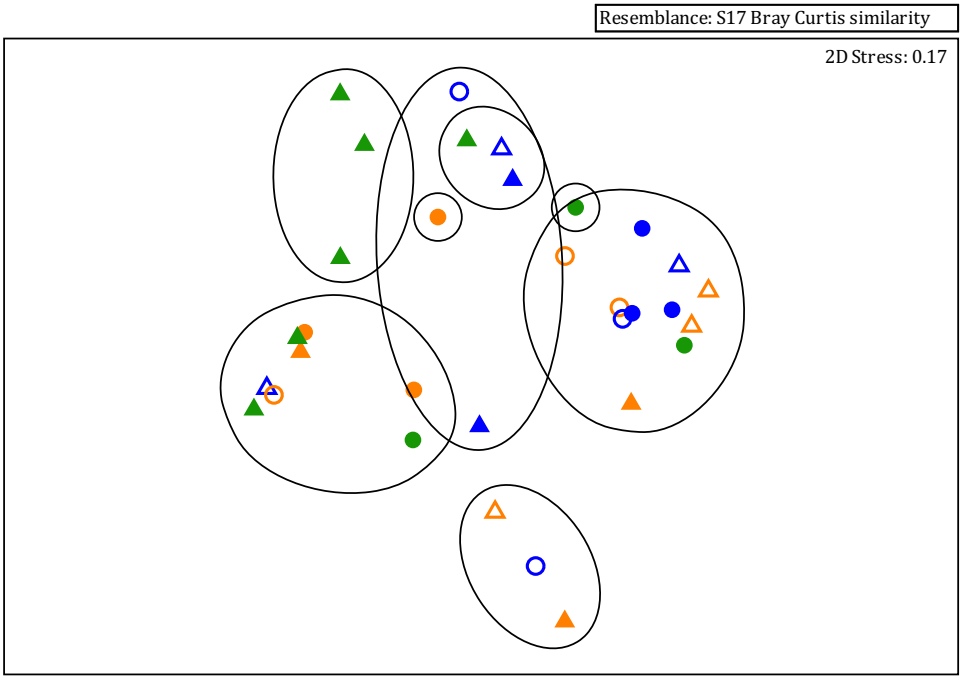

Figure 4.15: Ordination plots from NMDS scaling analysis of Bray Curtis similarities between phototrophic communities in microflume systems. Water (triangles) and sediment (circles) were analysed at the start of the experiment (green) and at 52 DAT in dark static (blue closed), dark flowing (blue open), illuminated static (orange closed), and illuminated flowing (orange open) microflume systems. Black lines represent a similarity threshold of 30 %.

After removal of the non-phototrophic OTUs (see Appendix III.6 for percentages of non-phototrophic and phototrophic OTUs amplified), there was a significant impact on the relative abundance of phototrophic taxa with microflume treatment in both the water and the sediment fractions ($p \leq 0.0001$).

In the water fraction (**Fig. 4.16.a**), there were significant differences between treatments in Charophyta, Chlorophyta, Cyanobacteria, Diatoms, and Golden Algae and there was a high range of divergence from the fresh samples in all microflumes. There were significantly ($p \leq 0.0001$) higher relative abundances of Charophyta in both dark static (94.2 %) and dark flowing (57.7 %) microflumes compared to the fresh river water and both illuminated microflume treatments (0.5 to 13.3 %). Additionally, dark static microflumes had a significantly ($p \leq 0.0001$) higher relative abundance compared to dark flowing microflumes. The illuminated static treatment had a significantly higher ($p \leq 0.05$)

Chlorophyta (73.6 %) relative abundance compared to the fresh river water and the other microflume treatments (1.9 to 56.7 %); however, illuminated treatments generally had higher Chlorophyta relative abundances and illuminated flowing microflumes (56.7 %) also had significantly ($p \leq 0.0001$) higher relative abundances compared to the two dark treatment microflumes (1.9 to 7.6 %). Fresh river samples, on the other hand, had an intermediate Chlorophyta relative abundance (29.0 %) and this was significantly different ($p \leq 0.001$) to the lower levels in the dark microflumes and the higher levels in the illuminated microflumes. Fresh river water also had significantly ($p \leq 0.01$) higher relative abundances of Diatoms (21.5 %) and Golden Algae (35.1 %) compared to the microflume treatments at 52 DAT (0.4 to 3.1 % and 0.4 to 18.4 %, respectively) and also significantly lower ($p \leq 0.05$) relative abundances of Cyanobacteria compared to the two illuminated microflumes at 52 DAT (15.8 to 14.5 %). Lastly, dark flowing microflumes had a significantly higher ($p \leq 0.05$) Golden Algae relative abundance (18.4 %) compared to illuminated flowing microflumes (0.4 %).

In the sediment fraction (**Fig. 4.16.b**), there were significant differences in Charophyta, Chlorophyta, Cyanobacteria, Diatoms, Moss and Land Plants, and Red Algae relative abundances between treatments, and the dark microflumes diverged the least from the fresh samples from the river. Illuminated static and illuminated flowing microflumes had significantly higher ($p \leq 0.05$) relative abundances of Chlorophyta (28.8 and 21.7 %, respectively) compared to fresh river samples and both dark treatment microflumes (3.3 to 7.5 %). Cyanobacteria relative abundance was highest in illuminated static microflumes at 52 DAT (44.5 %) and this was significantly higher compared to fresh river samples and all other microflume treatments ($p \leq 0.05$, 5.8 to 27.0 %). Additionally, illuminated flowing microflumes (27.0 %) had a significantly higher ($p \leq 0.05$) Cyanobacteria relative abundance compared to fresh samples and both dark treatment microflumes (5.8 to 12.0 %).

Diatom relative abundance was higher in fresh and dark treatment microflumes and lower in illuminated microflume treatments. Illuminated static microflumes had the lowest Diatom relative abundance (6.6 %) and this was significantly lower ($p \leq 0.05$) compared to fresh river samples and all other microflume treatments (25.2 to 40.4 %). Additionally, illuminated flowing microflumes had a significantly lower Diatom relative abundance ($p \leq 0.05$, 25.2 %) compared to fresh river samples (29.8 %) and dark static microflumes (40.4

%). Lastly, dark flowing microflumes had significantly ($p \leq 0.05$) higher relative abundances of Moss and Land Plants (19.8 %) and Red Algae (16.8 %) compared to illuminated static microflumes at 52 DAT (3.4 ad 0.7 %, respectively), as well as significantly higher ($p \leq 0.05$) Charophyta relative abundances (19.6 %) compared to fresh river samples and all other microflume treatments (1.5 to 4.1 %).

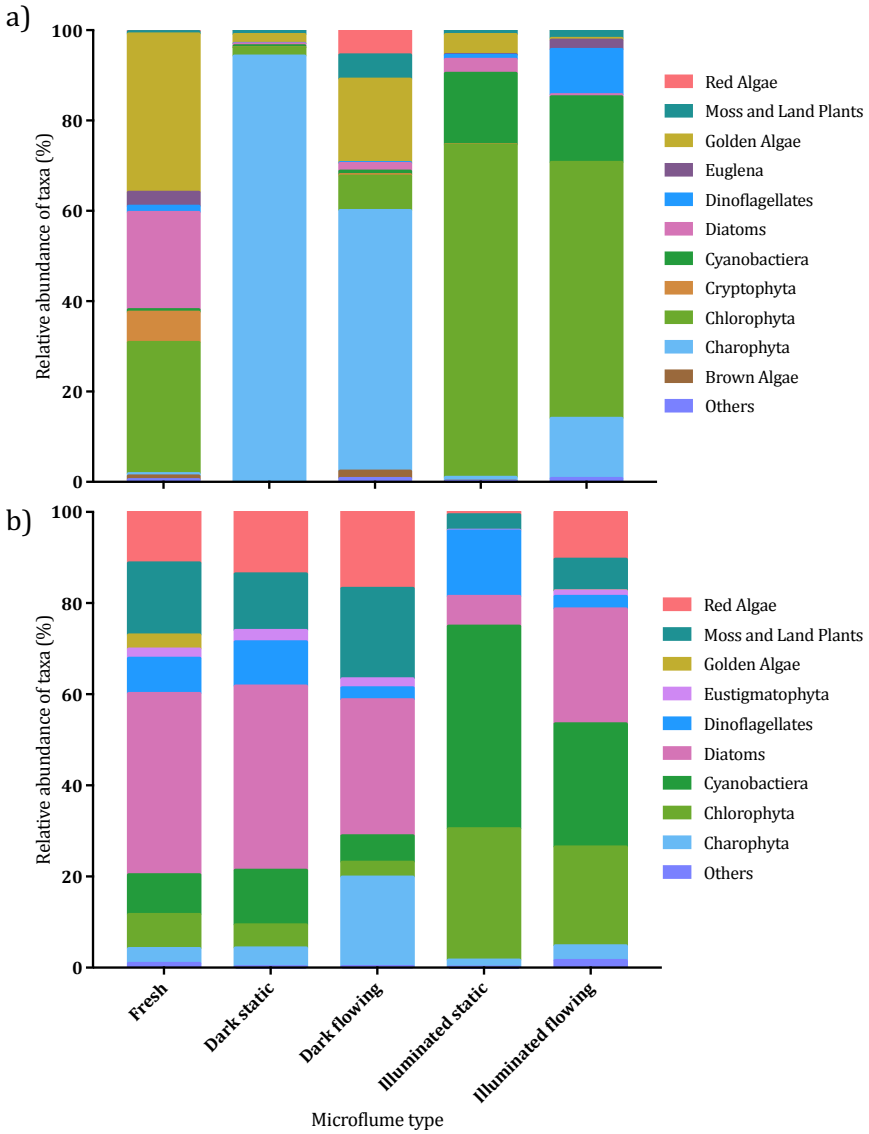

Figure 4.16: Relative abundance of phototrophic taxa between microflume systems in the water (a) and the sediment (b). Different phototrophic taxa are denoted by different colours and taxa making up < 1 % of the relative abundance are listed under *other*. Analysis was carried out on water and sediment at the beginning of the experiment and at 52 DAT.

There were no significant differences between treatments linked to any specific OTU. Microflumes were then split by fast dissipation (flowing and illuminated static microflumes) and slow dissipation (dark static microflumes). Only two phototrophic OTUs were significant between fast and slow dissipation categories, and these were both Spermatophyta (1025 and 981, Viridiplantae, $p \leq 0.0117$ and $p \leq 0.0269$, respectively), which had higher relative abundances in dark static microflumes (0.07 and 0.05 %, respectively). Apart from dark flowing microflumes, which contained 0.003 % of 981, these OTUs were not present in the other microflume treatments. Full breakdown of significant OTUs and their taxonomies can be found in Appendix III.6.

4.3.4.v Eukaryotic community composition of the microflume systems

There was a significant impact of microflume treatment on eukaryotic α diversity in both the water and the sediment fractions ($p \leq 0.0001$). In the water fraction (**Fig. 4.17.a**), there was no significant difference between the microflume treatments at 52 DAT (between 14.4 and 26.0); however, fresh samples had a significantly higher α diversity ($p \leq 0.01$, 75.1). In the sediment fraction (**Fig. 4.17.b**), fresh samples also had a significantly higher α diversity ($p \leq 0.001$, 173.6) compared to the treatments at 52 DAT; however, there was also a significant difference ($p \leq 0.05$) between illuminated static microflumes (46.7) and dark flowing microflumes (87.8).

There was a significant impact of microflume treatment on eukaryotic β diversity in both the water and the sediment fractions ($p \leq 0.001$). The sediment samples were more variable, which was evident from the higher R^2 value (0.73) compared to the water samples (0.62). In the water, although pairwise R^2 values were generally mid-range or low (< 0.6), tests showed that fresh samples were statistically different from both flowing and illuminated static treatments ($p \leq 0.023$, **Fig. 4.18**). In the sediment fraction, pairwise tests showed no significant difference between individual comparisons (mainly $p \leq 0.1000$) and most R^2 values were mid-range (0.5 to 0.6). Despite this, when comparing fresh samples to the samples at 52 DAT, R^2 values were higher (> 0.7) showing greater dissimilarity, with illuminated microflumes diverging further from the fresh samples than dark microflumes.

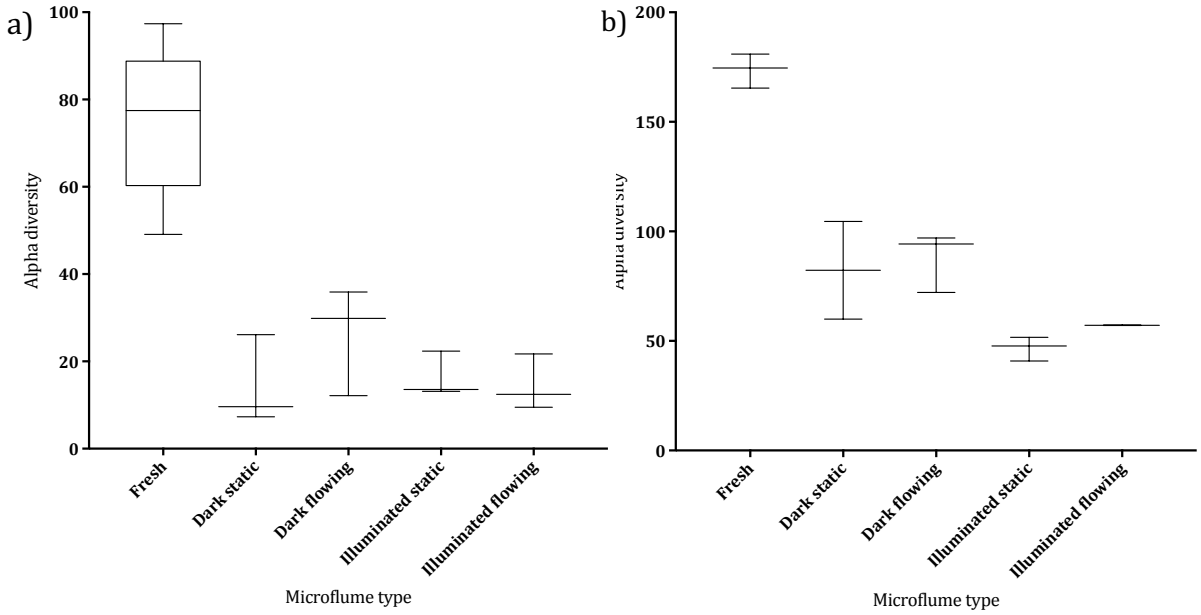

Figure 4.17: Alpha diversity of eukaryotic communities between microflume systems in the water (a) and the sediment (b). Fisher's α index was calculated from the observed eukaryotic species at the sample site and from each microflume system at 52 DAT, with the whiskers showing the minimum and maximum values and the middle lines showing the median values.

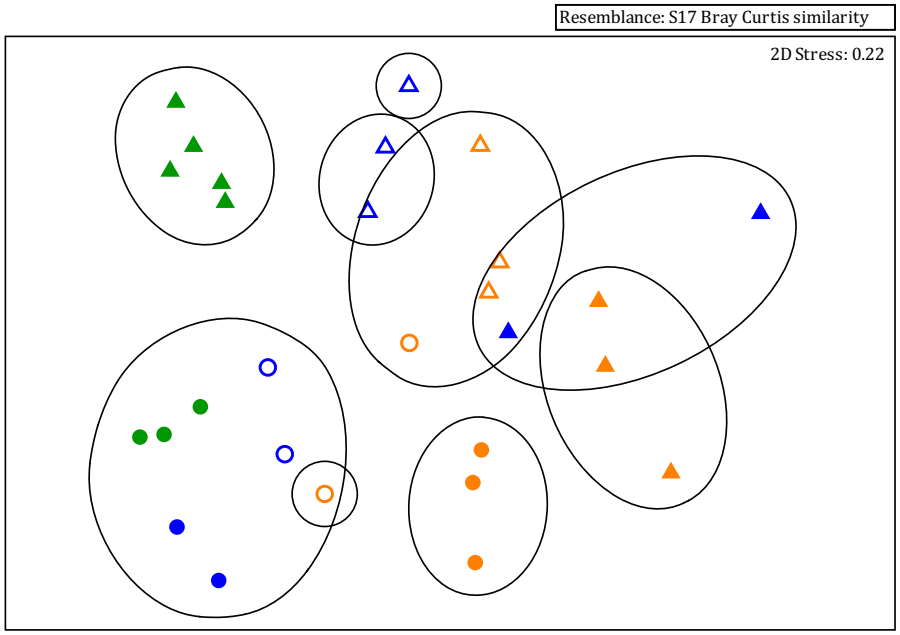

Figure 4.18: Ordination plots from NMDS scaling analysis of Bray Curtis similarities between eukaryotes in microflume systems. Water (triangles) and sediment (circles) were analysed at the start of the experiment (green) and at 52 DAT in dark static (blue closed), dark flowing (blue open), illuminated static (orange closed), and illuminated flowing (orange open) microflume systems. Black lines represent a similarity threshold of 30 %.

There was a significant impact of microflume treatment on the relative abundance of eukaryotic classes within both the water and the sediment fractions ($p \leq 0.0001$). The water fraction (**Fig. 4.19.a**) was less variable than the sediment fraction and there were significant differences between Nucletmycea, which include fungi, Alveolata, a group comprising of protists, and Chloroplastida and Stramenopiles, which are both phototrophic eukaryotes. The fresh samples from the river had a wider range of classes with higher relative abundances (> 1 %) and had significantly higher percentages of Chloroplastida ($p \leq 0.05$, 11.8 5) compared to dark systems, and a significantly higher relative abundance of Nucletmycea ($p \leq 0.0001$, 22.0 %) compared to static systems. In addition, fresh samples had a significantly higher relative abundance of Stramenopiles compared to all microflumes at 52 DAT ($p \leq 0.0001$, 40.2 %). Dark static microflumes diverged the most from the fresh sample and the eukaryotic relative abundance was dominated by Alveolata, and these microflumes had a significantly higher relative abundance of this class compared to other treatments ($p \leq 0.0001$, 80.5 %).

The relative abundance of Nucletmycea was significantly higher ($p \leq 0.0001$) in the flowing microflumes (34.3 and 40.4 % in dark and illuminated, respectively) compared to the static microflumes (2.4 and 5.3 % in dark and illuminated, respectively), and Chloroplastida relative abundance was significantly higher ($p \leq 0.0001$) in illuminated microflumes (24.6 and 28.0 % in static and flowing, respectively) compared to the dark microflumes. In addition, illuminated static microflumes also had a higher relative abundance of Stramenopiles ($p \leq 0.05$, 17.4 %) compared to dark static microflumes (5.7 %).

The sediment fraction was much more variable (**Fig. 4.19.b**) and there was a wider range of eukaryotic classes driving the differences between microflume treatments including, Holozoa, Nucletmycea, Alveolata, Rhizaria, Chloroplastida, Stramenopiles, and Rhodophyceae. The fresh samples had a significantly higher relative abundance of Holozoa ($p \leq 0.001$, 12.0 %) compared to the static and illuminated flowing microflumes at 52 DAT. In addition, they had a significantly higher relative abundance of Chloroplastida ($p \leq 0.0001$, 35.1 %) compared to the dark microflumes, and a significantly lower relative abundance of Rhizaria ($p \leq 0.0001$, 5.0 %), which are protists, compared to microflumes at 52 DAT.

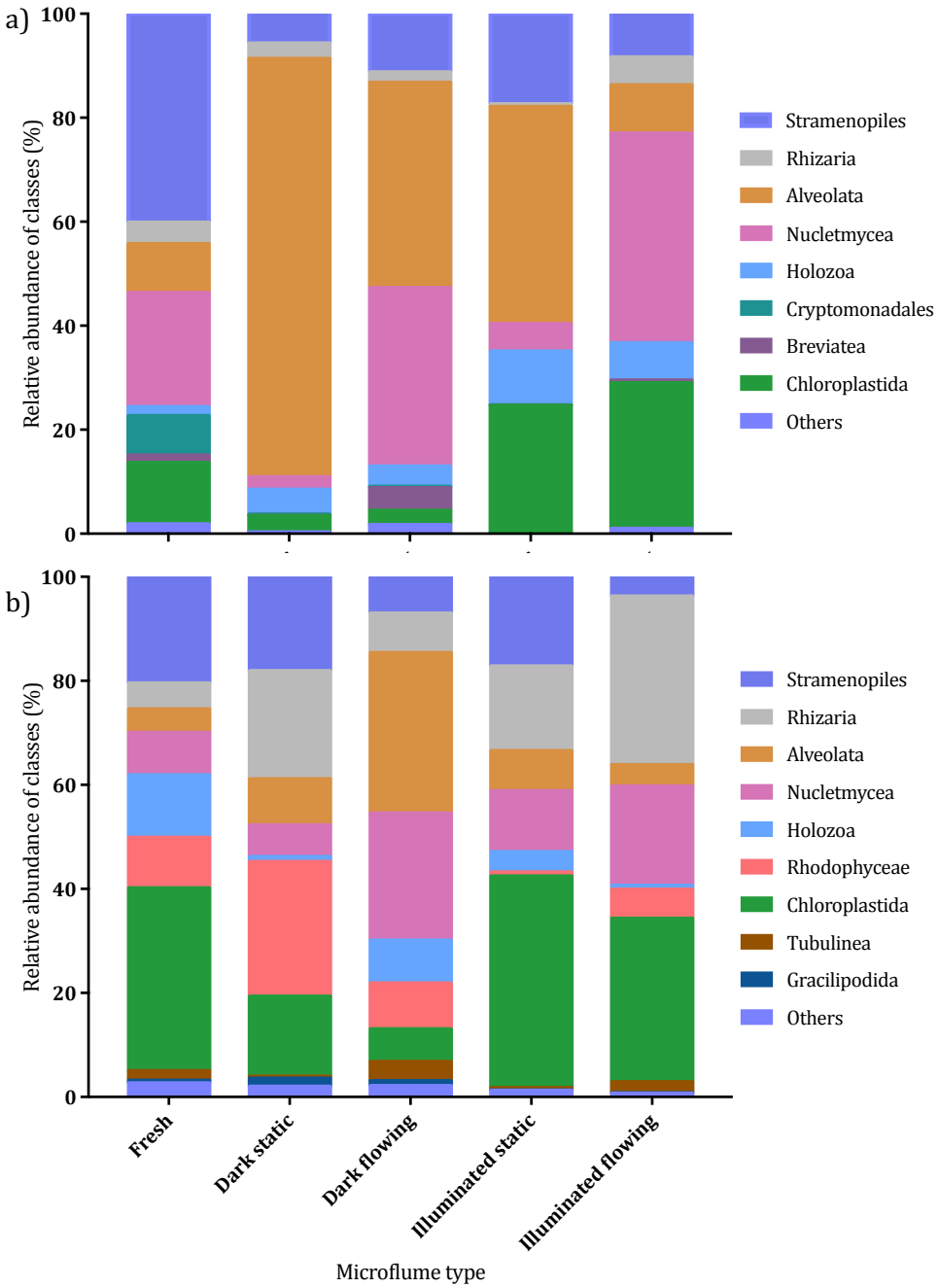

Figure 4.19: Relative abundance of eukaryotic classes between microflume systems in the water (a) and the sediment (b). Different eukaryotic classes are denoted by different colours and classes making up < 1 % of the relative abundance are listed under *other*. Analysis was carried out on water and sediment at the beginning of the experiment and at 52 DAT.

Illuminated microflumes had a significantly higher relative abundance of Chloroplastida ($p \leq 0.0001$, 40.7 and 31.4 % in static and flowing, respectively) compared to the dark treatments, and flowing microflumes also had a lower relative abundance of this

class (6.3 and 31.4 % in dark and illuminated, respectively) compared to their respective static treatments (15.4 and 40.7 %). In addition, flowing microflumes had higher relative abundances of Nucletmycea ($p \leq 0.0001$, 24.5 and 19.1 % in dark and illuminated, respectively) and lower relative abundances of Stramenopiles ($p \leq 0.001$, 7.0 and 3.6 % in dark and illuminated, respectively) compared to static microflumes.

Lastly, dark static microflumes had higher relative abundances of Rhodophyceae, a red algae class, ($p \leq 0.0001$, 25.9 %) compared to other treatments, and illuminated flowing microflumes had higher relative abundances of Rhizaria ($p \leq 0.0001$, 32.4 %) relative to other treatments. Dark flowing microflumes had higher relative abundances of Holozoa ($p \leq 0.05$, 8.3 %) compared to illuminated treatments and higher relative abundances of Alveolata ($p \leq 0.0001$, 30.8 %) compared to all other treatments.

There were no significant differences between treatments linked to any specific OTU. Microflumes were then split by fast dissipation (flowing and illuminated static microflumes) and slow dissipation (dark static microflumes). Only one OTU showed significance between dissipation categories and this was Magnoliophyta (775, Archaeplastida, $p \leq 0.0327$), which had a high relative abundance in dark static microflumes (0.06 %) and was not present in the other treatments. Full breakdown of significant OTUs and their taxonomies can be found in Appendix III.6.

4.4 DISCUSSION AND CONCLUSIONS

This study found that water flow had a bigger impact on isopyrazam dissipation than non-UV light at the microflume scale. In static systems, however, non-UV light had major impacts on dissipation and partitioning processes. Flow treatment impacted how phototrophic communities proliferated with higher concentrations in illuminated static microflumes. In these systems, these communities played a bigger role in dissipation relative to the flowing systems.

Microbial community composition in dark static microflumes diverged from the fresh samples more than the other treatments. Flowing and non-UV light treatments helped retain bacterial diversity in terms of species present in the water fraction, yet different communities developed depending on treatment. This suggests that there are different microbial mechanisms for dissipation with a number of species capable of metabolism. Isopyrazam dissipated in all systems, but environmental conditions impacted the time taken for communities capable of metabolism to proliferate, causing dissipation to occur at different rates between treatments.

4.4.1 Impact of mixing on dissipation and microbial communities

The impact of flowing water on the microflume treatments completely diminished the impact of non-UV light on isopyrazam dissipation, which has previously been seen in studies by Hand and Oliver (2010) and in Chapter 2 of this thesis. This is most likely due to the impact of mixing which can benefit microbial communities (Naudin *et al.*, 2001, Spain *et al.*, 1984). This can impact mass transport and increase the chance of microbes coming into contact with electron donors and acceptors or nutrients, which will allow proliferation. (Bauer *et al.*, 2008, Gantzer *et al.*, 1988, Kirchman *et al.*, 1989, Reynolds, 1994, Thullner *et al.*, 2002, Wetzel, 1993). This is evident in the higher NO_3- concentrations in flowing microflumes which indicates an increase in nitrifier microbial activity. Furthermore, water flow will impact the distribution of microbes in the systems, which is especially important in the dissipation process if it allows microbes capable of degradation to come into contact with pollutants (Sánchez-Pérez *et al.*, 2013).

Higher bacterial growth rates and degradation have been shown to occur at the water-sediment interface (Xia and Wang, 2008) and studies have shown the importance of water velocity and turbulence in aiding transfer between the two fractions (Chen *et al.*, 2008, Gualtieri, 2004, Higashino *et al.*, 2004, Hondzo, 1998). Substances can accumulate in the sediment, and there can also be transport back into the water column via the interface (Bonanni *et al.*, 1992, Chen *et al.*, 2008, Perelo, 2010, Shrestha *et al.*, 2016). This can include transport of nutrients, degrading bacteria, and environmental contaminants (Canuel and Martens, 1996, Hondzo, 1998, Rusch *et al.*, 2001).

It is likely that flowing systems are more homogenous regardless of light treatment and allow better dispersion (Bornette *et al.*, 1998, Vannote *et al.*, 1980, Williams *et al.*, 2003). This means exchange can occur at a higher rate and more isopyrazam can partition to the water column; this is evident especially in dark static systems were more isopyrazam partitioned to the sediment. This means it was not bioavailable to microbial degraders in the water column or at the water-sediment interface.

4.4.2 Impact of phototrophic biofilm in illuminated microflumes

The literature details that biofilm thickness is lower when water current is higher (Battin *et al.*, 2003a, Battin *et al.*, 2003b, Wetzel, 1993). It has also been noted that under higher turbulence, biofilm was more uniform covering the entire surface, but there was higher spatial variation at lower turbulence levels (Kugaorasatham *et al.*, 1992). This was seen in this experiment, with constant mixing in the illuminated flowing systems leading to an evenly distributed biofilm but, potentially due to velocity disturbances, it did not allow higher proliferation. In the illuminated static microflumes, however, phototrophic biofilms were able to grow more efficiently. Communities in illuminated static microflumes will be heavily impacted by light; illumination did play a role in isopyrazam dissipation in static microflumes, as in Hand and Oliver (2010) and Chapter 2 of this thesis, albeit at a slightly slower rate than the flowing microflumes. Phototrophic communities cannot proliferate as easily in a flowing environment, where other degraders may be more important.

Algae have the potential to sorb contaminants, including pesticides (Crum *et al.*, 1999, Friesen-Pankratz *et al.*, 2003), heavy metals (Holan and Volesky, 1992, Holan *et al.*,

1992, Mehta and Gaur, 2008, Rajfur and Klos, 2013, Rajfur *et al.*, 2013, Sandau *et al.*, 1996), and hydrocarbons (Headley *et al.*, 2008). Although biofilm on the glass surface was not taken into account in this study, biofilm in the water and on the sediment surface was assessed and included within the separate fractions. In illuminated static microflumes, it is likely that isopyrazam was sorbed to algal cells both within the water fraction, as there were also biofilms floating on top of the water surface, and on top of the sediment bed form. Biofilms additionally have the potential to release sorbed substances back into the water column (Flemming, 1995, Makris *et al.*, 2014). In these systems, isopyrazam may have been preferentially sorbed to the biofilm, degraded, and then metabolites released back into the water fraction. If degradation occurred quickly, it would explain why less isopyrazam was recovered from the sediment in illuminated static systems. An additional explanation could be from the biofilm acting as a barrier and clogging pores, thus decreasing connectivity between the water and the sediment fractions (Battin and Sengschmitt, 1999). Lastly, biofilms can also be responsible for nutrient cycling (Flemming, 1993, Writer *et al.*, 2011), which would account for the higher NO_3- concentrations compared to dark static microflumes.

4.4.3 Impact of microbial communities in isopyrazam dissipation

It is likely that the large abundance of phototrophic biofilm would have dominated the illuminated static systems and changed the microenvironment, including the abundance of other species (Raffaelli *et al.*, 1998). This could change the environment at the water-sediment interface and disrupt the transfer of nutrients (Paerl and Otten, 2013, Raffaelli *et al.*, 1998, Sunda *et al.*, 2006), especially the algal biofilms on top of the sediment bed which could intercept substances moving from the sediment to the water column (Valiela *et al.*, 1997). As phototrophic communities were impacted by flow conditions, it could have been more beneficial for non-phototrophic bacterial species, including degraders, to proliferate in flowing systems (Bauer *et al.*, 2008, Chapelle *et al.*, 1996, Gantzer *et al.*, 1988, Thullner *et al.*, 2002). In the illuminated flowing microflumes, there could also be other factors contributing to the lower abundance of phototrophic communities, such as bacteria modifying their environment so that it is detrimental to algal species. One example is aerobic respiration decreasing the concentration of dissolved oxygen in the water, which can inhibit some phototroph communities (Cole, 1982).

Relative to the flowing systems and illuminated static systems, the dark static microflumes showed marked differences in isopyrazam dissipation rate and microbial community composition. This was especially evident in the water fraction where the majority of the relative abundance was dominated by a single bacterial, phototrophic, and eukaryotic phylum – Proteobacteria, Charophyta, and Alveolata, respectively. Although Proteobacteria has been shown to have degradative capabilities (Marin, 2011, Parales, 2009), it is likely that biodegradation occurs due to the presence of microbial consortia rather than one single species (Arif *et al.*, 2012, Courtes *et al.*, 1995, Elias and Banin, 2012, Hoskeri *et al.*, 2014, Levanon, 1993, Lima *et al.*, 2003, Sørensen *et al.*, 2002). Due to the conditions in the dark static microflumes favouring these specific species, it led to a less diverse range of taxa present at higher relative abundances, which could reduce the community function. This is in contrast to the dark flowing microflumes. Although there are differences in community structure when compared to the illuminated microflumes, in the water there was a broader range of bacterial phyla present at higher relative abundances compared to the dark static microflumes; this included higher levels of Planctomycetes, Nitrospirae, and Gemmatimonadetes.

Relative abundance of certain phyla were significantly higher in some treatments, such as the phototrophs, Chlorophyta and Chloroplastida, in the illuminated microflumes and Actinobacteria and Gemmatimonadetes in the flowing microflumes. Within the separate illuminated treatments, flowing microflumes had higher levels of Diatoms in the sediment fraction, which are known to be adapted to flowing environments (Dorigo *et al.*, 2007, Reynolds *et al.*, 1994, Rodrigues and Bicudo, 2001). Illuminated static microflumes had higher levels of Verrucomicrobia and Cyanobacteria – Cyanobacteria was especially dominant in the sediment, likely due to the increase of surface biofilm. Regardless, as DNA analysis was only carried out at the beginning and end of the experiment, it will be impossible to determine what change in the microbial community occurred in illuminated static microflumes to enable them to have a similar dissipation rate as the flowing microflumes by 52 DAT, or the changes in the dark static community which causes an increase in dissipation after 24 DAT. Several OTUs were shown to be more abundant in dark static microflumes, such as PL-11B10 which is found in communities where hydrocarbon biodegradation occurs quickly (Shelton *et al.*, 2016) or in petroleum reservoir production

waters (Grabowksi *et al.*, 2005); however, analysis of OTUs within different treatments gave little insight into the differences in dissipation rate.

Faster dissipation occurred in microflumes with higher relative abundances of Actinobacteria and lower levels of Proteobacteria due to the proliferation of other phyla. Actinobacteria have been shown to be metabolically diverse and are capable of degradative abilities, including of cellulose, hydrocarbons, and pesticides, meaning they have valuable ecological functions (Chen *et al.*, 2016, De Schrijver and De Mot, 1999, Jung *et al.*, 2016, McCarthy and Williams, 1992). In the case of pesticides, although some species are able to completely mineralise pesticides, most degradation is reported to need consortia with co-metabolism and potentially even genetic transfer playing a role (De Schrijver and De Mot, 1999). This would explain why the higher dissipation was seen in microflumes containing a wider variety of bacterial phyla which were present at higher relative abundances. Similar to these results, other work on diesel contaminated microcosms also shows that Proteobacteria and Actinobacteria dominated the systems due to their competitiveness and degradative potential (Jung *et al.*, 2016). Although Proteobacteria abundance was lower in microflumes where dissipation was higher, they still made up a large majority of the total relative abundance of bacterial phyla.

Lastly, NO_3- concentrations increased with isopyrazam dissipation and there is evidence that nitrifying bacteria have the ability to biodegrade environmental contaminants; indeed, both Nitrospirae and Cyanobacteria can be responsible for nitrification and these are present in the dark flowing and illuminated microflume water fractions, respectively. This includes co-metabolism, with other non-nitrifying heterotrophs also playing a role in the degradation pathway (Batt *et al.*, 2006, Pérez *et al.*, 2005, Rasche *et al.*, 1990, Shi *et al.*, 2004). Nitrifying bacteria could play a direct role in degradation or they could have an indirect impact on degraders; bacteria can also use NO_3- for growth or as an electron acceptor (Moreno-Vivián *et al.*, 1999). In dark static microflumes, PO_4 concentrations increased after 24 DAT. Potentially this increase was due to a decrease in redox potential from reduced mixing in these microflumes, and this has been shown to increase phosphate concentration (Ann *et al.*, 1999). Nevertheless, isopyrazam dissipation increased with the increase in PO_4 concentration; PO_4 is vital for bacterial communities and is often a limiting factor in the freshwater environment (Kirchman, 1994). Some bacteria are able to solubilise

PO_4 and there have been links with these species and biodegradation of hydrocarbons (Bello-Akinosho *et al.*, 2016, DeSouza *et al.*, 1996).

Although it is not certain whether the increases in NO_3- and PO_4 in the different systems were directly linked to isopyrazam dissipation, it could be that different microbes or different mechanisms are responsible for the dissipation, explaining the dissimilarities in kinetics, macronutrient levels, and microbial communities between the three treatments.

4.4.4 Implications of the study

This work has enabled determination of differences in isopyrazam dissipation under more realistic conditions than is possible in standard OECD 308 tests. It has therefore given insight into the influence of variables which are absent from these regulatory tests on dissipation rate. OECD 308 tests are carried out at a much smaller scale and are usually performed statically and under dark conditions. This experiment has shown that flow, which is a key characteristic of water bodies in nature, even to some extent in static systems, is a powerful determinant of dissipation rate. Furthermore, this experiment has shown that although non-UV light plays a role in isopyrazam dissipation in static systems, it does not in flowing systems. This provides support for considering inclusion of a further range of environmental variables within laboratory testing regimes, depending on the source of the environmental samples e.g. static or moving water depending on whether the sample comes from a river or a lake.

Further work would be useful to determine sorption of isopyrazam to biofilms, non-extractable residues in the sediment, and mineralisation. This would require radiolabelled work and it would be a challenge to include on this larger scale. Even in more realistic microflume systems, it proves difficult to get an exact representation in the laboratory of the microbial communities present in the real environment. The phototrophic and eukaryotic relative abundance, in particular, diverged from the fresh samples, likely due to species preferring specific environmental conditions (e.g. light, temperature, etc.). Despite this, previous work has shown that a wide variety of phototrophic communities can degrade compounds (Thomas and Hand, 2012), so the fact that the community has diverged from the fresh sample does not necessarily mean that the dissipation rate is not relevant to the real

environment. The bacterial community of the illuminated flowing system, however, was a good mimic of the fresh water and sediment samples, and the data suggests that more realistic conditions, such as light and water flow, could allow better simulation of a river than the conditions currently used within OECD tests. The dark static microflumes in this experiment better resembled the conditions used in OECD 308 tests and, in this treatment, microbial community composition diverged from the fresh samples more than the other treatments, especially in the water fraction.

4.4.5 Conclusions

Non-UV light impacted isopyrazam dissipation in static microflumes. Phototrophic communities were also able to proliferate due to less turbulent conditions and these communities could have played a role in sorption and degradation of isopyrazam. Non-phototrophic communities were additionally impacted under light treatment, suggesting that the community as a whole was benefitted by the more inclusive community that the light treatment provides. Non-UV light had no effect on dissipation in flowing systems and flowing treatment proved to be more important in the dissipation process, impacting microbial activity and allowing dissipation to occur at a faster rate. This reflects the importance of mixing, which promotes contact between degraders and isopyrazam.

By the end of the experiment, flowing treatments and illuminated static microflumes had a similar level of isopyrazam dissipation and these treatments had a much broader range of taxa present at higher relative abundances compared to the dark static treatment. Biodegradation is unlikely to occur due to just a single species and an increase in the range of taxa present suggests there is an increase in community function. It seems likely from these results that several taxa will be capable of degrading isopyrazam; however, communities will proliferate at different rates depending on the environmental conditions. Therefore, different communities proliferate in the different microflume treatments and this is reflected in the isopyrazam dissipation rates.

CHAPTER 5 - GENERAL DISCUSSION

This thesis has explored the reproducibility and environmental realism of pesticide fate and transformation in regulatory-type tests and the role of the microbial community in these processes. Environmentally realistic variables not usually considered during regulatory studies were introduced to modified regulatory-type tests to assess the impact this would have on isopyrazam fate and transformation. The variables assessed were, non-UV light; temporal variation; sediment addition to microcosms; laboratory test system scale; and water flow. The major findings will be discussed below.

5.1 THE IMPACT OF NON-UV LIGHT ADDITION ON ISOPYRAZAM FATE AND TRANSFORMATION

The influence of non-UV light on both the microbial community and biodegradation was assessed in Chapters 2 and 4 in microcosms and microflumes, respectively. Test systems were incubated either under a non-UV light cycle, in order to eliminate photolysis but allow development of phototrophic communities, or total darkness. In Chapter 2, there was increased isopyrazam degradation in microcosms incubated under non-UV light compared to microcosms incubated under dark conditions, where there was very little degradation; this was most significant in water-sediment microcosms. On a larger more realistic scale in Chapter 4, there was no effect of non-UV light on isopyrazam dissipation in flowing systems; however, in static systems there was still significantly faster dissipation. This will be discussed more in section 5.5, but this is probably due to conditions in the illuminated static microflumes being more beneficial for phototrophic communities to proliferate.

Phototrophic communities are excluded from OECD tests and there is increasing evidence of the role these communities can play in the biodegradation of environmental pollutants. This can include direct metabolism by phototrophic communities, as in Lima *et al.* (2003) and Roldán *et al.* (1998), or an indirect role which could result from a number of mechanisms. Although Davies *et al.* (2013) found that there was an increase in degradation under non-UV light for some compounds, there was no correlation between chlorophyll *a* and degradation rate, suggesting that both phototrophic and heterotrophic communities contributed to degradation. Thomas and Hand (2012) also found that mixed phototrophic

and heterotrophic communities degraded compounds quicker than exclusively phototrophic communities. Particularly in Chapter 2, a number of non-phototrophic communities were significantly linked to faster degradation or mineralisation rates. Higher mineralisation rates at certain collection times were also not exclusive to illuminated treatments, suggesting heterotrophic communities may play more of a role in the final metabolic steps of isopyrazam degradation.

This thesis has only focused on the degradation of one compound, isopyrazam, and as has previously been shown by Davies *et al.* (2013), the impact of non-UV light on degradation is compound specific. This means that light may not stimulate degradation for all compounds. Nevertheless, OECD 308 and 309 tests are preferably carried out under dark conditions (OECD, 2002b, OECD, 2004) and the introduction of light to these studies would be more environmentally realistic, especially in environments such as surface water where there will be sunlight exposure. This thesis aimed to show the importance of phototrophic organisms in biodegradation processes and hence only non-UV light was used in these studies; however, it would also be beneficial to conduct experiments using light intensities representative of the real environment (e.g. including UV light) in order to determine the importance of phototrophic biodegradation when other degradation processes are also occuring simultaneously. One obstacle for regulations is the high variance in, for instance, light exposure, even across Europe (Seckmeyer *et al.*, 2008, World Energy Council, 2013). Nevertheless, regardless of whether light has a positive, negative, or no effect on fate and transformation, the inclusion of light in regulatory tests may make them more representative of natural systems; possibly a standard light intensity could be used across the guidelines so that there remains a level of control to the laboratory conditions.

5.2 THE IMPACT OF TEMPORAL VARIATION IN INOCULUM ON ISOPYRAZAM FATE AND TRANSFORMATION

The impact of temporal variation in environmental inoculum on isopyrazam degradation in laboratory test systems was assessed in Chapter 2. Only in illuminated treatments was there variation in isopyrazam degradation and mineralisation rates between inoculum collection times. In dark treatments, inoculum collection time only affected isopyrazam mineralisation rate. The OECD 308 and 309 guidelines do not prescribe the time

and place environmental inoculum should be collected stating, "the sample site should be selected in accordance with the purpose of the test in any given situation" (OECD, 2002b, OECD, 2004). This suggests that the time of year inoculum collection takes place should be at a time that the pesticide residues would be expected to be present in the environment. Considering pesticides might be applied multiple times within a cropping season (Caspell *et al.*, 2006, Okonya and Kroschel, 2015), or that residues might persist in the environment after application (Gavrilescu, 2005), a given pesticide could be present within the environment throughout the year.

Microbial communities, too, will change in time and space (Horner-Devine *et al.*, 2004, Palmisano *et al.*, 1991, Smoot and Findley, 2001) due to both abiotic factors, such as local climate and weather patterns (Crump *et al.*, 2009), and biotic factors, such as competition with other species, species drift, immigration, and extinction (Arif *et al.*, 2012, Elias and Banin, 2012, McGenity *et al.*, 2012, Nemergut *et al.*, 2013, Vellend, 2010). The fact that degradation of isopyrazam was not correlated with total mineralisation rate in the laboratory OECD 308 and 309 test systems, suggests that the metabolic characteristcs of the community changed over time. Studies have shown that variation in environmental inoculum is the main reason for differing results in biodegradation studies (Courtes *et al.*, 1995, Mezzanotte *et al.*, 2005), so it seems clear that inoculum only collected at a single time of year will not necessarily represent biodegradation potential within the environment.

Although the effect of temperature on biodegradation was not determined in this thesis, the work in Chapter 2 did indicate that water temperature at the time of collection could be an important factor in determining degradation potential of inoculum. Optimisation of temperature could be considered in order to increase environmental realism of regulatory studies. OECD 308 states that tests can be carried out between 10 and 30 ˚C, although 20 ˚C is deemed acceptable (OECD, 2002b). OECD 309 states that the standard laboratory temperature is between 20 and 25 ˚C; however, there can be consideration of using the average environmental temperature of the sample site (OECD, 2004). In Chapter 2, isopyrazam degradation was slower in the laboratory when temperature at the inoculum collection site was colder. In the laboratory, the standard temperature of 20 ˚C was used. At times of year when it was significantly colder than this in the environment, it may have taken the microbes present in the inoculum longer to acclimatise to these new conditions, which

were more extreme to those they were adapted to (Ranneklev and Bååth, 2001). Further work would need to be carried out to determine the effects of microbial acclimatisation on biodegradation rates in laboratory conditions; however, it would seem that using temperatures from the sample site should be more widely adopted in higher tier studies.

5.3 THE IMPACT OF SEDIMENT ADDITION ON ISOPYRAZAM FATE AND TRANSFORMATION

The addition of sediment only impacted isopyrazam degradation in illuminated microcosms in Chapter 2. OECD 308 focuses on the aquatic environment as a whole, including both water and sediment inocula (OECD, 2002b). OECD 309 studies are intended to mimic deeper water bodies and can include suspended sediment, but they lack the sediment substratum (OECD, 2004) that would be important for pesticide fate and transformation in shallow water bodies e.g. sediment sorption. Indeed, the work in this thesis has highlighted the importance of sediment in isopyrazam fate and transformation.

Sediment can be an important reservoir for microbial communities and nutrients, as well as a rich platform for both phototrophic and heterotrophic communities to proliferate (Uzarski *et al.*, 2004). There can also be important biogeochemical exchanges between the water and the sediment (Fang *et al.*, 2017, Sánchez-Pérez *et al.*, 2013). With the exclusion of sediment from OECD 309 tests, these characteristics and processes, which could have significant impacts on biodegradation, will be lost. Not only was isopyrazam degradation quicker in systems containing sediment, but the sediment also provides sorption sites for the compound, reducing the residence time in the water column. On the other hand, in the real environment, sorption to the sediment can reduce overall bioavailability and therefore subsequent biodegradation. Since these factors are not considered in OECD 309 guidelines, the usefulness of these tests does not extend to all water bodies.

5.4 THE IMPACT OF TEST SYSTEM SCALE ON ISOPYRAZAM FATE AND TRANSFORMATION

OECD tests are carried out on a small microcosm scale, with a minimum of 50 g of sediment and 150 mL water in OECD 308 tests (OECD, 2002b) and 100 mL water in OECD

309 tests (OECD, 2004). There is probably an optimum volume of environmental inoculum, after which an increase in microbial diversity is not seen. Indeed, Penton *et al.* (2016) suggests that samples as small as 10 g give optimal bacterial species diversity, while still having low variation between replicates. Although larger 100 g samples saw an increase in OTU number, this mainly consisted of singletons (Penton *et al.*, 2016). Therefore, if the purpose is to see an overall view of the microbial diversity present in the environment, lower sample sizes may be sufficient. Nevertheless, larger sample sizes may also include rare species, which could potentially be vital in terms of biodegradation; the literature certainly suggests that small volumes of environmental inoculum are unlikely to reflect the diversity and quantity of microorganisms and their metabolic potential seen in nature (Gartiser *et al.*, 2017, Kowalczyk *et al.*, 2015, Sturman *et al.*, 1995). The impact of microcosm scale was therefore analysed in Chapter 3 and, in Chapter 4, larger more realistic microflume systems were used as a way to compare the fate of isopyrazam in the microflumes to the smaller microcosm studies already carried out in Chapter 2.

In Chapter 3, differing sized microcosm systems were used with a 200-fold increase in inocula volume between the smallest and the largest test systems. In terms of isopyrazam recovery and DegT50, there was little difference between these microcosms, suggesting there is scope for smaller microcosms to be used as high-throughput tests. Nevertheless, there were significant differences in the fate and transformation processes between systems, with higher metabolite availability in the water fraction of large microcosms, and a higher NER percentage in small and medium microcosms. Without further analysis of whether the NER in the small and medium microcosms were biogenic in origin, it remains uncertain whether small scale tests can accurately predict transformation product formation.

Microflume systems in Chapter 4 increased test system size further, with a 365-fold increase from the microcosms used in Chapter 2. In common with the microcosms, the inclusion of light in the static microflume systems promoted dissipation relative to the dark static microflumes. Under the dark treatment, there was very little dissipation of isopyrazam at the microcosm scale (Chapter 2), but there was substantial dissipation in the dark treatment microflumes in Chapter 4, particularly in the flowing treatments. Although transformation products, NER, or mineralisation to CO_2 were not assessed in the

microflumes, the results suggests that scale of the test system impacts isopyrazam fate processes.

One of the key factors which could account for variation in isopyrazam degradation between the microcosm and microflume systems is differences in the volume of environmental inoculum in each system. This could have resulted in a larger range of microbial populations being present in the microflumes so that, even under dark conditions, the non-phototrophic communities present had the metabolic potential for isopyrazam degradation. Indeed, in Chapter 3, as test system size increased there was an increase in microbial α diversity in the sediment. When comparing the bacterial α diversity between microcosms in Chapter 2 and microflumes in Chapter 4, however, the microcosms actually had a significantly higher α diversity in both the water ($p \leq 0.0035$, **Fig. 5.1.a**) and the sediment fraction ($p \leq 0.0127$, **Fig. 5.1.b**) when pooled across all collection times. This is not unexpected as the microcosm experiments utilised material collected from eight collection times over two years, while material for the microflume experiment was obtained at one collection time only; therefore the microcosms will show the wide range of diversity present throughout the year. For β diversity (**Fig. 5.2**), however, there was a significant ($p \leq 0.001$) distinction between the two different sized systems in both the water and the sediment, with clustering according to test system.

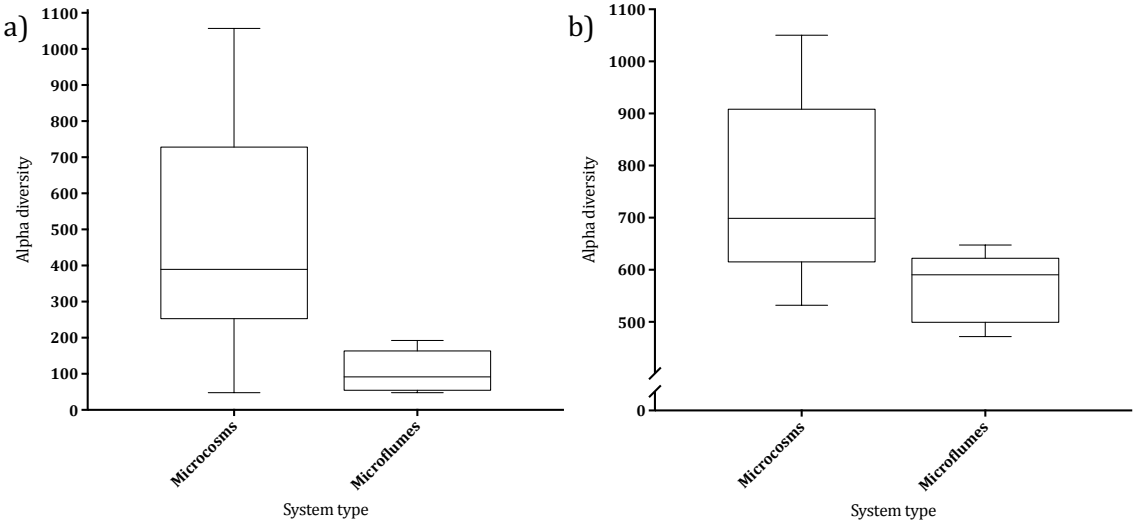

Figure 5.1: Alpha diversity of bacterial communities between dark microcosms and dark microflumes in the water (a) and the sediment (b). Fisher's α index was calculated from the observed bacterial species in dark microcosms and dark microflumes in the water (a) and the sediment (b). Whiskers show minimum and maximum values and middle lines show the median values.

Since there were significant differences in the bacterial community relative abundances between the dark static and dark flowing microflume treatments, a comparison to dark microcosms was not made. Analysis was carried out to determine whether any OTUs were significantly associated with either the dark microcosm or the dark microflume treatments. In the water fraction, there were six OTUs which were only present in the microflumes, and a further seven OTUs which were present in significantly higher relative abundances in the microflumes compared to the microcosms ($p \geq 0.0344$). In the sediment fraction, there were 92 OTUs only present in the microflumes, and a further 57 OTUs present in significantly higher relative abundances in the microflumes compared to the microcosms ($p \geq 0.0435$). There were no significant OTUs which were only present in the dark microcosms. Full breakdown of OTU relative abundance and taxonomies are shown in Appendix V.1. This suggests that in the larger volumes of environmental inoculum used for the microflume experiment, a wider range of species were present. This means that there was a higher likelihood that degrading communities were present to proliferate in the microflume systems, even under dark conditions.

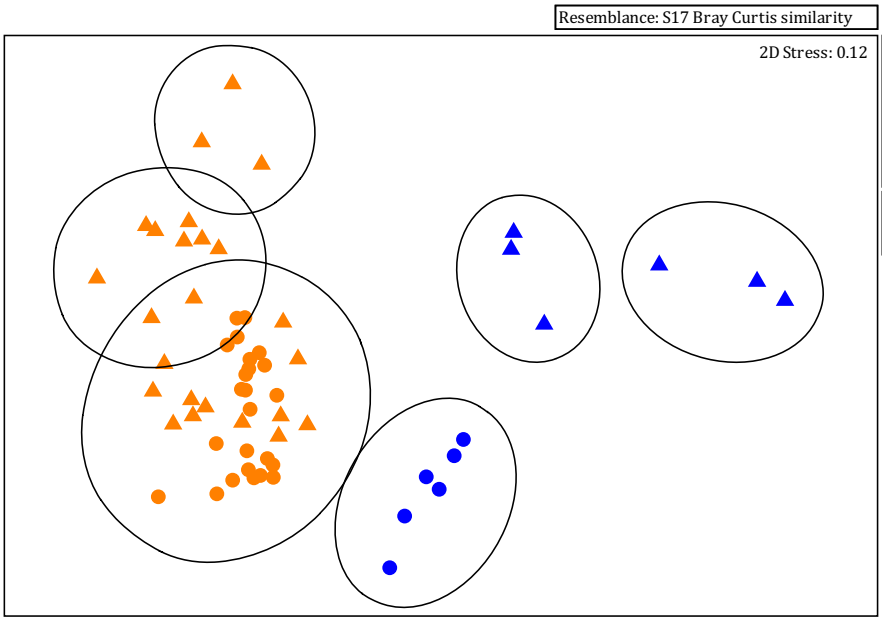

Figure 5.2: Ordination plots from NMDS scaling analysis of Bray Curtis similarities between bacteria in dark microcosm and dark microflume treatments. Water (triangles) and sediment (circles) were analysed at the end of each microcosm (orange) and microflume (blue) experiment. Black lines represent a similarity threshold of 30 %.

5.5 THE IMPACT OF WATER FLOW ON ISOPYRAZAM FATE AND TRANSFORMATION

OECD 308 studies are intended to simulate biodegradation across aquatic environments, this can include flowing systems, such as rivers or streams, or static systems, such as lakes or ditches. Even in static systems there can be turbulence from environmental factors, such as wind, rain, and runoff (Reynolds, 1994, Reynolds *et al.*, 1994). OECD 308 studies, however, are carried out statically, which means there is little consideration for flow velocity or sediment dynamics (Gartiser *et al.*, 2017, OECD, 2002b).

In Chapter 4, flow treatment was shown to have a bigger impact than non-UV light on biodegradation, with isopyrazam dissipation being quicker in flowing water treatments regardless of light treatment. In the flowing microflumes, this was likely due to phototrophic communities not proliferating as easily due to the turbulence from the water flow. In static systems, however, phototrophic biofilm was still able to flourish on the sediment surface so, in these systems, non-UV light still played a role in the dissipation process, showing that the species present were fundamentally capcable of degrading isopyrazam if the conditions allowed their proliferation. This is in line with several studies showing that biofilm is better adapted to growing in slower flow rates (Battin *et al.*, 2003a, Battin *et al.*, 2003b, Wetzel, 1993). In the flowing systems, however, due to a decrease in competition from phototrophic communities, the mixing in the systems likely enabled other non-phototrophic degraders to increase their population size due to increased chance of contact with electron donors and acceptors or nutrients (Bauer *et al.*, 2008, Gantzer *et al.*, 1988, Kirchman *et al.*, 1989, Reynolds, 1994, Thullner *et al.*, 2002, Wetzel, 1993). Subsequently, this would also increase the chance that degrading communities came into contract with the chemical (Sánchez-Pérez *et al.*, 2013).

This work has shown that water flow can impact microbial communities and this, in turn, can impact the way in which environmental pollutants are degraded in the environment. If these differences between microflume systems are consistent with the differences between flowing and static water systems in nature, it suggests that a single test is not representative of chemical environmental fate and transformation processes in all aquatic habitats.

5.6 RECOMMENDATIONS TO ENVIRONMENTAL FATE STUDIES AND INDUSTRY IMPLICATIONS

This thesis aimed to increase the realism of laboratory scale environmental fate studies. Based on isopyrazam biodegradation experiments, there are a number of modifications that could be suggested for higher tier environmental fate studies. This work also offers insight into non-standard tests that could be included in submissions to regulators, in order to provide further evidence of pesticide degradation in conditions that are more relevant to the environment, and the conditions encountered by a pesticide in the field.

Firstly, light-dark cycles should be considered in regulatory experimental design to better reflect the conditions in nature; it may be beneficial for a standard light intensity and daylight hour regime to be used in order to elimate variation across different regions at different times of year. Although studies carried out in dark conditions are important as they avoid interference from algal growth (OECD, 2002b), there should be an option to carry out tests in light-dark conditions in order to consider biodegradation by phototrophic communities, which may provide a key metabolic pathway in nature. Additionally, care should be taken in collection of environmental inoculum to ensure it represents temporal changes in the environment. For instance, this could include using inoculum from the same site but sampled in different seasons to represent this variation. Furthermore, flow velocity should be included if appropriate for the inoculum, e.g. if sampled from rivers or streams. Considering there will be differences between aquatic environments in microbial populations and therefore metabolic potential, the tests should reflect this rather than having one static test for all aquatic environments.

This work also provides evidence of the potential for high-throughput screening using small microcosms. Further work testing other compounds would need to be carried out, as well as determining whether this potential still exists when tests are carried out within the confines of the OECD tests (e.g. dark and static conditions). This would be cheaper, permit a high level of replication, and also could increase the possible number of variables assessed (Aichberger *et al.*, 2005, Carpenter, 1996, EPA, 2000, Khan and Zytner, 2011, Spain *et al.*, 1984). These controlled small-scale tests provide valuable insight into the main

degradation pathways for particular compounds. These processes could then be assessed further by industry (e.g. on a larger scale or under more realistic conditions) to evaluate whether processes determining the degradation of a particular pesticide at the small-scale reflect the processes in more environmentally relevant conditions. This could then be included in submission to regulators in order to provide additional evidence of pesticide degradation in conditions that the pesticide would encounter in the field.

5.7 FUTURE WORK

The work in this thesis highlights other areas for future research in order to better understand the effects increased environmental realism has on regulatory-type tests.

Firstly, this work has only been carried out with one compound, isopyrazam. Considering pesticide degradation is compound specific, the effects on degradation rate with an increase of environmental realism in the tests may be different for other compounds. Therefore, to get a better view of the effects of non-UV light, water flow, etc., similar studies should be conducted with other test compounds.

Radiochemical work carried out on the microflume scale would be difficult in terms of both logistics (e.g. decontamination of test systems and disposals) and economics (e.g. cost of larger quantities of radiochemical). Although sorption to the microflume systems was discounted as much as possible (see Appendix III.4), it would be beneficial to carry out radiolabelled microcosm studies comparing static (not on a shaker) and flowing (shaking to mimic a moderate flow) variables so that a complete mass balance can be generated. This would give insight into the degradation, rather than just the dissipation, processes between static and flowing water. Furthermore, it would allow assessment on whether the differences in dissipation rate are due to quicker generation of metabolites and mineralisation to CO_2, or formation of NER.

Temperature was not a variable evaluated in this thesis, but the work in Chapter 2 potentially highlighted the importance this could have on microbial communities when they are transferred from the environment to the laboratory. Additional work should be carried out to determine whether extreme changes in conditions, for instance transfer from a cold

winter environment to a much warmer laboratory, influence pesticide biodegradation in the laboratory. This would increase understanding into whether environmental inoculum should have a longer acclimatisation period to the new laboratory conditions, or whether more realistic temperatures should be used in the laboratory that mimic the sample site at the time of inoculum collection.

Lastly, further work should determine whether the microbial communities are comparable between the field and the laboratory after pesticide addition. Although the communities that develop under laboratory conditions may have the potential to degrade a compound, it is important to investigate whether these communities are similar in structure and composition to those that develop in the field, otherwise the tests will not reflect the potential field biodegradation rates.

REFERENCES

ABAD-FUENTES, A., CEBALLOS-ALCANTARILLA, E., MERCADER, J. V., AGULLÓ, C., ABAD-SOMOVILLA, A. & ESTEVE-TURRILLAS, F. A. 2015. Determination of succinate-dehydrogenase-inhibitor fungicide residues in fruits and vegetables by liquid chromaography-tandem mass spectometry - electronic supplementary material. *Analytical and Bioanalytical Chemistry,* 407**,** 4207-4211.

ABBASIAN, F., PALANISAMI, T., MEGHARAJ, M. & NAIDU, R. 2016. Microbial Diversity and Hydrocarbon Degrading Gene Capacity of a Crude Oil Field Soil as Determined by Metagenomics Analysis. *Biotechnology Progress,* 32**,** 638-648.

AGRICULTURAL DEVELOPMENT AND ADVISORY SERVICE 1986. The Analysis of Agricultural Materials: a manual of the analytical methods used by the Agricultural Development and Advisory Service/Ministry of Agriculture, Fisheries and Food*.,* Great Britain, Ministery of Agriculture Fisheries and Food.

AICHBERGER, H., HASINGER, M., BRAUN, R. & LOIBNER, A. P. 2005. Potential of preliminary test methods to predict biodegradation performance of petroleum hydrocarbons in soil. *Biodegradation,* 16**,** 115-125.

AKBARI, A. 2014. Bioremediation of Petroleum Hydrocarbons: Multi-scale Investigation of Effects of Pore Size and Role of Diurnal Temperature Changes. Doctor of Philosophy, McGill University.

ALEXANDER, M. 1981. Biodegradation of Chemicals of Environmental Concern. *Science,* 211**,** 132-138.

ALONSO-GUTIÉRREZ, J., FIGUERAS, A., ALBAIGÉS, J., JIMÉNEZ, N., VIÑAS, M., SOLANAS, A. M. & NOVOA, B. 2009. Bacterial Communities from Shoreline Evnironments (Costa de Morte, Northwestern Spain) Affected by the *Prestige* Oil Spill. *Applied and Environmental Microbiology,* 75**,** 3407-3418.

ALONSO-SÁEZ, L., GASOL, J. M., LEFORT, T., HOFER, J. & SOMMARUGA, R. 2006. Effect of Natural Sunlight on Bacterial Activity and Differential Sensitivity of Natural Bacterioplankton Groups in Northwestern Mediterranean Coastal Waters. *Applied and Environmental Microbiology,* 72**,** 5806-5813.

AMERICAN PUBLIC HEALTH ASSOCIATION 1995. Standard methods for the Examination of Water and Waste water: standard method 10200H. *American Public Health Association***,** 1-541.

ANDERSON, A.-M. 2005. Overview of Pesticide Data In Alberta Surface Waters Since 1995. *Environmental Monitoring and Evaluation Branch Alberta Environmental*, 1-172.

ANDERSON, T. A. & COATS, J. R. 2002. Enhanced Microbial Degradation of Pesticides. *In:* PIMENTEL, D. (ed.) *Encyclopedia of Pest Management.* New York: CRC Press.

ANDREINI, M. S. & STEENHUIS, T. S. 1990. Preferential Paths of Flow under Conventional and Conservation Tillage. *Geoferma,* 46**,** 85-102.

ANN, Y., REDDY, K. R. & DELFINO, J. J. 1999. Influence of redox potential on phosphorus solubility in chemically amended wetland organic soils. *Ecological Engineering,* 14**,** 169-180.

ANTONIOU, E., FODELIANAKIS, S., KORKAKAKI, E. & KALOGERAKIS, N. 2015. Biosurfactant production from marine hydrocarbon-degrading consortia and pure bacteria strains using crude oil as carbon source. *Frontiers in Microbiology,* 6**,** 1-14.

ARBIZU, P. M. 2015. *How can I do PerMANOVA pairwise contrasts in R?* [Online]. ResearchGate. Available: https://www.researchgate.net/post/How_can_I_do_PerMANOVA_pairwise_contrasts_in_R [Accessed May 26th 2017].

ARIAS-ESTÉVEZ, M., LÓPEZ-PERIAGO, E., MARTÍNEZ-CARBALLO, E., SIMAL-GÁNDARA, J., MEJUTO, J.-C. & GARCÍA-RÍO, L. 2008. The mobility and degradation of pesticides in soils and the pollution of groundwater resources. *Agriculture, Ecosystems & Environment,* 123**,** 247-260.

ARIF, I. A., BAKIR, M. A. & KHAN, H. A. 2012. Microbial Remediation of Pesticides. *In:* RATHORE, H. S., NOLLET ,L.M.L., (ed.) *Pesticides: Evaluation of Environmental Pollution.* Boca Raton: CRC Press.

ATWOOD, D. & PAISLEY-JONES, C. 2017. Pesticides Industry Sales and Usage: 2008 - 2012 Market Estimates. *US Environmental Protection Agency***,** 1-24.

AULD, D. S. & VALLEE, B. L. 1971. Kinetics of Carboxypeptidase A. pH and Temperature Dependence of Tripeptide Hydrolysis. *Biochemistry,* 10**,** 2892-2897.

BANSAL, O. P. 2012. Degradation of Pesticides. *In:* RATHORE, H. S. & NOLLET, L. M. L. (eds.) *Pesticides: Evaluation of Environmental Pollution.* Boca Raton, London, New York: CRC Press.

BÁRCENAS-MORENO, G., GÓMEZ-BRANDÓN, M., ROUSK, J. & BÅÅTH, E. 2009. Adaption of soil microbial communities to temperature: comparison of fungi and bacteria in a laboratory experiment. *Global Change Biology,* 15**,** 2950-2957.

BARGIELA, R., MAPELLI, F., ROJO, D., CHOUAIA, B., TORNÉS, J., BORIN, S., RICHTER, M., DEL POZO, M. V., CAPPELLO, S., GERTLER, C., GENOVESE, M., DENARO, R., MARTÍNEZ-MARTÍNEZ, M., FODELIANAKIS, S., AMER, R. A., BIGAZZI, D., HAN, X., CHEN, J., CHERNIKOVA, T. N., GOLYSHINA, O. V., MAHJOUBI, M., JAOUANIL, A., BENZHA, F., MAGAGNINI, M., HUSSEIN, E., AL-HORANI, F., CHERIF, A., BLAGHEN, M., ABDEL-FATTAH, Y. R., KALOGERAKIS, N., BARBAS, C., MALKAWI, H. I., GOLYSHIN, P. N., YAKIMOV, M. M., DAFFONCHIO, D. & FERRER, M. 2015. Bacterial population and biodegradation potential in chronically crude oil-contaminated marine sediments are strongly linked to temperature. *Scientific Reports,* 5**,** 1-15.

BARRETT, K. A. & MCBRIDE, M. B. 2005. Oxidative Degradation of Glyphosate and Aminomethylphosphonate by Manganese Oxide. *Environmental Science & Technology,* 39**,** 9223-9228.

BARRIA, C., MALECKI, M. & ARRAIANO, C. M. 2013. Bacteria adaption to cold. *Microbiology,* 159**,** 2437-2443.

BARRIUSO, E., BENOIT, P. & DUBUS, I. G. 2008. Formation of Pesticide Nonextractable (Bound) Residues in Soil: Magnitude, Controlling Factors and Reversibility. *Environmental Science & Technology,* 42**,** 1845-1854.

BASSEY, D. E. 2010. An investigation into the microbial degradation of benzyldimethyl hexadecylammoniumchloride used in oilfield chemical formulations*.* Doctor of Philosophy, Heriot-Watt University.

BATISSON, I., SANCELME, M., MALLET, C. & BESSE-HOGGAN, B. 2010. Fate and environmental impact of the recently marketed herbicide Mesotrione: coupling biological and chemical studies for a global overview. *In:* MENDEZ VILAS, A. (ed.) *Current Research Topics in Applied Microbiology and Microbial Biotechnology.* New Jersey, London, Singapore, Beijing, Shanghai, Hong Kong, Taipei, Chennai: World Scientific.

BATT, A. L., KIM, S. & AGA, D. S. 2006. Enhanced Biodegradation of Iopromide and Trimethoprim in Nitrifying Activated Sludge. *Environmental Science & Technology,* 40.

BATTIN, T. J., KAPLAN, L. A., NEWBOLD, J. D., CHENG, X. & HANSEN, C. 2003a. Effects of Current Velocity on the Nascent Architecture of Stream Microbial Biofilm. *Applied and Environmental Microbiology,* 69**,** 5443-5453.

BATTIN, T. J., KAPLAN, L. A., NEWBOLD, J. D. & HANSON, C. M. E. 2003b. Contributions of microbial biofilms to ecosystem processes in stream mesocosms. *Nature,* 426**,** 439-442.

BATTIN, T. J. & SENGSCHMITT, D. 1999. Linking Sediment Biofilm, Hydrodynamics, and River Bed Clogging: Evidence from a Large River. *Microbial Ecology,* 37**,** 185-196.

BAUER, R. D., MALOSZEWSKI, P., ZHANG, Y., MECKENSTOCK, R. U. & GRIEBLER, C. 2008. Mixing-controlled biodegradation in a toluene plume - Results from two-dimensional laboratory experiments. *Journal of Contaminant Hydrology,* 96**,** 150-168.

BEALES, N. 2004. Adaptation of Microorganisms to Cold Temperatures, Weak Acid Preservatives, Low pH, and Osmotic Stress: A Review. *Comprehensive Reviews in Food Science and Food Safety,* 3**,** 1-20.

BELL, T., JUCK, D., WHYTE, L. G. & GREER, C. W. 2013. Alteration of microbial community structure affects diesel biodegradation in an Arctic soil. *Federation of European Microbiological Societies Microbiology Ecology,* 85**,** 51-61.

BELLO-AKINOSHO, M., MAKOFANE, R., ADELEKE, R., THANTSHA, M., PILLAY, M. & CHIRIMA, G. J. 2016. Potential of Polycyclic Aromatic Hydrocarbon-Degrading Bacterial Isolates to Contribute to Soil Fertility. *BioMed Research International,* 2016**,** 1-10.

BENDING, G. D., LINCOLN, S. D. & EDMONDSON, R. N. 2006. Spatial variation in the degradation rate of the pesticides isoproturon, azoxystrobin and diflufenican in soil and its relationship with chemical and microbial properties. *Environmental Pollution,* 139**,** 279-287.

BENDING, G. D., LINCOLN, S. D., SØRENSEN, S. R., MORGAN, J. A. W., AAMAND, J. & WALKER, A. 2003. In-field spatial variability in the degradation of the phenyl-urea herbicide isoproturon is the result of interactions between degradative *Spingomonas* spp. and soil pH. *Applied and Environmental Microbiology,* 69**,** 827-834.

BERGSTRÖM, L. & STENSTRÖM, J. 1998. Environmental fate of chemicals in soil. *AMBIO: A Journal of the Human Environment* 27**,** 16-23.

BERNANKE, J. & KÖHLER, H.-R. 2008. The Impact of Environmental Chemicals on Wildlife Vertebrates. *In:* WHITACRE, D. M. (ed.) *Reviews of Environmental Contamination and Toxicology.* New York: Springer.

BEULKE, S., DUBUS, I. G., BROWN, C. D. & GOTTESBÜREN, B. 2000. Simulation of Pesticide Persistence in the Field on the Basis of Laboratory Data - A Review. *Journal of Environmental Quality,* 29**,** 1371-1379.

BEWICK, D. W. 1994. The Mobility of Pesticides in Soil - Studies to Prevent Groundwater Contamination. *In:* EBING, W. & BÖRNER, H. (eds.) *Chemistry of Plant Protection.* Berlin, Heidelberg, New York, London, Paris, Tokyo, Hong Kong, Barcelona, Budapest: Springer-Verlag.

BIRGANDER, J., ROUSK, J. & OLSSON, P. A. Impact of warm winters on microbial growth. European Geosciences Union General Assembly, 2014, Vienna. 1.

BLANC, F., GARRAUD, A. & MERLE, T. 2012. Syngenta presents its cereal fungicide innovation/isopyrazam or IZM. *Conférence Internationale sur les Maladies des Plantes.* Tours, France.

BÖCKELMANN, U., MANZ, W., NEU, T. R. & SZEWZYK, U. 2000. Characterization of the microbial community of lotic organic aggregates ('river snow') in the Elbe River of Germany by cultivation and molecular methods. *Frederation of European Microbiological Societies Microbiology Ecology,* 33**,** 157-170.

BOLGER, A. M., LOHSE, M. & USADEL, B. 2014. Trimmomatic: a flexible trimmer for Illumina sequence data. *Bioinformatics,* 30**,** 2114-2120.

BONANNI, P., CAPRIOLI, R., GHIARA, E., MIGNUZZI, C., ORLANDI, C., PAGANIN, G. & MONTI, A. 1992. Sediment and interstitial water chemistry of the Orbetello lagoon (Grosseto, Italy); nutrient diffusion across the water-sediment interface. *Hydrobiologia,* 235/236**,** 553-568.

BOOPATHY, R. 2000. Factors limiting bioremediation technologies. *Bioresource Technology,* 74**,** 63-67.

BORDE, X., GUIEYSSE, B., DELGADO, O., MUÑOZ, R., HATTI-KAUL, R., NUIGER-CHAUVIN, C., PATIN, H. & MATTIASSON, B. 2003. Synergistic relationships in algal-bacterial microcosms for the treatment of aromatic pollutants. *Bioresource Technology,* 86**,** 293-300.

BORGÅ, K., GABRIELSEN, G. W. & SKAARE, J. U. 2001. Biomagnification of organochlorines along a Barents Sea food chain. *Environmental Pollution,* 113**,** 187-198.

BORNETTE, G., ARMOROS, C. & LAMOUROUX, N. 1998. Aquatic plant diversity in riverine wetlands: the role of connectivity. *Freshwater Biology,* 39**,** 267-283.

BOUWER, H. & RICE, R. C. 1989. Effect of Water Depth in Groundwater Recharge Basins on Infiltration. *Journal of Irrigation and Drainage Engineering,* 115**,** 556-567.

BRABEC, K., ZAHRÁDKOVA, S., NĚMEJCOVÁ, D., PAŘIL, P., KOKEŠ, J. & JARKOVSKÝ, J. 2004. Assessment of organic pollution effect considering differences between lotic and lentic stream habitats. *Hydrobiologia,* 516**,** 331-346.

BRAKSTAD, O. D., LOFTHUS, S. & RIBICIC, D. 2017. Biodegradation of Petroleum Oil in Cold Marine Environments *In:* MARGESIN, R. (ed.) *Psychrophiles: From Biodiversity to Biotechnology.* Second ed. Berlin: Springer.

BRAKSTAD, O. D., THRONE-HOLST, M., NETZET, R., STOECKEL, D. M. & STLAS, R. M. 2015. Microbial communities related to biodegradation of dispersed Macondo oil at low seawater temperature with Norwegian coastal seawater. *Microbial Biotehnology,* 8**,** 989-998.

BREUER, F., JANZ, P., FARRELLY, E. & EBKE, K.-P. 2017. Environmental and structural factors influencing algal communities in small streams and ditches in central Germany. *Journal of Freshwater Ecology,* 32**,** 65-83.

BREUER, F., JANZ, P., FARRELLY, E. & EBKE, P. 2016. Seasonality of algal communities in small streams and ditches in temperate regions using delayed fluoresence. *Journal of Freshwater Ecology,* 31**,** 393-406.

BROCKMAN, F. J. & MURRAY, C. J. 1997. Subsurface microbiological heterogeneity: current knowledge, descriptive approaches and applications. *Federation of European Microbiological Societies Microbiology Reviews,* 20**,** 231-247.

BURROWS, H. D., CANLE, M., SANTABALLA, J. A. & STEENKEN, S. 2002. Reaction pathways and mechanisms of photodegradation of pesticides. *Journal of Photochemistry and Photobiology B: Biology,* 67**,** 71-108.

CÁCERES, T. P., MEGHARAJ, M. & NAIDU, R. 2008. Biodegradation of the Pesticide Fenamiphos by Ten Different Species of Green Algae and Cyanobacteria. *Current Microbiology,* 57**,** 643-646.

CALVERT, S. E. & PEDERSEN, T. F. 2010. Organic Carbon Accumulation and Preservation in Marine Sediments: How Important Is Anoxia? *In:* WHELAN, J. K. & FARRINGTON, J. W. (eds.) *Organic Matter: Productivity, Accumulation, and Preservation in Recent and Ancient Sediments.* New York, Oxford: Columbia University Press.

CANTY, M. N., HAGGER, J. A., MOORE, R. T. B., COOPER, L. & GALLOWAY, T. S. 2007. Sublethal impact of short term exposure to the organophosphate pesticide

azamethiphos in the marine mollusc *Mythilus edulis*. *Marine Pollution Bulletin,* 54**,** 396-402.

CANUEL, E. A. & MARTENS, C. S. 1996. Reactivity of recently deposited organic matter: Degradation of lipid compounds near the sediment-water interface. *Geochimica et Cosmochimica Acta,* 60**,** 1793-1806.

CAPORASO, J. G., KUCZYNSKI, J., STOMBAUGH, J., BITTINGER, K., BUSHMAN, F. D., COSTELLO, E. K., FIERER, N., PEÑA, A. G., GOODRICH, J. K., GORDON, J. I., HUTTLEY, G. A., KELLEY, S. T., KNIGHTS, D., KOENIG, J. E., LEY, R. E., LOZUPONE, C. A., MCDONALD, D., MUEGGE, B. D., PIRRUNG, M., REEDER, J., SEVINSKY, J. R., TURNBAUGH, P. J., WALTERS, W. A., WIDMANN, J., YATSUNENKO, T., ZANEVELD, J. & KNIGHT, R. 2010. QIIME allows analysis of high-throughput community sequencing data. *Nature Methods,* 7**,** 335-336.

CAPORASO, J. G., LAUBER, C. L., WALTERS, W. A., BERG-LYONS, D., HUNTLEY, J., FIERER, N., OWENS, S. M., BETLEY, J., FRASER, L., BAUER, M., GORMLEY, N., GILBERT, J. A., SMITH, G. & KNIGHT, R. 2012. Ultra-high-throughput microbial community analysis on the Illumina HiSeq and MiSeq platforms. *International Society for Microbial Ecology,* 6**,** 1621-1624.

CARLISLE, D. M. & CLEMENTS, W. H. 1999. Sensitivity and Variability of Metrics used in Biological Assessments of Running Water. *Environmental Toxicology and Chemistry,* 18**,** 285-291.

CARPENTER, S. R. 1996. Microcosm experiments have limited relevance for community and ecosystem ecology. *Ecology,* 77**,** 677-680.

CARSON, R. 1962. Silent Spring. London, New York, Camberwell, Ontario, New Dehli, Auckland, Rosebank: Mariner Books.

CARTER, A. 2000. How pesticides get into water - and proposed reduction measures. *Pesticide Outlook,* 11**,** 149-156.

CARVALHO, F. P. 2006. Agriculture, pesticides, food security and food safety. *Environmental Science & Policy,* 9**,** 685-692.

CASPELL, N., DRAKES, D. & O'NEILL, T. 2006. Pesticide Residue Minimisation Crop Guide: Tomatoes. *Food Standards Agency***,** 1-47.

CATFORD, J. 2008. Food security, climate change and heath promotion: opening up the streams not just helping out down stream. *Health Promotion International,* 23.

CETIN, B., OZER, S., SOFUOGLU, A. & ODABASI, M. 2006. Determination of Henry's law constants of organochlorine pesticides in deionized and saline water as a function of temperature. *Atmospheric Environment,* 40**,** 4538-4546.

CHAMBERS, P. A., PREPAS, E. E., HAMILTON, H. R. & BOTHWELL, M. L. 1991. Current velocity and its effects on aquatic macrophytes in flowing waters. *Ecological Applications,* 1**,** 249-257.

CHANDLER, I. D., GUYMER, I., PEARSON, J. M. & VAN EGMOND, R. 2016. Vertical variation of mixing within porous sediment beds below turbulent flows. *Water Resources Research,* 52**,** 3493-3509.

CHANSON, H. 2004. Hydraulics of Open Channel Flow: An Introduction. Amsterdam, Boston, Heidelberg, London, New York, Oxford, Paris, San Diego, San Francisco, Singapore, Sydney, Tokyo: Elsevier: Butterworth Heinemann.

CHAPELLE, F. H., BRADLEY, P. M., LOVLEY, D. R. & VROBLESKY, D. A. 1996. Measuring Rates of Biodegradation in a Contaminated Aquifer Using Field and Laboratory Methods. *Ground Water,* 34**,** 691-698.

CHAUSSONNERIE, S., SAAIDI, P.-L., UGARTE, E., BARBANCE, A., FOSSEY, A., BARBE, V., GYAPAY, G., BRÜLS, T., CHEVALLIER, M., COUTURAT, L., FOUTEAU, S., MUSELET, D., PATEAU, E., COHEN, G. N., FONKNECHTEN, N., WEISSENBACK, J. & LE PASLIER, D. 2016. Microbial Degradation of a Recalcitrant Pesticide: Chlordecone. *Frontiers in Microbiology,* 7**,** 1-12.

CHEN, P., ZHANG, L., GUO, X., DIA, X., LIU, L., XI, L., WANG, J., SONG, L., WANG, Y., ZHU, Y., HUANG, L. & HUANG, Y. 2016a. Diversity, Biogeography, and Biodegradation Potential of Actinobacteria in the Deep-Sea Sediments along the Southwest Indian Ridge. *Frontiers in Microbiology,* 7**,** 1-17.

CHEN, W., SONG, L., PENG, L., WAN, N., ZHANG, X. & GAN, N. 2008. Reduction in microcystin concentrations in large and shallow lakes: Water and sediment-interface contributions. *Water Research,* 42**,** 763-773.

CHEN, X., JIANG, H., SUN, X., ZHU, Y. & YANG, L. 2016b. Nitrification and denitrification by algae-attached and free-living microorganisms during a cyanobacterial bloom in Lake Taihu, a shallow Europhic Lake in China. *Biogeochemistry,* 131**,** 135-146.

CHENG, H.-M. & HWANG, D.-F. 1996. Photodegradation of Benthiocarb. *Chemistry and Ecology,* 12**,** 91-101.

CHENG, H. H. & KOSKINEN, W. C. 2010. Effects of "Aging" on Bioreactive Chemical Retention, Transformation, and Transport in Soil. *In:* XU, J. & HUANG, P. M. (eds.) *Molecular Environmental Soil Science at the Interfaces in the Earth's Critical Zone.* New York: Springer.

CHÉNIER, M. R., BEAUMIER, D., ROY, R., DRISCOLL, B. T., LAWRENCE, J. R. & GREER, C. W. 2003. Impact of Seasonal Variations and Nutrient Inputs on Nitrogen Cycling and Degradation of Hexadecane by Replicated River Biofilm. *Applied and Environmental Microbiology,* 69**,** 5170-5177.

CHOW, V. T. 1959. Open-Channel Hydraulics. New York, St. Louis, San Francisco, Auckland, Bogotá, Caracas, Colorado Springs, Hamburg, Lisbon, London, Madris, Mexico, Milan, Montreal, New Delhi, Oklahoma City, Panama, Paris, San Juan, São Paulo, Singapore, Sydney, Tokyo, Toronto: McGraw-Hill Book Company.

CLEMENTS, W. H. & NEWMAN, M. C. 2002. Community Ecotoxicity. *Hierarhical Ecotoxicology Mini Series.* Chichester: John Wiley & Sons, Ltd.

COAT, S., MONTI, D., LEGENDRE, P., BOUCHON, C., MASSAT, F. & LEPOINT, G. 2011. Organochlorine pollution in tropical rivers (Guadeloupe): Role of ecological factors in food web bioaccumulation. *Environmental Pollution,* 159**,** 1692-1701.

COATS, J. R. 1991. Pesticide Degradation Mechanisms and Environmental Activation. *Pesticide Transformation Products.* Washington, DC: Entomology Publications.

COLE, J. J. 1982. Interactions between bacteria and algae in aquatic ecosystems. *Annual Review of Ecology, Evolution, and Systematics,* 13**,** 291-314.

COMBER, M. & HOLT, M. 2010. Developing a set of reference chemicals for use in biodegradability tests for assessing the persistency of chemicals. *MCC Report: MCC/007***,** 1-90.

COMISAR, C. M., HUNTER, S. E., WALTON, A. & SAVAGE, P. E. 2008. Effect of pH on Ether, Ester, and Carbonate Hydrolysis in High-Temperature Water. *Industrial & Engineering Chemistry Research,* 47**,** 577-584.

COPLEY, S. D. 2009. Evolution of efficient pathways for degradation of anthropogenic chemicals. *Nature Chemical Biology,* 5**,** 559-566.

CORT, T., DAVIS, C. A., DAI, D., ILLANGASEKARE, T. H. & MUNAKATA-MARR, J. Intermediate-Scale Evaluation of Bioremediation Technologies in Heterogenous LNAPL-Contaminated Soil. Conference on Environmental Research, May 21-24 2001 Hazardous Substance Research Centre, Manhattan. 96-111.

CORTÉS-LORENZO, C., DEL MAR SÁNCHEZ-PEINADO, M., OLIVER-RODRÍGUEZ, B., VÍLCHEZ, J. L., GONZÁLEZ-LÓPEZ, J. J. & RODRÍGUEZ-DÍAZ, M. 2013. Two novel strains within the family *Caulobacteraceae* capable of degradation of linear alhylbenzene sulfonates as pure cultures. *International Biodeterioration & Biodegradation,* 85**,** 62-65.

COURTES, R., BAHLAOUI, A., RAMBAUD, A., DESCHAMPS, F., SUNDE, E. & DUTRIEUX, E. 1995. Ready biodegradability test in seawater: a new methodological approach. *Ecotoxicology and Environmental Safety,* 31**,** 142-148.

CRUM, S. J. H., VAN KAMMEN-POLMAN, A. M. M. & LEISTRA, M. 1999. Sorption of Nine Pesticides to Three Aquatic Macrophytes. *Archives of Environmental Contamination and Toxicology,* 37**,** 310-316.

CRUMP, B. C., PETERSON, B. J., RAYMOND, P. A., AMON, R. M. W., RINEHART, A., MCCLELLAND, J. W. & HOLMES, R. M. 2009. Circumpolar synchrony in big river bacterioplankton. *Proceedings of the National Academy of Sciences,* 106**,** 21208-21212.

CUI, Z., LAI, Q., DONG, C. & SHAO, Z. 2008. Biodiversity of polycyclic aromatic hydrocarbon-degrading bacteria from deep sea sediment of the Middle Atlantic Ridge. *Environmental Microbiology,* 10**,** 2138-2149.

DÆHLI, M., RANDALL, M. & HOLTEN, R. 2012. Evaluation of the plant protection product Bontima - cyprodinil + isopyrazam regarding application for authorisation. *Norwegian Scientific Committee for Food Safety***,** 1-51.

DAVIES, L. O., BRAMKE, I., FRANCE, E., MARSHALL, S., OLIVER, R., NICHOLS, C., SCHAFER, H. & BENDING, G. D. 2013a. Non-UV light influences the degradation rate of crop protection products. *Environmental Science & Technology,* 47**,** 8229-37.

DAVIES, L. O., SCHAFER, H., MARSHALL, S., BRAMKE, I., OLIVER, R. G. & BENDING, G. D. 2013b. Light structures phototroph, bacterial and fungal communities at the soil surface. *Public Library of Science ONE,* 8**,** e69048.

DAVIS, C., CORT, T., DAI, D., ILLANGASEKARE, T. H. & MUNAKATA-MARR, J. 2003. Effects of heterogeneity and experimental scale on the biodegradation of diesel. *Biodegradation,* 14**,** 373-384.

DE SCHRIJVER, A. & DE MOT, R. 1999. Degradation of Pesticides by Actinomycetes. *Critical Reviews in Microbiology,* 25**,** 85-119.

DEATH, R. G., FULLER, I. C. & MACKLIN, M. G. 2015. Resetting the river template: the potential for climate-related extreme floods to transform river geomorphology and ecology. *Freshwater Biology,* 60**,** 2477-2496.

DEBROAS, D., ENAULT, F., JOUAN-DUFOURNEL, I., BRONNER, G. & HUMBER, J.-F. 2011. Metagenomic Approach Studying the Taxonomic and Functional Diversity of the Bacterial Community in a Lacustrine Ecosystem. *In:* DE BRUIJN, F. J. (ed.) *Handbook of Molecular Microbial Ecology II: Metagenomics in Different Habitats.* New Jersey: Wiley-Blackwell.

DECHESNE, A., BADAWI, N., AAMAND, J. & SMETS, B. F. 2014. Fine scale spatial variability of microbial pesticide degradation in soil: scales, controlling factors, and implications. *Frontiers in Microbiology,* 5**,** 1-14.

DEFRA 2012. Observatory monitoring framework - indicator data sheet. 1-7.

DELGADILLO-MIRQUEZ, L., LOPES, F., TAIDI, B. & PAREAU, D. 2016. Nitrogen and phosphate removal from wastewater with a mixed microalgae and bacteria culture. *Biotechnology Reports,* 11**,** 18-26.

DELORENZO, M. E., SCOTT, G. I. & ROSS, P. E. 2001. Toxicity of Pesticides to Aquatic Microorganisms: A Review. *Environmental Toxicology and Chemistry,* 20**,** 84-98.

DESOUZA, M. J. B. D., NAIR, S., DAVID, J. J. & CHANDRAMOHAN, D. 1996. Crude oil degradation by phosphate-solubilizing bacteria. *Journal of Marine Biotechnology,* 4**,** 91-95.

DIAMOND, J. 1986. Overview: Laboratory Experiments, Field Experiments, and Natural Experiments *In:* DIAMOND, J. & CASE, T. J. (eds.) *Community Ecology.* New York: Harper and Row.

DÍAZ-RAVIÑA, M. & BÅÅTH, E. 1996. Development of Metal Tolerance in Soil Bacterial Communities Exposed to Experimentally Increased Metal Levels. *Applied and Environmental Microbiology,* 62**,** 2970-2977.

DICH, J., ZAHM, S. H., HANBERG, A. & ADAMI, H. O. 1997. Pesticides and cancer. *Cancer Causes Control,* 8**,** 420-443.

DIKSHITH, T. S. S. 1991. Carcinogenicity of Pesticides. *In:* DIKSHITH, T. S. S. (ed.) *Toxicology of Pesticides in Animals.* Boca Raton, Boston, Ann Arbor: CRC Press.

DONLAN, R. M. 2002. Biofilms: microbial life on surfaces. *Emerging Infectious Diseases,* 8**,** 881-890.

DORIGO, U., LEBOULANGER, C., BÉRARD, A., BOUCHEZ, A., HUMBERT, J. F. & MONTUELLE, B. 2007. Lotic biofilm community structure and pesticide tolerance along a contamination gradient in a vineyard area. *Aquatic Microbial Ecology,* 50**,** 91-102.

DOUGLAS, G. S., HARDENSTINE, J. H., LIU, B. & UHLER, A. D. 2012. Laboratory and Field Verification of a Method to Estimate the Extent of Petroleum Biodegradation in Soil. *Environmental Science & Technology,* 46**,** 8279-8287.

DU, K., ZHOU, B. & YUAN, R. 2017. Biodegradation of 2-methylisoborneol by single bacterium in culture media and river water environment. *International Journal of Environmental Studies,* 74**,** 399-411.

ECETOC 2003. Persistence of Chemicals in the Environment. *European Centre for Ecotoxicology and Toxicology of Chemicals,* Technical Report No. 90**,** 1-195.

ECETOC 2013. Environmental Exposure Assessment of Ionisable Organic Componds. *European Centre for Ecotoxicology and Toxicology of Chemicals,* Technical Report No. 123**,** 1-193.

EDGAR, R. C. 2010. Search and clustering orders of magnitude faster than BLAST. *Bioinformatics,* 26**,** 2460-2461.

EDGAR, R. C. 2013. UPARSE: highly accurate OTU sequences from microbial amplicon reads. *Nature Methods,* 10**,** 996-998.

EDGAR, R. C., HASS, B. J., CLEMENTE, J. C., QUINE, C. & KNIGHT, R. 2011. UCHIME improves sensitivity and speed of chimera detection. *Bioinformatics,* 27**,** 2194-2200.

EFSA 2012. Conclusion on the peer review of the pesticide risk assessment of the active substance isopyrazam. *European Food Safety Authority Journal,* 10**,** 1-110.

EL-SHEEKH, M. M., GHARIEB, M. M. & ABOU-EL-SOUOD, G. W. 2009. Biodegradation of dyes by some green algae and cyanobacteria. *International Biodeterioration,* 63**,** 699-704.

ELIAS, S. & BANIN, E. 2012. Multi-species biofilms: living with friendly neighbours. *Federation of European Microbiological Societies Microbiology*, 35**,** 990-1004.

ENVIRONMENT AGENCY 2003. Guidance on the monitoring of landfill Leachate, groundwater and surface water. TGNO2.

ENVIRONMENT AGENCY 2009. *Evnironment Agency Interactive Maps - River Quality* [Online]. Available: http://maps.environment-agency.gov.uk/wiyby/queryController?topic=riverquality&ep=2ndtierquery&lang=_e&layerGroups=2&x=425850.0&y=256320.0&extraClause=STRETCH_CODE~'05

4010164022'&extraClause=YEAR~2009&textonly=off&latestValue=2009&latestField=YEAR [Accessed January 7th 2016].

ENVIRONMENT AGENCY 2017a. *River Dene at Wellesbourne* [Online]. Environmental Agency. Available: https://flood-warning-information.service.gov.uk/station/2029# [Accessed 20/09/2017 2017].

ENVIRONMENT AGENCY 2017b. River Dene water monitoring temperatures (2010 - 2017). The National Archives. Contains public sector information licensed under the Open Government Licence v3.0, http://www.nationalarchives.gov.uk/doc/open-government-licence/version/3/.

EPA 2000. Engineered Approaches to *In Situ* Bioremediation of Chlorinated Solvents: Fundamentals and Field Applications. *Solid Waste and Emergency Response.* Washington, DC: United States Environmental Protection Agency.

EPA 2011. Pesticide Fact Sheet. *Office of Chemical Safety and Pollution Prevention*, 1-23.

EPSTEIN, S. S. 2013. The phenomenon of microbial uncultivability. *Current Opinion in Microbiology,* 16, 636-642.

EUROPEAN COMMISSION 1998. Council Directive 98/83/EC of 3 November 1998 on the Quality of Water intended for Human Consumption. *Official Journal of the European Communities*, 32-54.

EUROPEAN COMMISSION 2009a. Directive 2009/128/EC of the European Parliament and of the Council. *Official Journal of the European Union*, 71-86.

EUROPEAN COMMISSION 2009b. Regulation (EC) No 1107/2009. *Official Journal of the European Union*, 1-50.

EUROPEAN COMMISSION. 2013a. *Approval of active substances* [Online]. Available: https://ec.europa.eu/food/plant/pesticides/approval_active_substances_en [Accessed 08/09/2017 2017].

EUROPEAN COMMISSION 2013b. Commission Regulation (EU) No 283/2013. *Official Journal of the European Union*, 1-84.

EUROPEAN COMMISSION 2013c. Commission Regulation (EU) No 284/2013. *Official Journal of the European Union*, 85-152.

EVENSON, R. E. & GOLLIN, D. 2003. Assessing the Impact of the Green Revolution, 1960 to 2000. *Science,* 300, 758-762.

FANG, H., CAI, L., YANG, Y., JU, F., LI, X., Y., Y. & ZHANG, T. 2014. Metagenomic analysis reveals potential biodegradation pathways of persistent pesticides in freshwater and marine sediments. *Science of the Total Environment,* 470-471**,** 983-992.

FANG, H., CHEN, Y., HUANG, L. & HE, G. 2017. Analysis of biofilm bacterial communities under different shear stresses using size-fractionated sediment. *Scientific Reports,* 7**,** 1-14.

FAO 2002. International Code of Conduct on the Distribution and Use of Pesticides. *Food and Agriculture Organization*.

FEBRIA, C. M., FULTHORPE, R. R. & WILLIAMS, D. D. 2010. Characterizing seasonal changes in physiochemistry and bacterial commuity composition in hyporheic sediments. *Hydrobiologia,* 647**,** 113-126.

FENNER, K., CANONICA, S., WACKETT, L. P. & ELSNER, M. 2013. Evaluating Pesticide Degradation in the Environment: Blind Spots and Emerging Opportunities. *Science,* 341**,** 752-758.

FERA. 2017. *Pesticide Usage Surveys* [Online]. Food and Environment Research Agency. Available: https://secure.fera.defra.gov.uk/pusstats/surveys/index.cfm [Accessed 08/09/2017 2017].

FERGUSON, R. M. W., GONTIKAKI, E., ANDERSON, J. A. & WITTE, U. 2017. The Variable influence of Dispersant on Degradation of Oil Hydrocarbons in Subartic Deep-Sea Sediments at Low Temperatures (0-5 °C). *Scientific Reports,* 7**,** 1-13.

FERIS, K. P., RAMSEY, P. W., FRAZAR, C., RILLIG, M. C., GANNON, J. E. & HOLBEN, W. E. 2003. Structure and Seasonal Dynamics of Hyporheic Zone Microbial Communities in Free-Stone Rivers of the Western United States. *Microbial Ecology,* 46**,** 200-215.

FERRERA-RODRÍGUES, O., GREER, C. W., JUCK, D., CONSAUL, L. L., MARTÍNEZ-ROMERO, E. & WHYTE, L. G. 2012. Hydrocarbon-degrading potential of microbial communities from Arctic plants. *Journal of Applied Microbiology,* 114**,** 71-83.

FINNEGAN, C. J., VAN EGMOND, R. A., PRICE, O. R. & WHELAN, M. J. 2009. Continuous-flow laboratory simulation of stream water quality changes downstream of an untreated wastewater discharge. *Water Research,* 43**,** 1993-2001.

FISHEL, F. M. 2009. Pest Management and Pesticides: A Historical Perspective. *The Institute of Food and Agricultural Sciences,* PI219**,** 1-5.

FLEMMING, H.-C. 1993. Biofilms and Environmental Protection. *Water Science and Technology,* 27**,** 1-10.

FLEMMING, H.-C. 1995. Sorption sites in biofilms. *Water Science and Technology,* 32**,** 27-33.

FLENNER, C. K., PARSONS, J. R., SCHRAP, S. M. & OPPERHUIZEN, A. 1991. Influence of Suspended Sediment on the Biodegradation of Alkyl Esters of *p*-Aminobenzoic Acid. *The Bulletin of Environmental Contamination and Toxicology* 47**,** 555-560.

FLORES, E., MURO-PASTOR, A. M. & HERRERO, A. 1999. Cyanobacterial Nitrogen Assimilation Genes and NtcA-Dependent Control of Gene Expression. *In:* PESCHEK, G. A., LÖFFELHARDT, W. & SCHMETTERER, G. (eds.) *The Phototrophic Prokaryotes.* New York: Springer Science+Business Media, LLC.

FLURY, M. 1996. Experimental evidence of transport of pesticides through field soils - a review. *Journal of Environmental Quality,* 25**,** 25-45.

FOCUS 2006. Guidance document on estimating persistence and degradation kinetics from environmental fate studies on pesticides in EU registration: Report of the focus work group on degradation kinetics. *EC Document Reference Sanco/10058/2005 version 2.0***,** 434.

FRANK, M. P., GRAEBING, P. & CHIB, J. S. 2002. Effect of Soil Moisture and Sample Depth on Pesticide Photolysis. *Journal of Agricultural and Food Chemistry,* 50**,** 2607-2614.

FRANKE, C., STUDINGER, G., BERGER, G., BÖHLING, S., BRUCKMANN, U., COHORS-FRESENBORG, D. & JÖHNCKE, U. 1994. An Assessment of BIoaccumulation. *Chemosphere,* 29**,** 1501-1514.

FREDRICKSON, A. G. & STEPHANOPOULOS, G. 1981. Microbial Competition. *Science,* 213**,** 972-979.

FRIESEN-PANKRATZ, B. B., DOEBEL, C. C., FARENHORST, A. A. & GOLDSBOROUGH, L. G. 2003. Interactions Between Algea (*Selenastrum capricornutum*) and Pesticides: Implications for Managing Constructed Wetlands for Pesticide Removal. *Journal of Environmental Science and Health,* 2**,** 147-155.

GALITSKAYA, P., AKYMETZYANOVA, L. & SELIVANOVSKAYA, S. 2016. Biochar-carrying hydrocarbon decomposers promote degradation during the early stage of bioremediation. *Biogeosciences,* 13**,** 5739-5752.

GANTZER, C. J., RITTMANN, B. E. & HERRICKS, E. E. 1988. Mass Transport to Streambed Biofilms. *Water Research,* 22**,** 709-722.

GAO, J., WANG, Y., GAO, B., WU, L. & CHEN, H. 2012. Environmental Fate and Tranport of Pesticides. *In:* RATHORE, H. S. & NOLLET , L. M. L. (eds.) *Pesticides: Evaluation of Environmental Pollution.* Boca Raton, London, New York: CRC Press.

GARRY, V. F., HARKIN, M. E., ERICKSON, L. L., LONG-SIMPSON, L. K., HOLLAND, S. E. & BURROUGHS, B. L. 2002. Birth Defects, Season of Concenption, and Sex of Children Born to Pesticide Applicatiors Living in the Red River Valley of Minnesota, USA. *Environmental Health Perspectives,* 110**,** 441-449.

GARTISER, S., SCHNEIDER, K., SCHWARZ, M. A. & JUNKER, T. 2017. Assessment of environmental persistance: regulatory requirements and practical possibilities - available test systems, identification of technical constraints and indication of possible solutions *Texte 10/2017***,** 1-17.

GAULLIER, C., DOUSSET, S., BILLET, D. & BARAN, N. 2017. Is pesticide sorption by constructed wetland sediments governed by water level and water dynamics? *Environmental Science and Pollution Research,* Advanced online publication**,** 1-12.

GAULTIER, J., FARENHORST, A., CATHCART, J. & GODDARD, T. 2008. Degradation of [carboxyl-^{14}C] 2,4-D and [ring-U-^{14}C] 2,4-D in 114 agricultural soils as affected by soil organic carbon content. *Soil Biology and Biochemistry,* 40**,** 217-227.

GAVRILESCU, M. 2005. Fate of Pesticides in the Environment and its Bioremediation. *Engineering in Life Sciences,* 5**,** 497-526.

GHOSAL, D., GHOSH, S., DUTTA, T. K. & AHN, Y. 2016. Current State of Knowledge in Microbial Degradation of Polycyclic Aromatic hydrocarbons (PAHs): A Review *Frontiers in Microbiology,* 7**,** 1-27.

GOLDSTEIN, R. M., MALLORY, L. M. & ALEXANDER, M. 1985. Reasons for Possible failure of Inoculation to Enhance Biodegradation. *Applied and Environmental Microbiology,* 50**,** 977-983.

GOOGLE 2016. *Map data* [Online]. Available: https://www.google.co.uk/maps/@52.2064492,-1.6073383,14z [Accessed 7th January 2016].

GRABOWKSI, A., NERCESSIAN, O., FAYELLE, F., BLANCHET, D. & JEANTHON, C. 2005. Microbial diversity in production waters of a low-temperature biodegraded oil reservoir. *Federation of European Microbiological Societies Microbiology Ecology,* 54**,** 427-443.

GRAEBING, P., FRANK, M. P. & CHIB, J. S. 2003. Soil Photolysis of Herbicides in a Moisture- and Temperature-Controlled Environment. *Journal of Agricultural and Food Chemistry,* 51**,** 4331-4337.

GRAY, J. S. 2002. Biomagnification in marine systems: the perspective of an ecologist. *Marine Pollution Bulletin,* 45**,** 46-52.

GUALTIERI, C. 2004. Interaction Between Hydrodynamics and Mass-Transfer at the Sediment-Water Interface. *International Congress on Environmental Modelling and Software,* 41**,** 1-8.

GUENGERICH, F. P. & LIEBLER, D. C. 1985. Enzymatic activation of chemicals to toxic metabolites. *Critical Reviews in Toxicology,* 14**,** 259-307.

GUERRERO, M. A. & JONES, R. D. 1996. Photoinhibition of marine nitrifying bacteria. II. Dark recovery after monochromatic or polychromatic irradiation. *Marine Ecology Progress Series,* 141**,** 193-198.

HALL, E. K. & COTNER, J. B. 2007. Interactive effect of temperature and resouces on carbon cycling by freshwater bacterioplankton communities. *Aquatic Microbial Ecology,* 49**,** 35-45.

HALL, E. K., SINGER, G. A., KAINZ, M. J. & LENNON, J. T. 2010. Evidence for a temperature acclimation mechanism in bacteria: an empirical test of a membrane-mediated trade-off. *Functional Ecology,* 24**,** 898-908.

HALL-STOODLEY, L., COSTERTON, J. W. & STOODLEY, P. 2004. Bacterial biofilms: from the natural environment to infectious diseases. *Nature Reviews Microbiology,* 2**,** 95-108.

HAMAMURA, N., OLSON, S. H., WARD, D. M. & INSKEEP, W. P. 2006. Microbial Population Dynamics Associated with Crude-Oil Biodegradation in Diverse Soils. *Applied and Environmental Microbiology,* 72**,** 6316-6324.

HAND, L. H. & MORELAND, H. J. 2014. Surface water mineralization of isopyrazam according to OECD 309: observations on implementation of the new data requirement within agrochemical regulation. *Environmental Toxicology and Chemistry,* 33**,** 516-24.

HAND, L. H. & OLIVER, R. G. 2010. The behavior of isopyrazam in aquatic ecosystems: implementation of a tiered investigation. *Environmental Toxicology and Chemistry,* 29**,** 2702-12.

HAYNES, W. 2013. Tukey's Test. *In:* DUBITZKY, W., WOLKENHAUER, O., CHO, K. H. & YOKOTA, H. (eds.) *Encyclopedia of Systems Biology.* New York: Springer.

HAZELL, P. B. R. 2002. Green Revolution Curse or Blessing? *International Food Policy Research Institute*, 1-4.

HEADLEY, J. V., DU, J. L., PERU, K. M., GURPRASAD, N. & MCMARTIN, D. W. 2008. Evaluation of algal phytodegradation of petroleum naphthenic acids. *Journal of Environmental Science and Health,* 43**,** 227-232.

HERZFELD, D. & SARGENT, K. 2012. Private Pesticide Applicator Safety Education Manual. *Pesticide Safety & Environmental Education Program,* 19th Edition**,** 1-12.

HIBBING, M. E., FAQUA, C., PARSEK, R. & PETERSON, S. B. 2010. Bacterial competition: surviving and thriving in the microbial jungle. *Nature Reviews Microbiology,* 8**,** 15-25.

HICKMAN, L. 2012. What is the legacy of Rachel Carton's Silent Spring? *The Guardian*.

HIGASHINO, M., GANTZER, C. J. & STEFAN, H. G. 2004. Unsteady diffustional mass transfer at the sediment/water interface: Theory and significance for SOD measurment. *Water Research,* 38**,** 1-12.

HOAGLAND, R. E., ZABLOTOWICZ, R. M. & HALL, J. C. 2000. Pesticide Metabolism in Plants and Microorganisms: An Overview. *Pesticide Biotransformation in Plants and Microorganisms.* Washington, DC: American Chemical Society.

HOLAN, Z. R. & VOLESKY, B. 1992. Biosorption of Lead and Nickel by Biomass of Marine Algae. *Biotechnology and Bioengineering,* 43**,** 1001-1009.

HOLAN, Z. R., VOLESKY, B. & PRASETYO, I. 1992. Biosorption of Cadmium by Biomass of Marine Algae. *Biotechnology and Bioengineering,* 41**,** 819-825.

HONDZO, M. 1998. Dissolved oxygen transfer at the sediment-water interface in a turbulent flow. *Water Resources Research,* 34**,** 3525-3533.

HORNER-DEVINE, M. C., CARNEY, K. M. & BOHANNAN, B. J. M. 2004. An ecological perspective on bacterial biodiversity. *Proceedings of the Royal Society of London,* 271**,** 113-122.

HOSKERI, R. S., MULLA, S. I. & NINNEKAR, H. Z. 2014. Biodegradation of chloroaromatic pollutants by bacteria consortium immobilized in polyurethane foam and other matrices. *Biocatalysis and Agricultural Biotechnology,* 30**,** 390-396.

HOTTES, A. K., FREDDOLINO, P. L., KHARE, A., DONNELL, Z. N., LIU, J. C. & TAVAZOIE, S. 2013. Bacterial Adaption through Loss of Function. *Public Library of Science Genetics,* 9**,** 1-13.

HOYLE, B. L. & ARTHUR, E. L. 2000. Biotransformation of pesticides in saturated-zone materials. *Hydrogeology Journal,* 8**,** 89-103.

HUANG, W., PENG, P., YU, Z. & FU, J. 2003. Effects of organic matter heterogeneity on sorption and desorption of organic contaminants by soils and sediments. *Applied Geochemistry,* 18**,** 955-972.

HUDON, C. 1997. Impact of water level fluctuations on St. Lawrence River aquatic vegetation. *Canadian Journal of Fisheries and Aquatic Sciences,* 54**,** 2853-2865.

HULLAR, M. A. J., KAPLAN, L. A. & STAHL, D. A. 2006. Recurring Seasonal Dynamics of Microbial Communities in Stream Habitats. *Applied and Environmental Microbiology,* 72**,** 713-722.

HUNTER-CEVERA, J. C. 1998. The value of microbial diversity. *Current Opinion in Microbiology,* 1**,** 278-285.

HUTCHINS, S. R. 1991. Biodegradation of Monoaromatic Hydrocarbons by Aquifer Microorganisms Using Oxygen, Nitrate, or Nitrous Oxide as the Terminal Electron Acceptor. *Applied and Environmental Microbiology,* 57**,** 2403-2407.

JAVAID, M. K., ASHIQ, M. & TAHIR, M. 2016. Potential of Biological Agents in Decontamination of Agricultural Soil. *Scientifica,* 2016**,** 1-9.

JØRGENSEN, E. G. & NIELSEN, E. S. 1960. Effect of Daylight and of Artifical Illumination on the Growth of *Staphylococcus aureus* and Some Other Bacteria. *Physiologia Plantarum,* 13**,** 534-538.

JOUSSET, A., EISENHAUER, N., MERKER, M., MOUQUET, N. & SCHEU, S. 2016. High functional diversity stimulates diversification in experimental mirobal communities. *Science Advances,* 2**,** 1-7.

JUNG, J., PHILIPPOT, L. & PARK, W. 2016. Metagenomic and functional analyses of the consequences of reduction of bacteria diversity on soil functions and bioremediation in diesel-contaminated microcosms. *Scientific Reports,* 6**,** 1-10.

KAMRIN, M. A. 1997. Pesticide profiles: toxicity, environmental impact, and fate. Boca Raton, New York: CRC Press.

KARICKHOFF, S. W. 1984. Organic Pollutant Sorption in Aquatic Systems. *Journal of Hydraulic Engineering,* 110**,** 707-735.

KÄSTNER, M., NOWAK, K. M., MILTNER, A., TRAPP, S. & SCHÄFFER, A. 2014. Classification and Modelling of Nonextractable Residue (NER) Formation of Xenobiotics in Soil - A Synthesis. *Critial Reviews in Environmental Science and Technology,* 44**,** 2107-2171.

KÄSTNER, M., STREIBICH, S., BEYRER, M., RICHNOW, H. H. & FRITSCHE, W. 1999. Formation of Bound Residues during Microbial Degradation of [^{14}C]Antheracene in Soil. *Applied and Environmental Microbiology,* 65**,** 1834-1842.

KEITH, L. H. 1991. Environmental sampling and analysis: A practical guide. Boca Raton, London, New York, Washington, DC: Lewis Publishers.

KELLY, M. M. & ARNOLD, W. A. 2012. Direct and indirect photolysis of the phytoestrogens genistein and daidzein. *Environmental Science & Technology,* 46**,** 5396-5403.

KERTESZ, M. A. & MIRLEAU, P. 2004. The role of soil microbes in plant sulphur nutrition. *Journal of Experimental Botany,* 55**,** 1939-1945.

KHAN, A. A. & ZYTNER, R. G. A Meso-Scale Experimental Apparatus for Determining Bioventing Degradation Rates for Petroleum Hydrocarbons. 18th International Protoleum and Biofuels Environmental Conference, 2011, Houston, Texas.

KHAN, A. A. & ZYTNER, R. G. 2013. Degradation Rates for Petroleum Hydrocarbons Undergoing Bioventing at the Meso-Scale. *Bioremediation Journal,* 17**,** 159-172.

KHAN, A. A., ZYTNER, R. G. & FENG, Z. 2015. Establishing Correlations and Scale-Up Factor for Estimating the Petroleum Biodegradation Rate in Soil. *Bioremediation Journal,* 19**,** 32-46.

KHAN, S. T., HORIBA, Y., YAMAMOTO, M. & HIRAISHI, A. 2002. Members of the Family *Comamonadaceae* as Primary Poly(3-Hydroxybutyrate-co-3-Hydroxyvalerate)-Degrading Denitrifiers in Activated Sludge as Revealed by a Polyphasic Approach. *Applied and Environmental Microbiology,* 68**,** 3206-3214.

KIEBER, D. J. 2000. Photochemical Production of Biological Substrates. *In:* DE MORA, S., DEMERS, S. & VERNET, M. (eds.) *The Effects of UV Radiation in the Marine Environment.* Cambridge: Cambridge University Press.

KIRCHMAN, D., SOTO, Y. & VAN WAMBECK, F. 1989. Bacterial production in the Rhône River plume: effect of mixing on relationships among microbial assemblages. *Marine Ecology Progress Series,* 53**,** 267-275.

KIRCHMAN, D. L. 1994. The Uptake of Inorganic Nutrients by Heterotrophic Bacteria. *Microbial Ecology,* 28**,** 255-271.

KIRONOTO, B. A. & GRAF, W. H. 1994. Turbulence characteristics in rough uniform open-channel flow. *Proceedings of the Institution of Civil Engineers,* 106**,** 333-344.

KO, I., KIM, K.-W., LEE, C.-H. & LEE, K.-P. 2007. Effect of Scale-up and Seasonal Variation on Biokinetics in the Enhanced Bioremediation of Petroleum Hydrocarbon-contaminated Soil. *Biotechnology and Bioprocess Engineering,* 12**,** 531-541.

KOHLI, P., NAYYAR, N., SHARMA, A., SINGH, A. K. & LAL, R. 2016. *Algoripghagus roseus* sp. nov., isolated from a hexachlorocyclohexane-contaminated dumpsite. *International Journal of Systematic and Evolutionary Microbiology,* 66**,** 3558-3565.

KONSTANTINOU, I. K., ZARKADIS, A. K. & ALBANIS, T. A. 2001. Photodegradation of Selected Herbicides in Various Natural Waters and Soils under Environmental Conditions. *Journal of Environmental Quality,* 30**,** 121-130.

KOOKANA, R. S., BASKARAN, S. & NAIDU, R. 1998. Pesticide fate and behaviour in Australian soils in relation to contamination and management of soil and water: a review. *Australian Journal of Soil Research,* 36**,** 715-764.

KOOL, H. J. 1984. Influence of microbial biomass on the degradability of organic compounds. *Chemosphere,* 7**,** 751-761.

KOSTKA, J. E., PRAKASH, O., OVERHOLT, W. A., GREEN, S. J., FREYER, G., CANION, A., DELGARDIO, J., NORTON, N., HAZEN, T. C. & HUETTEL, M. 2011. Hydrocarbon-Degrading Bacteria and the Bacerial Community Response in Gulf of Mexico Beach Sands Impacted by the Deepwater Horizon Oil Spill. *Applied and Environmental Microbiology,* 77**,** 7962-7974.

KOWALCZYK, A., MARTIN, T. J., PRICE, O. R., SNAPE, J. R., VAN EGMOND, R. A., FINNEGAN, C. J., SCHÄFER, H., DAVENPORT, R. J. & BENDING, G. D. 2015. Refinement of biodegradation tests methodologies and the proposed utility of new microbial ecology techniques. *Ecotoxicology and Environmental Safety,* 111**,** 9-22.

KOWALCZYK, A., PRICE, O. R., VAN DER GAST, C. J., FINNEGAN, C. J., VAN EGMOND, R. A., SCHÄFER, H. & BENDING, G. D. 2016. Spatial and temporal variability in the potential of river water biofilms to degrade *p*-nitrophenol. *Chemosphere,* 164**,** 355-362.

KUFFNER, M., HAI, B., RATTEI, T., MELODELIMA, C., SCHLOTER, M., ZECHMEISTER-BOLTENSTERN, S., JANDL, R., SCHINDLBACHER, A. & SESSITSCH, A. 2012. Effects of season and experimental warming on the bacterial community in a temperate mountain forest soil assessed by 16S rRNA gene pyrosequencing. *Federation of European Microbiological Societies Microbiology Ecology,* 82**,** 551-562.

KUGAORASATHAM, S., NAGAOKA, H. & OHGAKI, S. 1992. Effect of Turbulence on Nitrifying Biofilms at Non-Limiting Substrate Conditions. *Water Research,* 26**,** 1629-1638.

KUMAR, R. V., KANNA, G. R. & ELUMALAI, S. 2017. Biodegradation of Polyehylene by Green Photosynthetic Microalgae. *Journal of Bioremediation & Biodegradation,* 8**,** 1-8.

LAIRD, D. A. & KOSKINEN, W. C. 2008. Triazine Soil Interactions. *In:* LEBARON, H. M., MCFARLAND, J. & BURNSIDE, O. C. (eds.) *The Triazine Herbicides.* San Diego, Amsterdan, Oxford: Elsevier.

LAMENDELLA, R., STRUTT, S., BORGLIN, S., CHAKRABORTY, R., TAS, N., MASON, O. U., HULTMAN, J., PRESTAT, E., HAZEN, T. C. & JANSSON, J. K. 2014. Assessment of the Deepwater Horizon oil spill impact on Gulf coast microbial communities. *Frontiers in Microbiology,* 5**,** 16-28.

LANGE, J., SCHEUTZ, T., GREGOIRE, C., ELSÄSSER, D., SCHULZ, R., PASSEPORT, E. & TOURNEBIZE, J. 2011. Multi-tracer experiments to characterise contaminant mitigation capacities for different types of artificial wetlands. *International Journal of Environmental Analytical Chemistry,* 91**,** 768-785.

LAPERTOT, M. E. & PULGARIN, C. 2006. Biodegradability assessment of several priority hazardous substances: Choice, application and relevance regarding toxicity and bacterial activity. *Chemosphere,* 65**,** 682-690.

LEBRERO, R., ÁNGELES, R., PÉREZ, R. & MUÑOZ, R. 2016. Toluene biodegradation in an algal-bacterial airlift photobioreactor: Influence of the biomass concentration and of the presence of an organic phase. *Journal of Environmental Management,* 1**,** 585-593.

LEFF, L. G., MCARTHUR, V. & SHIMKETS, L. J. 1992. Information Spiraling: Movement of Bacteria and Their Genes in Streams. *Microbial Ecology,* 24**,** 11-24.

LEOPOLD, L. B. 1970. An Improved Method for Size Distribution of Stream Bed Gravel. *Water Resoucres Research,* 6**,** 1357-1366.

LEVANON, D. 1993. Roles of fungi and bacteria in the mineralization of the pesticides atrazine, alachlor, malathion and carbofuran in soil. *Soil Biology and Biochemistry,* 25**,** 1097-1105.

LEW, S., LEW, M., BIEDUNKIEWICZ, A. & SZAREK, J. 2013. Impact of Pesticide Contamination on Aquatic Microorganism Populations in the Littoral Zone. *Archives of Environmental Contamination and Toxicology,* 64**,** 399-409.

LIMA, S. A. C., CASTRO, P. M. L. & MORAIS, R. 2003. Biodegradation of *p*-nitrophenol by microalgae. *Journal of Applied Phycology,* 15**,** 137-142.

LIN, Z., BAI, J., ZHEN, Z., LAO, S., LI, W., WU, Z., LI, Y., SPIRO, B. & ZHANG, D. 2016. Enhancing pentachlorophenol degradation by vermicomposting associated bioremediation. *Ecological Engineering,* 87**,** 288-294.

LINDE, C. D. 1994. Physico-Chemical Properties and Environmental Fate of Pesticides. *Environmental Protection Agency Environmental Hazards Assessment Program***,** 1-55.

LINDELL, M. J., GRANÉLI, H. W. & TRANVIK, L. J. 1996. Effects of sunlight on bacterial growth in lakes of different humic content. *Aquatic Microbial Ecology,* 11**,** 135-141.

LLORENS-BLANCH, G., BADIA-FABREGAT, M., LUCAS, D., RODRIGUEZ-MOZAZ, S., BARCELÓ, D., PENNANEN, T., CAMINAL, G. & BLÁNQUEZ, P. 2015. Degradation of pharmaceuticals from membrane biological reactor sludge with *Trametes versicolor*. *Environmental Science: Processes & Impacts,* 17**,** 429-440.

LODER, T. C. & REICHARD, R. P. 1981. The Dynamics of Conservative Mixing in Estuaries. *Estuaries,* 4**,** 64-69.

LUDWIG, W., STRUNK, O., WESTRAM, R., RICHTER, L., MEIER, H., YADHUKUMAR, BUCHNER, A., LAI, T., STEPPI, S., JOBB, G., FORSTER, W., BRETTSKE, I., GERBER, S., GINHART, A. W., GROSS, O., GRUMANN, S., HERMANN, S., JOST, R., KONIG, A., LISS, T., LUSSMANN, R., MAY, M., NONHOFF, B., REICHEL, B., STREHLOW, R., STAMATAKIS, A., STUCKMANN, N., VILBIG, A., LENKE, M., LUDWIG, T., BODE, A. & SCHLEIFER, K. H. 2004. ARB: a software environment for sequence data. *Nucleic Acids Research,* 32**,** 1363-1371.

LYAUTEY, E., JACKSON, C. R., CAYROU, J., ROLS, J.-L. & GARABÉTIAN, F. 2005. Bacterial Community Succession in Natural River Biofilm Assemblages. *Microbial Ecology,* 50**,** 589-601.

MACHEREY, A.-C. & DANSETTE, P. M. 2015. Biotransformations Leading to Toxic Metabolites: Chemical Aspect. *In:* WERMUTH, C., ALDOUS, D., RABOISSON, P. & ROGNAN, D. (eds.) *The Practice of Medicinal Chemistry.* 4th ed. Amsterdam, Boston, Heidelberg, London, New York, Oxford, Paris, San Diego, San Fransisco, Singapore, Sydney, Tokyo: Elsevier.

MADIGAN, M. T., MARTINKO, J. M., DUNLAP, P. V. & CLARK, D. P. 2009. Brock Biology of Microorganisms: San Francisco: Pearson Benhamin Cummings.

MAKRIS, K. C., ANDRA, S. S. & BOTSARIS, G. 2014. Pipe Scales and Biofilms in Drinking-Water Distribution Systems: Undermining Finished Water Quality. *Critial Reviews in Environmental Science and Technology,* 44**,** 1477-1523.

MALTSEVA, O., MCGOWAN, C., FULTHORPE, R. & ORIEL, P. 1996. Degradation of 2,4-dichlorophenoxyacetic acid by haloalkaliphilic bacteria. *Microbiology,* 142**,** 1115-1122.

MARIN, I. 2011. Proteobacteria. *In:* GARGAUD, M., AMILS, R., QUINTANILLA, J. C., CLEAVES, H. J., IRVINE, W. M., PINTI, D. L. & VISO, M. (eds.) *Encyclopedia of Astrobiology.* Berlin, Heidelberg: Springer.

MCCARTHY, A. J. & WILLIAMS, S. T. 1992. Actinomycetes as agents of biodegradation in the environment - a review. *Gene,* 115**,** 189-192.

MCDONALD, D., PRICE, M. N., GOODRICH, J., NAWROCKI, E. P., DESANTIS, T. Z., PROBST, A., ANDERSEN, G. L., KNIGHT, R. & HUGENHOLTZ, P. 2012. An improved Greengenes taxonomy with explicit ranks for ecological and evolutionary analyses of bacteria and archaea. *Multidisciplinary Journal of Microbial Ecology,* 6**,** 610-618.

MCDONALD, J. A. & RITTMANN, B. E. 1993. Performance Standards for In Situ Bioremediation. *Environmental Science & Toxicology,* 27**,** 1974-1979.

MCGENITY, T. J., FOLWELL, B. D., MCKEW, B. D. & SANNI, G. O. 2012. Marine crude-oil biodegradation: a central role for interspecies interactions. *Aquatic Biosystem,* 8**,** 1-19.

MCMURDIE, P. J. & HOLMES, S. 2013. phyloseq: An R Package for Reproducible Interactive Analysis and Graphics of Microbiome Census Data. *Public Library of Science ONE,* 8**,** 1-11.

MEGHARAJ, M., MADHAVI, D. R., SREENIVASULU, C., UMAMAHESWARI, A. & VENKATESWARLU, K. 1994. Biodegradation of Methyl Parathion by Soil Isolates of Microalgae and Cyanobacteria. *Bulletin of Environmental Contamination and Toxicology,* 53**,** 292-297.

MEHTA, S. K. & GAUR, J. P. 2008. Use of Algae for Removing Heavy Metal Ions from Wastewater: Progress and Prospects. *Critical Reviews in Biotechnology,* 25**,** 113-152.

MET OFFICE. 2017a. *Temperature, rainfall and sunshine time-series* [Online]. Met Office. Available: http://www.metoffice.gov.uk/climate/uk/summaries/actualmonthly [Accessed 13/07/17 2017].

MET OFFICE. 2017b. *Wellesbourne Climate* [Online]. Met Office. Available: https://www.metoffice.gov.uk/public/weather/climate/gcqbgxb2n [Accessed 20/09/2017 2017].

MEZZANOTTE, V., BERTANI, R., INNOCENTI, F. D. & TOSIN, M. 2005. Influence of inocula on the results of biodegradation tests. *Polymer Degradation and Stability,* 87**,** 51-56.

MILLER, D. 2008. Bed Bugs (Hemiptera: Climicidae: Cimex spp.). *In:* CAPINERA, J. L. (ed.) *Encyclopedia of Entomology.* 2nd ed. USA: Springer.

MILLIMAN, J. D. 2009. River Inputs. *In:* STEELE, J. H., THORPE, S. A. & TUREKIAN, K. K. (eds.) *Elements of Physical Oceanography.* Boston, Heidelberg, London, New York, Oxford, Paris, San Diego, San Francisco, Singapore, Sydney, Tokyo: Academic Press.

MISHAMANDANI, S., GUTIERREZ, T. & AITKEN, M. D. 2014. DNA-based stable isotope probing coupled with cultivation methods implicated *Methylophaga* in hydrocarbon degradation. *Frontiers in Microbiology,* 5**,** 172-180.

MORENO-VIVIÁN, C., CABELLO, P., MARTÍNEZ-LUQUE, M., BLASCO, R. & CASTILLO, F. 1999. Prokaryotic Nitrate Reduction: Molecular Properties and Functional Distinction among Bacterial Nitrate Reductases. *Journal of Bacteriology,* 181**,** 6573-6584.

MORRIS, C. E., BARDIN, M., BERGE, O., FREY-KLETT, P., FROMIN, N., GIRARDIN, H., GUINEBRETIÈRE, M.-H., LEBARON, P., THIÉRY, J. M. & TROUSSELLIER, M. 2002. Microbial Biodiversity: Approaches to Experimental Design and Hypothesis Testing in Primary Scientific Literature from 1975 to 1999. *Microbial and Molecular Biology Reviews,* 66**,** 592-616.

MORTLAND, M. M. & RAMAN, K. V. 1967. Catalytic hydrolysis of some organic phosphate pesticides by copper(II). *Journal of Agricultural and Food Chemistry,* 15**,** 163-167.

MULHOLLAND, P. J., STEINMAN, A. D., MARZOLF, E. R., HART, D. R. & DEANGELIS, D. L. 1994. Effect of periphyton biomass on hydraulic characteristics and nutrient cycling in streams. *Oecologia,* 98**,** 40-47.

NAKAMURA, F. M., GERMANO, M. G. & TSAI, S. M. 2014. Capacity of Armomatic Compound Degradation by Bacteria from Amazon Dark Earth. *Diversity,* 6**,** 339-353.

NAUDIN, J.-J., CAUWET, G., FAJON, C., ORIOL, L., TERZIĆ, S., DEVENON, J.-L. & BROCHE, P. 2001. Effect of mixing on microbial communities in the Rhone River plume. *Journal of Marine Systems,* 28**,** 203-227.

NAURA, M. 2014. ToolHab Decision Support System. *Tools for Managing Habitats.* GeoData Institute, University of Southampton: Environment Agency, SC060093, 1-51.

NEMERGUT, D. R., SCHMIDT, S. K., FUKAMI, T., O'NEILL, S. P., BILINSKI, T. M., STANISH, L. F., KNELMAN, J. E., DARCY, J. L., LYNCH, R. C., WICKEY, P. & FERRENBERG, S. 2013. Patterns and Processes of Microbial Community Assembly. *Microbiology and Molecular Biology Reviews,* 77**,** 342-356.

NIELSEN, E. G. & LEE, L. K. 1987. The Magnitude and Costs of Groundwater Contamination From Agricultural Chemicals: A National Perspective. *Resources and Technology Division, Economic Research Service***,** 1-38.

NING, J., BAI, Z., GANG, G., JIANG, D., HU, Q., HE, J., ZHANG, H. & ZHUANG, G. 2010. Functional assembly of bacteria communities with activity for the biodegradation of an organophosphorus pesticide in the rape phyllosphere. *Federation of European Microbiological Societies Microbiology Letters,* 306**,** 153-143.

NOWACK, B. & STONE, A. T. 2000. Degradation of Nitrilotris(methylenephosphonic Acid) and Related (Amino)Phosphonate Chelating Agents in the Presence of Manganese and Molecular Oxygen. *Environmental Science & Technology,* 34**,** 4759-4765.

NOWAK, K. M., GIRARDI, C., MILTNER, A., GEHRE, M., SCHÄFFER, A. & KÄSTNER, M. 2013. Contribution of microorganisms to non-extractable residue formation during biodegradation of ibuprofen in soil. *Science of the Total Environment,* 445-446**,** 377-384.

NOWAK, K. M., KÄSTNER, M., MILTNER, A., TRAPP, S. & SCHÄFFER, A. 2014. Non-extractable residues (NER) from xenobiotics in soil: a new classification and relevance in the risk assessment. *In Science Across Bridges, Borders and Boundaries.* Basel, Switzerland: SETAC-Europe.

NOWAK, K. M., MILTNER, A., GEHRE, M., SCHÄFFER, A. & KÄSTNER, M. 2011. Formation and Fate of Bound Residues from Microbial Biomass during 2,4-D Degradation in Soil. *Environmental Science & Technology,* 45**,** 999-1006.

NRFA. 2016. *54048 - Dene at Wellesbourne* [Online]. National River Flow Archive. Available: http://nrfa.ceh.ac.uk/data/station/meanflow/54048 [Accessed 20/09/2017 2017].

O'KELLEY, J. C. & DEASON, T. R. 1976. Degradation of Pesticides by Algae. *Ecological Research Series.* Georgia: United States Environmental Protection Agency

OECD 2002a. Test No. 307: Anerobic and Anaerobic Transformation in Soil. *OECD Guidelines for the Testing of Chemicals,* Section 3**,** 1-17.

OECD 2002b. Test No. 308: Aerobic and Anaerobic Transformation in Aquatic Sediment Systems. *OECD Guideline for the Testing of Chemicals*, 1-19.

OECD 2004. Test No. 309: Aerobic Mineralisation in Surface Water - Simulation Biodegradation Test. *OECD Guidelines for the Testing of Chemicals,* Section 3, 1-21.

OECD 2005. Proposal for Revised Introduction to the OECD Guidelines for Testing of Chemicals. *OECD Guidelines for Testing of Chemicals,* Section 3, 1-13.

OECD 2008a. Test No. 314: Simulation Tests to Assess the BIodegradability of Chemicals Discharged in Wastewater. *OECD Guidelines for the Testing of Chemicals,* Section 3, 1-51.

OECD 2008b. Test No. 316: Phototransformation of Chemicals in Water - Direct Photolysis. *OECD Guidelines for the Testing of Chemicals*, 1-53.

OKONYA, J. S. & KROSCHEL, J. 2015. A Cross-Sectional Study of Pesticide Use and Knowledge of Smallholder Potato Farmers in Uganda. *Hindawi Publishing Corporation,* 2015, 1-9.

OKSANEN, J., BLANCHET, F. G., FRIENDLY, M., KINDT, R., LEGENDRE, P., MCGLINN, D., MINCHIN, P. R., O'HARA, R. B., SIMPSON, G. L., SOLYMOS , P., STEVENS, M. H. H., SZOECS, E. & WAGNER, H. 2017. vegan: Community Ecology Package. *R* 2.4-4, 1-219.

OVERMANN, J. & GARCIA-PICHEL, F. 2006. The Phototrophic Way of Life. *In:* DWORKIN, M., FALKOW, S., ROSENBERG, E., SCHLEIFER, K. H. & STACKERBRANDT, E. (eds.) *The Prokaryotes.* 3rd ed. Singapore: Springer.

OYA, S. & VALOCCHI, A. J. 1998. Transport and biodegradation of solutes in stratified aquifers under enhanced in situ bioremediation conditions. *Water Resoucres Research,* 34, 3323-3334.

PAERL, H. W. & OTTEN, T. G. 2013. Harmful Cyanobacterial Blooms: Causes, Consequences, and Controls. *Microbial Ecology,* 65.

PAGGA, U. 1997. Testing Biodegradability with Standardized Methods. *Chemosphere,* 35, 2953-2972.

PALMISANO, A. C., SCHWAB, B. S. & MARUSCIK, D. A. 1991. Seasonal changes in mineralization of xenobiotic by stream microbial communities. *Canadian Journal of Microbiology,* 37, 939-948.

PARALES, R. E. 2009. Hydrocarbon Degradation by Betaproteobacteria. *In:* TIMMIS, K. N. (ed.) *Handbook of Hydrocarbon and Lipid Microbiology.* Berlin, Heidelberg: Springer Science and Business Media.

PARKIN, T. B. & SHELTON, D. R. 1991. Spatial and Temporal Variability of Carbofuran Degradation in Soil. *American Society of Agronomy,* 21**,** 672-678.

PARSONS, J. R. 1992. Influence of suspended sediment on the biodegradation of chlorinated dibenzo-*p*-dioxins. *Chemosphere,* 25**,** 1973-1980.

PATEL, V., SHARMA, A., LAL, R., AL-DHABI, N. A. & MADAMWAR, D. 2016. Response and resilience of soil microbial communities inhabiting in edible oil stress/contamination from industrial estates. *BMC Microbiology,* 16**,** 1-14.

PENTON, C. R., GUPTA, V. V. S. R., YU, J. & TIEDJE, J. M. 2016. Size Matters: Assessing Optimum Soil Sample Size for Fungal and Bacterial Community Structure Analyses Using High Throughput Sequencing of rRNA Gene Amplicons. *Frontiers in Microbiology,* 7**,** 1-11.

PERELO, L. W. 2010. Review: In situ and bioremedation of organic pollutants in aquatic sediments. *Journal of Hazardous Materials,* 117**,** 81-89.

PÉREZ, S., EICHHORN, P. & AGA, D. S. 2005. Evaluating the biodegradability of sulfamethazine, sulfamethoxazole, sulfathiazole, and trimethoprim at different stages of sewage treatment. *Environmental Toxicology and Chemistry,* 24**,** 1361-1367.

PESCE, S., MARTIN-LAURENT, F., ROUARD, N., ROBIN, A. & MONTUELLE, B. 2010. Evidence for adaption of riverine sediment microbial communities to diuron mineralization: incidence of runoff and soil erosion. *Journal of Soils and Sediments,* 10**,** 698-707.

PETERSEN, S. & KLUG, M. J. 1994. Effects of Sieving, Storage, and Incubation Temperature on the Phospholipid Fatty Acid Profile of a Soil Microbial Community. *Applied and Environmental Microbiology,* 60**,** 2421-2430.

PETTERSSON, M. & BÅÅTH, E. 2003. Temperature-dependent changes in the soil bacterial community in limed and unlimed soil. *Federation of European Microbiological Societies Microbiology Ecology,* 45**,** 13-21.

PHILIPPOT, L., SPOR, A., HÉNAULT, C., BRU, D., BIZOUARD, F., JONES, C. M., SARR, A. & MARON, P.-A. 2013. Loss in microbial diversity affects nitrogen cycling in soil. *The International Society for Microbial Ecology Journal,* 7**,** 1609-1619.

PIMENTEL, D. 2005. Environmental and economic costs of the application of pesticides primarily in the United States. *Environment, Development and Sustainability,* 7**,** 229-252.

PIRES, A. P. F., GUARIENTO, R. D., LAQUE, T., ESTEVES, F. A. & FARJALLA, V. F. 2014. The negative effects of temperature increase on bacterial respiration are indepentent of changes in community composition. *Environmental Microbiology Reports,* 6**,** 131-135.

PIRISI, F. M., CABRAS, P., GARAU, V. L., MELIS, M. & SECCHI, E. 1996. Photodegradation of Pesticides. Photolysis Rates and Half-Life of Pirimicarb and Its Metabolites in Reactions in Water and in Solid Phase. *Journal of Agricultural and Food Chemistry,* 44**,** 2417-2422.

PPDB. 2017. *General Information for Isopyrazam* [Online]. UK: University of Hertfordshire. Available: http://sitem.herts.ac.uk/aeru/ppdb/en/Reports/1449.htm [Accessed 19/09/17 2017].

QUAST, C., PRUESSE, E., YILMAZ, P., GERKEN, J., SCHWEER, T., YARZA, P., PEPLIES, J. & GLÖCKNER, F. O. 2013. The SILVA ribosomal RNA gene database project: improved data processing and web-based tools. *Nucleic Acids Research,* 41**,** 590-596.

RAFFAELLI, D. G., RAVEN, J. A. & POOLE, L. J. 1998. Ecological impacts of green microalgal blooms. *In:* ANSELL, A., BARNES, M., GIBSON, R. N. & BARNES, H. (eds.) *Oceanography and Marine Biology: An Annual Review.* London, Bristol, Pennsylvannia: UCL Press.

RAJFUR, M. & KLOS, A. 2013. Sorption of heavy metals in the biomass of alga *Palmaria palmata*. *Water Science and Technology,* 68**,** 1543-1549.

RAJFUR, M., KLOS, A. & WACLAWEK, M. 2013. Environmental Engineering IV. *In:* PAWLOWSKI, L. (ed.) *Equilibrium and studies on sorption of heavy metals from solutions by algae.* London: CRC Press.

RAMAKRISHNAN, B. 2012. Microbial Diversity and Degradation of Pollutants. *Bioremediation and Biodegradation,* 3**,** 1-3.

RANNEKLEV, S. B. & BÅÅTH, E. 2001. Temperature-Driven Adaption of the Bacterial Community in Peat Measured by Using Thymidine and Leucine Incorporation. *Applied and Environmental Microbiology,* 67**,** 1116-1122.

RASCHE, M. E., HYMAN, M. R. & ARP, D. J. 1990. Biodegradation of Halogenated Hydrocarbon Fumigants by Nitrifying Bacteria. *Applied and Environmental Microbiology,* 56**,** 2568-2571.

REUSCHENBACH, P., PAGGA, U. & STROTMANN, U. 2003. A critical comparison of respirometric biodegradation tests based on OECD 301 and related test methods. *Water Research,* 37**,** 1571-1582.

REYNOLDS, C. S. 1994. The long, the short and the stalled: on the attributes of phytoplankton selected by physical mixing in lakes and rivers. *Hydrobiologia,* 289**,** 9-21.

REYNOLDS, C. S., DESCY, J.-P. & PADISÁK, J. 1994. Are phytoplankton dynamics in rivers so different from those in shallow lakes? *Hydrobiologia,* 289**,** 1-7.

RIER, S. T. & STEVENSON, R. J. 2002. Effects of light, dissolved organic carbon, and inorganic nutrients on the relationship between algae and heterotrophic bacteria in stream periphyton. *Hydrobiologia,* 489.

RISER-ROBERTS, E. 1992. In Situ/On-Site Biodegradation of Refined Oils and Fuels (a Technology Review). *Naval Civil Engineering Laboratory* 1**,** 1-190.

RITCHIE, R. J. 2006. Consistent sets of spectrophotometric chlorophyll equations for acetone, methanol and ethanol solvents. *Photosynthesis Research,* 89**,** 27-41.

RODGERS-VIEIRA, E. A., ZHANG, Z., ADRION, A., GOLD, A. & AITKEN, M. D. 2015. Identification of Anthraquinone-Degrading Bacteria in Soil Contaminated with Polycyclic Aromatic hydrocarbons. *Applied and Environmental Microbiology,* 81**,** 3775-3781.

RODRIGUES, L. & BICUDO, D. D. C. 2001. Similarity among periphyton algal communities in a lentic-lotic gradient of the upper Paraná river floodplain, Brazil. *Brazillian Journal of Botany,* 24**,** 235-248.

RODRÍGUEZ-CRUZ, M. S., JONES, J. E. & BENDING, G. 2008. Study of the spatial variation of the biodegradation rate of the herbicide bentazone with soil depth using contrasting incubation methods. *Chemosphere,* 73**,** 1221-1215.

RODRÍGUEZ-CRUZ, M. S., JONES, J. E. & BENDING, G. D. 2006. Field-scale study of the variability in pesticide biodegradation with soil depth and its relationship with soil characteristics. *Soil Biology and Biochemistry,* 38**,** 2910-2918.

ROESELERS, G., VAN LOOSDRECHT, M. C. M. & MUYZER, G. 2008. Phototrophic biofilms and their potential applications. *Journal of Applied Phycology,* 20**,** 277-235.

ROLDÁN, M. D., BLASCO, R., CABALLERO, F. J. & CASTILLO, F. 1998. Degradation of *p*-nitrophenol by the phototrophic bacterium *Rhodobacter capsulatus*. *Archives of Microbiology,* 169**,** 36-42.

ROMERA, E., GONZÁLEZ, F., BALLESTER, A., BLÁZQUEX, L. & MUÑOZ, J. A. 2006. Biosorption with Algae: A Statistical Review. *Critical Reviews in Biotechnology,* 26**,** 223-235.

ROMERO, E., SCHMITT, P. & MANSOUR, M. 1994. Photolysis of Pirimicarb in Water under Natural and Simulated Sunlight Conditions. *Pesticide Science,* 41**,** 21-26.

RUSCH, A., FORSTER, S. & HUETTEL, M. 2001. Bacteria, diatoms and detritus in an intertidal sandflat subject to advective transport across the water-sediment interface *Biogeochemistry,* 55**,** 1-27.

RUTHERFORD, J. C. 1994. River Mixing. *In:* SYMADER, W. (ed.). Chichester: Wiley.

RUTTER, M. & NEDWELL, D. B. 1994. Influence of Changing Temperature on Growth Rate and Competition between Two Psychrotolerant Antarctic Bacteria: Competition and Survival in Non-Steady-State Temperature Environments. *Applied and Environmental Microbiology,* 60**,** 1993-2002.

SABATER, S., GUASH, H., RICART, M., ROMANÍ, A., VIDAL, G., KLÜNDER, C. & SCHMITT-JANSEN, M. 2007. Monitoring the effect of chemicals on biological communities. The biofilm as an interface. *Analytical and Bioanalytical Chemistry,* 387**,** 1425-1434.

SAHA, J. G., KARAPALLY, J. C. & JANZEN, W. K. 1971. Influence of the type of mineral soil on the uptake of dieldrin by wheat seedlings. *Journal of Agricultural and Food Chemistry,* 19**,** 842-845.

SÁNCHEZ-PÉREZ, J. M., MONTUELLE, B., MOUCHET, F., GAUTHIER, L., JULIEN, F., SAUVAGE, S., TEISSIER, S., DEDIEU, K., DESTRIEUX, D., VERVIER, P. & GERINO, M. 2013. Role of the hyporheic heterotrophic biofilm on transformation and toxicity of pesticides. *Annales de Limnologie - International Journal of Limnology,* 49**,** 87-95.

SANDAU, E., SANDAU, P., PULZ, O. & ZIMMERMANN, M. 1996. Heavy Metal Sorption by Marine Algae and Algal By-Products. *Acta Biotechnologica,* 16**,** 103-119.

SÄRKKÄ, J., KESKITALO, A. & LUUKKO, A. 1996. Temporal changes in concentration of radiocaesium in lake sediment and fish of southern Finland as related to environmental factors. *The Science of the Total Environment,* 191**,** 125-136.

SARTORY, D. P. 1982. Spectrophotometric analysis of chlorophyll *a* in freshwater phytoplankton. *Department of Water Affairs***,** 1-163.

SCHÜLE, E., MACK, D., SCHÜLER, S. & WIELAND, M. Polar Pesticide-Metabolites in Drinking and Mineral Water. European Pesticide Residue Workshop, 2008 Berlin, Germany.

SCHWARTZ, T., KOHNEN, W., JANSEN, B. & OBST, U. 2003. Detection of antibiotic-resistant bacteria and their resistance genes in wastewater, surface water, and drinking water biofilms. *Federation of European Microbiological Societies Microbiology Ecology,* 43**,** 325-335.

SCOW, K. M. 1982. Rate of biodegradation. *In:* LYMAN, W. J., REEHL, W. F. & ROSENBLATT, D. H. (eds.) *Handbook on Chemical Property Estimation Methods.* New York: McGraw-Hill.

SECKMEYER, G., PISSULLA, D., GLANDORF, M., HENRIQUES, D., JOHNSEN, B., WEBB, A., SIANI, A.-M., BAIS, A., KJELDSTAD, B., BROGNIEZ, C., LENOBLE, J., GARDINER, B., KIRSCH, P., KOSKELA, T., KAUROLA, J., UHLMANN, B., SLAPER, H., DEN OUTER, P., JANOUCH, M., WERLE, P., GRÖBNER, J., MAYER, B., DE LA CASINIERE, A., SIMIC, S. & CARVALHO, F. 2008. Variability of UV Irradiance in Europe. *Photochemistry and Photobiology,* 84**,** 172-179.

SEIBER, J. N. 2002. Environmental Fate of Pesticides. *In:* WHEELER, W. B. (ed.) *Pesticides in Agriculture and the Environment.* New York, Basel: CRC Press.

SEMPLE, K. T., DOICK, K. J., JONES, K. C., BURAUEL, P., CRAVEN, A. & HARMS, H. 2004. Defining Bioavailability and Bioaccessibility of Contaminated Soil and Sediment is Complicated. *Environmental Science & Technology,* 38**,** 228A-231A.

SEXTON, S. E. 2007. The Economics of Pesticides and Pest Control. *International Review of Environmental and Resource Economics,* 1**,** 271-326.

SHARPLEY, A. N. 1985. Depth of Surface Soil-runoff Interaction as Affected by Rainfall, Soil Slope, and Management. *Soil Science Society of America Journal,* 49**,** 1010-1015.

SHELTON, J. L., AKOB, D. M., MCINTOSH, J. C., FIERER, N., SPEAR, J. R., WARWICK, P. D. & MCCRAY, J. E. 2016. Environmental Drivers of Differences in Microbial Community Structure in Crude Oil Reservoirs across Methanogenic Gradient. *Frontiers in Microbiology,* 7**,** 1-12.

SHERWOOD, A. R. & PRESTING, G. G. 2007. Universal primers amplify a 23S rDNA plastid marker in eukaryotic algae and cyanobacteria. *Journal of Phycology,* 43**,** 605-608.

SHI, J., FUJISAWA, S., NAKAI, S. & HOSOMI, M. 2004. Biodegradation of natural and synthetic estrogens by nitrifying activated sludge and ammonia-oxidizing bacterium *Nitrosomonas europaea*. *Water Research,* 38**,** 2323-2330.

SHRESTHA, P., JUNKER, T., FENNER, K., HAHN, S., HONTI, M., BAKKOUR, R., DIAZ, C. & HENNECKE, D. 2016. Simulation Studied to Explore Biodegradation in Water-Sediment Systems: From OECD 308 to OECD 309. *Environmental Science & Technology,* 50**,** 6856-6864.

SIMMONS, D. B. D. & WALLSCHLÄGER, D. 2005. A critical review of the biogeochemistry and ecotoxicology of selenium in lotic and lentic environments. *Environmental Toxicology and Chemistry,* 24**,** 1331-1343.

SIMON, M. & WÜNSCH, C. 1998. Temperature control of bacterioplankton growth in a temperate large lake. *Aquatic Microbial Ecology,* 16**,** 119-130.

SINGH, D. K. 2012. Metabolism or Degradation of Pesticides: Phase I and Phase II Reactions. *In:* SINGH, D. K. (ed.) *Pesticide Chemistry and Toxicology.* Bentham eBooks.

SINGH, R., PAUL, D. & JAIN, R. K. 2006. Biofilms: implications in bioremediation. *Trends in Microbiology*, 14**,** 389-397.

SJØHOLM, O. R., AAMAND, J., SØRENSEN, J. & NYBROE, O. 2010. Degrader density determines spatial variability of 2,6-dichlorobenzamide mineralisation in soil. *Environmental Pollution,* 158**,** 292-298.

SMOOT, J. C. & FINDLEY, R. H. 2001. Spatial and Seasonal Variation in a Reservoir Sedimentary Microbial Community as Determined by Phospholipid Analysis *Microbial Ecology,* 42**,** 350-358.

SØRENSEN, S. R., RONEN, Z. & AAMAND, J. 2002. Growth in Coculture Stimulates Metabolism of the Phenylurea Herbicide Isoproturon by *Sphingomonas* sp. Strain SRS2. *Applied and Environmental Microbiology,* 68**,** 3478-3485.

SPAIN, J. C., VAN VELD, P. A., MONTI, C. A., PRITCHARD, P. H. & CRIPE, C. R. 1984. Comparison of *p*-Nitrophenol Biodegradation in Field and Laboratory Test Systems. *Applied and Environmental Microbiology,* 48**,** 944-950.

STEWART, E. J. 2012. Growing Unculturable Bacteria. *Journal of Bacteriology,* 194**,** 4151-4160.

STOATE, C., BOATMAN, N. D., BORRALHO, R. J., RIO CARVALHO, C., DE SNOO, G. R. & EDEN, P. 2001. Ecological impacts of arable intensification in Europe. *Journal of Environmental Management,* 63**,** 337-365.

STOECK, T., BASS, D., NEBEL, M., CHRISTEN, R., JONES, M. D. M., BREINER, H.-W. & RICHARDS, T. A. 2010. Multiple marker parallel tag environmental DNA sequencing

reveals a highly complex eukaryotic community in marine anoxic water. *Molecular Ecology,* 19**,** 21-31.

STOKSTAD, E. 2013. Pesticides Under Fire For Risks to Pollinators. *Science,* 340**,** 674-676.

STORCK, V. 2016. Assessment of the environmental fate of pesticides and their ecotoxicological impact on soil microorganisms. Doctor of Philosophy, National Institute of Agronomical Research.

STRAVS, M. A., POMATI, F. & HOLLENDER, J. 2017. Exploring micropollutant biotransformation in three freshwater phytoplankton species. *Environmental Science Processes & Impacts,* 19**,** 822-832.

STREIT, B. 1992. Bioaccumulation processes in ecosystems. *Experientia,* 48**,** 955-970.

STUART, M. E., MANAMSA, K., TALBOT, J. C. & CRANE, E. J. 2011. Emerging contaminants in groundwater. *British Geological Survey,* (OR/11/013)**,** 1-111.

STURMAN, P. J., STEWART, P. S., CUNNINGHAM, A. B., BOUWER, E. J. & WOLFRAM, J. H. 1995. Engineering scale-up of insitu bioremediation processes: a review. *Journal of Contaminant Hydrology,* 19**,** 171-203.

SUN, G., ZHANG, X., HU, Q., ZHANG, H., ZHANG, D. & LI, G. 2015. Biodegradation of Dichlorodiphenyltrichloroethanes (DDTs) and Hexachlorocyclohexanes (HCHs) with Plant and Nutrients and Their Effects on the Microbial Ecological Kinetics. *Microbial Ecology,* 69**,** 281-292.

SUNDA, W. G., GRANELI, E. & GOBLER, C. J. 2006. Positive feedback and the development and persistence of ecosystem disruptive algal blooms. *Journal of Phycology,* 42**,** 963-974.

SYLVANIA 2007. Product selected: F70W/865. 0001095 F70W/865**,** 1.

SYNGENTA. 2017a. *SDHI chemistry* [Online]. Syngenta. Available: http://www.isopyrazam.com/izm-sdhi-technology.html [Accessed 19/09/17 2017].

SYNGENTA. 2017b. *Unique Double Binding Properties* [Online]. Syngenta. Available: http://www.isopyrazam.com/izm-double-binding.html#&panel1-1 [Accessed 19/09/17 2017].

SZABÓ, K. E., ITOR, P. O. B., BERTILSSON, S., TRANVIK, L. & EILER, A. 2007. Importance of rare and abundant populations for the structure and functional potential of freshwater bacterial communities. *Aquatic Microbial Ecology,* 47**,** 1-10.

TAKAGI, K., FUJII, K., YAMAZAKI, K., HARADA, N. & IWASAKI, A. 2012. Biodegradation of melamine and its hydroxy derivatives by a bacterial consortium containing a novel *Nocardioides* species. *Applied Microbiology and Biotechnology,* 94**,** 1647-1656.

TALWAR, M. P. & NINNEKAR, H. Z. 2015. Biodegradation of pesticide profenofos by the free and immobilized cells of *Pseudoxanthomonas suqonensis* strain HNM. *Journal of Basic Microbiology,* 55**,** 1094-1103.

TANABE, A., MITOBE, H., KAWATA, K., YASUHARA, A. & SHIBAMOTO, T. 2001. Seasonal and Spatial Studies on Pesticide Residues in Surface Waters of the Shinano River in Japan. *Journal of Agricultural and Food Chemistry,* 49**,** 3847-3852.

TAYLOR, E. L., HOLLEY, A. G. & KIRK, M. 2007. Pesticide Development: a Brief Look at the History. *Southwen Regional Extention Forestry* 1-7.

TEJERINE-GARRO, F. L., MALDONADO, M., IBAÑEZ, C., PONT, D., ROSET, N. & OBERDORFF, T. 2005. Effects of Natural and Anthropogenic Environmental Changes on Riverine Fish Assemblages: a Framework for Ecological Assessment of Rivers. *Brazilian Archives of Biology and Technology,* 48**,** 91-108.

TEKRONY, D. M. 1976. Applicator Training Manual for: Seed Treatment Pest Control. *University of Kentucky, College of Agriculture,* 1-14.

THOMAS, K. A. & HAND, L. H. 2011. Assessing the potential for algae and macrophytes to degrade crop protection products in aquatic ecosystems. *Environmental Toxicology and Chemistry,* 30**,** 622-31.

THOMAS, K. A. & HAND, L. H. 2012. Assessing the metabolic potential of phototrophic communities in surface water environments: fludioxonil as a model compound. *Environmental Toxicology and Chemistry,* 31**,** 2138-46.

THOMPSON, H., ANGELOVA, A., BOWLER, B., JONES, M. D. M. & GUTIERREZ, T. 2017. Enhanced crude oil biodegradative potential of natural phytoplankton-associated hydrocarbonoclastic bacteria. *Environmental Microbiology,* Advanced online publication**,** 1-51.

THORNTON, S. F. & WILSON, R. D. 2008. Principles and Practice for the Collection of Representative Groundwater Samples. *CL:AIRE Technical Bulletin* [Online], TB3.

THOUAND, G., DURAND, M.-J., MAUL, A., GANCET, C. & BLOK, H. 2011. New concepts in the evalutation of biodegradation/persistance of chemical substances using a microbial inoculum. *Frontiers in Microbiology,* 2**,** 1-6.

THOUAND, G., FRIANT, P., BOIS, F., CARTIER, A., MAUL, A. & BLOCK, J. C. 1995. Bacterial inoculum density and probability of para-nitrophenol biodegradability test response. *Ecotoxicology and Environmental Safety,* 30**,** 274-282.

THULLNER, M., MAUCLAIRE, L., SCHROTH, M. H., KINZELBACK, W. & ZEYER, J. 2002. Interaction between water flow and spatial distribution of microbial growth in a two-dimensional flow field in saturated porous media. *Journal of Contaminant Hydrology,* 58**,** 169-189.

TIMEANDDATE.COM. 2017. *Coventry, England, United Kindgom - Sunrise, Sunset, and Daylength* [Online]. Available: https://www.timeanddate.com/sun/uk/coventry [Accessed 13/07/17 2017].

TORSTENSSON, N. T. L. 1980. Role of microorganisms in decomposition. *In:* HANCE, R. J. (ed.) *Interactions Between Herbicides and the Soil.* London: European Weed Research Society, Academic Press.

UZARSKI, D. G., STRICKER, C. A., BURTON, T. M., KING, D. K. & STEINMAN, A. D. 2004. The importance of hyporheic sediment respiration in several mid-order Michigan rivers: comparison between methods in estimates of lotic metabolism. *Hydrobiologia,* 518**,** 47-57.

VALIELA, I., MCCLELLAND, J., HAUXWELL, J., BEHR, P. J., HERSH, D. & FOREMAN, K. 1997. Macroalgal blooms in shallow estuaries: Controls and ecophysiological and ecosystem consequences. *Limnology and Oceanography,* 42**,** 1105-1118.

VAN GEMERDEN, H. & BEEFTINK, H. H. 1983. Ecology of Phototrophic Bacteria. *In:* ORMEROD, J. G. (ed.) *The Phototrophic Bacteria: Anaerobic Life in the Light.* Berkeley, Los Angeles: University of California Press.

VANNOTE, R. L., MINSHALL, G. W., CUMMINS, K. W., SEDELL, J. R. & CUSHING, C. E. 1980. The River Continuum Concept. *Canadian Journal of Fisheries and Aquatic Sciences,* 37**,** 130-137.

VELLEND, M. 2010. Conceptual Synthesis in Community Ecology. *The Quarterly Review of Biology,* 85**,** 183-206.

VIÑAS, M., J., S., ESPUNY, M. E. & SOLANAS, A. M. 2005. Bacterial Community Dynamics and Polycyclic Aromatic hydrocarbon Degradation during bioremediation of Heavily Creosote-Contaminated Soil. *Applied and Environmental Microbiology,* 71**,** 7008-7018.

VINCENT, W. F. & JAMES, M. R. 1996. Biodiversity in extreme aquatic environments: lakes, ponds and streams of the Ross Sea sector, Antarctica. *Biodiversity and Conservation,* 5**,** 1451-1471.

VON DER WEID, I., MARQUES, J. M., CUNHA, C. D., LIPPI, R. K., DOS SANTOS, S. C. C., ROSADO, A. S., LINS, U. & SELDIN, L. 2007. Identification and biodegradation potential of a novel strain of *Dietzia cinnamea* isolated from a petroleum-contaminated tropical soil. *Systematic and Applied Microbiology,* 30**,** 331-339.

VON KARMAN, T. 1930. Mechanische Ähnlichkeit und Turbulenz. *Nachrichten von der Gesellschaft der Wissenschaften zu Göttingen, Fachgruppe 1 (Mathematik),* 5**,** 58-76. English translation: VON KARMAN, T. 1931. Mechanical Similitude and Turbulence. *Technical memorandums National Advisory Committee for Aeronautics*, 611, 1-21.

VRYZAS, Z., VASSILIOU, G., ALEXOUDIS, C. & PAPADOPOULOU-MOURKIDOU, E. 2009. Spatial and temporal distribution of pesticide residues in surface waters in northeastern Greece. *Water Research,* 43**,** 1-10.

WALDROP, M. P. & FIRESTONE, M. K. 2006. Response of Microbial Community Composition and Function to Soil Climate Change. *Microbial Ecology,* 52**,** 716-724.

WALKER, A., JURADO-EXPOSITO, M., BENDING, G. D. & SMITH, V. J. R. 2001. Spatial variability in the degradation rate of isoproturon in soil. *Environmental Pollution,* 111**,** 407-415.

WALKER, D. 2006. Adaption and Survival. *In:* BROWN, H. (ed.) *Science Essentials. Biology.* London: Evans.

WALLACE, D. F., HAND, L. H. & OLIVER, R. G. 2010. The role of indirect photolysis in limiting the persistence of crop protection products in surface waters. *Environmental Toxicology and Chemistry,* 29**,** 575-581.

WANG, H., WANG, B., DONG, W. & HU, X. 2016. Co-acclimation of bacterial communities under stresses of hydrocarbons with different structures. *Scientific Reports,* 6**,** 1-12.

WANG, Y., RIESS, R., NEMATI, M., HILL, G. & HEADLEY, J. 2008. Scale-up impacts on mass transfer and bioremediation of suspended naphthalene particles in bead mill bioreactors. *Bioresource Technology,* 99**,** 8143-8150.

WANG, Y., ZHANG, R., HE, Z., VAN NOSTRAND, J. D., ZHENG, Q., ZHOU, J. & JIAO, N. 2017. Functional Gene Diversity and Metabolic Potential of the Microbial Community in an Estuary-Shelf Environment. *Frontiers in Microbiology,* 8**,** 1-12.

WATSON, J. R. 1977. Seasonal Variation in the Biodegradation of 2,4-D in River Water. *Water Research,* 11**,** 153-157.

WEBER, J. B., WILKERSON, G. G. & REINHARDT, C. F. 2004. Calculating pesticide sorption coefficients (K_d) using selected soil properties. *Chemosphere,* 55**,** 157-166.

WETZEL, R. G. 1993. Microcommunities and microgradients: linking nutrient regeneration, microbial mutualism, and high sustained aquatic primary production. *Netherlands Journal of Aquatic Ecology,* 27**,** 3-9.

WHIPPLE, K. & CROSBY, B. 2004. 12.163 Surface Processes and Landscape Evolution. *Massachusetts Institute of Technology: MIT OpenCourseWare.* https://ocw.mit.edu.

WHITE, C. A. & FRANKS, A. L. 1978. Introduction. *In:* ENVIRONMENTAL PROTECTION AGENCY (ed.) *Demonstration of Erosion and Sediment Control Technology: Lake Tahoe Region of California.* Ohio: California State Water Resources Control Board.

WHITE, P. A., KALFF, J., RASMUSSEN, J. B. & GASOL, J. M. 1991. The Effect of Temperature and Algal Biomass on Bacterial Production and Specific Growth Rate in Freshwater and Marine Habitats. *Microbial Ecology,* 21**,** 99-118.

WHITTAKER, R. H. 1972. Evolution and Measurement of Species Diversity. *Taxon,* 21**,** 213-251.

WILLIAMS, P., WHITFIELD, M., BIGGS, J., BRAY, S., FOX, G., NICOLET, P. & SEAR, D. 2003. Comparative biodiversity of rivers, streams, ditches and ponds in an agricultural landscape in Southern England. *Biological Conservation,* 115**,** 329-341.

WINCHESTER, P. D., HUSKINS, J. & YING, J. 2009. Agrichemicals in surface water and birth defects in the United States. *Acta Pædiatrica,* 98**,** 664-669.

WINSLEY, T. J., SNAPE, I., MCKINLAY, J., STARK, J., VAN DORST, J. M., JI, M., FERRARI, B. C. & SICILIANO, S. D. 2014. The ecological controls on the prevalence of candidate division TM7 in polar regions. *5,* 345.

WIPA, C. & FA-AROONSAWAT, S. 2008. Biodegradation of Organophosphate Pesticide Using Recombinant Cyanobacteria with Surface- and intracellular-Expressed Organophosphorus Hydrolase. *Journal of Microbiology and Biorechnology,* 18**,** 946-951.

WORLD ENERGY COUNCIL 2013. Solar. *World Energy Resources,* 8**,** 1-28.

WRITER, J. H., RYAN, J. N. & BARBER, L. B. 2011. Role of Biofilms in Sorptive Removal of Steroidal Hormones and 4-Nonylphenol Compounds from Streams. *Environmental Science & Technology,* 45**,** 7275-7283.

XIA, X. & WANG, R. 2008. Effect of sediment particle size on polycyclic aromatic hydrocarbon biodegradation: importance of the sediment-water interface. *Environmental Toxicology and Chemistry,* 27**,** 119-125.

XIA, X., ZHOU, Z., ZHOU, C., JIANG, G. & LIU, T. 2011. Effects of Suspended Sediment on the Biodegradation and Mineralization of Phenanthrene in River Water. *Journal of Environmental Quality,* 40**,** 118-125.

XIN-YU, L., ZHEN-CHENG, S., XU, L., CHENG-GANG, Z. & HUI-WEN, Z. 2010. Assessing the effects of acetochlor on soil fungal communities by DGGE and clone library analysis. *Ecotoxicology,* 19**,** 1111-1116.

YANG, S., WEN, X., SHI, Y., LIEBNER, S., JIN, H. & PERFUMO, A. 2016. Hydrocarbon degraders establish at the cost of microbial richness, abundance and keystone taxa after crude oil contamination in permafrost environments. *Scientific Reports,* 6**,** 1-13.

YANG, S., WEN, X., ZHAO, L., SHI, Y. & JIN, H. 2014. Crude Oil Treatment Leads to Shift of Bacterial Communities in Soils from the Deep Active Layer and Upper Permafrost along the China-Russia Crude Oil Pipeline Route. *Public Library of Science ONE,* 9**,** 1-10.

YANG, Z. F., XIA, X. H., HUANG, G. H., ZHOU, J. S. & RONG, X. 2008. Effect of Sediment on the biodegradation of Petroleum Contaminants in Natural Water. *Petroleum Science and Technology,* 26**,** 868-886.

YE, Y.-F., MIN, H. & DU, Y.-F. 2004. Characterization of a strain of *Sphingobacterium* sp. and its degradation to herbicide mefenacet. *Journal of Environmental Sciences,* 16**,** 343-347.

YOUIDRAW, L. 2016. *YouiDraw Drawing* [Online]. YouiDraw. [Accessed 27/10/2016 2016].

YOUNES, M. & GALAL-GORCHEV, H. 2000. Pesticides in Drinking Water - A Case Study. *Food and Chemical Toxicology,* 38**,** S87-S90.

YU, X.-Y., YING, G.-G. & KOOKANA, R. S. 2009. Reduced plant uptake of pesticides with biochar additions to soil. *Chemosphere,* 76**,** 665-671.

YUDELMAN, M., RATTA, A. & NYGAARD, D. 1998. Pest Management and Food Production: Looking to the Future. *Food, Agriculture, and the Environment Discussion Paper 25.* Washington: International Food Policy Research Institute.

ZHANG, S., QIU, C. B., ZHOU, Y., KIN, Z. P. & YANG, H. 2011. Bioaccumulation and degradation of pesticide fluroxypyr are associated with toxic tolerance in green alga *Chlamydomonas reinhardtii*. *Ecotoxicology,* 20**,** 337-347.

APPENDICES

APPENDIX I - CHAPTER 1 FURTHER METHODS AND SUPPORTING DATA

I.1 Environmental realism of the test conditions

For illuminated systems, lights were on for 16 hours per day and the experiment was controlled at 20 ± 2 °C. Both of these are more typical for summer months but are within the daylight (timeanddate.com, 2017) and temperature (Met Office, 2017a) ranges usually seen in the United Kingdom. The fluorescent 70 W daylight blubs (F70W/865 T8 6 ft, Fusion Lamps, UK) had a low transmission below 400 nm (**Fig. I.1**), however, LEE226 filters (Transformation Tubes, UK) also covered the bulbs. This was to ensure that there was a transmission of less than 50 % radiation at a wavelength of 410 nm, and minimal transmission at wavelengths below 390 nm. This ensured that photolysis was limited and that any effect from the light treatment was due to its impact on the microbial communities. The transmission spectra for the filters can be seen in **Figure I.2**. The average light intensity across the shaker was 1.66 x 10^4 lux, which is within the range of light intensities taken at the sample site for the experiments in this thesis.

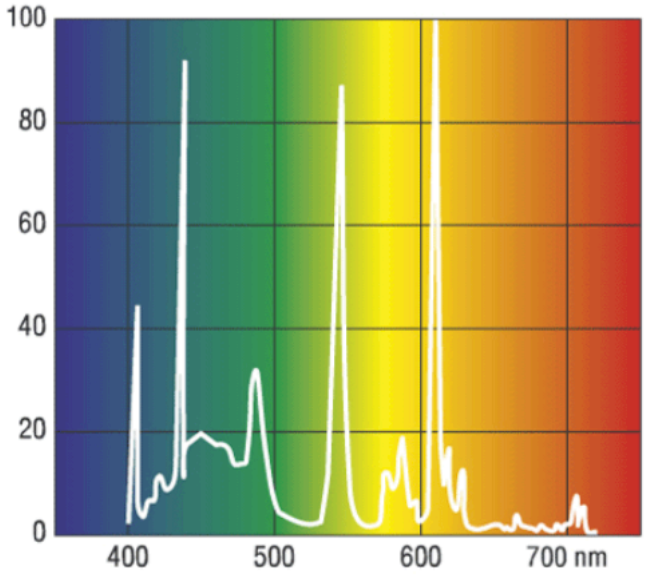

Figure I.1: Transmission spectra for fluorescent daylight bulbs. Transmission below 400 nm was limited with these bulbs, however, the LEE226 filters were additionally used as an extra precaution (Sylvania, 2007).

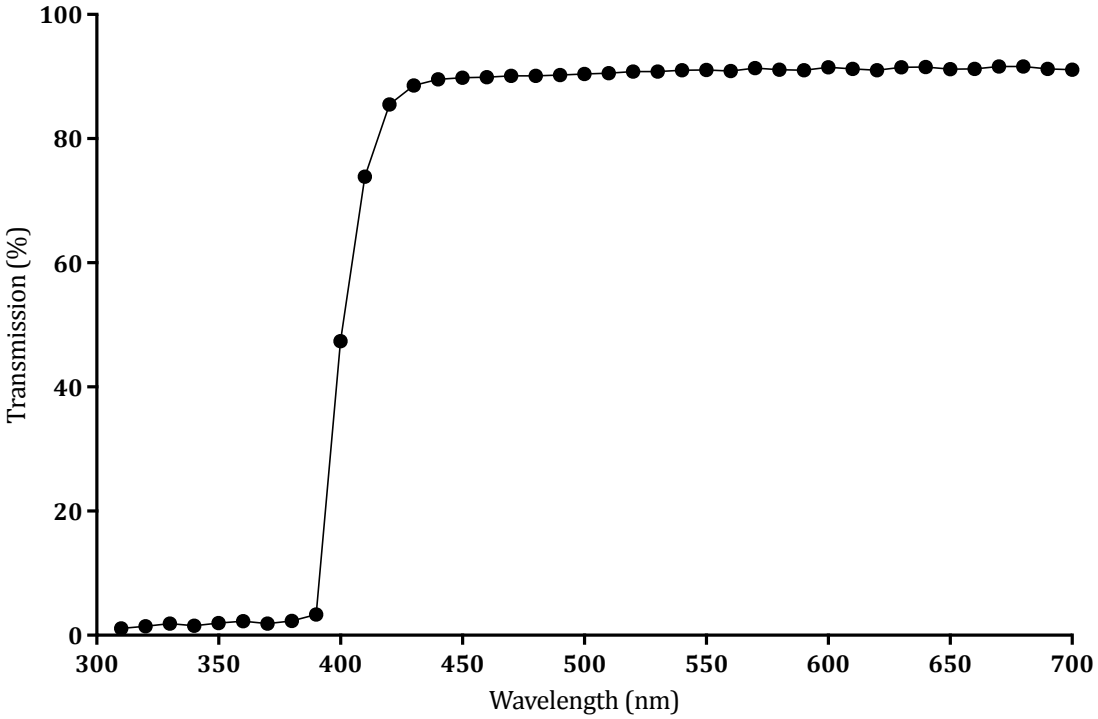

Figure I.2: Transmission spectra for LEE226 filters supplied by Transformation Tubes, United Kingdom. The filters covered the lights and ensured that transmission of wavelengths essential for photolysis were limited.

For the water velocity, the actual measurements from the river (from all sampling sessions in this thesis) gave a depth mean velocity (u_d) of 86 mm/s and an average water depth of 0.31 m. The bottom roughness parameter (z_o) of the sediment bed can be approximated using equation (1), where particle size distribution (d_{50}) has been estimated as 10 mm for rough bed conditions (Leopold, 1970).

$$z_o = d_{50} / 30$$
$$z_o = 10 / 30 \quad (1)$$
$$z_o = 0.3$$

The Law of the Wall (von Karman, 1930) shown in equation (2), gives the cross-sectionally averaged velocity (u), where u^* (86 mm/s / 20 = 4.33 mm/s) is the shear velocity generated by multiplying the u_d by the transverse mixing coefficient (taken as 20 using Rutherford (1994)), k is Von Karman's Constant (0.4), z_o is the bottom roughness parameter

(0.3 from equation (1)), and z is the depth height at a particular velocity (Kironoto and Graf, 1994, Whipple and Crosby, 2004).

$$u = \frac{u*}{k} ln \frac{z}{z_o} \quad (2)$$

Values of increasing water depth were substituted in as z ranging from 1 to 352.5 mm to give the vertical profile chart shown in **Figure I.3**, with u on the x-axis and z on the y-axis.

<u>Microcosm measurements and shaker settings</u>

Mass of water sample = 0.08 kg

Microcosm radius = 0.035 m

Revolutions per minute (rpm) of shaker = 50 rpm

Revolution per second (rps) of shaker = 50 / 60 = 0.83 rps

Velocity of shaker in radians = 2π * shaker rps = 5.24 radians/s

The central axis (I) of the microcosm can be calculated by equation (3), where M is mass of water and R is the radius of the microcosm.

$$I = ½MR^2 \quad (3)$$

$$I = ½ * 0.08 * 0.035^2$$

$$I = 0.000049 \text{ kg/m}^2$$

The kinetic energy (K) of the rotation on the shaker can be calculated by equation (4), where I is the central axis and ω is the angular velocity.

$$K = ½I\omega^2 \quad (4)$$

$$K = ½ * 0.000049 * 5.24^2$$

$$K = 0.00067 \text{ J}$$

The average velocity of the shaker can be calculated by equation (5) where M is the mass of water and V is the velocity.

$$K = ½MV^2 \quad (5)$$

$$0.00067 = ½ * 0.08 * V^2$$

$$0.00067 = 0.04 * V^2$$

$$0.01675 = V^2$$

$$V = 0.12942 \text{ m/s} = \underline{129.42 \text{ mm/s}}$$

Therefore, according to the vertical profile in **Figure I.3**, the water velocity in the microcosms was faster than would be expected at the mean river depth. Nevertheless, as the depth could be higher than the mean, and because the river water velocity will be dynamic spatially and temporally, the water velocity in the microcosms is deemed realistic.

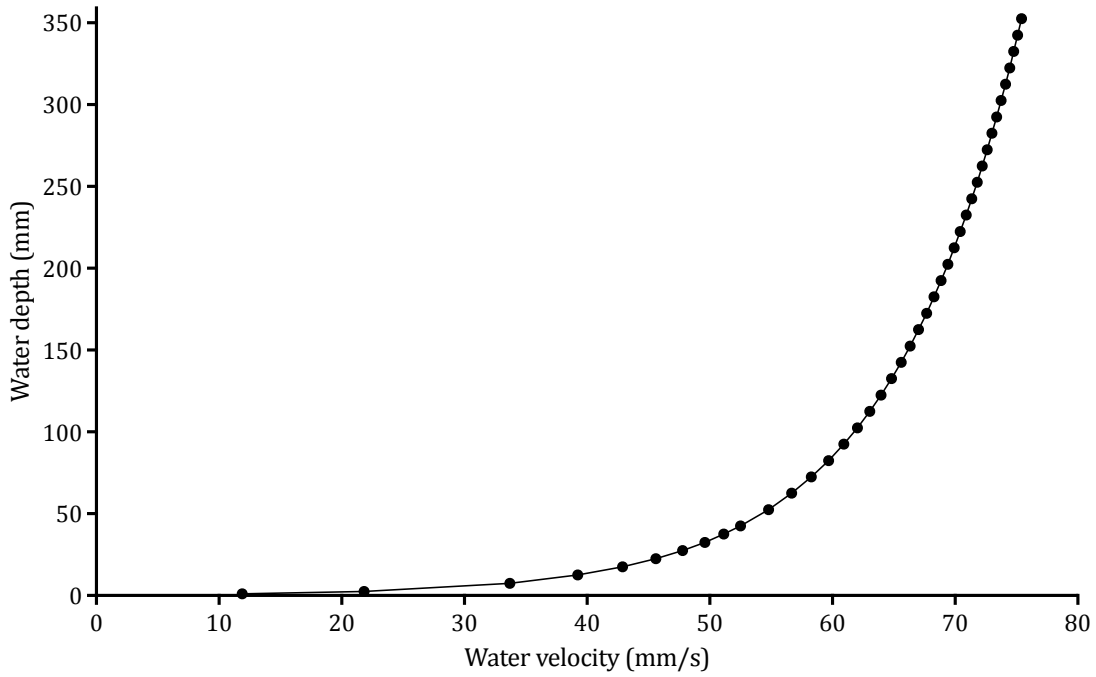

Figure I.3: Velocity profile of River Dene, Wellesbourne, United Kingdom. The velocity profile of the sample site created using values from the Law of the Wall equation.

I.2 Example mass balance calculations

Radioactivity from the Liquid Scintillation Counting (LSC) analysis of each fraction – water (including acetonitrile rinse), sediment extract, NER, and NaOH traps – was summed together to determine the mass balance of each microcosm. Example calculations can be seen in **Table I.1** and an average mass balance over an entire time course can be seen in **Figure I.4**.

Table I.1: Example mass balance calculations. Mass balance calculations taken from winter 2015 at 36 DAT for each microcosm treatment.

Microcosm (DAT/ treatment)	Fraction (% of applied radioactivity)				
	Water	Sediment extract	NER in sediment	Mineralised	Total
36 Illuminated water-sediment	25.0	63.5	2.2	1.2	91.9
36 Dark water-sediment	20.8	73.3	2.5	0.8	97.4
36 Illuminated water-only	90.8	N/A	N/A	1.5	92.3
36 Dark water-only	96.7	N/A	N/A	1.0	97.7

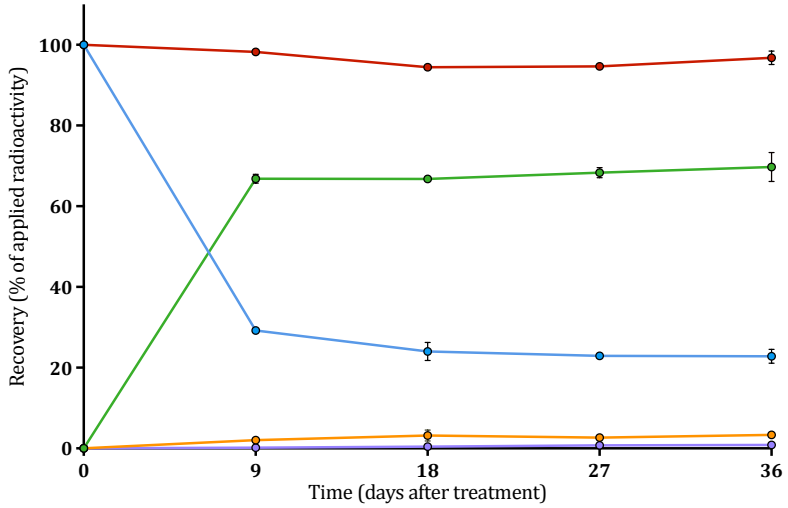

Figure I.4: Average mass balance in dark water-sediment microcosms in winter 2015 over 36 days. Average mass balance in the water (blue), sediment extract (green), sediment NER (orange), and mineralisation (purple), to make up the total mass balance (red). Error bars show ± standard deviation.

I.3 Solid Phase Extraction methodology for isopyrazam aqueous samples

The methodology was supplied by Syngenta, Jealott's Hill International Research Centre, United Kingdom and used Oasis HLB 60 mg 3 mL capacity SPE cartridges (Waters Ltd., UK). Sep-Pak reservoir and adapters (Waters Ltd., UK) were used to hold larger volumes of sample if needed.

Cartridges were placed in a Whatman 12 port SPE vacuum manifold (GE Healthcare, UK) and conditioned by applying 2 mL methanol (HPLC grade, Fischer Scientific, UK) followed by 2 mL pure water (HPLC grade, VWR Chemicals, UK). Aqueous samples were acidified before loading onto the cartridges by adding the equivalent of 200 μL concentrated acetic acid glacial (Fischer Scientific, UK) per 60 mL sample. This helped with the retention of metabolites.

Aqueous samples were loaded onto the cartridge at a maximum load rate of 2 mL/min with gentle vacuum pressure using an N 035.3 AN.18 diaphragm pump (KNF Neuberger, UK). Sample vessels were then rinsed with 2 mL water (HPLC grade, VWR Chemicals, UK) and this was used to rinse the cartridges. Excess water was removed from the cartridge with gentle vacuum pressure using an N 035.3 AN.18 diaphragm pump (KNF Neuberger, UK), but it was ensured that cartridges were not dried out.

Glass collection tubes were placed under the cartridge drain ports and stop taps were closed. 3 mL methanol (HPLC grade, Fischer Scientific, UK) was added to the cartridges and the solvent was allowed to soak in for a few minutes before eluting. Cartridges were retained until analysis was complete, as the elution step could be repeated if sample recovery was low. The methanol was evaporated to dryness and re-dissolved in 50:50 acetonitrile (HPLC grade, Fischer Scientific, UK) and water (HPLC grade, VWR Chemicals, UK) mobile phase.

I.4 Example concentration calculations

Water and sediment extracts were both concentrated so that there was approximately 1500 Bq in the 1 mL sample post-concentration ready for HPLC analysis. As

described in section 2.2.5, in the water, isopyrazam was concentrated using SPE and, in the sediment extracts, evaporation under nitrogen was used. It was ensured that between 90 and 110 % of the radioactivity from the original aliquot taken for concentration was recovered after concentration. Example calculations can be found in **Table I.2**.

Table I.2: Example concentration calculations in water and sediment samples. Concentration calculations taken from winter 2015 for each microcosm treatment. *Rad.*, *conc.* and *rec.* are shorthand for *radioactivity*, *concentration*, and *recovery*, respectively.

Microcosm (DAT/ treatment)	Sample type	Rad. in sample (Bq/g)	Amount concentrated (g)	Rad. in sample aliquot (Bq)	Rad. post-conc. (Bq)	Rec. post-conc. (%)
9 Illuminated water-sediment	Water	121.9	12.9	1570.3	1545.1	98.6
9 Dark water-sediment	Water	141.9	10.6	1503.1	1444.6	96.1
9 Illuminated water-only	Water	444.6	3.4	1498.4	1476.0	98.5
9 Dark water-only	Water	438.0	3.4	1506.8	1429.3	94.9
27 Illuminated water-sediment	Sediment Extract	180.0	8.5	1530.0	1554.6	101.6
36 Dark water-sediment	Sediment Extract	206.7	7.2	1488.1	1623.8	109.1

I.5 Isopyrazam High-Performance Liquid Chromatography method

Syngenta supplied the HPLC protocol for the compound, isopyrazam. A Lichrosphere RP-18e μm column (4.0 x 250 mm, Agilent Technologies, US) was used with a column temperature of 20 °C and the radiodetector had a dwell time of 6 seconds. Mobile phases consisted of 0.2 % acetic acid glacial (Fischer Scientific, UK) (mobile phase A) and acetonitrile (HPLC grade, Fischer Scientific, UK) (mobile phase B). The gradient elution can be seen in **Table I.3**. The flow rate was 1 mL/minute with a ratio of mobile phase to scintillation fluid of 1:1. The expected retention time of isopyrazam was 23 to 26 minutes and chromatograms were analysed using Laura software (version 4, LabLogic, UK).

Table I.3: HPLC elution gradient of mobile phases in analysis of isopyrazam. Mobile phase A is 0.2 % acetic acid glacial and mobile phase B is acetonitrile.

Time in run (minutes)	Mobile phase A (%)	Mobile phase B (%)
0	90	10
5	90	10
25	30	70
27	10	90
30	10	90
32	90	10
35	90	10

Radiolabelled standards were run on the HPLC and analysed using Laura software (version 4, LabLogic, UK). The isopyrazam retention time was between 29 and 31 minutes (**Fig. I.5**) and this confirmed that the peak seen in the samples at this time was also isopyrazam. Both water and sediment from each time point within each collection time was analysed by HPLC. Chromatograms were analysed using Laura software (version 4, LabLogic, UK) and examples can be seen in **Figures I.6** and **I.7**.

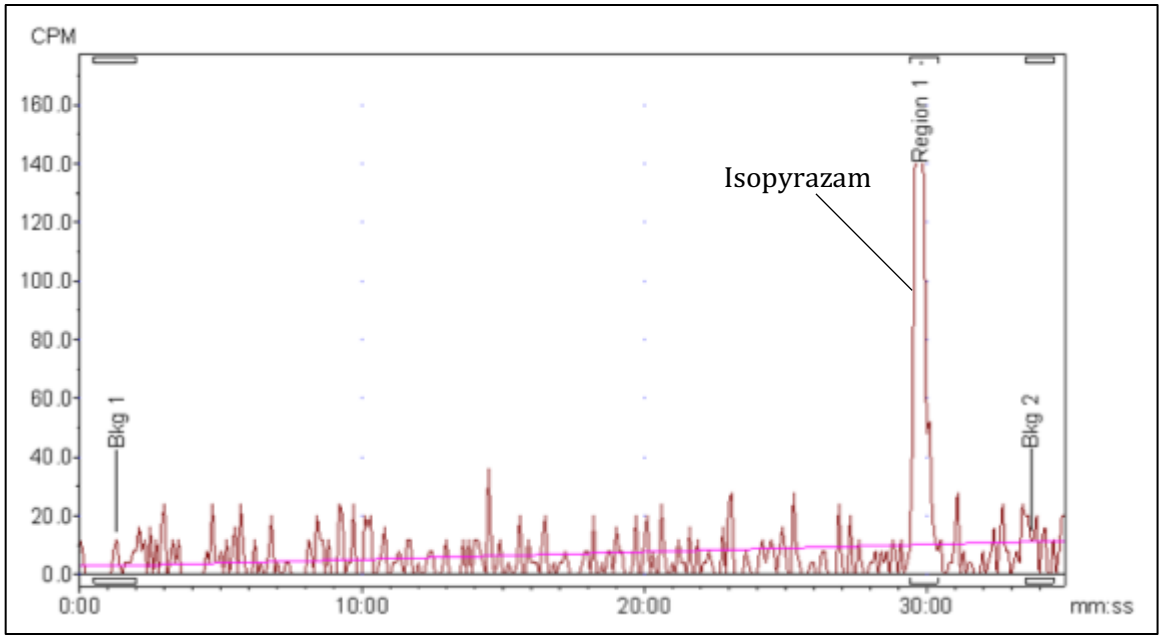

Figure I.5: Chromatogram of radiolabelled isopyrazam standard. Chromatograms were generated using Laura software (version 4, LabLogic, UK) and the isopyrazam retention time was between 29 and 31 minutes (annotated).

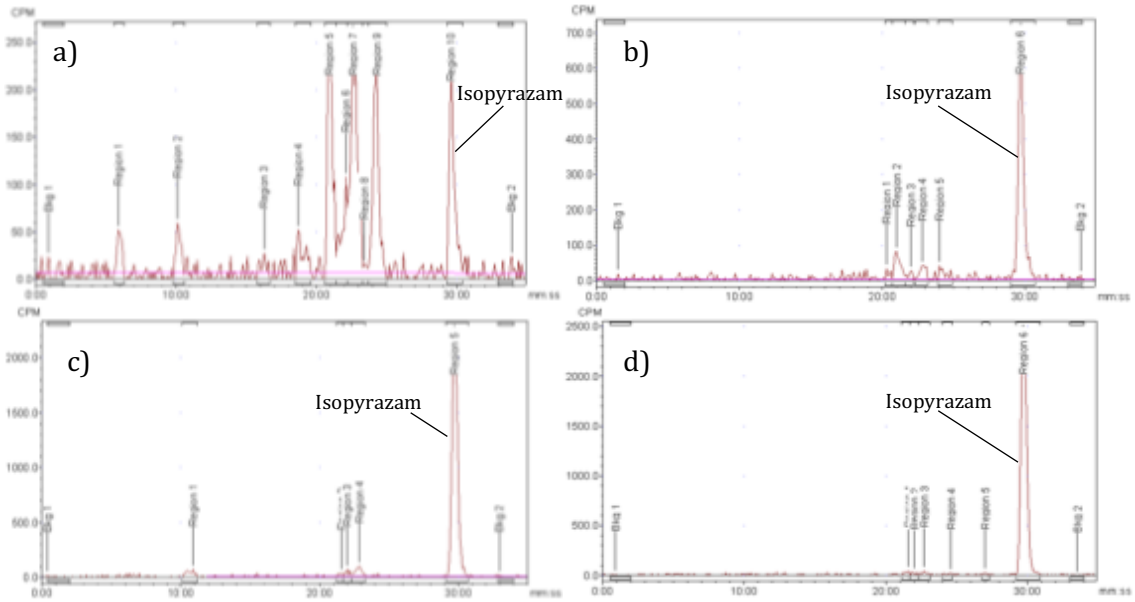

Figure I.6: Example chromatograms from the water fraction in illuminated water-sediment (a), dark water-sediment (b), illuminated water-only (c), and dark water-only (d) microcosms from summer 2014 at 36 DAT. Chromatograms were generated using Laura software (version 4, LabLogic, UK) and the isopyrazam retention time was between 29 and 31 minutes. Isopyrazam peaks are annotated and all other peaks were classified as metabolites.

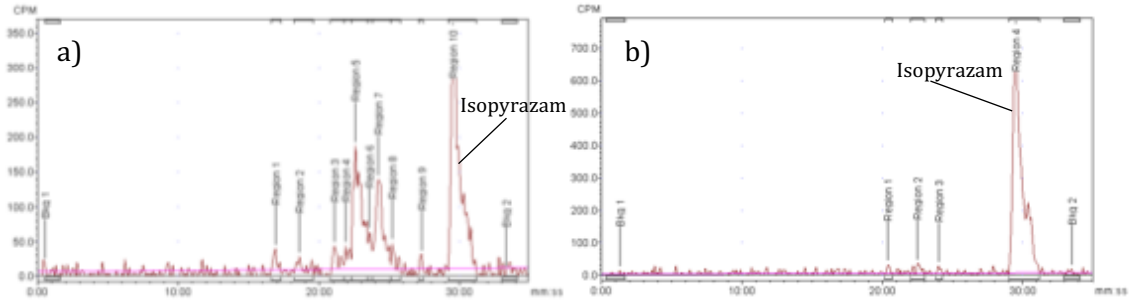

Figure I.7: Example chromatograms from the sediment fraction in illuminated water-sediment (a) and dark water-sediment (b) microcosms from autumn 2015 at 36 DAT. Chromatograms were generated using Laura software (version 4, LabLogic, UK) and the isopyrazam retention time was between 29 and 31 minutes. Isopyrazam peaks are annotated and all other peaks are classified as metabolites.

I.6 Supporting data

Isopyrazam decline curves, outlining the data described in **Figures 2.7** and **2.8**, are shown in **Figure I.8**, however, data is split by individual collection times to better shown the impact of microcosm type on isopyrazam decline. The DegT50 data is shown in **Tables I.4** and **I.5** (examples of SFO model fits shown in **Figure I.9**) and tends to follow the trend seen in the decline curve data. The DegT50 data was used for illuminated water-sediment microcosm analysis, however, for the other microcosm treatments, the DegT50 was beyond the duration of the study so was difficult to extrapolate from. For the majority of the other microcosm treatments, acceptance requirements outlined in section 2.2.8 were not met, this was especially the case of the r^2 values suggesting that there isn't a correlation between the observed and expected values. This suggests that SFO is not the best-fit model for these treatments.

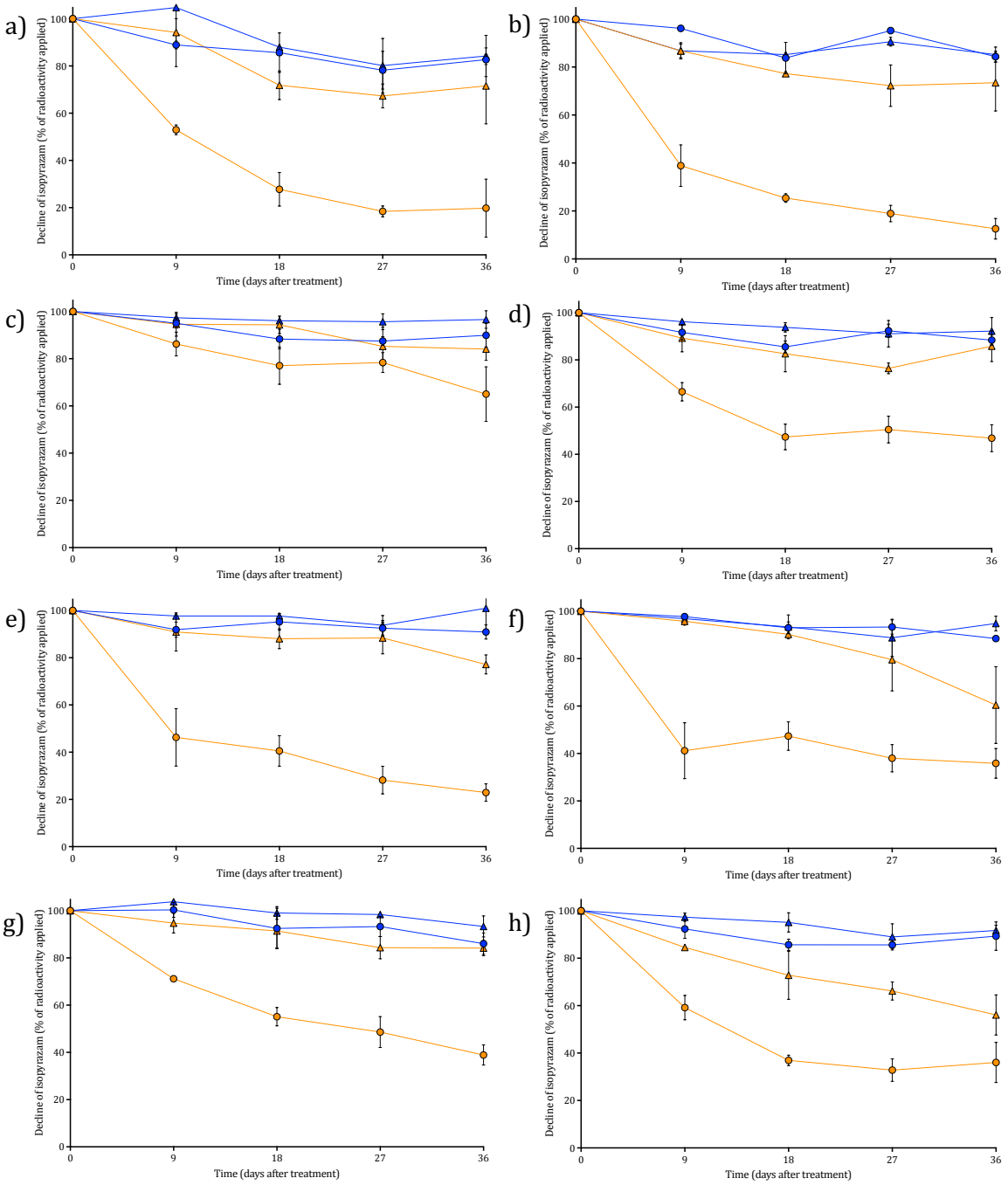

Figure I.8: Degradation of isopyrazam in different collection times as a percentage of the radioactivity originally applied. Degradation of isopyrazam in illuminated water-sediment (orange circles), dark water-sediment (blue circles), illuminated water-only (orange triangles), and dark water-only (blue triangles) microcosm treatments in summer 2014 (a), autumn 2014 (b), winter 2015 (c), spring 2015 (d), summer 2015 (e), autumn 2015 (f), winter 2016 (g), and spring 2016 (h). Error bars show ± standard deviation.

Table I.4: DegT50 and rate constant estimates from CAKE for microcosm treatments at each collection time. SFO kinetic models were used for all data and 95 % confidence intervals calculated for the rate constant. k_1 denotes the first-order kinetics rate constant and *CI* denotes *confidence interval*.

Sample (collection time/year/microcosm)	DegT50 (days)	k_1	Lower 95 % CI	Upper 95 % CI
Summer '14 illuminated water-sediment	11.1	0.064	0.051	0.074
Summer '14 dark water-sediment	116	0.006	0.003	0.009
Summer '14 illuminated water-only	57.8	0.012	0.007	0.017
Summer '14 dark water-only	101.0	0.007	0.001	0.013
Autumn '14 illuminated water-sediment	9.0	0.077	0.062	0.092
Autumn '14 dark water-sediment	117.0	0.004	0.001	0.007
Autumn '14 illuminated water-only	72.7	0.010	0.006	0.013
Autumn '14 dark water-only	211.0	0.003	0.001	0.006
Winter '15 illuminated water-sediment	64.4	0.011	0.007	0.015
Winter '15 dark water-sediment	203.0	0.003	0.002	0.005
Winter '15 illuminated water-only	139.0	0.005	0.003	0.007
Winter '15 dark water-only	714.0	0.001	-7.7×10^{-5}	0.002
Spring '15 illuminated water-sediment	27.7	0.025	0.018	0.033
Spring '15 dark water-sediment	251.0	0.003	0.002	0.005
Spring '15 illuminated water-only	126.0	0.006	0.002	0.009
Spring '15 dark water-only	278.0	0.002	0.001	0.004
Summer '15 illuminated water-sediment	14.1	0.049	0.037	0.062
Summer '15 dark water-sediment	334.0	0.002	4.7×10^{-4}	0.004
Summer '15 illuminated water-only	115.0	0.006	0.003	0.009
Summer '15 dark water-only	2960.0	2.4×10^{-4}	-0.002	0.002
Autumn '15 illuminated water-sediment	20.0	0.035	0.020	0.049
Autumn '15 dark water-sediment	215.0	0.003	0.002	0.004
Autumn '15 illuminated water-only	58.3	0.012	0.007	0.017
Autumn '15 dark water-only	316.0	0.002	-5.5×10^{-5}	0.004
Winter '16 illuminated water-sediment	25.3	0.027	0.024	0.031
Winter '16 dark water-sediment	170.0	0.004	0.002	0.006
Winter '16 illuminated water-only	134.0	0.005	0.003	0.007
Winter '16 dark water-only	335.0	0.002	0.001	0.004
Spring '16 illuminated water-sediment	17.4	0.040	0.030	0.050
Spring '16 dark water-sediment	195.0	0.004	0.001	0.006
Spring '16 illuminated water-only	43.9	0.016	0.012	0.019
Spring '16 dark water-only	236.0	0.003	0.001	0.005

Table I.5: Kinetic model and acceptance requirements for DegT50 and rate constant estimates from CAKE for microcosm treatments at each collection time. SFO kinetic models were used for all data and key acceptance requirements are goodness of fit (χ^2), correlation between the observed and expected values (r^2), and the probability that the rate constant was significantly different to zero (Prob. > t). * denotes values that have failed the acceptance requirements outlined in section 2.2.8. *Prob.* denotes *probability*, and k_1 denotes the first-order kinetics rate constant.

Sample (collection time/year/microcosm)	Model	χ^2 (%)	r^2	Prob. > t (k_1)
Summer '14 illuminated water-sediment	SFO	8.9	0.950	1.3×10^{-8}
Summer '14 dark water-sediment	SFO	3.2	0.580 *	4.5×10^{-4}
Summer '14 illuminated water-only	SFO	5.6	0.647 *	1.5×10^{-4}
Summer '14 dark water-only	SFO	4.4	0.318 *	1.5×10^{-2}
Autumn '14 illuminated water-sediment	SFO	12.7	0.954	2.6×10^{-8}
Autumn '14 dark water-sediment	SFO	4.1	0.420 *	4.4×10^{-3}
Autumn '14 illuminated water-only	SFO	3.4	0.693 *	5.5×10^{-5}
Autumn '14 dark water-only	SFO	3.7	0.393 *	5.8×10^{-5}
Winter '15 illuminated water-sediment	SFO	3.2	0.742	2.0×10^{-5}
Winter '15 dark water-sediment	SFO	2.2	0.544 *	8.0×10^{-4}
Winter '15 illuminated water-only	SFO	1.5	0.627 *	2.2×10^{-4}
Winter '15 dark water-only	SFO	0.8	0.234 *	3.3×10^{-2}
Spring '15 illuminated water-sediment	SFO	10.6	0.8066	3.3×10^{-6}
Spring '15 dark water-sediment	SFO	2.3	0.467 *	2.4×10^{-3}
Spring '15 illuminated water-only	SFO	4.7	0.444 *	2.9×10^{-3}
Spring '15 dark water-only	SFO	1.0	0.469 *	2.4×10^{-3}
Summer '15 illuminated water-sediment	SFO	13	0.881	5.1×10^{-7}
Summer '15 dark water-sediment	SFO	1.8	0.374 *	7.6×10^{-3}
Summer '15 illuminated water-only	SFO	2.4	0.639 *	1.8×10^{-4}
Summer '15 dark water-only	SFO	2.0	0.004 *	4.1×10^{-1} *
Autumn '15 illuminated water-sediment	SFO	19.4 *	0.689 *	9.5×10^{-5}
Autumn '15 dark water-sediment	SFO	0.9	0.809	2.5×10^{-6}
Autumn '15 illuminated water-only	SFO	4.8	0.673 *	1.3×10^{-4}
Autumn '15 dark water-only	SFO	2.2	0.251 *	2.8×10^{-2}
Winter '16 illuminated water-sediment	SFO	4.4	0.953	5.4×10^{-10}
Winter '16 dark water-sediment	SFO	1.7	0.545 *	8.7×10^{-4}
Winter '16 illuminated water-only	SFO	1.1	0.699 *	5.2×10^{-5}
Winter '16 dark water-only	SFO	1.7	0.424 *	4.5×10^{-3}
Spring '16 illuminated water-sediment	SFO	12.5	0.875	4.8×10^{-7}
Spring '16 dark water-sediment	SFO	3.1	0.447 *	2.9×10^{-3}
Spring '16 illuminated water-only	SFO	1.3	0.894	6.8×10^{-8}
Spring '16 dark water-only	SFO	1.4	0.551 *	7.6×10^{-4}

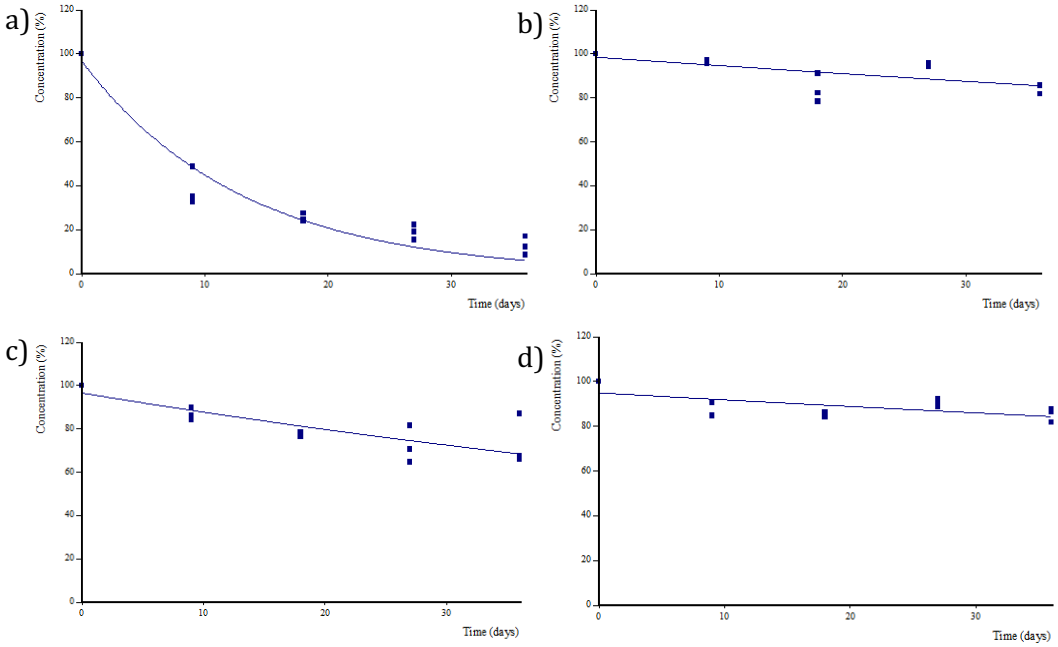

Figure I.9: Example kinetic model fits from CAKE analysis for each microcosm treatment. SFO kinetic model fits for the autumn 2014 collection time in illuminated water-sediment (a), dark water-sediment (b), illuminated water-only (c), and dark water-only (d) microcosms. The dots are individual observations and the line shows the fit.

Macronutrient concentration in the water was measured at each time point within a collection time; however, **Figures I.10** and **I.11** only show the concentrations in the fresh samples from the river and from each microcosm at 36 DAT. For NO_3- concentration (**Fig. I.10**), there was a significant impact ($p \leq 0.0001$) of microcosm type. A Tukey multiple comparisons test showed that dark water-sediment microcosms contained significantly more ($p \leq 0.0001$) NO_3- compared to the fresh samples and illuminated water-sediment, illuminated water-only, and dark water-only treatments. In dark water-sediment microcosms, concentrations ranged between 26.1 and 128.0 mg/L. Although the other microcosm treatments were variable in terms of water NO_3- concentration and there were increases and decreases throughout each collection time within the 36 days, the concentrations at the end of the experiment were not significant when compared to each other. This suggests that dark water-sediment microcosms contained higher populations of nitrifying bacteria. Although light is important for nitrification, some nitrifying bacteria have been shown to recover from photoinhibition (Guerrero and Jones, 1996). Phototrophic communities may utilise NO_3- (Flores *et al.*, 1999) in the illuminated microcosms. In dark

water-sediment microcosms, these communities are not able to proliferate to utilise the NO_3- produced, which may explain the higher concentrations in these treatments.

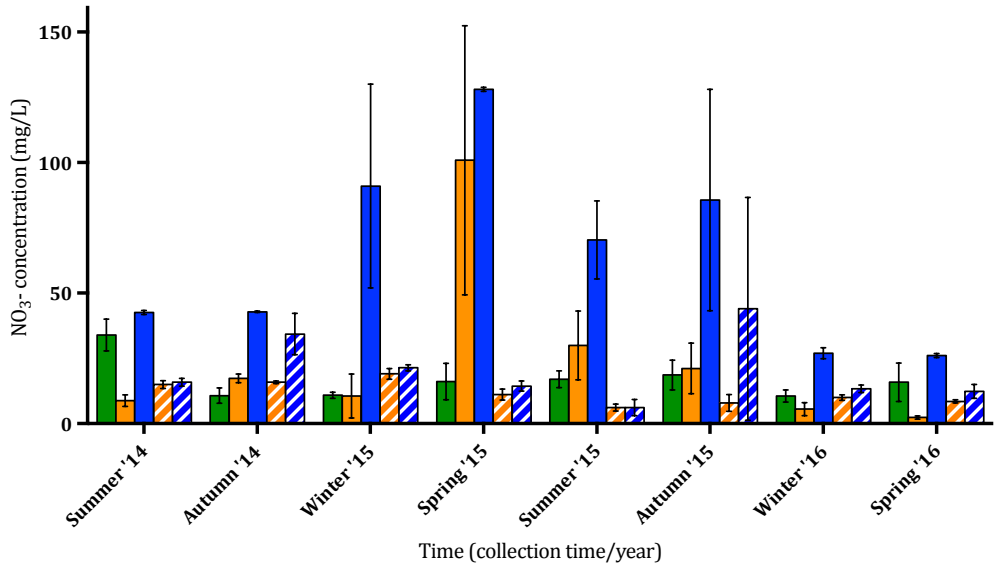

Figure I.10: Water NO_3- concentration of the fresh samples and at the end of each collection time. NO_3- concentration in the water was quantified using an NO_3- test kit (Hach, UK) on the fresh samples from the river (green) and in illuminated water-sediment (solid orange), dark water-sediment (solid blue), illuminated water-only (dashed orange), and dark water-only (dashed blue) microcosms. Microcosm concentrations are from the end of the experiment at 36 DAT and error bars show ± standard deviation.

For PO_4 concentration (**Fig. I.11**), there were no significant differences between collection times in any of the microcosm treatments ($p \leq 0.4762$). There was, however, a significant impact of treatment ($p \leq 0.0002$) and a Tukey multiple comparisons test showed that although there was not a significant difference in water PO_4 concentration between the four microcosm treatments, there was a significant difference between the fresh sample concentrations and of that in the microcosms. PO_4 concentrations ranged between 1.0 and 3.0 mg/L in the fresh water and, in general, this decreased in all microcosm treatments by 36 DAT. Some microcosms do significantly increase in PO_4 concentration from the fresh water, for instance in spring 2016, there was an increase in water-sediment systems from 1.3 mg/L to 1.6 and 2.3 mg/L in the illuminated and dark treatment microcosms, respectively. This suggests that the microbial communities within the microcosms are all active, regardless of whether isopyrazam is degraded and communities, especially microalgae, have been shown to convert phosphates into biomass (Delgadillo-Mirquez *et al.*, 2016)

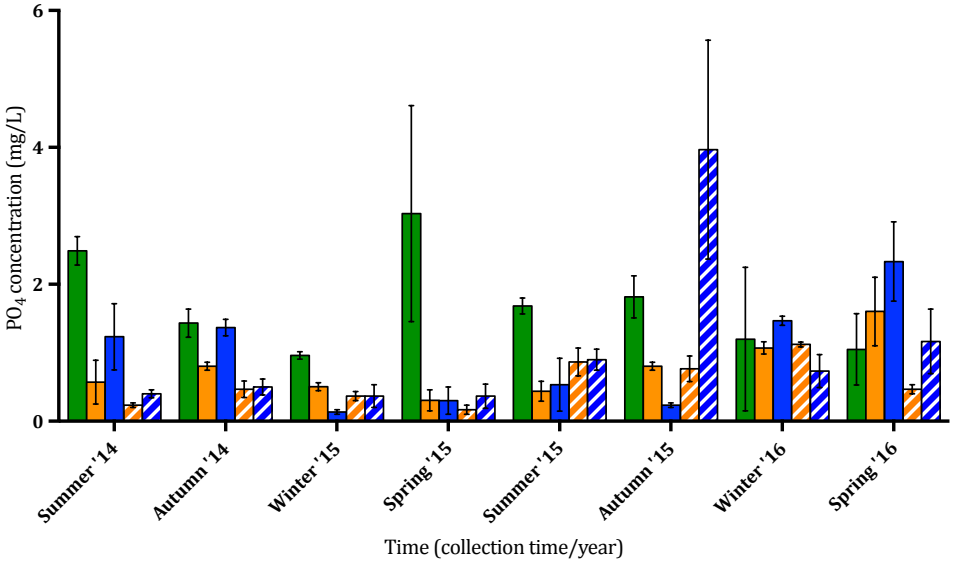

Figure I.11: Water PO_4 concentration of the fresh samples and at the end of each collection time. PO_4 concentration in the water was quantified using an Orthophosphate PO_4 test kit (Hach, UK) on the fresh samples from the river (green) and in illuminated water-sediment (solid orange), dark water-sediment (solid blue), illuminated water-only (dashed orange), and dark water-only (dashed blue) microcosms. Microcosm concentrations are from the end of the experiment at 36 DAT and error bars show ± standard deviation.

Bacteria concentration in the water was variable over the time course of the experiment. In illuminated water-sediment microcosms this ranged between 6.3 x 10^1 and 8.2 x 10^5 CFU/µL by 36 DAT, and in dark water-sediment microcosms between 9.9 x 10 and 3.3 x 10^5 CFU/µL depending on the collection time. In illuminated water-only microcosms, this ranged between 4.7 x 10^1 and 83.9 x 10^4 CFU/µL by the end of the experiment, and in dark water-only systems between 1.1 x 10^2 and 4.8 x 10^5 CFU/µL depending on the collection time. There was no significant impact of collection time on the concentration of bacteria in the water ($p \leq 0.6767$) regardless of both light treatment or sediment addition in the microcosms (**Fig. I.12**). There was, however, a significant impact of time ($p \leq 0.0006$) as bacteria concentration fluctuated throughout the time course within each treatment. This does not take into account the types of bacteria present and only accounts for the bacteria that could be cultured using the media and incubation conditions outlined in section 2.2.7.ii.

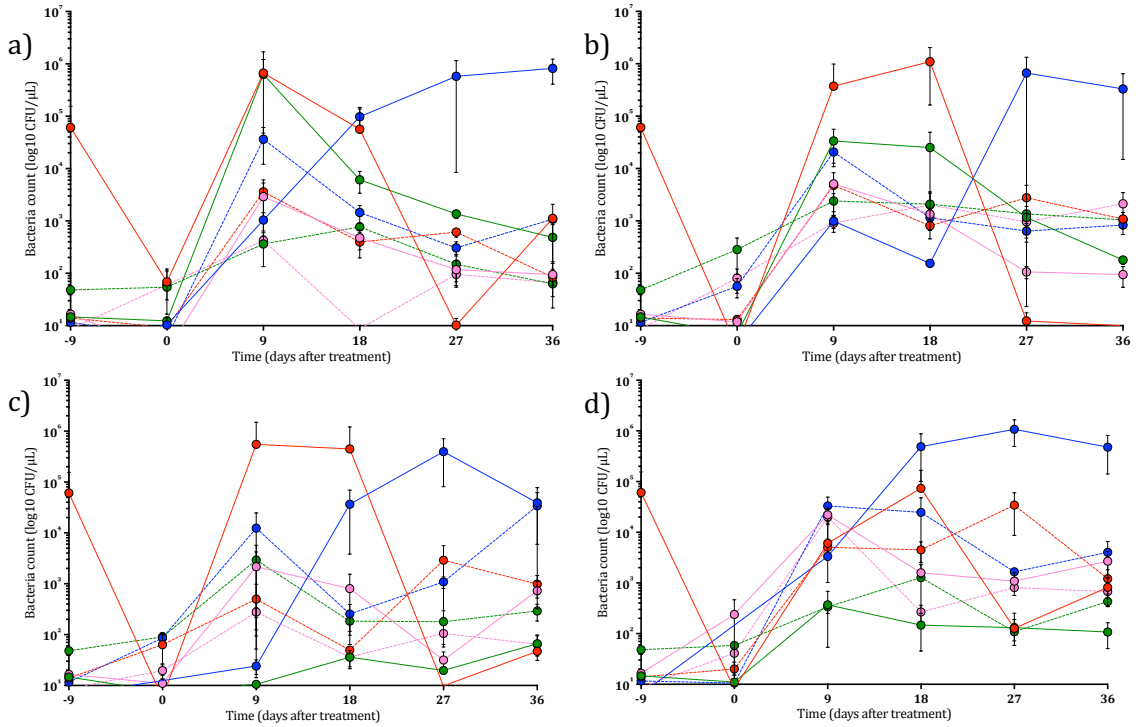

Figure I.12: Concentration of bacteria in the water fraction of different microcosm treatments. Bacteria concentration in the water fraction was quantified using R2A agar across time points at different collection times. Microcosm treatments were illuminated water-sediment (a), dark water-sediment (b), illuminated water-only (c), and dark water-only (d). Collection times were summer (red), autumn (blue), winter (green), and spring (pink), with the first year of each collection time denoted by a solid line and the second year by a dashed line. Error bars show ± standard deviation.

Pooled data of microbial analysis results is shown in section 2.3.4. The full breakdown of DNA analysis data can be found in the following figures; bacterial α diversity between different treatments at each collection time (**Fig. I.13**); bacterial β diversity within different treatments at each collection time (**Fig. I.14**); bacteria phyla relative abundances within different treatments at each collection time (**Fig. I.15**); phototrophic α diversity between different treatments at each collection time (**Fig. I.16**); phototrophic β diversity within different treatments at each collection time (**Fig. I.17**); total relative abundance of phototrophic and non-phototrophic OTUs amplified form the 23S rRNA gene at each collection time (**Fig. I.18**); and phototrophic taxa relative abundances within different treatments at each collection time (**Fig. I.19**).

Taxonomies of OTUs showing significance to particular DegT50s are shown in **Table I.6** and their relative abundances between each DegT50 rate is shown in **Table I.7**. Taxonomies of OTUs showing significance to collection times with high mineralisation (summer 2014 and winter 2015) are shown in **Table I.8** and their relative abundances compared to collection times with low mineralisation in **Table I.9**.

The raw sequence data (.fastq files) and metadata are stored at the National Centre for Biotechnology Information (NCBI) Sequence Read Archive (SRA). They are recorded under the study accession number SRP132448. In addition to the bacterial and phototrophic data discussed in this thesis, library preparation using the 18S rRNA gene was also carried out for the fresh water and sediment samples taken from the river to investigate eukaryotic community structure and diversity; these data are also stored under the same study accession number. Sequences for OTUs showing significance to particular DegT50 or mineralisation rates are stored at the NCBI GenBank database and accession numbers are given in **Tables I.6** and **I.8**.

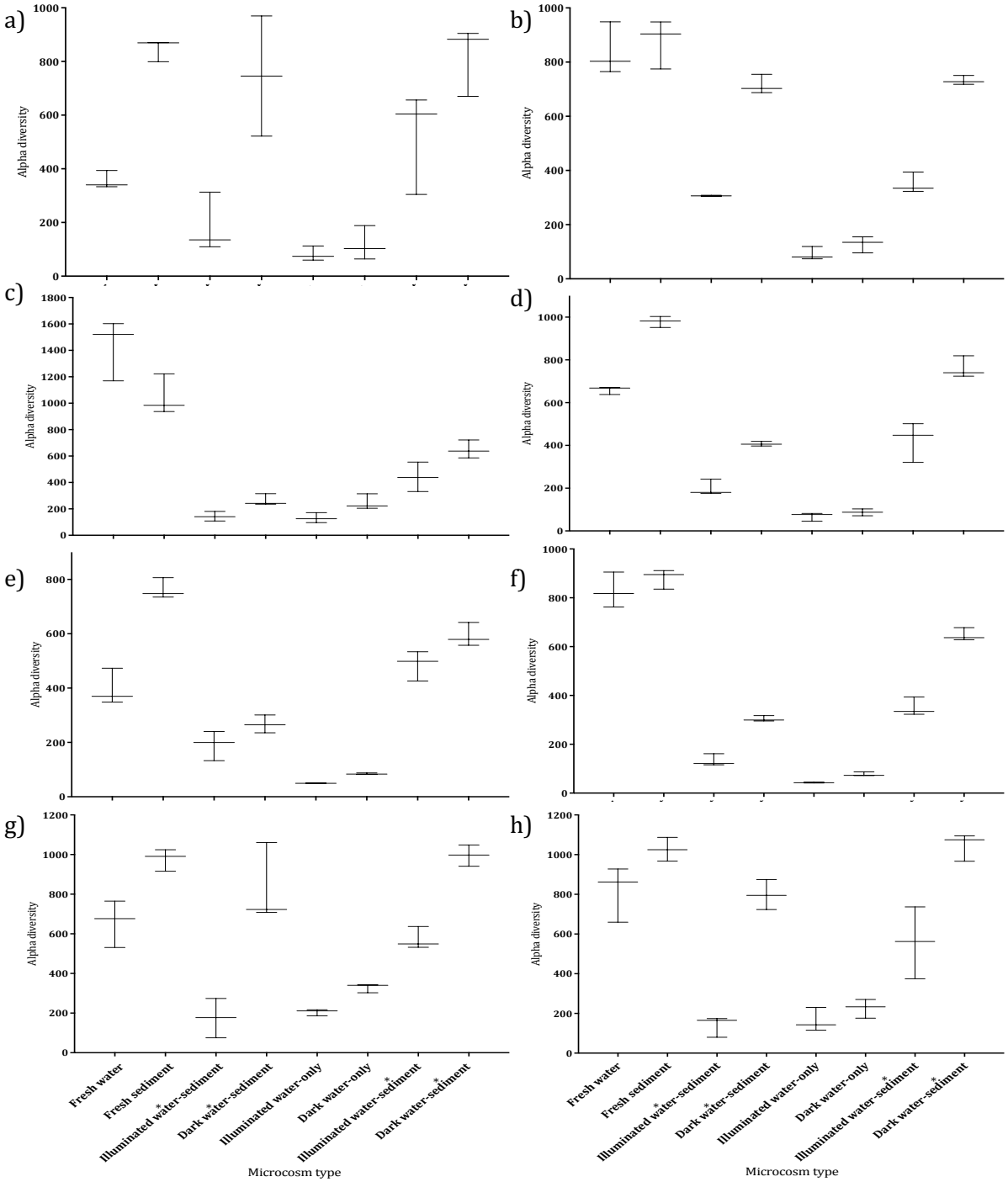

Figure I.13: Alpha diversity of bacterial communities in the different microcosm treatments across collection times. Fisher's α index was calculated from the observed bacterial species in fresh water and sediment, illuminated water-sediment, dark water-sediment, illuminated water-only, and dark water-only microcosms in summer 2014 (a), autumn 2014 (b), winter 2015 (c), spring 2015 (d), summer 2015 (e), autumn 2015 (f), winter 2016 (g), and spring 2016 (h). Whiskers show the minimum and maximum values, middle lines the median values, and * over *water* or *sediment* in the water-sediment systems indicates the sample type.

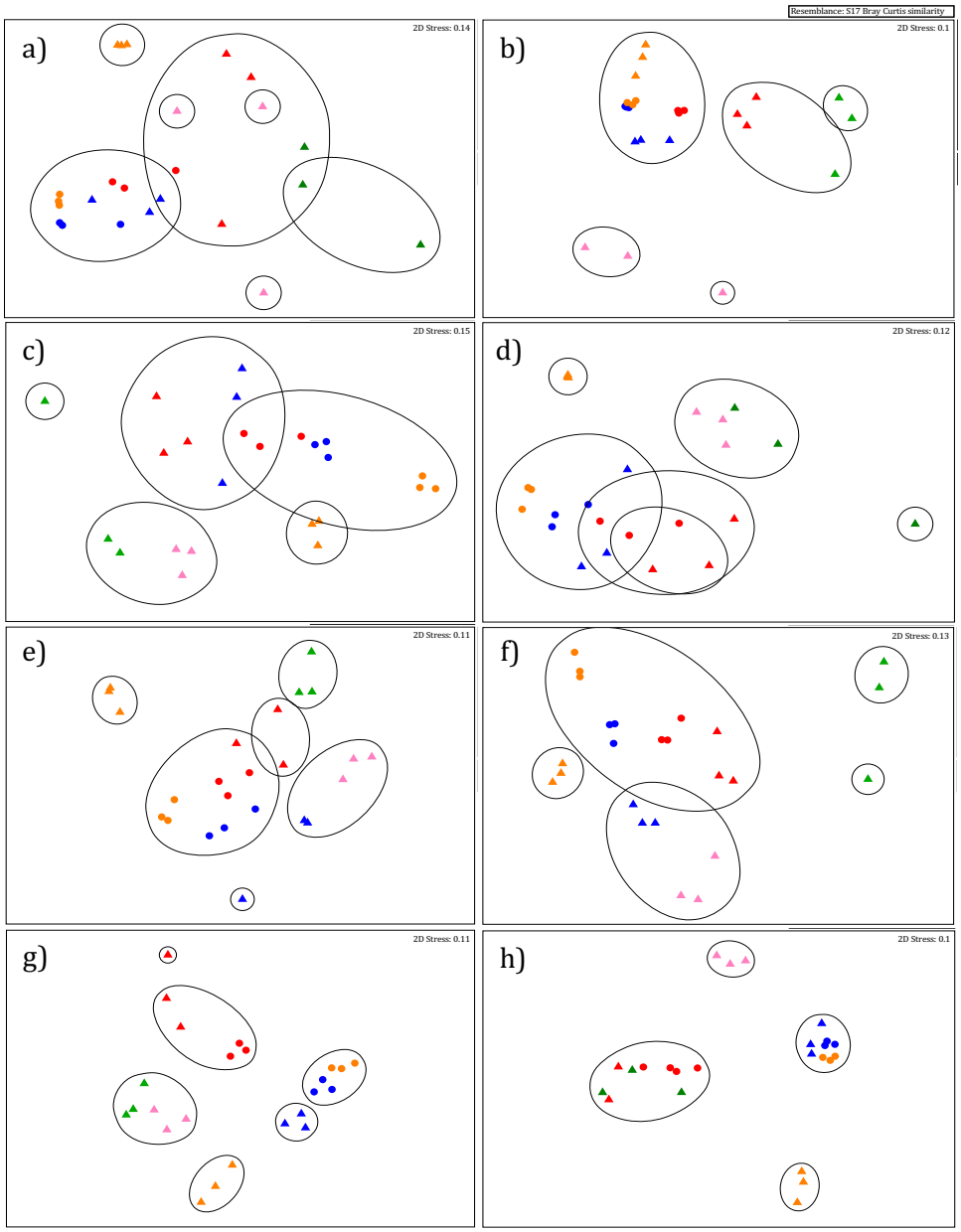

Figure I.14: Ordination plots from NMDS analysis of Bray Curtis similarities for bacterial communities between microcosms at each collection time. Water (triangles) and sediment (circles) were analysed from the sample site (orange), and illuminated water-sediment (red), dark water-sediment (blue), illuminated water-only (green), and dark water-only (pink) microcosms at 36 DAT. Analysis was carried out in summer 2014 (a), autumn 2014 (b), winter 2015 (c), spring 2015 (d), summer 2015 (e), autumn 2015 (f), winter 2016 (g), and spring 2016 (h). Black lines show 35 % ((a), (c), (f)), 40 % ((b), (d), (e)), or 50 % ((g), (h)) similarity.

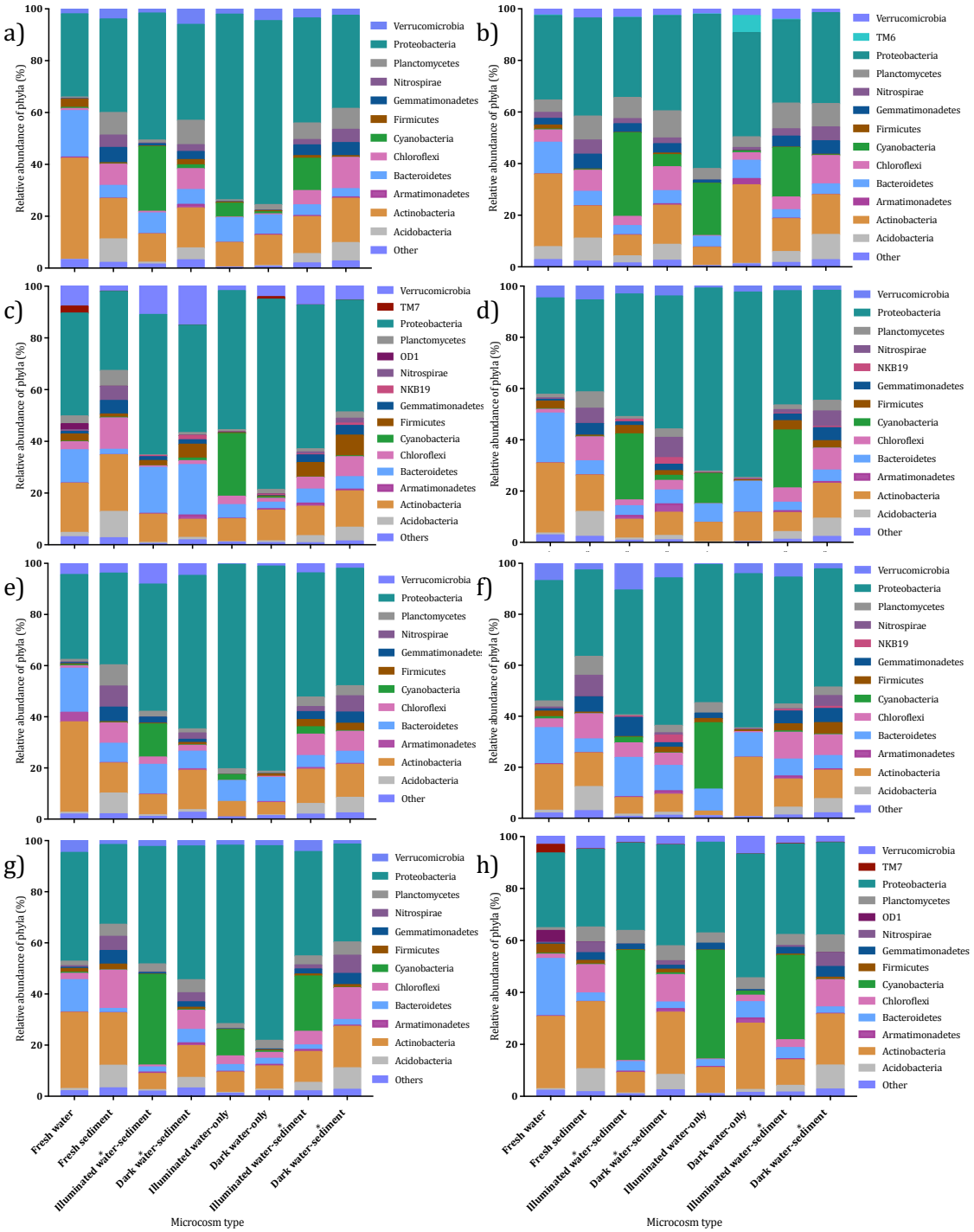

Figure I.15: Relative abundance of bacterial phyla between fresh samples and different microcosm treatments in water and sediment at each collection time. Different bacterial phyla are donated by different colours and phyla making up < 1 % of the relative abundance are listed under *other*. Analysis was carried out on fresh river samples and at 36 DAT on both water and sediment samples in summer 2014 (a), autumn 2014 (b), winter 2015 (c), spring 2015 (d), summer 2015 (e), autumn 2015 (f), winter 2016 (g), and spring 2016 (h). * over *water* or *sediment* in the water-sediment systems indicated the sample type.

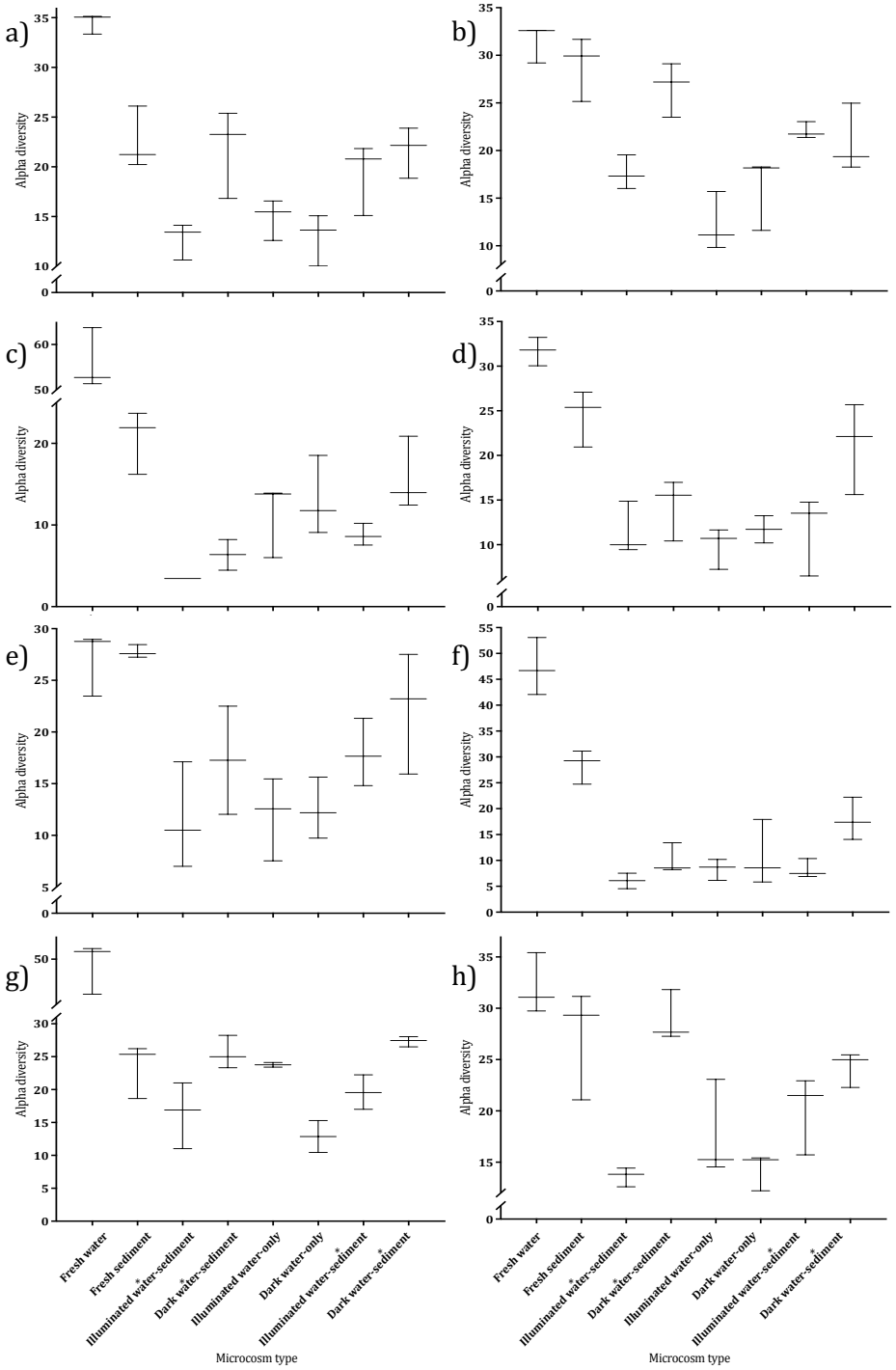

Figure I.16: Alpha diversity of phototrophic communities in the different microcosm treatments across collection times. Fisher's α index was calculated from the observed phototrophic species in fresh water and sediment, illuminated water-sediment, dark water-sediment, illuminated water-only, and dark water-only microcosms in summer 2014 (a), autumn 2014 (b), winter 2015 (c), spring 2015 (d), summer 2015 (e), autumn 2015 (f), winter 2016 (g), and spring 2016 (h). Whiskers show the minimum and maximum values, middle lines the median values, and * over *water* or *sediment* in the water-sediment systems indicates the sample type.

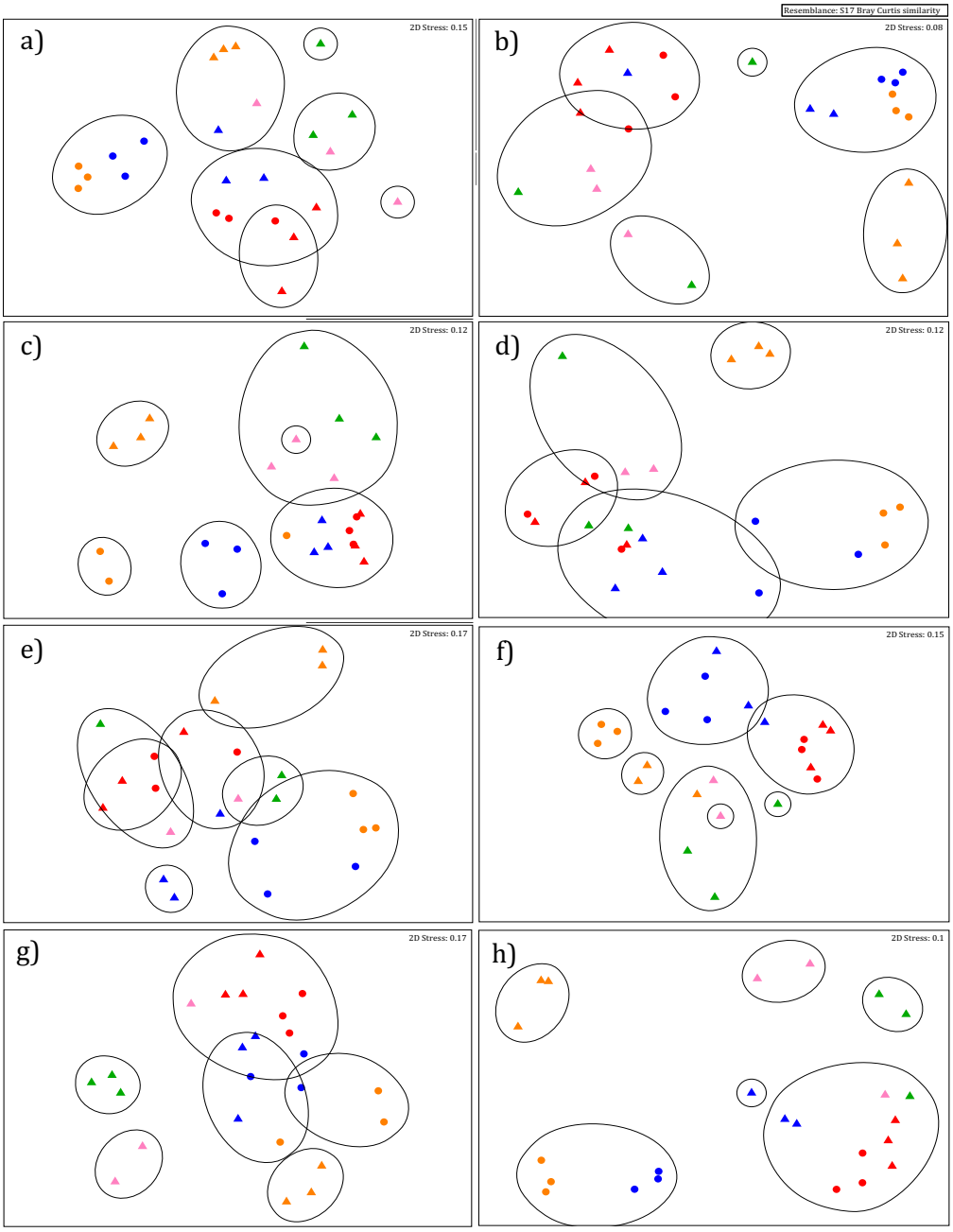

Figure I.17: Ordination plots from NMDS scaling analysis of Bray Curtis similarities for phototrophic communities between microcosms at each collection time. Water (triangles) and sediment (circles) were analysed from the sample site (orange), and illuminated water-sediment (red), dark water-sediment (blue), illuminated water-only (green), and dark water-only (pink) microcosms at 36 DAT. Analysis was carried out in summer 2014 (a), autumn 2014 (b), winter 2015 (c), spring 2015 (d), summer 2015 (e), autumn 2015 (f), winter 2016 (g), and spring 2016 (h). Black lines show 25 % (f), 30 % ((a), (c), (d), (e), (g)), or 50 % ((b), (h)) similarity.

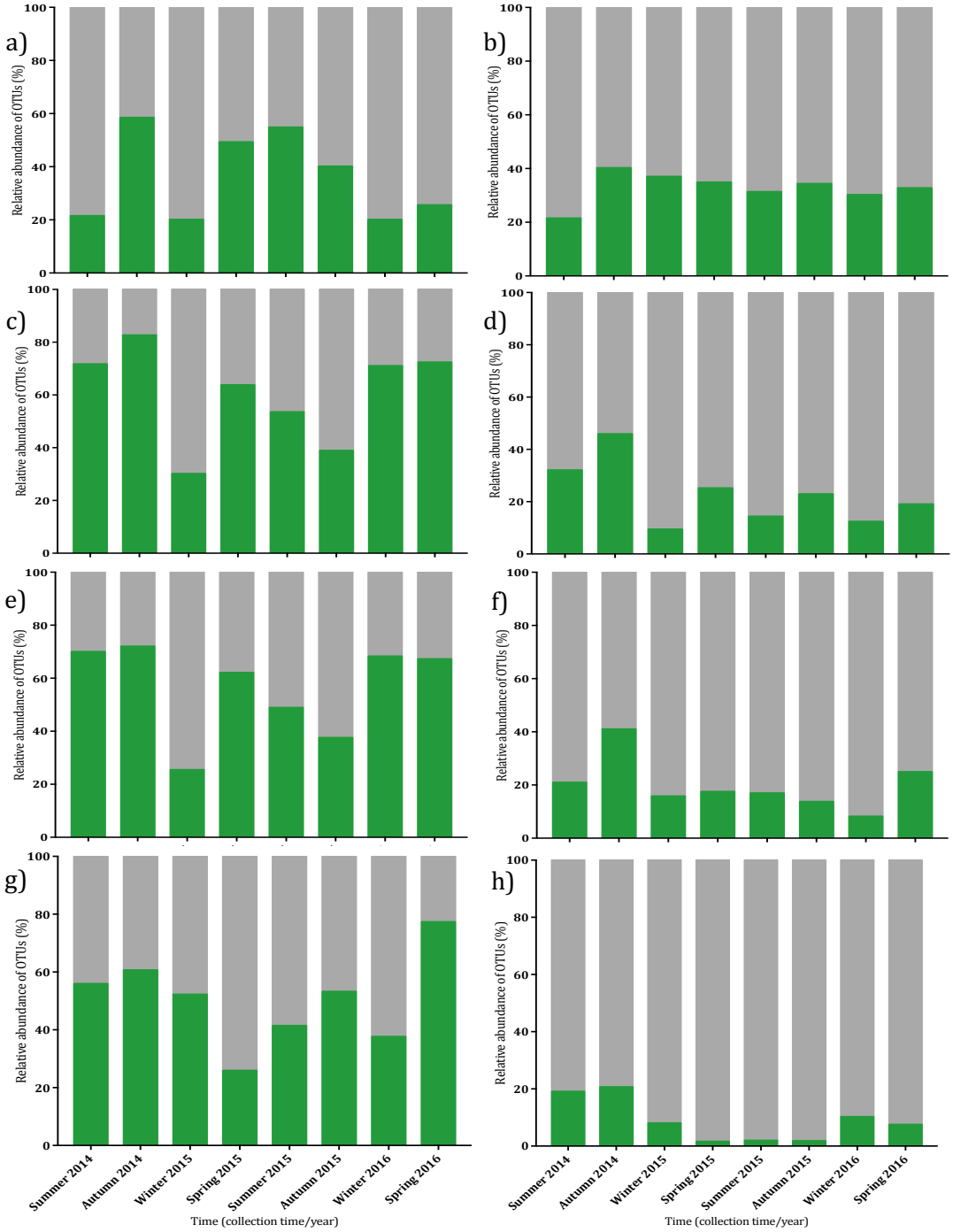

Figure I.18: Relative abundance of total phototrophic communities between collection times in fresh samples and microcosm treatments. Abundance of phototrophic (green) and non-phototrophic (grey) communities amplified from the 23S rRNA gene. Analysis was carried out on fresh river water (a), fresh sediment (b), water in illuminated water-sediment (c) and dark water-sediment (d) microcosms, sediment in illuminated water-sediment (e) and dark water-sediment (f) microcosms, and in illuminated water-only (g) and dark water-only (h) microcosms.

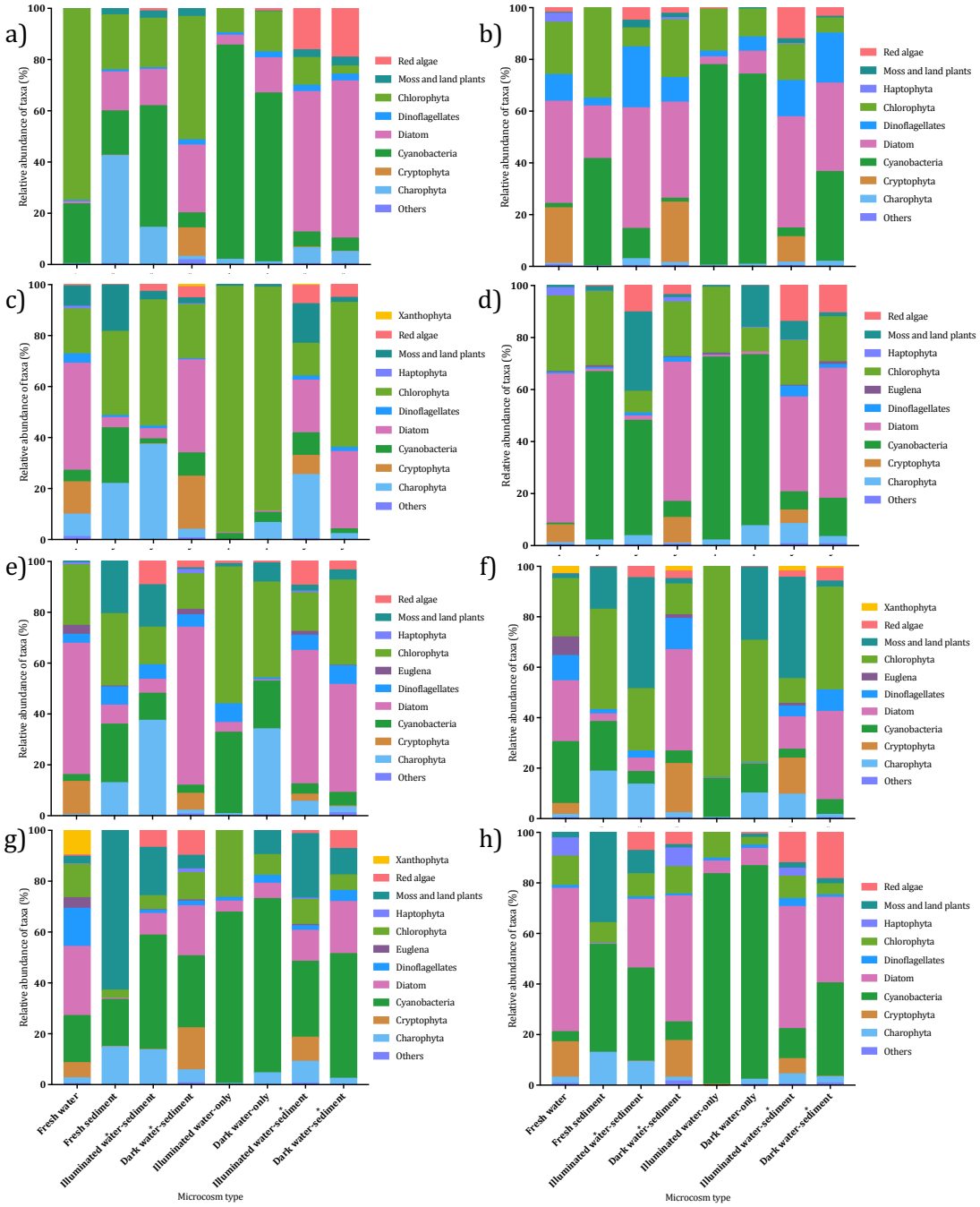

Figure I.19: Relative abundance of phototrophic taxa between fresh samples and different microcosm treatments at each collection time. Different phototrophic taxa are donated by different colours and taxa making up < 1 % of the relative abundance are listed under *other*. Analysis was carried out on fresh river samples and at 36 DAT on both water and sediment samples in summer 2014 (a), autumn 2014 (b), winter 2015 (c), spring 2015 (d), summer 2015 (e), autumn 2015 (f), winter 2016 (g), and spring 2016 (h). * over *water* or *sediment* in the water-sediment systems indicated the sample type.

Table I.6: Taxonomy and significance of OTUs significant to specific DegT50 rates. OTUs showing significance when split by DegT50 rate. Family level is given where possible, however, if not classified, the next taxonomic rank is stated. *(B)* and *(P)* next to the OTU number denotes whether it is amplified from the 16S or the 23S rRNA gene, respectively. Sequences can be found at the NCBI GenBank database with the given accession number.

OTU number	Genbank accession number	Phyla	Family (unless otherwise stated)	Significance
1217 (B)	MG947392	Proteobacteria	Gammaproteobacteria (class)	$p \leq 4.0 \times 10^{-5}$
2427 (B)	MG947393		Halomonadaceae	$p \leq 0.0012$
69 (B)	MG947394		Sphingomonadaceae	$p \leq 0.0077$
370 (B)	MG947395		Sinobacteraceae	$p \leq 0.0094$
2994 (B)	MG947396			$p \leq 0.0313$
10240 (B)	MG947397		Piscirickettsiaceae	$p \leq 0.0095$
4258 (B)	MG947398		Rhodospirillaceae	$p \leq 0.0005$
9316 (B)	MG947399		BD7-3 (order)	$p \leq 0.0173$
2290 (B)	MG947400	TM7	TM7-1 (class)	$p \leq 9.3 \times 10^{-5}$
3046 (B)	MG947401	Bacteroidetes	Saprospirales (order)	$p \leq 0.0447$
202 (B)	MG947402	Cyanobacteria	Pseudanabaenaceae	$p \leq 0.0028$
8333 (B)	MG947403			$p \leq 0.0147$
15 (P)	MG948642			$p \leq 0.0243$
84 (B)	MG947404		Xenococcaceae	$p \leq 0.0146$
809 (B)	MG947405			$p \leq 0.0485$
6064 (B)	MG947406		Synechococcaceae	$p \leq 0.0183$
1530 (P)	MG948643			$p \leq 0.0409$
607 (B)	MG947407	Actinobacteria	Actinomycetales (order)	$p \leq 0.0058$
995 (B)	MG947408	Acidobacteria	Holophagales (order)	$p \leq 0.0082$
1788 (B)	MG947409	Chlamydiae	Parachlamydiaceae	$p \leq 0.0384$
148 (P)	MG948644	Viridiplantae	Sphaeropleales	$p \leq 0.0203$
3317 (P)	MG948645		Pseudendoclonium	$p \leq 0.0309$
12 (P)	MG948646		Chlorellaceae	$p \leq 0.0195$

Table I.7: Relative abundance of OTUs significant to specific DegT50 rates. Relative abundance of OTUs showing significance while split by DegT50 rate. *(B)* and *(P)* next to the OTU number denotes whether it is amplified from the 16*S* or the 23S rRNA gene, respectively.

OTU number	Relative abundance in each DegT50 rate (%)			
	Fast	Medium	Medium-slow	Slow
1217 (B)	0.1	0	0.001	0
2427 (B)	0.04	0.001	0	0
69 (B)	1.1	0.004	0	0
370 (B)	0.2	0.03	0.03	0
2994 (B)	0.03	0.002	0	0
10240 (B)	0.03	0.0006	0	0
4258 (B)	0	0	0	0.04
9316 (B)	0	0	0.001	0.09
2290 (B)	0.03	0	0.003	0
3046 (B)	0	0.003	0	0.04
202 (B)	2.5	0.1	0.4	0.008
8333 (B)	0.3	0.01	0.03	0.003
15 (P)	8.6	0.8	0.6	0.3
84 (B)	1.7	0.06	0.3	0
809 (B)	0.07	0.001	0	0
6064 (B)	3.1	0.06	0.01	0
1530 (P)	5.4	0.5	0.2	0
607 (B)	0.5	0.03	0.04	0.006
995 (B)	0.06	0	0.001	0
1788 (B)	0.02	0	0.003	0
148 (P)	0.9	0.02	0	0
3317 (P)	0.3	0	0	0
12 (P)	0.2	10.3	3.8	31.6

Table I.8: Taxonomy and significance of OTUs significant to collection times with high mineralisation. OTUs showing significance in collection times with high mineralisation (summer 2014 and winter 2015). Family level is given where possible, however, if not classified, the next taxonomic rank is stated. *(B)* and *(P)* next to the OTU number denotes whether it is amplified from the 16S or the 23S rRNA gene, respectively. Sequences can be found at the NCBI GenBank database with the given accession number.

OTU number	GenBank accession number	Phyla	Family (unless otherwise stated)	Significance
175 (B)	MG947410	Proteobacteria	Sphingomonadaceae	$p \leq 6.1 \times 10^{-10}$
20496 (B)	MG947411		Sinobacteraceae	$p \leq 2.0 \times 10^{-5}$
395 (B)	MG947412			$p \leq 0.0002$
1672 (B)	MG947413		Xanthomonadaceae	$p \leq 3.8 \times 10^{-5}$
1875 (B)	MG947414		Chromatiaceae	$p \leq 0.0006$
19569 (B)	MG947415		Alphaproteobacteria (class)	$p \leq 0.0023$
2401 (B)	MG947416		Caulobacteraceae	$p \leq 0.0111$
84 (B)	MG947418	Cyanobacteria	Xenococcaceae	$p \leq 0.0001$
11264 (B)	MG947417			$p \leq 0.0007$
18 (P)	MG948647		Synechococcus	$p \leq 1.9 \times 10^{-9}$
51 (B)	MG947419	Bacteroidetes	Cyclobacteriaceae	$p \leq 0.001$
1127 (B)	MG947421		Saprospiraceae	$p \leq 1.3 \times 10^{-8}$
43 (B)	MG947420			$p \leq 1.5 \times 10^{-7}$
632 (B)	MG947422		Chitinophagaceae	$p \leq 0.0009$
17859 (B)	MG947423	Actinobacteria	Microbacteriaceae	$p \leq 1.5 \times 10^{-8}$
12298 (B)	MG947424			$p \leq 3.6 \times 10^{-5}$
4236 (B)	MG947425	Verrucomicrobia	Verrucomicrobiaceae	$p \leq 0.0076$
149 (B)	MG947426			$p \leq 0.0407$
258 (B)	MG947427	Firmicutes	Erysipelotrichaceae	$p \leq 0.0186$
115 (P)	MG948649	Viridiplantae	Chlamydomonadaceae	$p \leq 1.3 \times 10^{-5}$
3317 (P)	MG948651		Pseudendoclonium	$p \leq 8.0 \times 10^{-5}$
5014 (P)	MG948652		Chlorellales	$p \leq 3.3 \times 10^{-6}$
12 (P)	MG948648			$p \leq 3.6 \times 10^{-5}$
949 (P)	MG948650		Tracheophyta	$p \leq 2.1 \times 10^{-5}$

Table I.9: Relative abundance of OTUs significant at collection times with higher mineralisation. Relative abundance of OTUs showing significance when split by high (summer 2014 and winter 2015) and low mineralisation. *(B)* and *(P)* next to the OTU number denotes whether it is amplified from the 16S or the 23S rRNA gene, respectively.

Collection time with high mineralisation	OTU number	Relative abundance (%)	
		High mineralisation	Low mineralisation
Summer 2014	175 (B)	0.8	0.002
	20496 (B)	0.09	0.004
	395 (B)	0.4	0.04
	1672 (B)	0.01	0.0008
	1872 (B)	0.1	0.004
	84 (B)	1.2	0.07
	11264 (B)	0.1	0.007
	18 (P)	7.5	0.3
	51 (B)	1.1	0.05
	115 (P)	0.8	0.04
	3317 (P)	0.2	0.02
Winter 2015	1127 (B)	0.09	0
	43 (B)	2	0.05
	632 (B)	0.06	0.02
	17859 (B)	0.3	0.002
	12298 (B)	0.06	0.005
	19569 (B)	0.02	0.0008
	2401 (B)	0.1	0.01
	4236 (B)	0.4	0.02
	149 (B)	0.6	0.1
	258 (B)	0.5	0.08
	5014 (P)	1.8	0.3
	12 (P)	16.7	2.9
	949 (P)	0.2	0

APPENDIX II – CHAPTER 3 FURTHER METHODS AND SUPPORTING DATA

II.1 Example mass balance calculations

Radioactivity from the LSC analysis of each fraction – water (including acetonitrile rinse), sediment extract, NER, and NaOH traps – was summed together to determine the mass balance of each microcosm. Throughout the experiment, mass balance was above 90 % showing methodology was robust; example calculations can be seen in **Table II.1**. Average mass balance over the entire time course for each microcosm can be seen in **Figure II.1**.

Table II.1: Example mass balance calculations. Mass balance calculations taken from 43 DAT for each microcosm treatment.

Microcosm (DAT/ treatment)	Fraction (% of applied radioactivity)				
	Water	Sediment extract	NER in sediment	Mineralised	Total
43 Small	34.1	41.7	16.1	0.10	92.0
43 Medium	30.7	45.0	18.4	0.03	94.1
43 Large	43.3	54.1	2.9	0.01	100.3

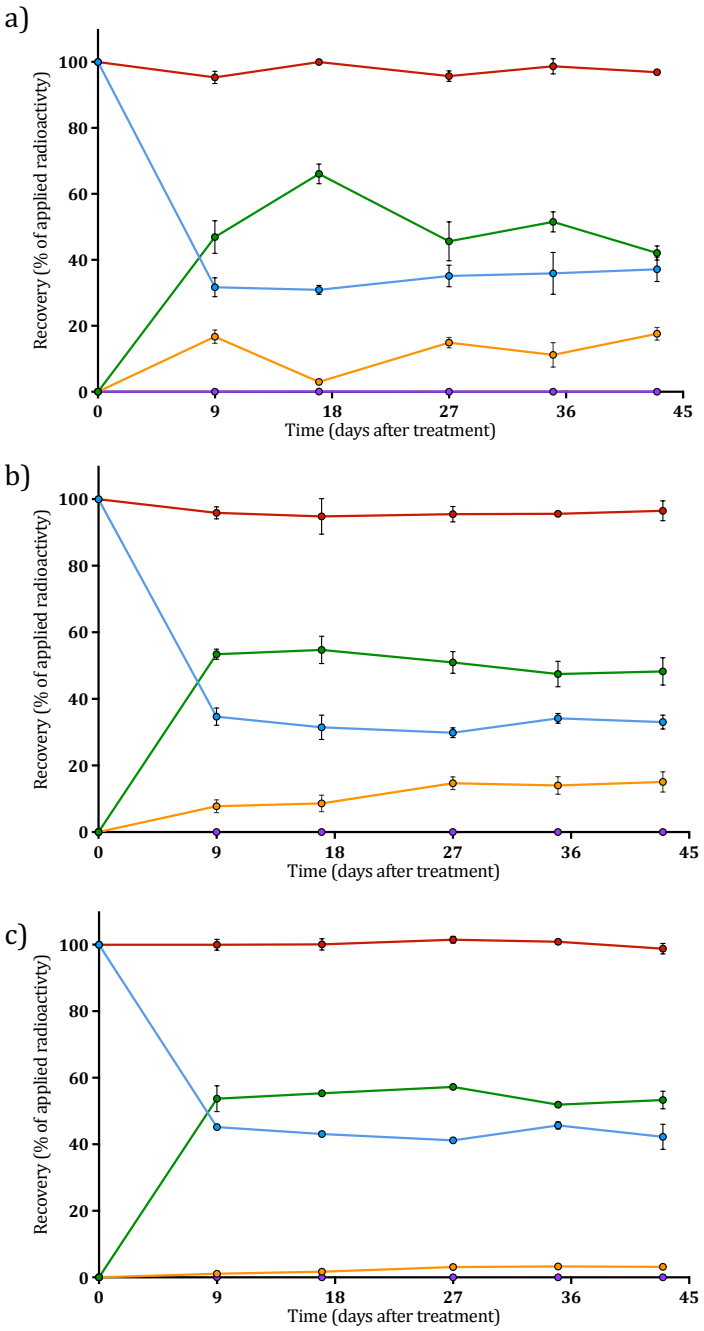

Figure II.1: Average mass balance in microcosm treatments over 43 days. Average mass balance in small (a), medium (b), and large (c) microcosms in the water (blue), sediment extract (green), sediment NER (orange), and mineralisation (purple), to make up the total mass balance (red). Error bars show ± standard deviation.

II.2 Confirmation of isopyrazam Thin-Layer Chromatography band

A non-radiolabelled isopyrazam standard was also applied to each TLC plate. After elution, the plate was visualized under UV (254 nm) light so that the standard could be seen and the band was marked. It was then measured how far the standard had run (measuring from the centre of the band) in relation to the solvent. From this, the retention factor (Rf) value was calculated. The isopyrazam band from the samples could be determined by corresponding it to the isopyrazam standard based on similar Rf values. Rf values were calculated using the formula below. The Rf values can be seen in **Table II.2**. The Rf value of the standards averaged 0.74 and the sample band suspected to be isopyrazam averaged 0.76. There are likely to be slight differences in Rf value depending on the conditions at the time of elution, however, this confirms that the band suspected to be isopyrazam was accurate. A comparison between the standard (**Fig. II.2.a**) and the isopyrazam band from the samples (**Fig. II.2.b**) can be seen in **Figure II.2**.

$$Rf = \text{distance travelled}_{\text{compound}} / \text{distance travelled}_{\text{solvent}}$$

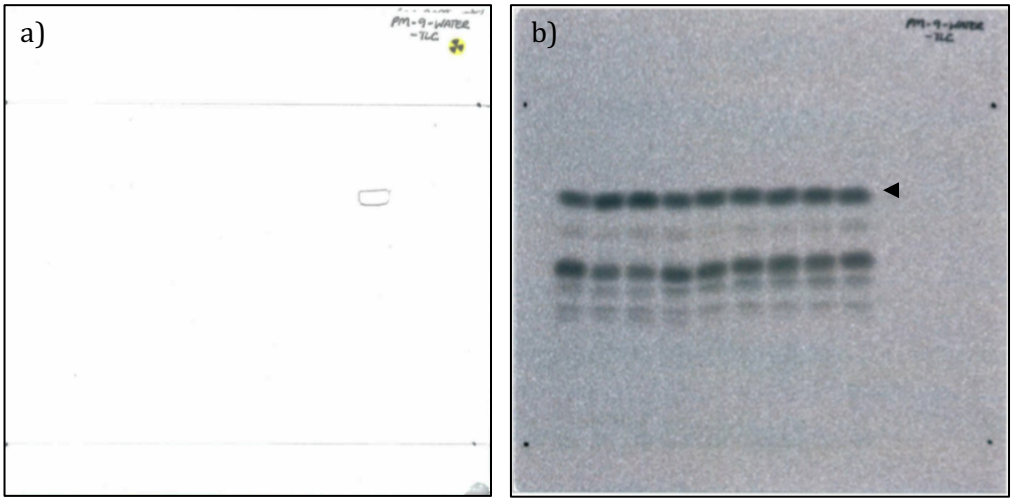

Figure II.2: Comparison between isopyrazam standard (a) and the band corresponding to isopyrazam in the radioluminogram (b). The isopyrazam standard band is marked on the plate after visualizing under UV light (a). From the Rf values, it was then determined which band in the radioluminogram corresponded to isopyrazam (b). The TLC plates are from 9 DAT and contain the water samples. The isopyrazam bands are marked by the black arrow in (b).

Table II.2: Rf values of both the isopyrazam standards and the band suspected to be isopyrazam from the samples. Rf values were calculated both for the isopyrazam standard and for the samples. *W* denotes TLC plates containing *water* samples and *S* those containing *sediment* samples. The difference in distance travelled between the isopyrazam standard and the samples is because the standard was measured directly from the marking on the TLC plate, whereas, the samples were measured from a printed copy of the radioluminograms. *SD* denotes *standard deviation*.

TLC plate (DAT/ sample type)	Isopyrazam standard			Samples		
	Solvent distance (cm)	Standard distance (cm)	Rf value	Solvent distance (cm)	Isopyrazam distance (cm)	Rf value
0 DAT W	13.90	9.85	0.71	11.50	8.20	0.71
9 DAT W	13.80	10.00	0.72	11.50	8.25	0.72
9 DAT S	14.00	10.55	0.75	13.00	9.90	0.76
17 DAT W	14.30	10.85	0.76	11.60	9.20	0.79
17 DAT S	14.20	10.80	0.76	11.40	9.05	0.79
27 DAT W	14.00	10.25	0.73	11.60	8.55	0.74
27 DAT S	14.00	10.60	0.76	11.70	8.75	0.75
35 DAT W	13.40	10.20	0.76	11.50	8.25	0.72
35 DAT S	14.00	10.25	0.73	11.70	9.05	0.77
43 DAT W1	14.00	10.25	0.73	11.50	8.65	0.75
34 DAT W2	14.00	10.55	0.75	11.80	8.90	0.75
43 DAT S1	14.10	10.15	0.72	12.30	9.85	0.80
43 DAT S2	14.00	10.15	0.73	11.80	9.00	0.76
Mean			0.74			0.76
SD			0.02			0.03

II.3 Thin-Layer Chromatography chromatogram example analysis

Analysis of the chromatograms from the radioluminograms were evaluated on AIDA software (version 3, Fujifilm, Japan). Each region was marked and then the background region subtracted to determine the percentage of the total region of interest in each band. Example chromatograms can be seen in **Figure II.3**.

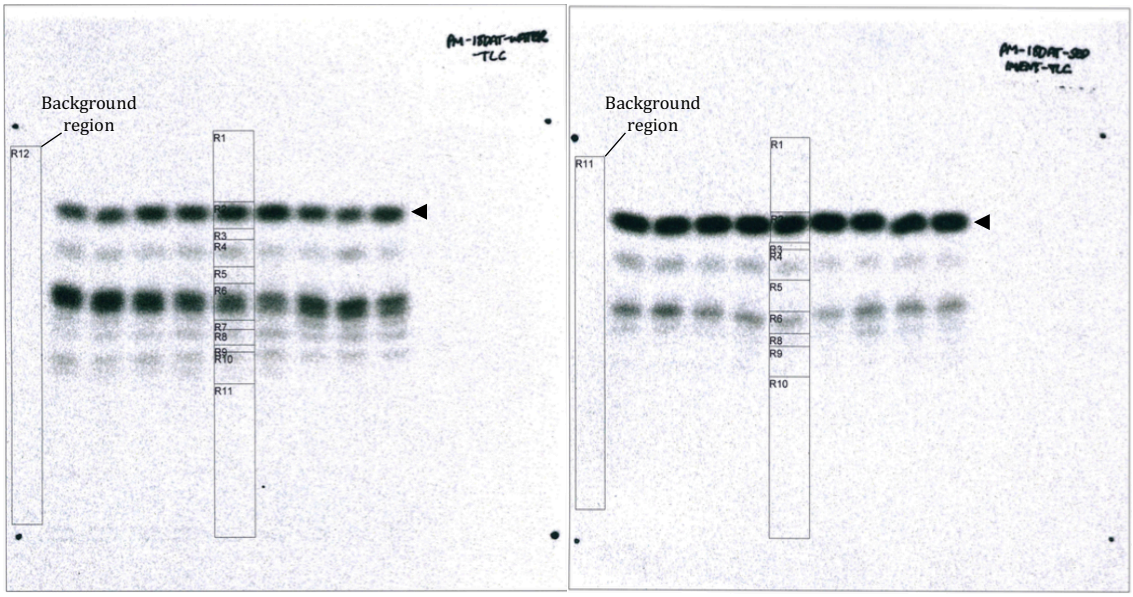

Figure II.3: Example chromatogram analysis in the water (a) and the sediment (b) fractions. Analysis for 18 DAT medium microcosms. The *R* corresponds to *region*. Region 12 and 11 are the background regions (annotated) in (a) and (b), respectively, and region 2 is the isopyrazam band (black arrow). Analysis was carried out on AIDA software (version 3, Fujifilm, Japan).

Table II.3: Region of interest percentages from chromatogram analysis in the water and the sediment fractions. Analysis for 18 DAT medium microcosms as in **Figure II.3**. Analysis was carried out on AIDA software (version 3, Fujifilm, Japan).

Region of interest (water)	Percentage (%) (water)	Region of interest (sediment)	Percentage (%) (sediment)
1	0.56	1	2.62
2	42.61	2	80.37
3	0.35	3	0.36
4	5.83	4	4.9
5	1.18	5	1.82
6	37.67	6	7.14
7	1.84	8	1.48
8	3.06	9	1.23
9	0.75	10	0.07
10	4.59	11	0
11	1.56		
12	0		

II.4 Supporting data

DegT50 and rate constant estimates met the acceptance requirements outlined in section 2.2.8 for SFO kinetic models. **Table II.4** outlines the requirement data for this experiment and examples of the SFO kinetic model fits can be seen in **Figure II.4**.

Table II.4: Kinetic model and acceptance requirements for DegT50 and rate constant estimates from CAKE for the microcosm treatments. SFO kinetic models were used for all data and key acceptance requirements are goodness of fit (χ^2), correlation between the observed and expected values (r^2), and the probability that the rate constant was significantly different to zero (Prob. > t). *Prob.* denotes *probability*, and k_1 denotes the first-order kinetics rate constant..

Microcosm scale	Model	χ^2 (%)	r^2	Prob. > t (k_1)
Small	SFO	12.0	0.8120	3.5×10^{-7}
Medium	SFO	9.27	0.8563	3.1×10^{-8}
Large	SFO	8.4	0.8993	9.1×10^{-9}

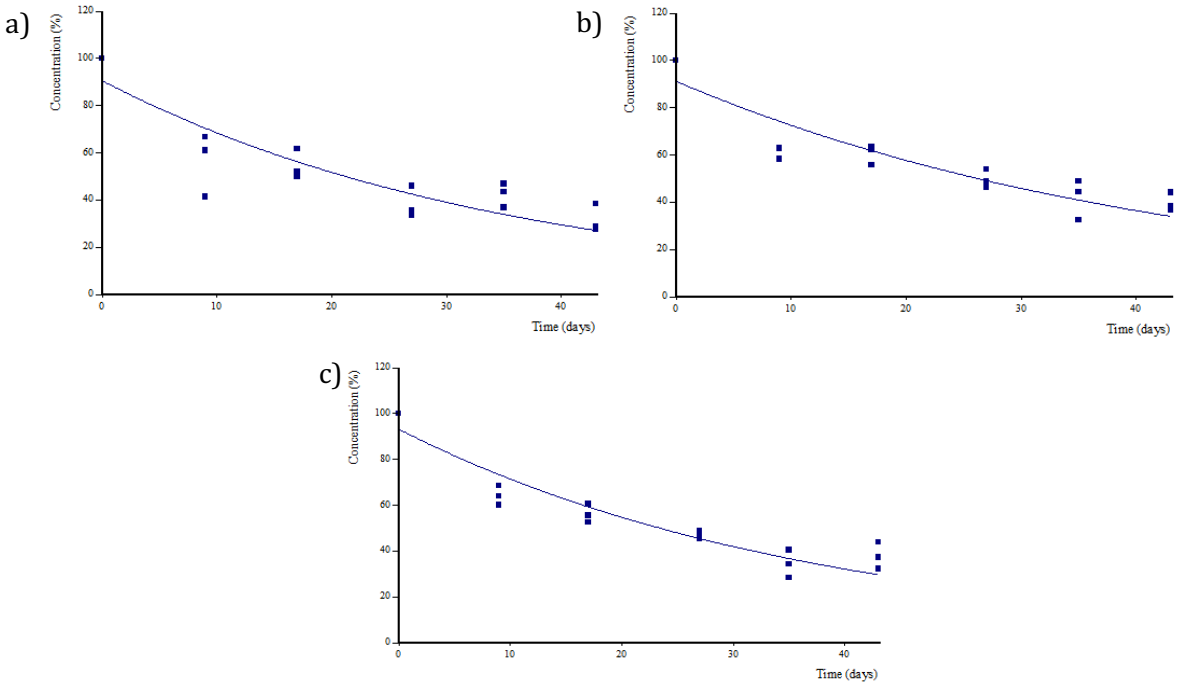

Figure I.4 Example kinetic model fits from CAKE analysis for each microcosm treatment. SFO kinetic model fits for the small (a), medium (b), and large (c) microcosm treatments. The dots are individual observations and the line shows the fit.

The raw sequence data (.fastq files) and metadata are stored at the NCBI SRA. They are recorded under the study accession number SRP132294.

In the water fraction, there was no significant impact on total abundance of phototrophic OTUs based on microcosms treatment ($p \leq 0.0793$, **Fig. II.5.a**). In the sediment fraction (**Fig. II.5.b**), however, there was a significant impact on phototrophic OTU abundance and microcosm treatment ($p \leq 0.0007$), with fresh samples having significantly less ($p \leq 0.01$, 15.3 %) compared to the microcosm samples at the end of the experiment (57.0 to 60.6 %).

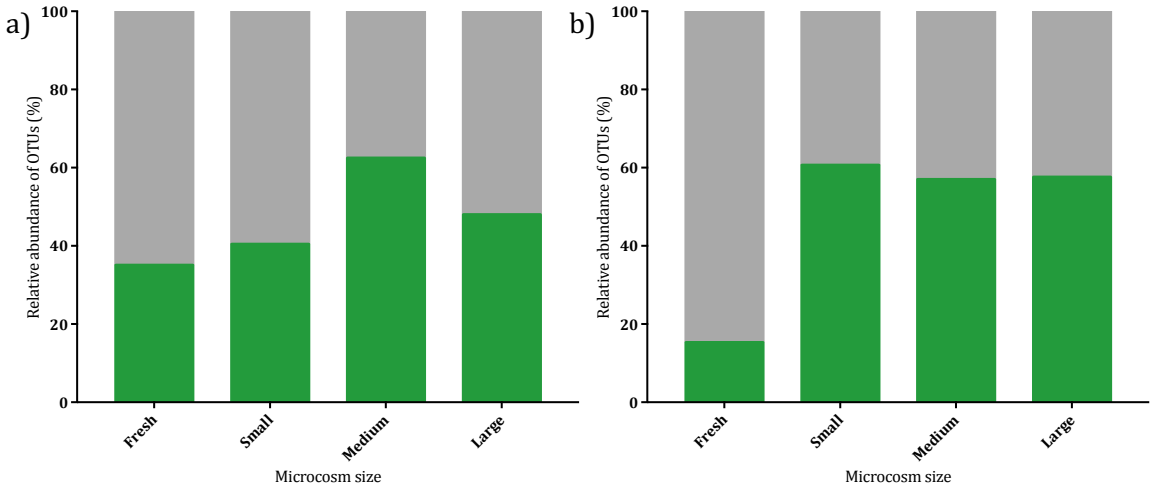

Figure II.5: Relative abundance of total phototrophic communities between microcosm treatments in the water (a) and the sediment (b). Abundance of phototrophic (green) and non-phototrophic (grey) communities amplified from the 23S rRNA gene. Analysis was carried out on water and sediment at the beginning of the experiment and at 43 DAT.

APPENDIX III – CHAPTER 4 FURTHER METHODS AND SUPPORTING DATA

III.1 Isopyrazam Liquid Chromatography-Mass Spectrometry methodology

A Poroshell 120 EC-C18 2.7 μm column (2.1 x 50 mm, Agilent Technologies, US) with a column temperature of 40 °C was used. Mobile phases consisted of 0.2 % acetic acid glacial (Fischer Scientific, UK) (mobile phase A) and acetonitrile (HPLC grade, Fischer Scientific, UK) (mobile phase B). The elution gradient can be seen in **Table III.1**.

The flow rate was 0.1 mL/min with an expected retention time of isopyrazam between 7 and 8 minutes. Chromatograms were analysed using DataAnalysis software (version 4.2, Brucker, US). Mass transitions of 360 *m/z* and 340 *m/z* were used (**Table III.2**) and monitoring carried out in Multiple Reaction Monitoring (MRM) mode (**Table III.3**).

Table III.1: LC-MS elution gradient of mobile phases in analysis of isopyrazam. Mobile phase A is 0.2 % acetic acid glacial and mobile phase B is acetonitrile.

Time in run (min)	Percentage of mobile phase A	Percentage of mobile phase B
0	85	15
5	5	95
6	5	95
7	85	15
10	85	15

Table III.2: LC-MS mass transitions. Monitoring for mass transitions of 360 *m/z* and 340 *m/z*.

Ion	Isolation mass (*m/z*)	Mass isolation width (*m/z*)	Fragmentation amplitude (V)
Precursor	360	5	1
Product	340	5	1

Table III.3: LC-MS monitoring. Monitoring was carried out in MRM mode.

Multiple Reaction Monitoring (MRM) conditions	
Capillary voltage	4500 V
Capillary exit	500 V
Ion Charge Control (ICC) target	80,000
Maximum Accumulation Time	150 ms
Collision gas	Helium
Collision energy	1.0 V

Isopyrazam standards were run on the LC-MS and analysed using DataAnalysis (version 4.2, Bruker, US) software. The isopyrazam retention time was between 7 and 8 minutes (**Fig. III.1**, peaks 6 and 10) and the two separate peaks corresponded to the different isomeric forms (*syn* and *anti*) of isopyrazam – these were analysed together for assessing the peak area. This confirmed that the peak seen in the samples at this time was also isopyrazam. Both water and sediment from each time point was analysed by LC-MS and examples can be seen in **Figure III.2**. Chromatograms were analysed using DataAnalysis software (version 4.2, Bruker, US) taking the total peak area of the peak corresponding to isopyrazam. If both isomer peaks were present, these were analysed together to give a total peak area, however, both peaks were not always present.

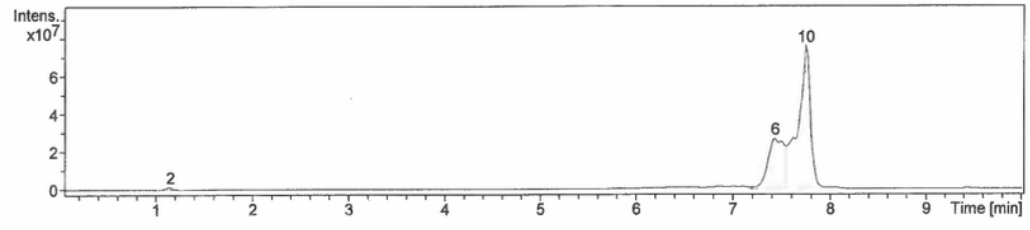

Figure III.1: Chromatogram of isopyrazam standard. Chromatograms were generated and analysed using DataAnalysis software (version 4.2, Bruker, US) and the isopyrazam retention time was between 7 and 8 minutes (peaks 6 and 10).

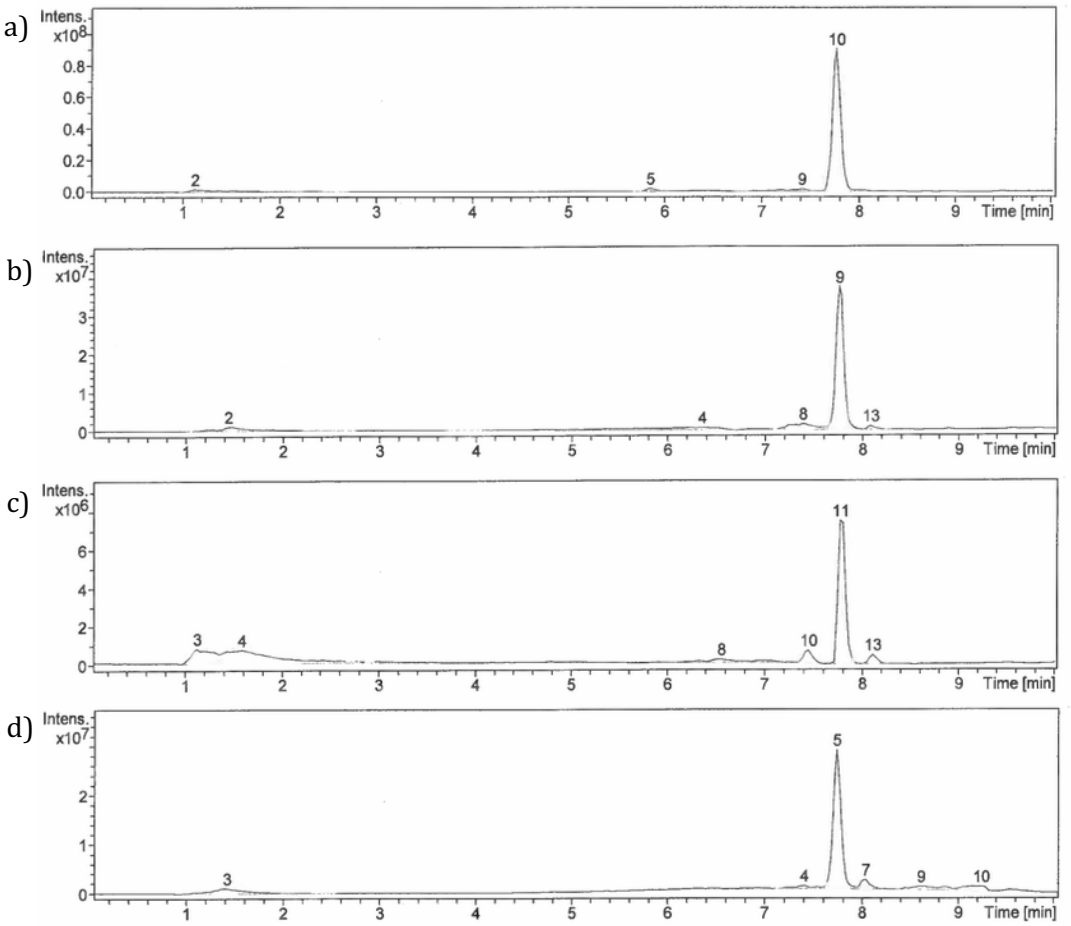

Figure III.2: Chromatogram of water (a) and sediment (b) from dark static microflumes at 10 DAT and water (c) and sediment (d) from dark flowing microflumes at 52 DAT. Chromatograms were generated and analysed using DataAnalysis software (version 4.2, Bruker, US) and the isopyrazam retention time was between 7 and 8 minutes. Both isomer peaks were analysed together (9 and 10 in (a), 8 and 9 in (b), 10 and 11 in (c), and 4 and 5 in (d)), if present, to give a total peak area.

III.2 Random sampling site locations

Sampling sites were marked on the frame of the flume at 20 cm intervals. Sampling locations for both the water and the sediment were randomly generated to avoid any bias in where the sample was taken from, however, areas near the flow inlet and outlet were avoided due to potential discrepancies from turbulence. The locations can be seen in **Figure III.3**. Duplicate sample sites at each sampling point can be seen in **Table III.4**.

-	I	J	K	L	M	N	O	P	-
-	A	B	C	D	E	F	G	H	-

Figure III.3: Location of random sampling sites. Sites were marked at 20 cm intervals so that random sampling could be allocated. 20 cm at either end was left un-sampled in case of discrepancies from turbulence.

Table III.4: Random sampling locations. Two water and sediment cores were taken at random locations at each time point.

DAT	Water sample site		Sediment sample site	
10	F	O	C	E
24	M	N	L	M
34	H	K	H	I
45	B	I	N	O
52	D	L	F	J

III.3 Environmental realism of the test conditions

Light intensity measured from the top of the length of the flume channel averaged 8.2 x 10^3 lux. This was lower than seen at the sample site for this experiment; however, was within the range of light intensities seen at the sample site while sampling for other experiments (Chapter 2), so was deemed realistic. For illuminated systems, fluorescent 70 W daylight bulbs (F70W/865 T8 6ft, Fusion Lamps, UK) were on for 16 hours with LEE226 filters (Transformation Tubes, UK) covering the bulbs, and the experiment was controlled at 20 ± 2 °C; the environmental realism of these conditions are discussed in Appendix I.1. For the water velocity, the velocity profile of the sampling site can be found in **Figure I.2** in Appendix I.1. Water velocity in the microflumes averaged at 30 mm/s and, given the water depth of the flumes (120 mm), the water velocity in the real environment should be almost double this. Despite this, the water velocity seen in the flumes is within the range that would be seen in nature at certain water depths, and the velocity is still higher compared to that in the static microflumes, enabling a comparison between the two treatments.

III.4 Evidence and tests to determine sorption to the system

Despite not being able to generate a mass balance, tests were carried out to ensure sorption to the system, especially the pipework, was not an issue. The amount of isopyrazam extracted from the system needed to be as true as possible without taking into account bound residues and mineralisation of the compound, which could not be obtained without using radiochemical. To investigate losses to the flume walls, tests were performed with river water and sediment in the same way as in Chapter 4, but for a shorter duration (14 days). Tests carried out prior to this in pure water without sediment showed that data was very variable if sampled within a few days of isopyrazam addition, as systems had not equilibrated. In this test, sampling points were therefore spread further apart at 3, 6, 10, and 14 DAT. Isopyrazam analysis was carried out as in Chapter 4. These tests proved that the methodology recovered an acceptable amount of isopyrazam (**Fig. III.4**). Although there was dissipation in the flowing systems, in the static systems about 100 % was recovered throughout the duration of the time course. This suggested that there was no issue with sorption to the sides of the microflumes. In addition, in small scale microcosm studies, sorption to the glassware was only an issue in water-only microcosms, whereas in water-sediment microcosms, sorption to the glassware only averaged 1.9 % (Chapter 3 –

acetonitrile rinse counted in the water fraction) due to preferential sorption to the sediment fraction. As the microflumes contained sediment, it was assumed that this would also be the case here.

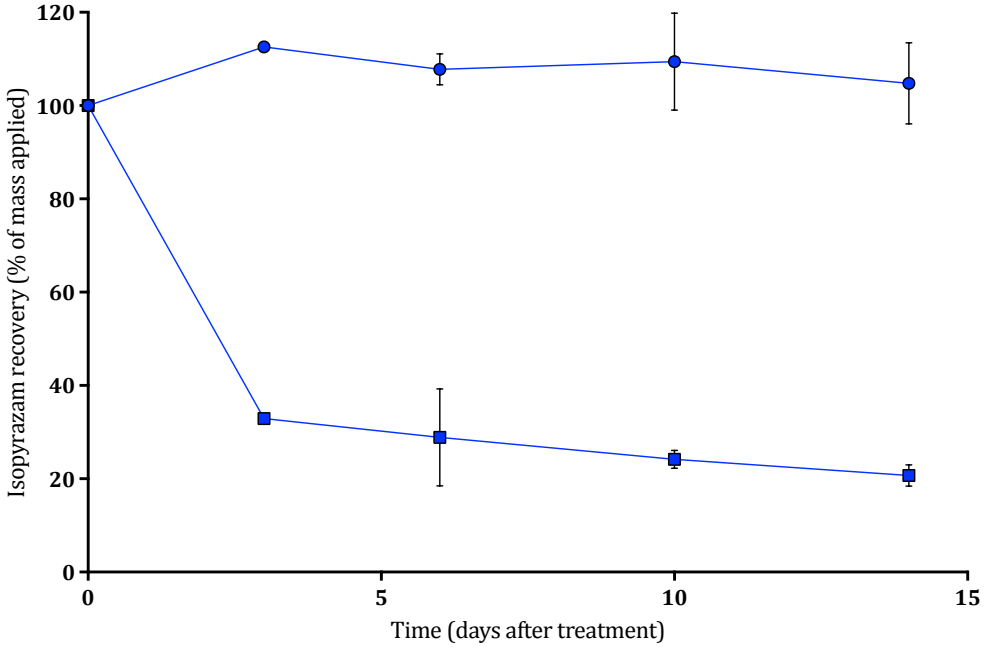

Figure III.4: Dissipation of isopyrazam in microflume test systems as a percentage of the mass originally applied. Dissipation of isopyrazam in dark static (blue circles) and dark flowing (blue squares) microflume test systems. Error bars show ± standard deviation.

At this stage, it was assumed that the dissipation in the flowing microflume systems could be due to sorption to the pipework. Therefore, tests were carried out using radiolabelled isopyrazam, used in Chapters 2 and 3, to determine sorption to plastic and stainless-steel piping. Sections of pipe were placed in water containing [^{14}C]-isopyrazam and the recovery from the water fraction assessed. At the end of the time course, glassware and pipes were also rinsed with acetonitrile (HPLC grade, Fischer Scientific, UK) and results were added to the recovery. For the plastic pipe, isopyrazam quickly dissipated from the water fraction (**Fig. III.5**) and, although the pipe rinse recovered 58.3 % of the compound, total recovery was only 64.2 %, suggesting that a proportion of the isopyrazam was irreversibly sorbed. For the stainless-steel pipe, however, losses of isopyrazam from the water were significantly lower and only 13.2 % was recovered from the pipework at the end of the experiment (total recovery of 119.1 %). As well as this, for this test, the pipe was fully submerged in the water rather than only the inside of the pipe being in contact with the

chemical, so sorption can be assumed to be less than in this test study. This showed that the stainless-steel pipe was the best choice for the microflume study and that sorption of isopyrazam to the material was minimal.

Finally, one last possibility in the flowing microflumes was sorption to the chiller, which was attached along the pipework. Without fully dismantling the chiller, which was not feasible, it was not possible to test the sorption to the inside of the chiller with radiochemical. To counteract this, tests were carried out to determine how long a single molecule of isopyrazam would spend in the pipework. This was carried out by injecting a dye, Rhodamine Water Tracing Dye (Sigma-Aldrich, US), at the microflume inlet and placing a Cyclops-7F™ Submersible Sensor (Turner Designs, US) at the outlet to determine the residence time in the pipework. A LogBox Data Logger (Novus, Brazil) was used to collect the data and this was imported and collected in LogChart II software (Novus, Brazil). It was determined that the dye re-emerged after 9.4 seconds (i.e. its residence time in both the pipework and the chiller itself) and, as detailed below, if the chiller made up 57.7 % of the pipework, then a single molecule only remained 5.4 seconds within the chiller. Because of this, it was assumed that even if there was some sorption to the chiller, due to the short residence time it should not contribute to the amount of sorption seen in the flowing systems and, therefore, it was assumed that this was true dissipation. As detailed above, sorption to the sediment was probably the main fate of the pesticide. In addition, in Chapter 4 there was also dissipation in the static systems, whereas in these preliminary tests there was very little, suggesting that in the actual test when under the light treatment and when incubated for longer, dissipation could occur – as recovery had previously been acceptable, it was assumed that the recovery generated in the experiment was real.

Surface area of the pipe work without the chiller

Total height (h) of pipe work = 335 cm

Radius (r) of pipe = 1.2 cm

Surface area of pipe = $2\pi rh + 2\pi r^2 = 2 * \pi * 1.2 * 335 + 2 * \pi * 1.44 =$ 2534.9 cm^2

Surface area of the chiller

Volume (v) of water that will fit into the chiller = 1982.5 cm^3

Radius (r) of chiller pipe = 1.15 cm

Height (h) of total chiller pipe = $v/\pi r^2$ = 1982.5 / π * 1.3225 = 477.2 cm

It is assumed that the chiller has a coiled pipe as the height is greater than the chiller.

Surface area of chiller pipe = $2\pi rh + 2\pi r^2$ = 2 * π * 1.15 * 477.2 + 2 * π * 1.3225 = <u>3456.4 cm²</u>

<u>Total surface area of pipe work including chiller</u>

2534.9 cm² + 3456.4 cm² = 5991.3 cm²

3456.4 cm² / 5991.3 cm² * 100 = <u>57.7 %</u>

<u>Residence time in the chiller</u>

Total residence time in the pipe work = 9.4 seconds

Chiller makes up 57.7 % of the total pipe work

9.4 second * 0.577 = <u>5.4 seconds</u>

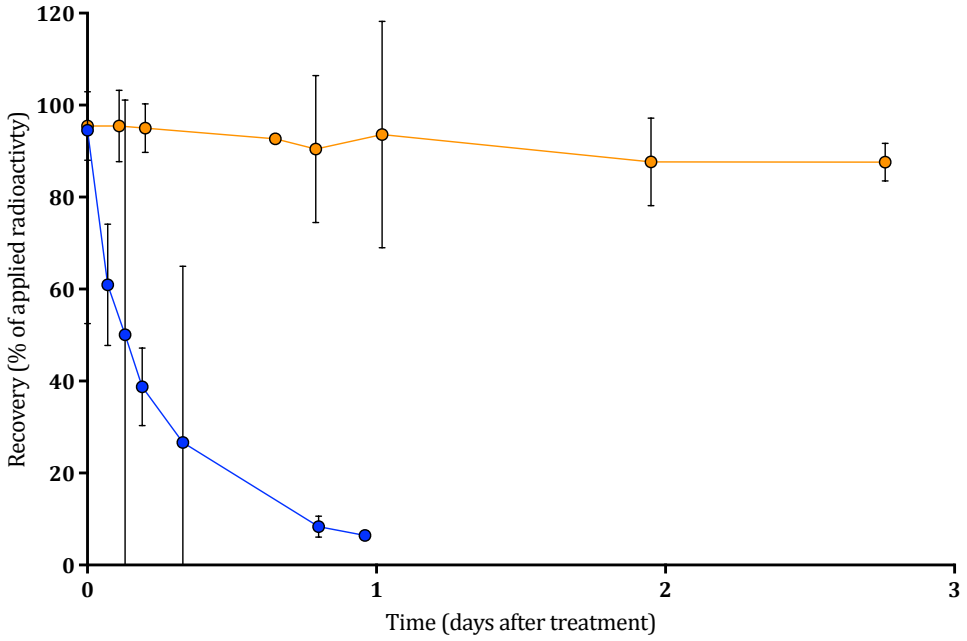

Figure III.5: Sorption of isopyrazam to different types of piping. Plastic (blue) and stainless steel (orange) piping was placed in water containing isopyrazam and the recovery from the water assessed to determine the amount sorbed to the pipework. Error bars show ± standard deviation.

III.5 Microflume system recovery example calculations

Example microflume system recovery calculations are from replicate 1 in the dark flowing microflume treatment at 52 DAT. Correction factors for the water and sediment samples extracted from the microflume were calculated to work out the proportion of sample taken from the entire system. Static microflume systems were 200 cm in length, so different calculations were used for these systems. At each time point, triplicate injections of standards were analysed on the LC-MS, and the averages used to create a standard curve (**Fig. III.6**). The equation of the line was used to determine the concentration of isopyrazam present in the samples. This and the correction factors were used to determine the total recovery of isopyrazam in the systems (**Tables III.5** to **III.7**). In this example, the equation of the standard curve is $y = 7 * 10^6 x$, so peak intensities from the LC-MS analysis of the water and sediment samples were divided by $7 * 10^6$ to determine the isopyrazam concentration in the samples.

Microflume system measurements

Width (w) of flowing microflume = 10 cm

Height (h) of flowing microflume = 20 cm

Length (l) of flowing microflume = 240 cm

Volume = whl = 10 cm * 20 cm * 240 cm

Volume = 48,000 cm^3 = 48 L

Isopyrazam addition to microflume system

Dark flowing microflume replicate 1 water volume = 32,364 cm^3

Expected mass added of isopyrazam for 0.1 mg/L = 3,200 µg

Actual mass added of isopyrazam from LC-MS analysis = 4,000 µg

Water sampling correction factor

Diameter of sampling device = 0.83 cm

Radius of sampling device = 0.42 cm

Radius^2 of sampling device = 0.17 cm^2

Surface area of sampling device = πr^2 = π * 0.17 = 0.54 cm^2

Length of microflume = 240 cm

Height of water = 10 cm

Surface area of water in the microflume = lh = 240 cm * 10 cm = 2,400 cm^2

Proportion of water in each sample = (0.54 cm^2 / 2400 cm^2) * 100 = 0.02 %

Correction factor for mass of isopyrazam recovered in each sample = 100 / 0.02 = **4,435.73**

Sediment sampling correction factor

Diameter of sampling device = 3.5 cm

Radius of sampling device = 1.75 cm

Radius^2 of sampling device = 3.06 cm^2

Surface area of sampling device = πr^2 = π * 3.06 = 9.62 cm^2

Length of microflume = 240 cm

Height of water = 10 cm

Surface area of sediment in the microflume = lh = 240 cm * 10 cm = 2,400 cm^2

Proportion of sediment in each sample = (9.62 cm^2 / 2400 cm^2) * 100 = 0.40 %

Correction factor for mass of isopyrazam recovered in each sample = 100 / 0.40 = **249.45**

Table III.5: Recovery calculations from the water fraction in dark flowing microflumes at 52 DAT. The recovery was calculated for dark flowing microflume replicate 1 at 52 DAT. To determine the sample concentration, peak intensities were divided by 7 * 10^6 from the equation of the linear trend line of the standard curve. The correction factor was also used to determine the total isopyrazam mass in the water of the microflume. *Conc.* is shorthand for *concentration*.

Sample weight (g)	Sample density (g/mL)	Sample volume (mL)	Peak intensity (AU)	Sample conc. (µg/L)	Average sample conc. (µg/L)	Sample mass (µg)	Microflume mass (µg)	Total in water fraction (%)
7.83	0.93	7.83 / 0.93 = 8.42	44196945	6.31	6.45	6.45 * 8.42 /1000 = 0.05	0.05 * 4,435.73 = 241.00	241.00 / 4,000 *100 = 6.00
			45521866	6.50				
			45800039	6.54				

Table III.6: Recovery calculations from the sediment fraction in dark flowing microflumes at 52 DAT. The recovery was calculated for dark flowing microflume replicate 1 at 52 DAT. To determine the sample concentration, peak intensities were divided by 7 * 10^6 from the equation of the linear trend line of the standard curve. The correction factor was also used to determine the total isopyrazam mass in the sediment of the microflume. *Conc.* is shorthand for *concentration*.

Sample weight (g)	Sample density (g/mL)	Sample volume (mL)	Peak intensity (AU)	Sample conc. (µg/L)	Average sample conc. (µg/L)	Sample mass (µg)	Microflume mass (µg)	Total in sediment fraction (%)
92.89	0.87	92.89 / 0.93 = 106.77	125031864 115299352 117163576	17.86 16.47 16.74	17.02	17.02 * 106.77 / 1000 = 1.82	1.82 * 249.45 = 453.40	453.40 / 4,000 *100 = 11.3

Table III.7: Total isopyrazam microflume recovery in dark flowing microflumes at 52 DAT. The total microflume recovery was calculated from the total recovery in both the water and the sediment fractions.

Total in water fraction (%)	Total in sediment fraction (%)	Total microflume recovery (%)
6.00	11.3	17.3

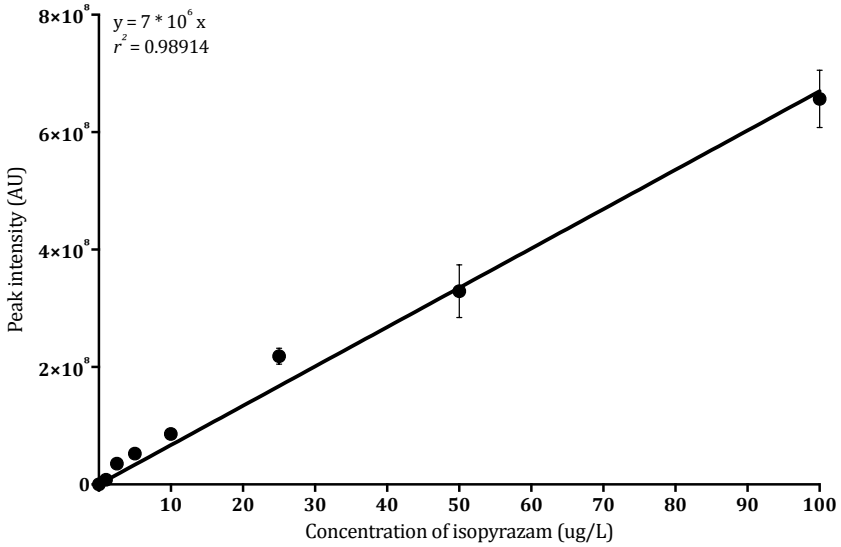

Figure III.6: Standard curve for isopyrazam standards. Isopyrazam standards were ran on the LC-MS to determine a standard curve. The equation was used to determine the concentration of isopyrazam in the water and sediment samples from the microflume systems. High r^2 values indicate a good fit of the linear trend line.

III.6 Supporting data

DT50 and rate constant estimates are outlined in section 2.2.8 for SFO kinetic models. The requirement data for this experiment is outlined in **Table III.8** and examples of the SFO kinetic model fits can be seen in **Figure III.7**.

Table III.8: Kinetic model and acceptance requirements for DT50 and rate constant estimates from CAKE for the microflume treatments. SFO kinetic models were used for all data and key acceptance requirements are goodness of fit (χ^2), correlation between the observed and expected values (r^2), and the probability that the rate constant was significantly different to zero (Prob. > t). * denotes values that have failed the acceptance requirements outlined in section 2.2.8, *Prob.* denotes *probability*, and k_1 denotes that degradation was according to first-order kinetics.

Microflume treatment	Model	χ^2 (%)	r^2	Prob. > t (k_1)
Dark static	SFO	15.9 *	0.6083 *	1.2×10^{-4}
Dark flowing	SFO	17.6 *	0.8543	5.4×10^{-7}
Illuminated static	SFO	13.9	0.9108	1.2×10^{-8}
Illuminated flowing	SFO	20.4 *	0.8663	5.1×10^{-7}

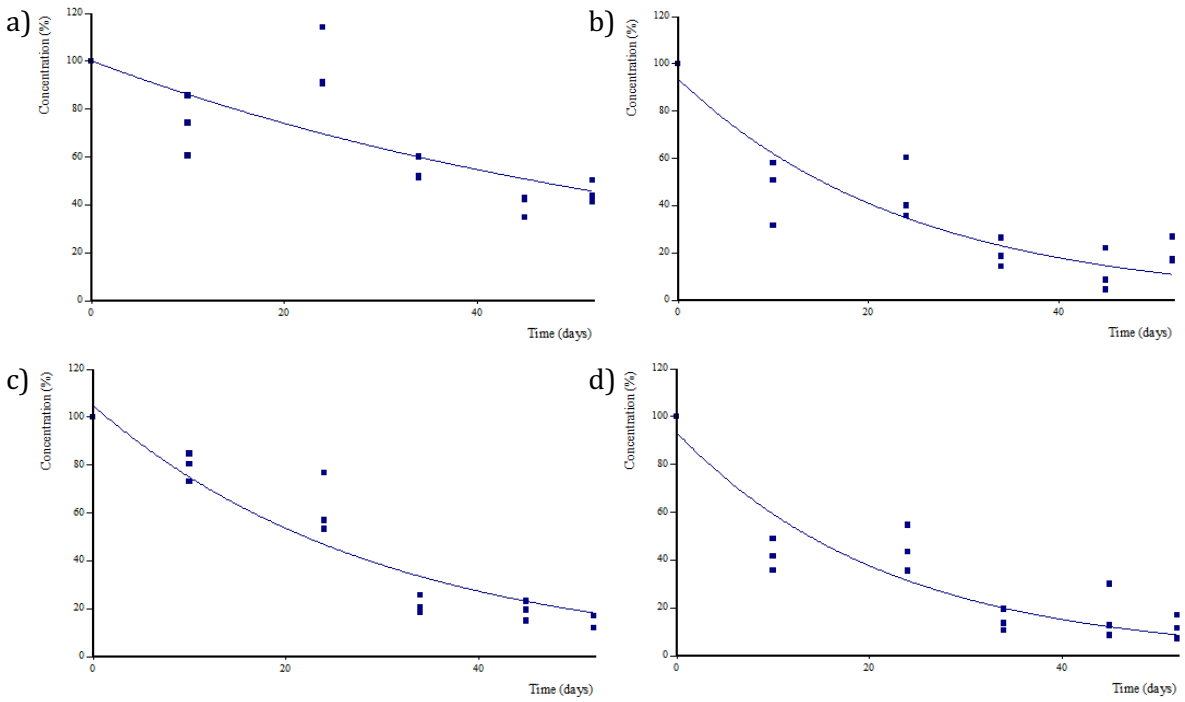

Figure III.7: Example kinetic model fits from CAKE analysis for each microflume treatment. SFO kinetic model fits for dark static (a), dark flowing (b), illuminated static (c), and illuminated flowing (d) microflume treatments. The dots are individual observations and the line shows the fit.

There was a significant impact of microflume treatment on water pH in the microflumes ($p \leq 0.0217$, **Fig. III.8**), with dark flowing systems having a slightly lower pH, fluctuating between 6.9 and 7.9. This was only significantly different to dark static microflumes, and the pH in the other microflumes fluctuated between 7.4 and 8.2 across the time course. Although statistical tests showed significance, pH fluctuated in all microflume treatments, which is evident from the large standard deviation (**Fig. III.8**), and there were no clear links to suggest that treatment influenced water pH.

There was a significant impact of microflume treatment on PO_4 concentration in the water ($p \leq 0.05$, **Fig. III.9**). Dark static microflumes had significantly higher PO_4 concentrations compared to illuminated static ($p \leq 0.05$) and illuminated flowing ($p \leq 0.01$) systems, increasing to 1.8 mg/L by 34 DAT, although the concentration did decrease again by 52 DAT. In both illuminated systems, PO_4 concentration was low throughout the time course at around 2.7 mg/L, however, dark flowing systems had slightly higher levels of

around 4.7 mg/L after 24 DAT. Despite this, the other microflumes were not significantly different to one another.

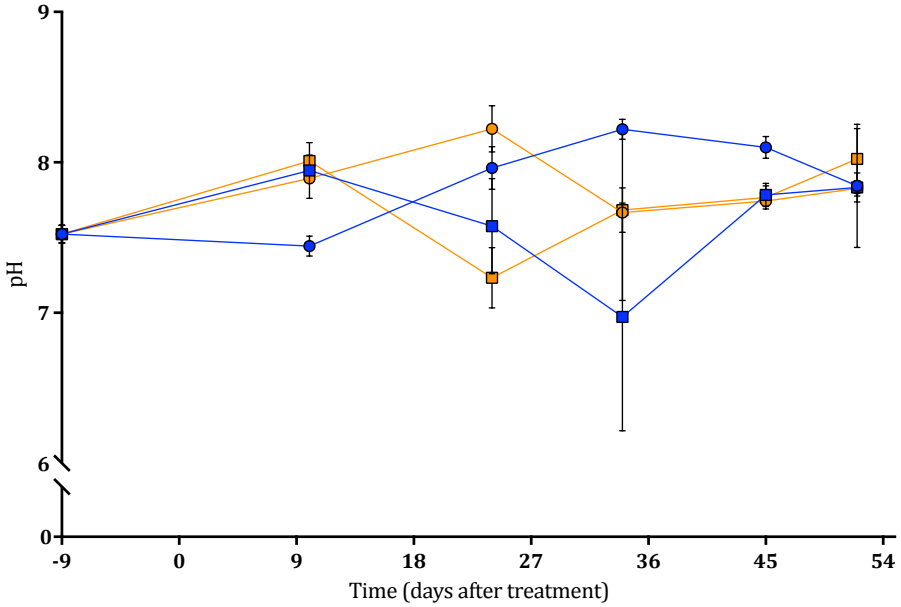

Figure III.8: pH of water in microflume systems. The pH of the water was measured at each time point in dark static (blue circles), dark flowing (blue squares), illuminated static (orange circles), and illuminated flowing (orange squares) microflume systems. Error bars show ± standard deviation.

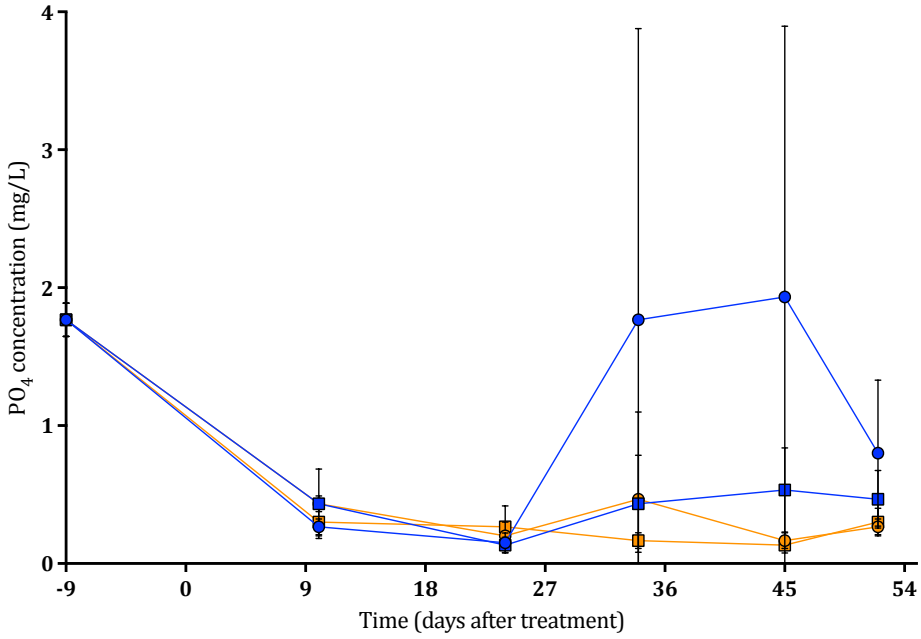

Figure III.9: Water concentration of PO_4 in microflume systems. PO_4 concentration of the water was measured at each time point in dark static (blue circles), dark flowing (blue squares), illuminated static (orange circles), and illuminated flowing (orange squares) microflume systems. Error bars show ± standard deviation.

Microflume treatment did not have a significant impact overall on the concentration of bacteria in the water fraction (**Fig. III.10**). There was an increase in all systems by 9 DAT, but this then decreased in both illuminated systems. In dark flowing microflumes, this increase continued to 24 DAT but then decreased, and by 45 DAT illuminated static, dark flowing, and illuminated flowing microflumes all had a similar bacteria water concentration of around 33.6 CFU/µL. In dark static microflumes, there was a greater increase of bacteria, reaching 1.2 x 10^5 CFU/µL by 24 DAT, then concentrations slowly decreased.

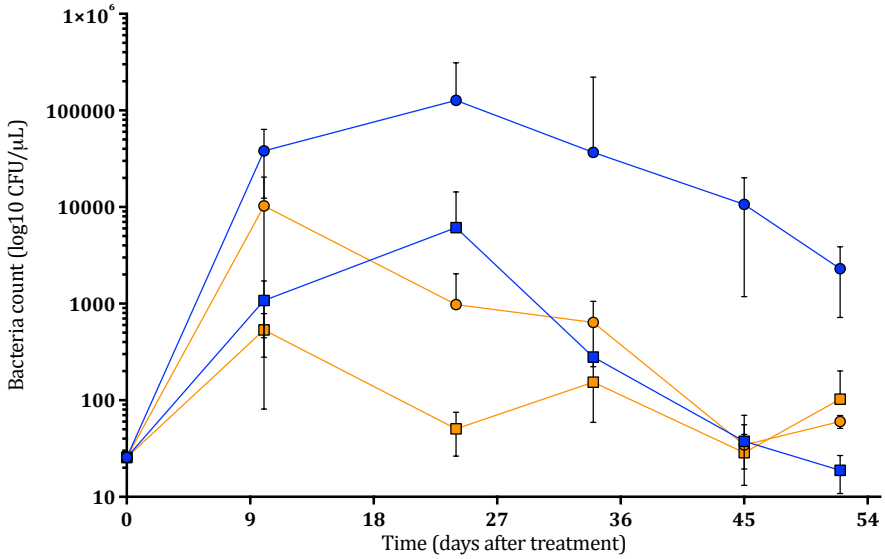

Figure III.10: Concentration of bacteria in the water of microflume systems. Bacteria concentration of the water was analysed using R2A agar at each time point in dark static (blue circles), dark flowing (blue squares), illuminated static (orange circles), and illuminated flowing (orange squares) microflume systems. Error bars show ± standard deviation.

The raw sequence data (.fastq files) and metadata are stored at the NCBI SRA. They are recorded under the study accession number SRP132456. Sequences for significant OTUs are stored at the NCBI GenBank database and accession numbers are given in **Table III.9**.

There was a significant difference between microflume treatments and the total abundance of phototrophic OTUs amplified from the 23S rRNA gene in both the water ($p \leq 0.0106$, **Fig. III.11.a**) and the sediment ($p \leq 0.0001$, **Fig. III.11.b**) fractions. In the water fraction, there was higher abundances in fresh (43.4 %) and illuminated static microflumes (49.8 %), with the latter being statistically significant compared to dark flowing microflumes ($p \leq 0.05$, 13.8 %). In the sediment fraction (**Fig. III.11.b**), illuminated static ($p \leq 0.0001$,

61.4 %) and illuminated flowing ($p \leq 0.05$, 46.4 %) microflumes had a significantly higher phototrophic relative abundance compared to fresh and dark microflume samples. Illuminated static microflumes also had a significantly higher ($p \leq 0.01$) relative abundance compared to illuminated flowing microflumes.

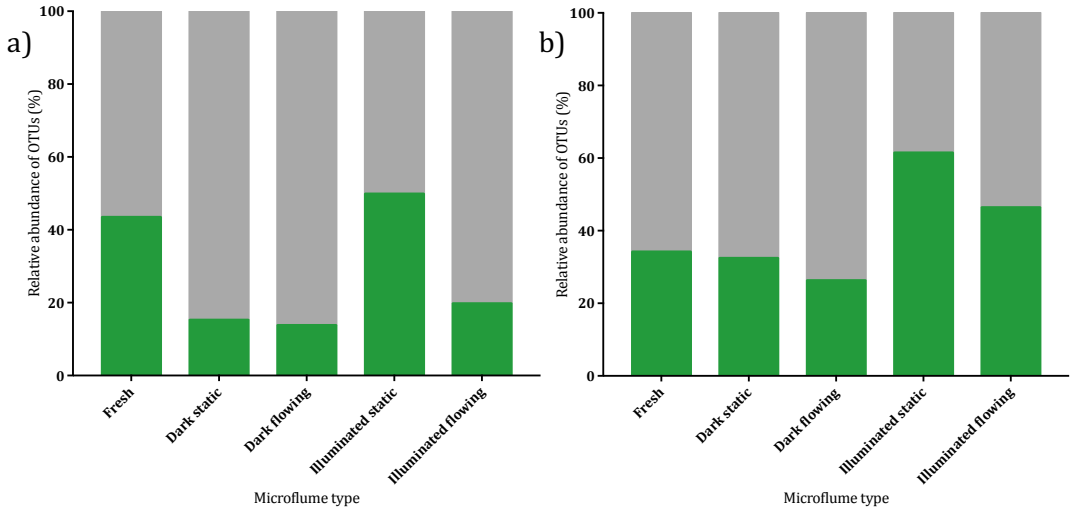

Figure III.11: Relative abundance of total phototrophic communities between microflume systems in the water (a) and the sediment (b). Abundance of phototrophic (green) and non-phototrophic (grey) communities amplified from the 23S rRNA gene. Analysis was carried out on water and sediment at the beginning of the experiment and at 52 DAT.

Multiple OTUs were described as being attributed to specific microflume treatments. The lowest taxonomic classification and the relative abundances in each treatment can be found in **Table III.9**.

Table III.9: Relative abundance of OTUs and their lowest taxonomic classification in microflume treatments. *B*, *P*, and *E* determines whether the OTU is *bacterial*, *phototrophic*, or *eukaryotic*, respectively. The letters *o*, *f*, *g*, and *s* determines whether the classification is *order*, *family*, *genus*, or *species*, respectively. The microflume treatments are denoted by *DS*, *DF*, *IS*, and *IF* for *dark static*, *dark flowing*, *illuminated static*, and *illuminated flowing*, respectively. Sequences can be found at the NCBI GenBank database with the given accession number.

OTU number	GenBank accession number	Lowest taxonomic classification	Relative abundance of OTU (%)			
			DS	DF	IS	IF
1013 (B)	MG947428	GZKB119 (f)	0.07	0.0	0.0	0.0
1049 (B)	MG947429	PL-11B10 (o)	0.1	0.0	0.003	0.0
1025 (P)	MG948654	Caryophyllaceae (f)	0.07	0.003	0.0	0.0
981 (P)	MG948653	Brassicaceae (f)	0.05	0.0	0.0	0.0
775 (E)	MG920570	*Brassica rapa* (g,s)	0.06	0.0	0.0	0.0

APPENDIX IV – DNA ISOLATION AND QUANTIFICATION METHODOLOGY

Isolation and quantification of DNA from water and sediment samples was carried out in Chapters 2 to 4. The methodology used throughout the experiments will be detailed below.

IV.1 DNA isolation

Water samples were filtered on Whatman 0.2 μm pore size and 47 mm diameter Anodisc filters (GE Healthcare, UK) in Chapters 2 and 3, and 0.2 μm pore size and 47 mm diameter PES filters (Sartorius Stedim Biotech, Germany) in Chapter 4. Filters and sediment were frozen at -80 °C until use. FastDNA™ SPIN Kit for Soil (MP Biomedicals, US) and the FastPrep® Instrument (MP Biomedicals, US) were used to isolate DNA according to the manufacturer's protocol. All reagents and tubes mentioned in this section were supplied with the above kit. All centrifuge steps were performed at 14,000 x *g*.

The water filters or 500 mg of thawed sediment were added to a Lysing Matrix E tube and 978 μL sodium phosphate buffer and 122 μL MT buffer were added to it. The samples were then homogenized in the FastPrep® for 40 seconds at a speed setting of 6.0. Samples were centrifuged for 10 minutes to pellet the debris and the supernatant transferred to a clean 2 mL microcentrifuge tube. To the samples, 250 μL of Protein Precipitation Solution (PPS) was added, and then the tubes were inverted by hand 10 times to mix. Samples were centrifuged for 5 minutes to pellet the precipitate and then supernatant was transferred to a clean 15 mL tube. The binding matrix was re-suspended and 1 mL was added to the supernatant in the 15 mL tubes. These were placed on a rotary shaker for 2 minutes to allow DNA binding, and then placed in the rack to allow the silica matrix to settle for 3 minutes.

500 μL was removed and discarded from the samples and the binding matrix was re-suspended in the remaining supernatant. 750 μL of the supernatant was added to a SPIN™ Filter and centrifuged for 1 minute. The catch tube was emptied and this was repeated with the remaining 750 μL of supernatant. The remaining pellet in the matrix was re-suspended by adding 500 μL SEWS, using the force of the liquid from the pipette tip. Samples were

centrifuged for 1 minute and the catch tube emptied, then without any addition of liquid, samples were centrifuged again for 2 minutes to allow the matrix to dry from any residual wash. The catch tube was discarded and replaced with a new, clean catch tube.

The SPIN™ Filter was allowed to air dry for 10 minutes at room temperature and then the binding matrix was gently re-suspended by adding 60 µL of DNase/Pyrogen-Free Water (DES), which had been heated at 55 °C for 5 minutes prior to use. Samples were centrifuged for 1 minute to bring the eluted DNA into the clean catch tube.

IV.2 DNA quantification

DNA samples were quantitated using the Qubit® 2.0 (Invitrogen, US) high sensitivity (HS) fluorometric quantitation protocol according to the manufacture's guidelines. A master mix containing 199 µL dsDNA HS buffer (Invitrogen, US) and 1 µL of dsDNA HS reagent (Invitrogen, US) per sample was made up in a clean tube. The mixture was briefly vortexed, and 195 µL added to clean Qubit sample tubes (Invitrogen, US). 5 µL of DNA sample was then added to the tubes. Two standards were made up containing 190 µL of the master mix and 10 µL of respective standards (Standard #1 and Standard #2 (Invitrogen, US)). All samples were vortexed and incubated at room temperature for 2 minutes. Firstly, standards were inserted into the Qubit® 2.0 fluorometer (Invitrogen, US) to create a calibration curve. Samples were then analysed in the same way and compared against the curve to determine DNA concentration.

IV.3 Illumina MiSeq amplicon library preparation

Three library preparations were carried out across the Chapters; these were 16S, 23S, and 18S rRNA genes to investigate bacterial, phototrophic, and eukaryotic community structure and diversity, respectively. 16S and 23S rRNA gene library preparation was carried out in Chapters 2 to 4, whereas 18S rRNA gene library preparation was only carried out in Chapter 4.

Water used in the library preparation was Just Water double distilled molecular biology grade water (Microzone Limited, UK). The polymerase used during the PCR

reactions was Q5® Hot Start High-Fidelity DNA polymerase 2x Master Mix (New England Biolabs, US) and will be from now on referred to as Q5®. 96-well plates were centrifuged at 1000 x *g* for 1 minute before and after use to ensure that samples were collected in the bottom of the wells. Plates were stored at -20 °C between stages.

IV.3.1 Normalisation

DNA samples were normalised to 1 ng/mL using a 96-well plate. Each DNA sample was diluted using an appropriate volume of water, however, any samples lower than 1 ng/mL in concentration were left neat.

IV.3.2 Amplicon PCR

Table IV.1: Primers and adapters used for MiSeq library construction.

Target	Region	Primer sequence	Fragment size (bp)
Bacterial	16S	515f - 5' - GTGCCAGCMGCCGCGGTAA 806r - 5' – GGACTACHVGGGTWTCTAAT	291
Phototrophic	23S	rV f1 - 5' - GGACAGAAAGACCCTATGAA rV r1 - 5' – TCAGCCTGTTATCCCTAGAG	410
Eukaryote	18S	V41f - 5' - CCAGCASCYGCGGTAATWCC V4r - 5' - ACTTTCGTTCTTGATYRA	500 - 600
Transposase sequences	-	f – 5' – TCGTCGGCAGCGTCAGATGTGTATAAGAGACAG r – 5' – GTCTCGTGGGCTCGGAGATGTGTATAAGAGACAG	32/33

Primers were designed so that Nextera XT transposase sequences were added to the published amplicon primer sequences. Bacterial primer sets were used as in Caporaso *et al.*

(2012), phototrophic primer sets as in Sherwood and Presting (2007), and eukaryotic primer sets as in Stoeck *et al.* (2010). Primer sequences were HPLC purified, and ordered from Sigma-Aldrich, US (**Table IV.1**).

A master mix of Q5®, BSA (Sigma-Aldrich, US), and respective primer sets were prepared (**Table IV.2**) and briefly vortexed. BSA was not used for 18S rRNA genes, and was substituted for water instead. 16 µL of master mix was aliquoted into the desired number of wells across a 96-well plate. 10 µL of template DNA sample from IV.3.1 were added to the appropriate wells, and the pipette was used to mix the sample. This resulted in a final reaction volume of 26 µL and PCR plates were sealed with a foil lid (Thermo Scientific, US).

Samples were amplified using a GeneAmp PCR System 9700 (Applied Biosystems, US). For bacterial primers, the following temperature programme was used; 98 °C for 30 seconds, followed by 25 cycles of 98 °C for 10 seconds, 50 °C for 15 seconds, and 72 °C for 20 seconds. There was then a final hold stage of 72 °C for 5 minutes, before cooling to 4 °C. For the phototrophic primers, the following temperature programme was used; 94 °C for 20 seconds, followed by 25 cycles of 94 °C for 20 seconds, 55 °C for 30 seconds, and 72 °C for 30 seconds. There was then a final hold stage of 72 °C for 10 minutes, before cooling at 4 °C. Finally, for the eukaryotic primers, the following temperature programme was used; 95 °C for 5 minutes, followed by 15 cycles of 95 °C for 3 minutes, 53 °C for 30 seconds, and 72 °C for 30 seconds, then 20 cycles of 95 °C for 30 seconds, 48 °C for 30 seconds, and 72 °C for 30 seconds. There was then a final hold stage of 72 °C for 10 minutes, before cooling to 4 °C.

Table IV.2: Reaction mixture components for amplicon PCR. BSA was not used for 18S rRNA genes and was substituted for water instead.

Reaction components	Volume per reaction (µL)
DNA template (1 µg/mL)	10
Q5®	13
BSA/water	0.4
Forward Primer (10 µM)	1.3
Reverse Primer (10 µM)	1.3

IV.3.3 PCR purification

The PCR purification step separated free primers and primer dimer species from the amplicons and used Agencourt AMPure XP beads (Beckman Coulter, UK). The AMPure XP beads were bought to room temperature and then vortexed for 30 seconds to ensure that the beads were evenly dispersed. The amplicon PCR plate was centrifuged at 1000 x *g* for 1 minute to collect the product at the bottom of the wells. 36 µL of the beads were added to each well (1.4 times the volume of the amplicon PCR reaction volume) and mixed by pipetting up and down ten times. The plate was incubated at room temperature for 5 minutes and then placed on a magnetic stand (Alpaqua, US) for 4 minutes until the supernatant had cleared.

While still on the magnetic stand, the supernatant was removed and discarded from each well. A mixture of 40 mL ethyl alcohol (200 proof, Sigma-Alrich, US) and 10 mL water (molecular biology grade, 5 Prime, Germany) was prepared and, while still on the magnetic stand, 200 µL was added to each well. The plate was incubated at room temperature for 30 seconds and then the supernatant removed and discarded. This was carried out twice in total. Plates were examined and any liquid still visible was removed. Plates were left to air-dry for 10 minutes whilst still on the magnetic stand.

After the incubation, the plate was removed from the stand and 40 µL of EB buffer (Qiagen, Germany) was added to each well and mixed ten times using the pipette. The plate was incubated at room temperature for 1 minute and then placed on the magnetic stand for 3 minutes until the supernatant had cleared. 35 µL of the supernatant was transferred to a new 96-well PCR plate and this was placed on a white surface to check there had been no carry over of AMPure beads. If any wells were brown in colour, they were transferred back to the original plate and left on the magnetic stand for a further 2 minutes before re-transferring. Plates were then sealed with a foil lid (Thermo Scientific, US) and centrifuged to collect the libraries at the bottom of the wells.

Libraries were run on a 1 % 96-well agarose gel (Hi-Res Standard, Geneflow Ltd., UK) for 10 minutes at 100 V to check if the purification had been successful. Sections IV.3.2 and IV.3.3 were repeated if any samples had not amplified.

IV.3.4 Index PCR

Illumina sequencing adapters and unique dual indices were added to the purified PCR products using index primers from the Nextera XT Index Kit v2 (Oligonucleotide sequences © 2007 – 2013 Illumina Inc., US).

A master mix was prepared consisting of 13 µL of Q5® and 4 µL water per reaction. 17 µL of master mix was added to each well of a 96-well plate. Index primers were arranged in a TruSeq Index Plate Fixture (Illumina, US), with forward i5 index primers aligned by row and reverse i7 primers aligned by column. 2.5 µL of forward i5 index primer was added to corresponding wells from 1 to 12, and 2.5 µL of the reverse i7 index primer was added to the corresponding wells from A to H. 4 µL of the purified PCR product from section IV.3.3 was added to the appropriate well and mixed by pipetting ten times. This left a final reaction mixture of 26 µL and the plate was covered with foil (Thermo Scientific, US) and centrifuged at 1000 x *g* for 1 minute.

Libraries were amplified using a GeneAmp PCR System 9700 (Applied Biosystems, US) using the following temperature programme; 95 °C for 3 minutes, followed by 8 cycles of 98 °C for 20 seconds, 55 °C for 15 seconds, and 72 °C for 15 seconds. There was then a final step of 72 °C for 5 minutes, then cooling to 4 °C. The plate was centrifuged again and a sub-sample of the libraries were tested on a 1 % agarose gel (Hi-Res Standard, Geneflow Ltd., UK) for 30 minutes at 100 V to check the size had shifted with the addition of the adapters and indices.

IV.3.5 SequalPrep™ normalisation

A normalisation step was carried out using the SequalPrep™ Normalisation Plate Kit (Invitrogen, US). 20 µL of SeuqalPrep™ Normalisation Binding Buffer (Invitrogen, US) was aliquoted into the wells of a SequalPrep™ Normalisation Plate (Invitrogen, US). 20 µL of the Index PCR product was added to the wells and mixed using the pipette. The plate was covered in foil (Thermo Scientific, US) and centrifuged at 1000 x *g* for 1 minute. The plate was then incubated at room temperature for 1 hour to allow binding of the DNA to the plate surface.

The liquid was then removed and discarded from the wells, making sure not to scrape the sides of the wells. 50 µL of SequalPrep™ Normalisation Wash Buffer (Invitrogen, US) was added to the wells and mixed by pipetting in order to improve the removal of contaminants. The buffer is then completely removed and discarded.

20 µL of SequalPrep™ Normalisation Elution Buffer (Invitrogen, US) was added to the wells and mixed by pipetting. The plate was covered in foil and centrifuged as before, then left to incubate at room temperature for 5 minutes.

IV.3.6 Pooling

Purified DNA was then pooled and transferred to a 1.5 mL micro-centrifuge tube. The tube was vortexed to mix and then briefly centrifuged. DNA concentration of the pooled library was quantified as in section IV.2 using the Qubit® 2.0 (Invitrogen, US) high sensitivity (HS) fluorometric quantitation protocol. The sample was then diluted or concentrated until they reached a 4 nM concentration. A 50 µL sample of pooled libraries was sent for sequencing.

IV.3.7 Sequencing details

Sequencing was carried out by the Genomics Facility at the University of Warwick, Coventry, United Kingdom. The final concentration of the pooled library was 4 nM and the library was sequenced using the MiSeq Reagent Kit v3 600-cycle (Illumina, US).

IV.3.8 Bioinformatic analyses

The Illumina MiSeq automatically de-multiplexed the raw sequences. Trimmomatic (version 0.35, Bolger *et al.* (2014)) was used to remove any low-quality bases from the ends of the sequence. USEARCH and UPARSE software (Edgar, 2010, Edgar, 2013) was then used for the remaining steps of the bioinformatic analysis. Assembling of the paired-end reads was carried out by the alignment of the forward and reverse reads, trimming primers, and quality filtering using the -fastq_maxee 0.5 command. Unique sequences were sorted by abundance and any singletons in the data were then discarded. A minimum identify

threshold was set at 97 % and sequences were clustered to OTUs using the –cluster_otus command, which also filters chimeras. For additional chimera filtering, the GOLD database (Edgar *et al.*, 2011) was used for 16S rRNA genes and *de novo* chimera checks in the UPARSE pipeline were used for 23S and 18S rRNA genes. QIIME (version 1.8, Caporaso *et al.* (2010)), as well as the Greengenes reference database (McDonald *et al.*, 2012) for 16S rRNA sequences and the ARB SILVA 119 LSU Ref database (Quast *et al.*, 2013) for 23S and 18S rRNA sequences, were used to assign taxonomies.

For 16S and 18S rRNA reads, the OTU table was split by taxonomy and then only bacterial or eukaryotic sequences were retained, respectively. For 16S rRNA reads, sequences of mitochondrial or chloroplast origin were removed. Samples were rarefied to an even sampling depth and this was determined ad-hoc to ensure that an acceptable number of sequences were maintained, yet the maximum number of samples possible were included. Samples which contained fewer sequences per sample than this value were discarded.

For 23S rRNA reads, however, there were a large number of OTUs which were left unassigned and taxonomy assignment was carried out by alignment in ARB (Ludwig *et al.*, 2004). Sequences were aligned against *Escherichia coli* 0157 and inserted into a SILVA 119 LSU Ref tree using parsimony criteria. Any sequences not assigned as phototrophs were unmarked. Organisms of close phylogenetic distance from the reads were selected from the tree and the alignment of the unassigned sequences were refined. The position of each sequence in the tree was then used to assign a taxonomy to each OTU based on their closest neighbour. The taxonomies were inputted into the original OTU table. The OTU table was rarefied, as with the 16S and 18S rRNA reads, and the total percentage of phototrophic taxa was determined. The original OTU table was then filtered so that only phototrophic taxa were retained and any eukaryotic samples assigned as “Metazoa” were removed. Rarefaction was carried out on this filtered OTU table – this was generally at a much lower level due to the small number of reads in the dark treatment samples.

APPENDIX V – GENERAL DISCUSSION SUPPORTING DATA

V.1 Supporting data

Sequences for OTUs showing significance between the dark microcosms and the dark microflumes are shown in **Tables V.1** and **V.2**. Sequences are stored at the NCBI GenBank database and accession numbers are given in **Tables V.1** and **V.2**.

Table V.1: Relative abundances of OTUs and their lowest taxonomic classification in the water fraction in dark microcosm and microflume treatments. The letters *c*, *f*, *g*, and *s* determines whether the classification is *class*, *family*, *genus*, or *species*, respectively. Sequences can be found at the NCBI GenBank database with the given accession number.

OTU number	GenBank accession number	Lowest taxonomic classification	Relative abundance of OTU (%)	
			Microcosms	Microflumes
410	MG947430	Bacteriovoracaceae (f)	0.0	0.26
3363	MG947431	Rubrivivax (g)	0.0	0.23
188	MG947432	Aquimonas (g)	0.0	0.26
4511	MG947433	Rhodobacter (g)	0.0	0.04
1954	MG947434	Comamonadaceae (f)	0.0	0.09
512	MG947435	Christensenellaceae (f)	0.0	0.16
24	MG947436	Sinobacteraceae (f)	0.0008	0.84
195	MG947437	TSBW08 (c)	0.0008	0.17
146	MG947438	Prosthecobacter debontii (g.s)	0.0008	0.50
4568	MG947439	Luteolibacter (g)	0.0008	0.37
1439	MG947440	Comamonadaceae (f)	0.003	1.55
132	MG947441	Luteolibacter (g)	0.002	0.48
2426	MG947442	Simplicispira (g)	0.002	4.78

Table V.2: Relative abundances of OTUs and their lowest taxonomic classification in the sediment fraction in dark microcosm and microflume treatments. The letters *c*, *o*, *f*, *g*, and *s* determines whether the classification is *class*, *order*, *family*, *genus*, or *species*, respectively. Sequences can be found at the NCBI GenBank database with the given accession number.

OTU number	GenBank accession number	Lowest taxonomic classification	Relative abundance of OTU (%)	
			Microcosms	Microflumes
3974	MG947573	Sphingomonadales (o)	0.0	0.02
636	MG947491	wb1_P06 (f)	0.0	0.04
4774	MG947588	JG30-KF-CM45 (o)	0.0	0.03
2390	MG947542	Gaiellaceae (f)	0.0	0.03
4363	MG947580	mb2424 (f)	0.0	0.03
870	MG947505	125ds10 (f)	0.0	0.03
3692	MG947565	Nocardioidaceae (f)	0.0	0.04
445	MG947475	agg27 (o)	0.0	0.03
744	MG947500	CCU21 (o)	0.0	0.03
892	MG947511	*Geothrix* (g)	0.0	0.03
238	MG947454	CCU21 (o)	0.0	0.14
543	MG947483	Betaproteobacteria (c)	0.0	0.04
4588	MG947583	Comamonadaceae (f)	0.0	0.23
4996	MG947589	Rhodospirillales (o)	0.0	0.08
3865	MG947569	MND1 (o)	0.0	0.07
492	MG947480	*Thauera* (g)	0.0	0.09
625	MG947490	Sinobacteraceae (f)	0.0	0.06
2827	MG947554	Ellin6529 (c)	0.0	0.21
3310	MG947559	Solirubrobacterales (o)	0.0	0.05
2030	MG947538	*Dechloromonas* (g)	0.0	0.09
798	MG947501	CCU21 (o)	0.0	0.04
1680	MG947534	Isosphaeraceae (f)	0.0	0.04
4749	MG947587	Ellin6067 (o)	0.0	0.05
871	MG947506	Anaerolineae (c)	0.0	0.05
920	MG947515	*4-29* (g)	0.0	0.09
3597	MG947562	Gemm-1 (c)	0.0	0.05
1027	MG947520	*Rhodoplanes* (g)	0.0	0.08
218	MG947452	Rhizobiales (o)	0.0	0.18
246	MG947456	A4b (f)	0.0	0.14
285	MG947461	Sinobacteraceae (f)	0.0	0.18
309	MG947463	0319-6A21 (f)	0.0	0.12
320	MG947466	Gaiellaceae (f)	0.0	0.26
409	MG947474	Hyphomicrobiaceae (f)	0.0	0.07
458	MG947478	Hyphomicrobiaceae (f)	0.0	0.17
577	MG947487	Dolo_23 (f)	0.0	0.10
4554	MG947582	*Nitrospira* (g)	0.0	0.07
3246	MG947558	*Agromyces* (g)	0.0	0.32
664	MG947493	iii1-15 (o)	0.0	0.06
5037	MG947590	Ellin6529 (c)	0.0	0.15

OTU number	GenBank accession number	Lowest taxonomic classification	Relative abundance of OTU (%)	
			Microcosms	Microflumes
4625	MG947584	Ellin6529 (c)	0.0	0.12
3380	MG947561	Sinobacteraceae (f)	0.0	0.25
917	MG947514	MVS-107 (o)	0.0	0.06
4053	MG947576	CCU21 (o)	0.0	0.08
234	MG947453	*DA101* (g)	0.0	0.20
1954	MG947536	Comamonadaceae (f)	0.0	0.13
322	MG947467	Syntrophobacteraceae (f)	0.0	0.17
323	MG947468	Gemm-1 (c)	0.0	0.23
2991	MG947556	Ellin6529 (c)	0.0	0.30
2006	MG947537	Phycisphaeraceae (f)	0.0	0.02
2219	MG947541	[Pedosphaerales] (o)	0.0	0.02
2723	MG947552	*Pirellula* (g)	0.0	0.02
1624	MG947532	JG30-KF-CM45 (o)	0.0	0.02
2950	MG947555	[Pedosphaerales] (o)	0.0	0.02
832	MG947503	d113 (o)	0.0	0.02
875	MG947508	*Cellulomonas xylanilytica* (g.s)	0.0	0.03
4091	MG947578	Pirellulaceae (f)	0.0	0.04
2432	MG947545	iii1-15 (o)	0.0	0.02
532	MG947481	PRR-10 (f)	0.0	0.06
953	MG947518	125ds10 (f)	0.0	0.02
3625	MG947564	Sinobacteraceae (f)	0.0	0.02
2543	MG947549	*Pseudomonas* (g)	0.0	0.02
1291	MG947526	0319-7L14 (o)	0.0	0.03
3935	MG947572	Xanthomonadaceae (f)	0.0	0.03
1316	MG947529	EB1017 (f)	0.0	0.04
900	MG947512	*Gemmata* (g)	0.0	0.03
4064	MG947577	RB40 (f)	0.0	0.04
2439	MG947546	Haliangiaceae (f)	0.0	0.04
1111	MG947523	iii1-15 (o)	0.0	0.05
355	MG947470	*Luteolibacter* (g)	0.0	0.03
571	MG947486	*Pseudonocardia* (g)	0.0	0.07
1487	MG947530	Gaiellales (o)	0.0	0.03
4512	MG947581	*Luteolibacter* (g)	0.0	0.03
1601	MG947531	B07_WMSP1 (o)	0.0	0.03
804	MG947502	CL500-15 (o)	0.0	0.03
856	MG947504	[Methylacidiphilae] (c)	0.0	0.03
879	MG947509	JG30-KF-CM45 (o)	0.0	0.03
907	MG947513	Myxococcales (o)	0.0	0.04
951	MG947517	Anaerolineae (c)	0.0	0.03
1085	MG947522	Rhodocyclaceae (f)	0.0	0.04
3797	MG947568	iii1-15 (o)	0.0	0.04
361	MG947471	*Kribbella* (g)	0.0	0.17
1235	MG947525	EB1017 (f)	0.0	0.04
690	MG947496	PRR-10 (f)	0.0	0.04
695	MG947497	Gemm-1 (c)	0.0	0.03
5093	MG947591	Sphingomonadaceae (f)	0.0	0.05

OTU number	GenBank accession number	Lowest taxonomic classification	Relative abundance of OTU (%)	
			Microcosms	Microflumes
4653	MG947585	Rhodocyclaceae (f)	0.0	0.04
2083	MG947539	Gaiellaceae (f)	0.0	0.03
981	MG947519	envOPS12 (o)	0.0	0.04
449	MG947476	Desulfobulbaceae (f)	0.0	0.14
3922	MG947571	Gaiellaceae (f)	0.0	0.15
680	MG947495	SB-34 (o)	0.0	0.10
4016	MG947575	Nocardioidaceae (f)	0.0	0.05
455	MG947475	Nitrospiraceae (f)	0.0008	0.08
553	MG947484	*Planctomyces* (g)	0.0008	0.06
474	MG947479	Gemmatimonadetes (c)	0.0008	0.08
253	MG947458	*Nitrospira* (g)	0.0008	0.31
46	MG947443	Pseudomonadaceae (f)	0.0008	1.51
2709	MG947551	RB40 (f)	0.0008	0.23
622	MG947489	AKYG1722 (o)	0.0008	0.11
115	MG947446	Gemm-1 (c)	0.0008	0.62
134	MG947448	Solirubrobacterales (o)	0.0008	0.23
310	MG947464	C111 (f)	0.0008	0.37
2540	MG947548	Actinomycetales (o)	0.0008	0.05
2555	MG947550	CCU21 (o)	0.0008	0.08
2413	MG947543	Rhizobiales (o)	0.0008	0.09
114	MG947445	Rhodospirillales (o)	0.0008	0.19
1827	MG947535	koll13 (f)	0.0008	0.04
362	MG947472	SB-1 (f)	0.0008	0.05
1300	MG947527	Betaproteobacteria (c)	0.0008	0.05
886	MG947510	Solibacterales (o)	0.0008	0.04
1034	MG947521	Rhizobiales (o)	0.0008	0.04
4002	MG947574	Ellin6529 (c)	0.0008	0.03
1676	MG947533	PRR-12 (c)	0.0008	0.02
1178	MG947524	Syntrophobacteraceae (f)	0.0008	0.02
2773	MG947553	Solirubrobacterales (o)	0.002	0.04
1301	MG947528	0319-7L14 (o)	0.002	0.06
950	MG947516	Ellin6529 (c)	0.002	0.07
3792	MG947567	Ellin6529 (c)	0.002	0.14
259	MG947459	Alphaproteobacteria (c)	0.002	0.22
298	MG947462	Gitt-GS-136 (c)	0.002	0.13
337	MG947469	DS-18 (o)	0.002	0.09
314	MG947465	Cytophagaceae (f)	0.002	0.16
3232	MG947557	Comamonadaceae (f)	0.002	0.36
4661	MG947586	*Nitrospira* (g)	0.002	0.17
3363	MG947560	*Rubrivivax* (g)	0.002	0.60
175	MG947450	Gaiellales (o)	0.002	0.26
874	MG947507	Sediment-1 (o)	0.002	0.03
621	MG947488	H39 (o)	0.002	0.05
165	MG947449	*Streptomyces* (g)	0.002	0.43
240	MG947455	C111 (f)	0.002	0.09
651	MG947492	SHA-26 (c)	0.002	0.06

OTU number	GenBank accession number	Lowest taxonomic classification	Relative abundance of OTU (%)	
			Microcosms	Microflumes
713	MG947498	0319-6A21 (f)	0.002	0.05
2123	MG947540	EB1017 (f)	0.002	0.05
559	MG947485	PK29 (o)	0.002	0.06
743	MG947499	iii1-15 (o)	0.002	0.05
3875	MG947570	*Aminobacter* (g)	0.002	0.03
125	MG947447	Rhizobiales (o)	0.003	0.08
4344	MG947579	*Gallionella* (g)	0.002	0.13
538	MG947482	JG30-KF-CM45 (o)	0.002	0.06
265	MG947460	Sediment-1 (o)	0.003	0.20
2426	MG947544	*Simplicispira* (g)	0.002	0.82
208	MG947451	CCU21 (o)	0.004	0.18
251	MG947457	*4-29* (g)	0.003	0.21
3714	MG947566	Intrasporangiaceae (f)	0.004	0.23
47	MG947444	*Candidatus Brocadia* (g)	0.003	0.57
670	MG947494	CV106 (f)	0.002	0.04
385	MG947473	Acidimicrobiales (o)	0.003	0.10
2445	MG947547	DS-18 (o)	0.002	0.05
3608	MG947563	Ellin6075 (f)	0.002	0.03